Assessment of the biological risks associated to the use of biosolids and wastewater

Claudia Sanz Lanzas

UPC CSIC
Consejo Superior de Investigaciones Científicas

Assessment of the biological risks associated to the use of biosolids and wastewater

Claudia Sanz Lanzas

Doctoral thesis by compendium of publications

Ph.D. program in Marine Sciences

Supervised by

Dr. Benjamí Piña and

Dr. Laia Navarro-Martín

Department of Enviromental Toxicology

Institute of Enviromental Assessment and Water Research (IDAEA-CSIC)

Barri de Gràcia, 2023

Table of contents

List of figures

Chapter One: General introduction

Chapter Two: Biological risks associated to biosolids reuse in agriculture

Chapter Three: Biological risks associated to wastewater effluents. Role of SAT technologies

Chapter Four: General discussion and conclusions

Supporting information

List of tables

Chapter One: General introduction

Chapter Two: Biological risks associated to biosolids reuse in agriculture

Chapter Three: Biological risks associated to wastewater effluents. Role of SAT technologies

Supporting information

List of abbreviations

AB: antibiotics

ABC: ATP-binding cassette

ABPs: Animal by-products not intended for human consumption

AhR: Aryl hydrocarbon receptor

AMR: Antimicrobial resistance

AOP: Adverse Outcome Pathway

AR: Antibiotic Resistance

ARB: Antibiotic Resistant Bacteria

ARGs: Antibiotic Resistant Genes

AWM: Agricultural waste management

cDNA: Complementary DNA

CE: Circular Economy

CEC: Contaminants of Emerging Concern

Ct: Quantification cycle

DEGs: Differentially Expressed Genes

DME: Drug-metabolizing enzymes

EC: European Commission

ED: Endocrine Disruption

EDCs: Endocrine Disrupting Chemicals

ERA: Environmental Risk Assessment

EU: European Union

FAOSTAT: Food and Agriculture Organization Corporate Statistical Database

KE: key event

LCA: Life cycle analysis

MAR: Managed Aquifer Recharge

MGEs: Mobile Genetic Elements

MIE: Molecular initiation event

mRNA: messenger RNA molecules

MSW: Municipal Solid Waste

NBS: nature-based-solutions

NGS: Next-Generation Sequencing

OECD: Organization for Economic Co-operation and Development

OFMSW: Organic Fraction of Municipal Solid Waste

OM: outer membrane

PBPs: penicillin binding proteins

PCR: Polymerase Chain Reaction

PG: peptidoglycan

PNEC: Predicted no-effect concentration

RB: reactive barriers

REACH (Registration, Evaluation, Authorization and Restriction of Chemicals)

RT-qPCR: Real time quantitative Polymerase Chain Reaction

SAT: Soil Aquifer Treatment

SDS: Safety Data Sheet

tRNA: Transfer RNA

UWM: Urban waste management

WHO: World Health organization

WWTP: Waste Water Treatment Plants

ZFIN: Zebrafish Information Network

Abstract

The circular economy is an emerging concept presented as a solution to counteract the damage caused by the linear economic scheme followed in the past decades. It is based on the principle of "closing the life cycle" and seeks, through reuse and revaluation, to extend the value of products, materials, and resources, such as water and energy, minimizing the generation of waste. In this context, the European Union (EU) aims to build a food system that could work under all circumstances, ensuring a safe and sustainable food and water supply for all citizens by applying circularity. Ensuring the availability of water and fertilizers for agriculture is probably the major challenge for achieving this goal. In this respect, the EU contemplates the use of effluents collected from water treatment plants (WWTP) for irrigation or aquifer recovery. Similarly, the use of solid waste such as sludge from WWTPs, the organic fraction of urban solid waste (OFMSW), or livestock waste, at different processing levels, is a promising alternative to mineral/chemical fertilization, promoting a self-sustainable, circular food system. However, the use of these recycled materials is not free from risks. They contain hazards of emerging concern including Contaminants of Emerging Concern (CECs) (like prescription drugs, endocrine disruptors and antibiotics) as well as different microbial hazards (not only pathogens, which are legally regulated and tested, but also antibiotic resistant bacteria known to spread the resistance to different antibiotics to the microbiomes from waterbodies, soils, and crops). Upcoming legislations that aim to promote and regulate their use agree on the fact that the main challenge relies on correctly assessing their associated risks for environmental and human health. This thesis aims to evaluate the biological activities associated to livestock wastes, OFMSW and WWTP effluents and associated biosolids in order to determine their potential hazards and the level of exposure for the environment and for the general population in the context of their use. For this purpose, we specifically evaluated the impact of organic fertilization on agroecosystems through ABs, ARGs and ARBs transmission and microbiome modulation monitoring. Moreover, we assessed the impact linked to WWTP effluents through the screening of ARGs and ARBs and associated toxic activities. Consequently, we developed an environmental risk analysis framework associated to biosolids and wastewater reuse considering the occurrence of the monitored hazards and their potential impacts on exposed environments. In the studies included in this thesis we observed that the selective pressure posed by the analyzed organic fertilizers was enough to favor the soil colonization by antibiotic-resistant bacteria and to increase horizontal gene transfer (HGT) in both target soils and crops. The fact that this impact appeared transient highlights the importance of respecting fertilization rates and the time elapsing from fertilization to harvest. Moreover, the processing of wastes favoring bacterial succession appeared as a valuable tool to reduce this risk. On the other hand, we detected high loads of both chemical and microbial hazards in WWTP effluents, underscoring the need of tertiary treatments able to reduce them in order to ensure a safe reuse of wastewater. In this regard, Soil Aquifer Treatment (SAT) technologies appeared in our studies as cost-effective alternatives to other tertiary treatments given their efficiency on removing biological (particularly ARG loads) and chemical hazards and their potential ability to promote the displacement of gut-related, copiotrophic bacteria by groundwater-like microbiomes, enhancing in this way the removal of ARGs, CECs and toxic activities.

Resum

L'economia circular és un concepte emergent que es presenta com una solució per contrarestar els danys causats per l'esquema econòmic lineal en les últimes dècades. Es basa en el principi de "tancar el cicle de vida" i busca, a través de la reutilització i la revaloració, allargar la vida i el valor de productes, materials i recursos, com l'aigua i l'energia, minimitzant la generació de residus. En aquest context, la Unió Europea (UE) té com a objectiu construir un sistema alimentari resilient, garantint un subministrament d'aliments i aigua segur i sostenible per a tots els ciutadans aplicant els principis de la circularitat. Assegurar la disponibilitat d'aigua i fertilitzants per a l'agricultura és probablement el gran repte per assolir aquest objectiu. En aquest sentit, la UE contempla l'ús d'efluents de les estacions de depuració d'aigües residuals (EDAR) per al reg o la recuperació d'aqüífers. De la mateixa manera, l'ús de residus sòlids com els fangs de les EDAR, la fracció orgànica dels residus sòlids urbans (FORM) o els residus ramaders, a diferents nivells de processament, és una alternativa prometedora a la fertilització mineral/química, promovent un sistema alimentari autosostenible i circular. No obstant això, l'ús d'aquests subproductes no està exempt de riscos químics i biològics. Això és degut a què en la composició d'aquests efluents i residus es poden detectar concentracions (rellevants) de contaminants emergents (CE) (com ho són els medicaments, els disruptors endocrins i els antibiòtics), així com la presència d'altres vectors de contaminació d'origen microbià (no només patògens regulats, sinó també bacteris resistents als antibiòtics coneguts per propagar la resistència a diferents antibiòtics a través dels microbiomes aquàtics i dels sòls i cultius). L'elaboració de polítiques que tenen com a objectiu promoure i regular el seu ús identifiquen la l'avaluació de riscos associats a la salut ambiental i humana com el principal repte. Aquesta tesi té com a objectiu avaluar les activitats biològiques associades als residus ramaders, FORM i efluents d'EDAR i biosòlids associats per tal de determinar els seus riscos potencials i el nivell d'exposició per al medi ambient i per a la població en general en el context del seu ús. Amb aquesta finalitat, hem avaluat específicament l'impacte de la fertilització orgànica en els agroecosistemes mitjançant la transmissió d'ABs, ARGs i ARBs i el monitoratge de la modulació del microbioma. A més, hem avaluat l'impacte vinculat als efluents de les EDAR mitjançant el cribratge d'ARGs i ARBs i activitats tòxiques associades. En conseqüència, aquset treball ha desenvolupat un marc d'anàlisi de riscos ambientals associat als biosòlids i a la reutilització d'aigües residuals tenint en compte l'ocurrència dels perills monitoritzats i els seus impactes potencials en els ambients exposats. En els estudis inclosos en aquesta tesi hem observat que la pressió selectiva que exerceixen els fertilitzants orgànics analitzats és suficient per afavorir la colonització del sòl per bacteris resistents als antibiòtics i per augmentar la transferència horitzontal de gens (THG) tant en sòls diana com en cultius. El fet que aquest impacte sigui transitori posa de manifest la importància de respectar les freqüències d'aplicació de fertilitzant als sòls i el temps transcorregut des de la fertilització fins a la collita. A més, s'ha identificat que el processament de residus afavorint la successió bacteriana és una eina molt valuosa/efectiva/útil per reduir aquest risc. D'altra banda, hem detectat altes càrregues de riscos tant químics com microbians als efluents de les EDAR, fet que evidencia la necessitat de tractaments terciaris capaços de reduir-los per garantir una reutilització segura de les aigües residuals. En aquest sentit, les tecnologies basades en la recàrrega artificial d'aqüífers (SAT) apareixen als nostres estudis com a alternatives rendibles i comparables a altres tractaments terciaris donada la seva eficiència en l'eliminació de riscos biològics (particularment ARG) i químics i la seva capacitat potencial per promoure el desplaçament de bacteris copiotròfics e intestinals per microbiomes semblants als de les aigües subterrànies, potenciant d'aquesta manera l'eliminació d'ARGs, CECs i activitats tòxiques associades.

CHAPTER ONE.

GENERAL INTRODUCTION

General introduction

Sanz, Claudia[1] Navarro-Martin, Laia[1;] Piña, Benjamin[1]

1) IDAEA-CSIC, Jordi Girona, 18. E-08034, Barcelona, Spain.

1. The end of the linear model

World´s population is rapidly increasing at an unsustainable rate, which translates into environmental damage, human health deterioration, impaired social structures and a deep depletion of resources. Historically, the main consumers of resources have been largely concentrated in the most developed regions, whereas materials have been sourced globally. As a consequence, the industrial nations have enjoyed a huge abundance of both materials and energy (Sariatli, 2017). Since materials have traditionally been cheaper than human labor, the producers have been motivated to adopt business models that relied on their extensive use. In consequence, the cheap material/expensive labor relationship translated into a rejection of recycling, reducing and waste reuse (Sariatli, 2017).

In the late 80's, circular economy (CE) emerged as a "life savior" to repair the damage caused by the linear economic scheme followed in the past decades (Winans et al., 2017). CE goes far beyond the 3Rs (reduce, reuse, recycle) adopting the 6Rs paradigm: reduce, reuse, recycle, redesign, remanufacture and recover. CE is based on three main principles: eliminate waste and pollution, circulate products and materials (at their highest value) and regenerate nature. It emphasizes on waste recycling, post consumerism and development of waste-based closed loops within

a company or among different manufacturers and consumers groups (Sakai et al., 2011). Nonetheless, CE is not usually applied equally amongst countries. For instance, the CE concept is used in China as a tool for new technology development and for the upgrading of existing equipment (Winans et al., 2017). Meanwhile, in North America and the European Union (EU), corporations apply this concept mainly for waste management with the aim to conduct life cycle analysis (LCA) studies on their products (Winans et al., 2017). Despite being around for a while, the CE concept is still being explored in many countries and its tools are evolving but do not always evaluate the social or community context in which these initiatives occur (Wang et al., 2012).

Circular economy is composed by two different kind of waste cycles: the technical and the biological (Ellen MacArthur Foundation, **Figure 1**). The technical cycle allocates non-biodegradable wastes (metals, rare-earth metals, plastics, polymers) that can be ideally recovered and feed back into the system by, for example, chemical or physical recycling. On the other hand, the biological cycle allocates wastes that are biodegradable (food waste, sewage sludge...) and that can be reused by the system itself following a strategy in which we restore nutrients into the biosphere while rebuilding natural capital (Peck et al., 2015). This thesis focuses on the wastes allocated on the biological waste cycle. This cycle, based mainly in regeneration, aims to counteract our past extractive and consumptive behavior by the collection and reintegration of biological waste (Sariatli, 2017).

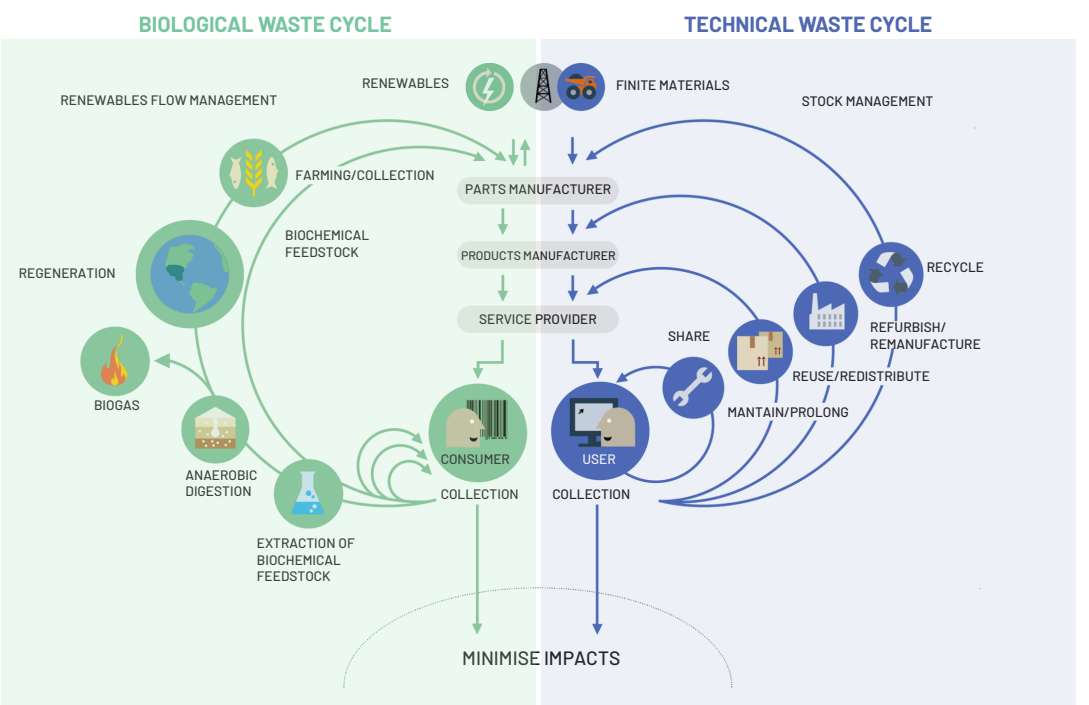

Figure 1. Circular economy systems diagram. Adapted from Ellen MacArthur Foundation[1].

1 https://ellenmacarthurfoundation.org/circular-economy-diagram

2. Europe and the circular biological waste cycle

The EU's Circular Economy Action Plan focuses on making crucial sectors circular with a special emphasis on the food, water and nutrients sector. In order to create a sustainable food system under a circular perspective, this plan contemplated the design of The Farm to Fork Strategy (COM/2020/381). This strategy, finally approved in 2020, aims to build a food system that could work under all circumstances, able to safeguard food security and protect the environment and human health and to ensure a sufficient supply of affordable food for all citizens. To achieve this goal, this framework considers a revision of EU pesticides legislation, a new EU animal welfare legislation, plans to address food waste, tackle food fraud and food labelling, a carbon farming initiative and the reform of the EU farm system. Its key goals for 2030 are a 50% reduction in the use and risk of pesticides, a 50% reduction in antimicrobials sales used for farmed animals and aquaculture, at least a 20% reduction in the use of chemical fertilizers and a 25% of agricultural land to be used for organic farming. The last three goals are deeply interconnected and are of special interest in the context of this thesis.

Firstly, the aim to reduce antimicrobial sales derives from their heavy misuse in animal and human healthcare systems over the past decades. Antimicrobials inappropriate use, led to the apparition and spreading of bacterial strains increasingly recalcitrant to medical treatment commonly called Antibiotic Resistant Bacteria (ARB). Antimicrobial Resistance (AR) causes annually an estimate of 35.000 and 33.000 human deaths in the US[1] and the EU[2] respectively. Therefore, there is an urgent need to counteract antimicrobials misuse, which can be achieved by a drastic reduction of sales. Secondly, the aim of reducing the use of chemical fertilizers derives from their proven adverse effect on soil's fertility and productivity, due to their intensive application in agriculture (EEA/PUBL/2022/023). Moreover, chemical fertilizers have a deep environmental impact, as they are obtained from non-renewable sources and are ineffectively absorbed by soils, becoming a major source of air, soil and water pollution, another reason for seeking their reduction (EEA/PUBL/2022/023).

In the context of the works carried in this thesis, these two objectives align with the last objective of promoting organic farming. According to The Farm to Fork Strategy, this type of farming represents a solution to chemical fertilization since it promotes the use of organic wastes as fertilizers, valorizing residues and simultaneously providing farmers with an important supply of high-quality nutrients and organic matter. Nonetheless, there are several hazards linked to organic waste fertilization that have the potential to impact animal and human health. Organic wastes can contain viral and bacterial pathogens and toxicants that could represent a risk for exposed farmers, livestock and consumers. Moreover, there is growing evidence of the role of organic fertilizers in increasing the occurrence and transmission of ARB in the exposed matrices (soil, crops and ultimately consumers) (Cerqueira et al., 2019; Tadić et al., 2021).

Regarding circularity around water reuse, the EU recognized in their Water Reuse Regulation (2022/C 298/01) that over-abstraction is the major cause of water stress, highlighting the agricultural and domestic sectors as the main water consumers. As a response, this regulation proposes the regeneration of wastewater as the best alternative to water abstraction. According with this document, the reuse of treated wastewater could improve the environment's status both quantitatively, by alleviating pressure substituting abstraction, and qualitatively, by avoiding the discharge from Waste Water Treatment Plants (WWTP) to sensitive areas. Moreover, when

[1] https://www.cdc.gov/drugresistance/national-estimates.html
[2] https://ec.europa.eu/commission/presscorner/detail/en/IP_22_6951

Table 1. Yearwise production (tons) of different wastes in the five continents. Adapted from Noor et al., (2020) with data from FAOSTAT[1].

Year	Country	Primary Fruit	Primary vegetables	Cereals crops	Citrus fruit	Manure
2000	Africa	6,81E+04	4,46E+04	1,05E+05	1,17E+04	1,90E+07
2010	Africa	9,31E+04	6,60E+04	1,58E+05	1,59E+04	2,52E+07
2017	Africa	1,09E+05	7,99E+04	1,89E+05	1,97E+04	2,98E+07
2000	America	1,39E+05	7,21E+04	5,21E+05	5,40E+04	6,81E+06
2010	America	1,50E+05	7,60E+04	6,22E+05	4,62E+04	6,85E+06
2017	America	1,61E+05	8,07E+04	7,54E+05	4,50E+04	6,94E+06
2000	Asia	2,79E+05	4,81E+05	8,15E+05	2,97E+04	3,83E+07
2010	Asia	4,29E+05	6,90E+05	1,01E+06	5,55E+04	4,27E+07
2017	Asia	5,10E+05	8,34E+05	1,21E+06	7,08E+04	4,65E+07
2000	Europe	8,37E+04	8,42E+04	3,83E+05	1,01E+04	1,56E+07
2010	Europe	7,63E+04	8,84E+04	4,04E+05	1,13E+04	1,37E+07
2017	Europe	7,67E+04	9,63E+04	5,20E+05	1,06E+04	1,35E+07
2000	Oceania	6,19E+03	3,31E+03	3,50E+04	6,72E+02	5,74E+06
2010	Oceania	7,09E+03	3,32E+03	3,44E+04	5,65E+02	4,59E+06
2017	Oceania	8,06E+03	3,32E+03	5,08E+04	5,47E+02	4,56E+06
Average value		1,47E+05	1,80E+05	4,54E+05	2,55E+04	1,86E+07

compared to desalination or water transfer practices, wastewater reuse requires lower investments in infrastructure and less energy to operate, contributing to reduce greenhouse gas emissions (Valhondo et al., 2020). This regulation also states that regenerated wastewater can be considered a reliable source of water supply for agriculture, since it is independent from droughts or weather variability and able to cover peaks of water demand.

As with organic fertilization, there are several biological risks attached to the reuse of wastewater that, without the proper regeneration practices, can potentially translate into ARB transmission or wild-life and human exposures to a wide range of pollutants (Kasonga et al., 2021; Petrie et al., 2015). In fact, the Water Reuse Regulation (2022/C 298/01) points out the necessity for the optimization of tools that allow the monitoring of biological risks along with the development of optimal wastewater treatments to ensure a safe reuse.

The main strategy carried by the Spanish government in the context of waste circularity is the Spanish Bioeconomy Strategy published by the Ministry of Agriculture, Fisheries and Food in 2015 adopting the EU's Circular Economy Action Plan. This strategy recognizes that, the Spanish agri-food chain is currently inefficient, since it generates high loads of crop residues and a wide range of by-products that are directly discarded. It also acknowledges the big amount of waste produced by human activity itself estimating in 159 million tones the amount of organic waste generated annually in Spain. Like EU's Farm to Fork Strategy, this document also promotes the reuse of organic wastes by means of organic fertilization and highlights the immediate need of a proper management and reuse of wastewater. It underscores how the reuse of organic by-products and wastewater will promote the development of rural regions and its interaction with urban areas as long as the sustainability and safety of their reuse can be guaranteed. From both, European

[1] https://www.fao.org/faostat/en/#search/excreted%20manure%20data

and Spanish perspectives, there is a need of a generation of an agro-urban mosaic, which actors collaborate in a way that circular economy settles in the two models.

3. Agricultural vs urban wastes

The current expansion of agricultural production translates into high amounts of waste from primary fruits and vegetables, cereals and citrus production (**Table 1**). However, the highest agricultural waste generated worldwide is animal manure, with a yearly average generation of more than 18.5 million tones (**Table 1**). Manure is mainly originated in farms, poultry houses and slaughterhouses as reflected in the Food and Agriculture Organization Corporate Statistical Database survey of excreted manure (N content) for the five continents (FAOSTAT, 2017) (**Figure 2**). Sheep and goats, cattle, swine, poultry and birds' manure contribute to the highest percentages of generated manure worldwide from which only a low percentage is being recycled (Meena, 2021). Therefore, further efforts to efficiently reuse agricultural waste are urgently needed (Meena, 2021). As acknowledged in the Spanish Bioeconomy Strategy, the expansion of agricultural production is mainly due to an uncontrolled population growth, which in turn leads to unmanageable loads of urban waste biomass. The main contributors to urban waste are residences, industries and hospitals, with wastewaters as their biological waste with higher environmental impact (Fereja & Chemeda, 2022).

With more than half percent of world´s population living in urban areas and a predicted rise in the urbanization rate of 1.5 times in 2045, an increase of 70% in urban waste is expected (Noor et al., 2020). That implies that the amount of waste generated in urban areas will increase double than the rate of urbanization itself. Moreover, models estimate that 60% of developing countries are expected to be urban and will accommodate 93% of world´s population by 2030 (Kubanza & Simatele, 2016). The fact that 31% of lower income countries do not have a proper access to waste collection translates into 93% of their waste being regularly disposed in open and unmanaged dumpsites. These numbers, added to the weak institutional capacities, limited budgets, inadequate infrastructure, and corruption will prohibit a sustainable urban development in these countries (Breukelman et al., 2019; Cohen, 2006;

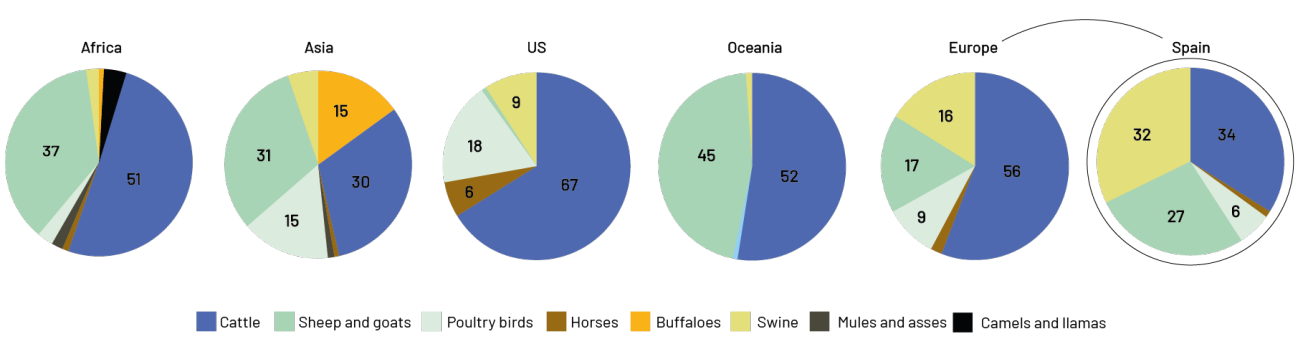

Figure 2. Excreted manure (N content) for the five continents in 2017. Data from FAOSTAT[1].

[1] https://www.fao.org/faostat/en/#search/excreted%20manure%20data

Zhang, 2016).

In this context, efforts need to be centered in (1) optimizing agricultural waste management (AWM) practices on a global scale and (2) improving urban waste management (UWM) by addressing the interconnexions between urbanization and urban governance, especially in developing countries (Kubanza & Simatele, 2016).

3.1 Limitations and methods for agricultural waste reuse

Optimizing AWM practices is a long-term task that starts with the identification of the wastes subjected to recycling. According with the Waste Framework Directive (2008/98/EC), an agricultural waste is considered candidate for recycling if it meets the following requirements:

1. The recovered substance will be used for specific purposes

2. There is a market or demand for the recovered substance

3. The substance meets the technical requirements for the specific purposes and complies with the existing legislation and the rules applicable to products

4. The use of the substance will not generate global adverse impacts for the environment or health

Amongst the different agricultural wastes, the European regulation (EC) no. 1069/2009 specifically legislates the handling and reuse of animal by-products not intended for human consumption (ABPs). It establishes the sanitary and hygienic standards applicable to ABPs and their products derivatives to avoid risks to human and animal health and preserve the safety of the food chain. Also, it classifies ABPs into three categories, based on the level of risk posed to human and animal health and establishes the conditions of disposal and use for each category. Specifically, in section 2 entitled "Fertilizers and soil amendments of organic origin" states that the fertilizers and soil amendments derived from agricultural waste can be sold and used if they have been through pressure sterilization or other disinfection procedures to safeguard public and animal health.

Spain regulates ABPs with the Royal Decree 1528/2012 (BOE-A-2012-14165) adopting these EU Regulations. In line with the EU, the Spanish Senate approved in March 29th of 2022 the bill "Waste and Contaminated Soil Bill for a Circular Economy" (C.DIP 205765 29/03/2022) that advocates for a proper composting and digestion of agricultural waste for its use in agriculture. In this bill, compost is defined as "sanitized and stabilized organic amendment obtained from controlled aerobic and thermophilic biological treatment of separately collected biodegradable waste" and digestate as "organic material obtained from the anaerobic biological treatment of separately collected biodegradable waste". This bill states that competent authorities must promote the use of properly elaborated compost and digestate in the agricultural sector as a contribution to the saving of mineral fertilizers, if possible. The use of compost and digestate is advisable as long as a low carbon/nitrogen ratio (lower than 10) and a high pH (6.0 – 7.0) can be ensured in order to increase the value and safety of the fertilizer. In this framework, an ideal composting process is described as a combination of nitrogen-rich residues (vegetable crop residues) with carbon-rich bulking agents (e.g., straw, poplar bark, wood chips, heath biomass) in order to optimize the carbon/nitrogen ratio, decrease the moisture content and minimize nitrogen losses.

Interestingly, the direct application of untreated agricultural waste to target soils remains unrecommended, but not prohibited, in these guidelines, on the grounds of its proven

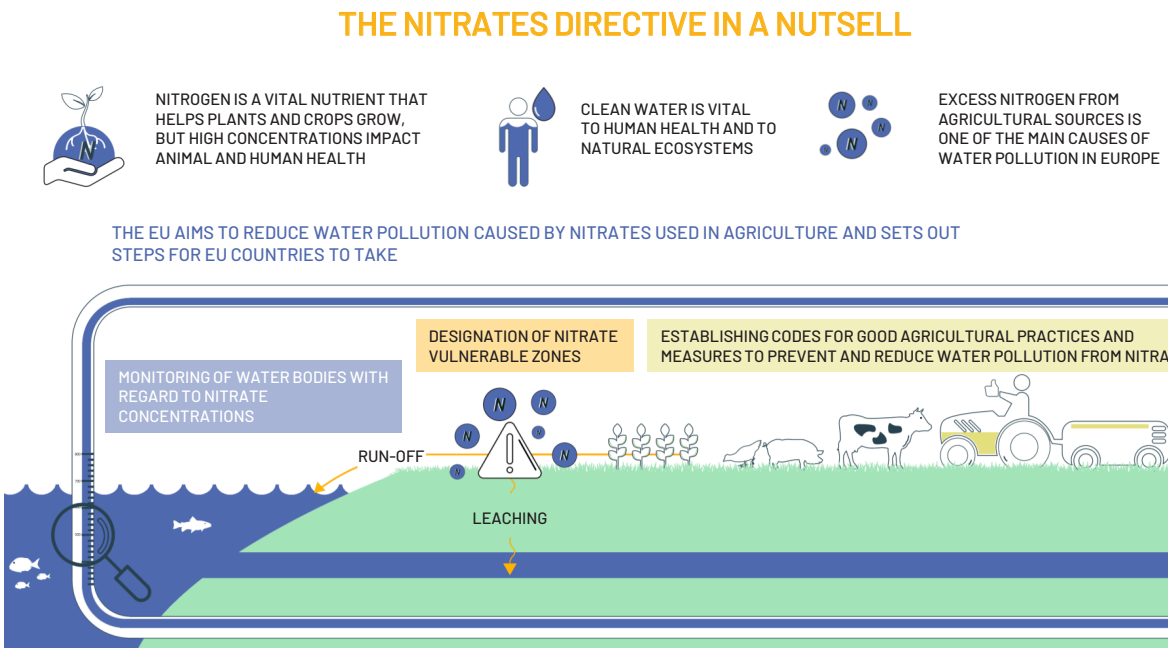

Figure 3. The Nitrates Directive in a nutshell[1].

phytotoxicity, viscosity, odor, slow decomposition rate, and high nitrate loads (Abdullahi et al., 2008). The latter received special emphasis in Europe since 2013 with the Nitrates Directive (91/676/EEC). This directive aims to protect water bodies against pollution caused by nitrates from agricultural sources and includes recommendations about nutrient management and a safe use of organic fertilizers (composted, digested or as last option, raw) (**Figure 3**). It recommends the application of fertilizers following the crop's nutrients requirement, taking into account the nitrogen and phosphorus content and applying them to a maximum annual fertilization rate. This document specifies that prior to any fertilization, the target soil must be tested to tailor fertilizer's nutrients around its needs. It also states that it is crucial that the application of the organic fertilizer takes place within 100 to 200 m of any water abstraction point and that a low emission spreading equipment is used when applied raw. Finally, it also recommends a proper storage of fertilizers in order to avoid leakages at all costs and a 12-month interval between application and crop harvest in the case of products normally consumed raw.

It is worth mentioning that on December 2nd of 2021, the EC decided to refer Spain to the Court of Justice of the EU due to a poor implementation of the Nitrates Directive[2]. The Commission sent a Letter of Formal Notice to Spain in November 2018 and a Reasoned Opinion in June 2020 highlighting Spain's failure to comply with the Nitrates Directive requirements. It states that despite some limited progress, Spain must still take additional measures to prevent eutrophication since the measures established to date have failed to achieve the objectives of the Directive. In addition, Spain should review and further designate Nitrate Vulnerable Zones in seven regions (Castilla y León, Extremadura, Galicia, Islas Baleares, Islas Canarias, Madrid and Comunidad Valenciana). This letter included all the necessary mandatory elements in the Action Programmes for five regions (Aragón, Castilla-La Mancha, Castilla y León, Extremadura and Madrid) and takes additional measures for the four regions where the measures set in place have proven to be insufficient (Aragón, Castilla-La Mancha, Castilla y León and Murcia). This fact reveals the urgent necessity of a proper management and treatment of the organic fertilizers used in Spain before their

[1] https://ec.europa.eu/environment/water/water-nitrates/index_en.html
[2] https://ec.europa.eu/commission/presscorner/detail/en/ip_21_6265

field application.

Some examples of properly managed organic fertilizers appear in the 'Practical guidelines for the use of agricultural wastes, co-products and by-products' elaborated during the project Agrocycle[1] (June 2016 – May 2019) were they characterized relevant organic waste streams (i.e, cattle manure, poultry litter, olive waste) in order to promote their use as soil amendments. The Agriclose[2] project, in which we collaborated during the development of this thesis, is another example of well managed pig manure-based fertilizers. This project aimed to promote new and safe fertilization strategies to improve the management of pig manure-based subproducts due the lack of regulations and certifications for their application in Catalonia (Spain). By the end of the project, more than one million m^3 of treated slurry was used safely for primary fruits and cereal crops fertilization.

3.2 Limitations and methods for urban solid waste use

The first efforts of Europe towards the improving of their urban waste management (UWM) started with the Waste Statistics Regulation in 2002 (EC/2150/2002), which generated data statistics about the recovery and waste management practices of different urban sectors. It wasn´t until 2018 that the EU issued the Landfill Directive (EU/2018/850) to regulate the urban solid waste that reaches landfills while preventing/reducing the adverse environmental and human health effects derived from their disposal. Despite this legislative effort, 47% of the annual 3.2 billion tons of urban solid waste is currently landfilled, with construction and demolition sectors as the major generators. Around 31% of the total urban solid waste is incinerated with household waste as the main source. This altogether implies that only the 22% of this waste is being recycled while the 78% is being incinerated and mostly landfilled (Noor et al., 2020; Zeller et al., 2019).

Also in 2018, a revision of the Waste Framework Directive 2008/98/EC started in order to force Member States (at the latest in 2023 December 31st) to separate and recycle their urban solid waste at the source, or to collect them separately without mixing them with other types of waste. This revision states that sorting the urban solid waste at source will help the subsequent separation processes (magnetic, pneumatic and water concentration (Wang et al., 2015). Some uses for the processed urban solid waste are also stated in this revision, like the building of green bricks for construction by mixing selected crushed solid wastes or the selection of organic compounds for their posterior use as methane (by fermentation) or electricity source (after sulfur and CO_2 removal and further drying). Another use for urban biological wastes, like WWTP sludge or the Organic Fraction of Municipal Solid Waste (OFMSW), could be their use as urban solid waste-based fertilizers in agriculture as proposed in the DAMA[3] project with which we also collaborated in this thesis.

4. Water scarcity and water reuse

As earlier introduced, water scarcity has become a major constraint to socio-economic development and a threat to populations prosperity worldwide. This problematic has a multi-faceted nature that englobes population increase, water availability (with its inter- and intra-annual variability) and water use (Liu et al., 2017). It seems obvious that water use cannot exceed water availability, but the reality is that while water use is increasing, water availability is shrinking due to both the depletion of fossil groundwater reservoirs and the increasing pollution of these reservoirs (Boretti & Rosa, 2019). As a result, many countries are

[1] https://www.agrocycle.eu
[2] https://agriclose.eu/en/
[3] https://damaproject.es/

experiencing water scarcity, especially in coastal areas densely populated with a high urbanization rate. The gentle nature-based-solutions (NBS) to regulate water use proposed by the World Water Assessment Program[1] in 2018 including the limitation of population and economic growth are quite impractical to solve this problem. Despite the EU efforts to highlight the potential of wastewater regeneration in order to counteract water scarcity, 80% of industrial and municipal wastewaters worldwide are currently being released untreated due to the rapid urbanization and the high cost of wastewater treatment (Noor et al., 2020). This results in a growing deterioration of water quality and availability and has detrimental impacts on human health and ecosystems. The optimization of more cost-efficient and environmentally friendly ways to regenerate wastewater appears as a clear current challenge.

4.1 Limitations and methods for urban wastewater reuse.

The EU published in 2022 a set of guidelines for a safer reuse of treated urban wastewater for agricultural irrigation (Regulation 2022/C 298/01). These guidelines included an introduction to the earlier mentioned Water Reuse Regulation that will set out minimum water quality parameters and mandatory risk evaluation and long-term monitoring. This new Regulation will include legislation from the Water Framework Directive (WFD) 2000/60/EC, the Groundwater Directive (GWD) 2006/118/EC, the Environmental Quality Standards Directive (EQSD) 2008/105/EC, the Nitrates Directive (91/676/EEC) and, where applicable, the Bathing Water Directive (BWD) 2006/7/EC and Drinking Water Directive (DWD) 2020/2184.

In the context of this thesis, the most interesting part of this upcoming regulation is the wastewater reuse risk evaluation. Article 5 (1) sets out how the competent authority will be ultimately responsible for ensuring the establishment of a risk management plan, addressing production, supply and use of reclaimed water. Some of the main elements in this plan are hazard identification (pathogens and pollutants) and potential hazardous events discovery associated with the wastewater reuse. The risk management plan must identify populations and environments potentially exposed to each identified hazard and the potential associated health risks for each receptor (people, animals, crops or plants, other terrestrial biota, aquatic biota and soils) in each exposure route (**Figure 4**). Aligned with this, installing/developing an environmental monitoring system is another key element of this strategy, which will allow to control the release and potential effect of the identified pollutants in the exposed environmental receptors.

The relevance of all the stated requirements for a specific wastewater reuse system in agriculture will depend on the types of cultivation (e.g. production of foodstuff or feedstuff), agricultural practices and the type of agricultural field. **Figure 5** shows a graphical example of how to determine which directive or regulation applies to a given water reuse system, evaluating potential interactions of the reclaimed water with the environmental matrices (freshwater resources) due to accidental leakages or via run-off from the irrigated field. The figure also illustrates the regulations and directives that might apply, depending on the agricultural practices.

Among the different wastewater reclamation systems available (advance oxidation, wetland-based treatments, membrane-based systems) Managed Aquifer Recharge (MAR) appear as a cost-effective green technology (**Figure 6**). MAR allows groundwater-dependent regions to maintain, enhance and protect their water resources with a limited use of energy and materials by the purposeful recharge of wastewater to aquifers (Dillon et al., 2019). These

[1] https://www.unwater.org/publications/world-water-development-report-2018

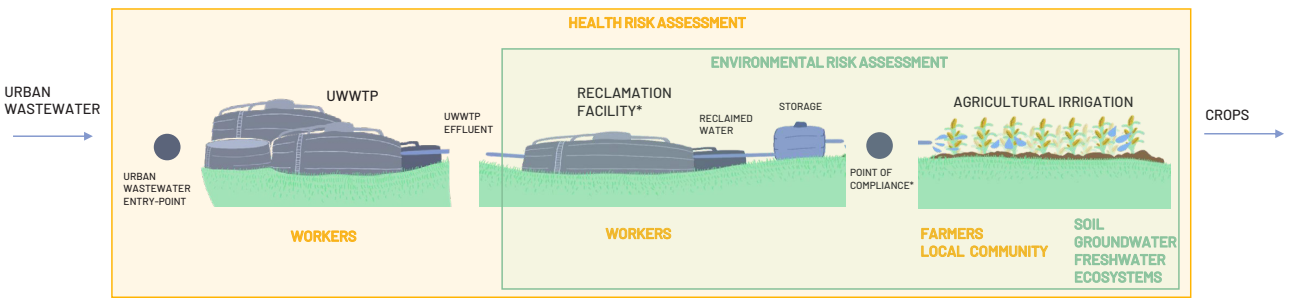

Figure 4. Main elements of a water reuse system, identifying receptors in the risk assessment. *Reclamation Facility: any urban WWTP or other facility that further treats urban wastewater that is fit for a use specified in section 1 of annex 1 of the 741/2020 Regulation; *Point of Compliance: the point where a reclamation facility operator Delivers reclaimed water to the next actor in the chain. In this image the reclaimed water is delivered directly to the end-users, but in other situations it may be delivered to a distribution operator or a storage operator. Adapted from Regulation 2022/C 298/01.

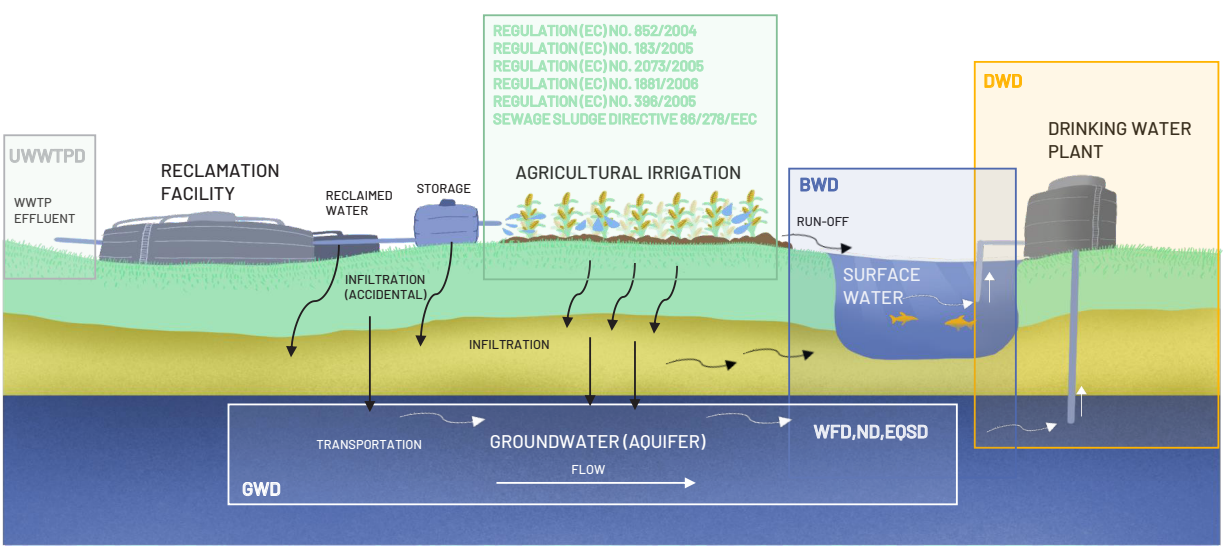

Figure 5. Graphic example of (1) how to identify applicable directives and regulations in a water reuse system, based on potential pathways taken by reclaimed water to the surrounding environments (surface water and groundwater) and (2) regulations and directives that could apply to the subsequent agricultural irrigation, depending on specific agricultural practices. UWWTPD: Urban Wastewater Treatment Directive, DWD: Drinking Water Directive; BWD: Bathing Water Directive (if surface water is used for bathing activities); GWD: Groundwater Directive; WFD: Water Framework Directive; EQSD: Environmental Quality Standard Directive; ND: Nitrate Directive (if water reuse scheme falls into Nitrate Vulnerable Zone (NVZ)). Adapted from: "Guidelines to support the application of Regulation 2020/741 on minimum requirements for water reuse" (2022/C 298/01).

techniques have become quite popular in recent years and have many advantages like their 1) low implementation cost, 2) low water loss due to evaporation when compared to surface reservoirs, 3) ability to infiltrate large volumes of water from different sources, including river or stream waters, urban and agricultural runoff and treated municipal wastewater (Alam et al., 2021), 4) contribution to aquifer recovery. Wastewater regeneration and aquifer recharge in MAR systems can be achieved following different strategies like dune infiltration, bank infiltration or Soil Aquifer Treatment (SAT) (Alam et al., 2021, **Figure 6**). MAR practices have proven to prevent storm runoff and soil erosion, preserve environmental flows in streams/rivers, mitigate flood and flood-derived damages, control saline intrusion, reduce land subsidence and have a hydraulic control of contaminant plumes. However, they suffer from some limitations as clogging, uncertainty in aquifer hydraulics, as well as potential damage to aquifers and other operational issues (Gruetzmacher & Kumar, 2012). A pilot scale example of MAR through SAT strategies was built during the RESTORA[1] project, with which we also collaborated in this work. In this project, the recharge basins from the SAT systems were optimized with different organic substrates in order to accelerate regeneration resulting in an efficient removal of hazards and a high-quality outflow water.

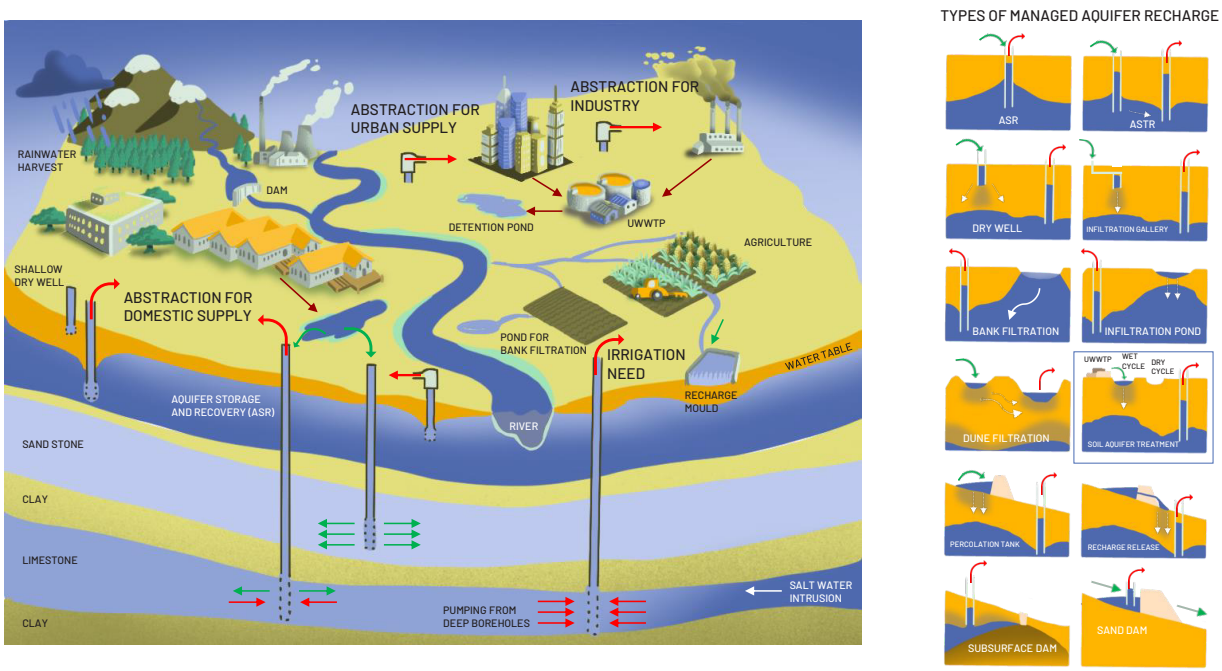

Figure 6. Different managed aquifer recharge techniques based on the type of aquifer, topography, land use, and intended uses of the recovered water. ASR stands for aquifer storage and recovery and ASTR stands for aquifer storage transport and recovery. Adapted from Alam et al., (2021).

[1] https://restora.h2ogeo.upc.edu/

5. Hazards associated to the use of biosolids and wastewaters

Europe and Spain advocate for agro-urban waste and wastewater reuse, but the fact that ensuring its safety is always highlighted, reveals their concern about their associated chemical and biological hazards. The term chemical hazard refers to any non-biological substance (i.e, food additives, pesticides, drugs) that can have a detrimental impact on life or health (Urben, 2017). On the other hand, a biological hazard can be described as a biological substance (i.e, pathogens, ARB, viruses) that might pose a threat to the health of exposed living organisms (Shroder, 2015). Some members from both groups are currently legislated due to their proven and well-characterized impact (priority hazards) but most of them are currently unregulated since they have been recently discovered and/or their impacts are still being assessed (emerging hazards).

5.1 Priority hazards

The first attempt to regulate the spreading of chemical hazards (within the industrial context) in a standard manner across Europe came with the REACH (Registration, Evaluation, Authorization and Restriction of Chemicals) regulation. REACH[1] was created in 2007 in order to improve the protection of human and environmental health from the risks posed by exposure to chemicals, promoting alternative methods for the hazard assessment of substances.

REACH was specifically designed for companies to identify and manage the risks associated to the substances they manufacture and market in the EU. Companies have to register the chemical compounds or the mixture of compounds they use and the products they manufacture in order to get the European Chemicals Agency (ECHA) approval for their use, sale or import. The detailed information about the physical and chemical properties of the substances as well as the identification of the risks attached to their use, must be provided in a Safety Data Sheet (SDS). The hazard identification provided in the SDS is mainly based on general toxicity tests data (ECHA, 2020). REACH applies to all chemical substances, from those used in industrial processes to those present in daily items, including cleaning products, paints, clothes, furniture and electrical appliances. The annex II of the REACH Regulation was amended in July 2020 (ECHA, 2020) in order to make mandatory the declaration of all substances that exist in different nanoforms as well as those that have potential endocrine disrupting properties (according to the 2017/2100 and 2018/605 Regulations).

Despite this legislative effort to reduce the use and spreading of industrial hazardous substances, many regulated compounds like different chemicals and active substances of biocidal products and plant protection products have been frequently detected in surface waters, groundwaters or soils across Europe (Oelkers, 2021). In order to monitor and prevent harmful substances reaching water bodies, the Water Framework Directive (2008/105/EC) created a list of "priority substances" using data from REACH and a big collection of ecotoxicological studies (Oelkers, 2021). The list (amended in 2013 with the Directive 2013/39/EU) currently contains 45 priority substances like plant protection products, biocides, metals, flame retardants, amongst others (**Table 2**). Like REACH regulated compounds, priority substances still appear above environmental quality standards in water bodies (Ribeiro et al., 2016).

Some priority substances like Persistent Organic Pollutants (POPs), pesticides and heavy metals have been detected in wastewaters and biosolids, seriously compromising their safe and legal reuse/disposal (Möller & Schultheiß, 2015; You

[2] https://echa.europa.eu/regulations/reach/understanding-reach.

Table 2. Priority list published in the Directive 2013/39/EU.

Number	CAS number	Name of priority substance
1	15972-60-8	Alachlor
2	120-12-7	Anthracene
3	1912-24-9	Atrazine
4	71-43-2	Benzene
5	not applicable	Brominated diphenylethers
6	7440-43-9	Cadmium and its compounds
7	85535-84-8	Chloroalkanes, C10-13
8	470-90-6	Chlorfenvinphos
9	2921-88-2	Chlorpyrifos (Chlorpyrifos-ethyl)
10	107-06-2	1,2-dichloroethane
11	75-09-2	Dichloromethane
12	117-81-7	Di(2-ethylhexyl)phthalate (DEHP)
13	330-54-1	Diuron
14	115-29-7	Endosulfan
15	206-44-0	Fluoranthene
16	118-74-1	Hexachlorobenzene
17	87-68-3	Hexachlorobutadiene
18	608-73-1	Hexachlorocyclohexane
19	34123-59-6	Isoproturon
20	7439-92-1	Lead and its compounds
21	7439-97-6	Mercury and its compounds
22	91-20-3	Naphthalene
23	7440-02-0	Nickel and its compounds
24	not applicable	Nonylphenols
25	not applicable	Octylphenols
26	608-93-5	Pentachlorobenzene
27	87-86-5	Pentachloropheno
28	not applicable	Polyaromatic hydrocarbons (PAH)
29	122-34-9	Simazine
30	not applicable	Tributyltin compounds
31	12002-48-1	Trichlorobenzenes
32	67-66-3	Trichloromethane (chloroform)
33	1582-09-8	Trifluralin
34	115-32-2	Dicofol
35	1763-23-1	Perfluorooctane sulfonic acid and its derivatives (PFOS)
36	124495-18-7	Quinoxyfen
37	not applicable	Dioxins and dioxin-like compounds
38	74070-46-5	Aclonifen
39	42576-02-3	Bifenox
40	28159-98-0	Cybutryne
41	52315-07-8	Cypermethrin
42	62-73-7	Dichlorvos
43	not applicable	Hexabromocyclododecanes (HBCDD)
44	76-44-8/ 1024-57-3	Heptachlor and heptachlor epoxide
45	886-50-0	Terbutryn

et al., 2020). High loads of nitrates are also present in biosolids (Paramashivam et al., 2017) and wastewaters (Stjepanović et al., 2019) and ,despite not being considered priority substances, they are regulated by the Nitrates Directive 91/676/EEC which could also compromise their reuse without proper treatment. Regarding the regulation of biological hazards, in a wastewater and biosolid reuse context, only the monitoring of pathogens is currently mandatory. For instance, the regulation 2019/1009/EU in its consolidated version from August 16th 2022, set limits to the presence of *Salmonella* spp and *Escherichia coli* or Enterococcaceae in organic fertilizers and organo-mineral fertilizers and the Water Reuse Regulation 2020/741 establishes minimum quality requirements, including minimal frequencies of monitoring for the presence of *Escherichia coli, Legionella* spp and intestinal nematodes in wastewater intended for agricultural irrigation.

In light of the current legislative framework, the first approach to ensure a safe reuse of biosolids and wastewaters should start with the monitoring of priority substances, nitrate and pathogen loads in both the matrices themselves and the impacted environmental compartments. Subsequently, a screening and impact evaluation of the rest of emerging hazards should take place.

5.2 Emerging hazards

Contaminants of Emerging Concern

A Contaminant of Emerging Concern (CEC) can be defined as any pollutant of anthropogenic origin that "is not currently included in routine monitoring programs, which may be candidate for future regulation depending in research on its (eco) toxicity, potential health effects, public perception and occurrence in various environmental compartments" (Yadav et al., 2021). Drinking water, reservoirs, lakes, and rivers play a major role in CECs dissemination (Yadav et al., 2021), resulting on a widespread distribution across many environmental compartments. Some examples of widespread CECs are summarized in **Table 3**. Derived from their production, distribution, and use in domestic and industrial activities, CECs travel through various pathways potentially contaminating air, ground/surface waters and soil, impairing simultaneously aquatic and terrestrial ecosystems and human health (**Figure 7**). Complex mixtures of airborne CECs reach the atmosphere daily where they transform, appearing more toxic and up to an order-of-magnitude more persistent than their respective parent forms (Q. Liu et al., 2021). Industries, agriculture, hospitals and household wastewaters are also potentially polluted with complex mixtures of unregulated compounds that travel unaltered through WWTPs reaching ground/surface waters (**Figure 7**, Yadav et al., 2021). At the same time, soil acts as a sink of different CECs from different sources, like landfill leachates or agricultural run-off, with potentially high impacts on soil productivity and soil organisms (Bender & van der Heijden, 2015; W. Zhang et al., 2020). In turn, plants growing in these polluted soils may also act as CEC vectors (Yadav et al., 2021). The complexity of the discharges/emissions aligned with the different propagation patterns of CECs lead to subsequent synergistic, antagonistic or additive effects on exposed humans and ecosystems (Tran et al., 2017).

One of the best described health effects derived from the exposure to CECs and many regulated compounds is their potential for Endocrine Disruption (ED). Endocrine Disruptor Chemicals (EDCs) are defined by the World Health Organization (WHO) as "any exogenous substance or mixture that alters function(s) of the endocrine system and consequently causes adverse health effects in an intact organism, or its progeny, or (sub)populations". These negative effects can be exerted by a number of different mechanisms, being the ability of many EDCs to mimic, inhibit

Table 3. Examples of widespread CECs. Adapted from Salimi et al., (2017).

Classes	Used as	Examples
Pharmaceuticals and personal care products (PPCPs)		
Analgesics	Pain reliever	Acetaminophen and acetylsalicylic
Anti-epileptic drugs	Anticonvulsant	Carbamazepine and primidone
Antihyperlipidemics	Lipid regulators	Gemfibrozil, clofibric acid, and fenofibric acid
Non-steroidal anti-inflammatory drugs	Anti-inflammatory	Diclofenac, ibuprofen, ketoprofen, and naproxen
Synthetic hormones	Hormonal treatment	17α-estradiol, 17α-ethinylestradiol
Antimicrobials	Antibiotic	Erythromycin, sulfamethoxazole, and tetracycline
	Antiseptic	Triclosan, biphenylol, and chlorophene
Polycyclic musks	Fragrances	Hexahydrohexamethyl-cyclopentabenzopyran
Other	Insect repellant	DEET
	Fragrances	Acetophenone
	Stimulant	Caffeine
Endocrine-Disrupting Chemicals (EDCs)		
Steroids	Natural human estrogen	17β-estradiol
	Metabolite	Estrone
Alkylphenols	Manufacture of household and industrial products	Nonylphenol and octylphenol
Polyaromatic compounds	Additives	Polychlorinated biphenyls and brominated flame retardants
Others	By-products of various industrial and combustion processes	Dioxins and furans
Flame Retardants (FRs)		
Halogen-containing flame retardants (fluorine, chlorine, bromine, or iodine)	FRs	Brominated bisphenols and phenols
Phosphorus-based FRs	FRs	Elemental red phosphorus and inorganic phosphates
Melamine FRs	FRs	Melamine cyanurate
Inorganic hydroxides FRs	FRs	Aluminum hydroxide and magnesium hydroxide
Borate FRs	FRs	Sodium borate and boric acid
Pesticides		
Carbamates	Herbicides, insecticides, and fungicide	Carbendazim, benomyl, and carbaryl
Chloroacetanilides	Preemergent herbicides	Metolachlor and alachlor
Chlorophenoxy acids	Herbicides	Bentazone and triclopyr
Organochlorines	Insecticides	DDT, dieldrin, endrin, and endosulfan
Organophosphates	Insecticides	Diazinon, malathion, and chlorpyrifos
Pyrethroids	Insecticides	Biphenthrin, cypermethrin, and esfenvalerate
Triazines	Herbicides	Atrazine, cyanazine, and simazine
Artificial Sweeteners (ASWs)		
Artificial sweeteners	Sugar substitutes	Acesulfame
		Sucralose
		Saccharin
		Cyclama
		Aspartame
		Neotame
		Neohesperidine dihydrochalcone

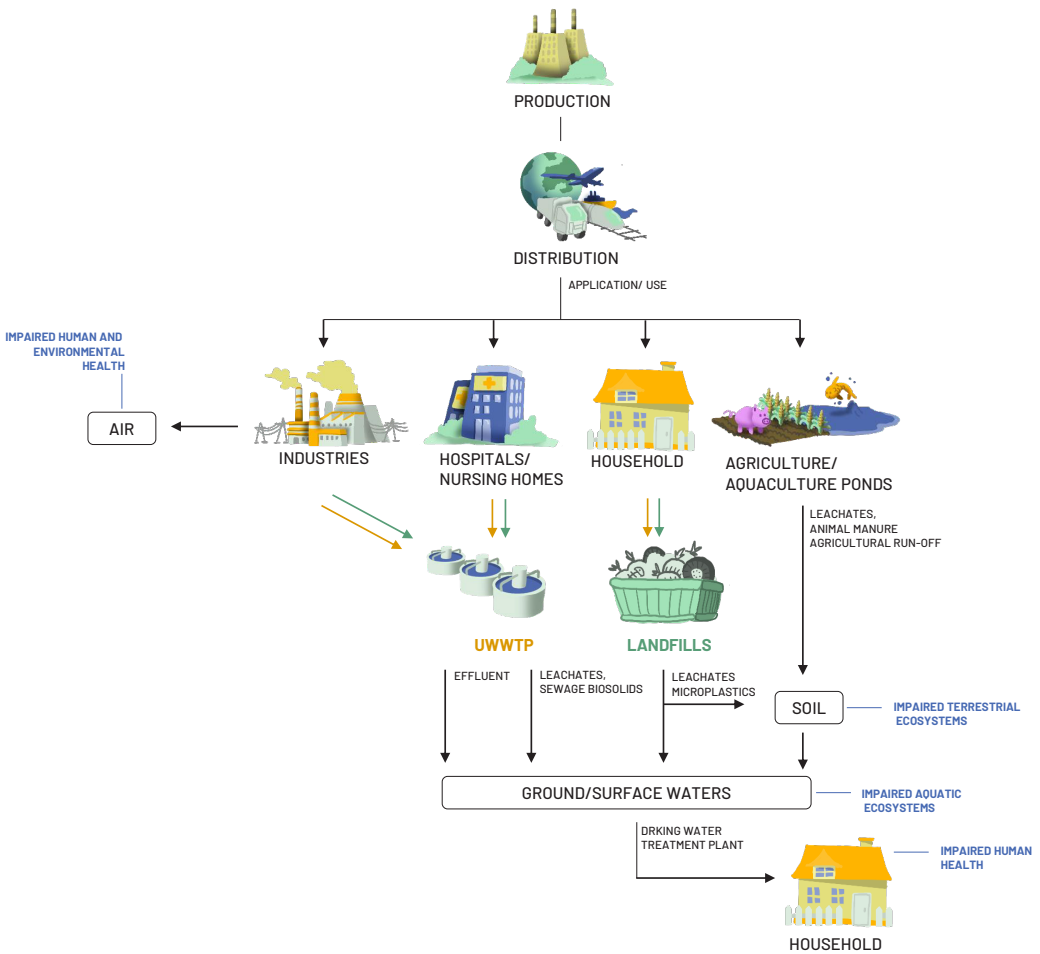

Figure 7. Sources and potential pathways of CECs distribution across environmental compartments. Adapted from Yadav et al., (2021).

or interfere with the action of natural hormones one of the most relevant (Wuttke et al., 2010). Derived from this interference, ED can take place in the shape of estrogenicity, androgenicity, obesity, lipid and adipogenesis dysregulation, thyroid dysregulation, steroid-related pathways alteration, infertility, developmental problems and several other metabolic syndromes (Robitaille et al., 2022). EDCs are structurally very diverse, from compounds like organochlorines, polybrominated flame retardants, perfluorinated substances, alkylphenols, phthalates, pesticides to polycyclic aromatic hydrocarbons, solvents and some metals (Wuttke et al., 2010). One of the main sources of EDCs to the environment is municipal wastewater discharge, since these compounds are not completely removed during treatment (Sumpter, 2005). Different examples of EDCs present in WWTP discharges are: naturally synthesized steroid hormones like estrogen (estradiol, estriol, estrone) and progesterone, artificial synthetic estrogens or androgens such as ethynylestradiol, Norgestrel and Trenbolone, phytoestrogens including isoflavonoids and coumestrol or industrial compounds like bisphenol A or nonylphenol (Benotti et al., 2009). Other sources of EDCs in the environment include agricultural and urban run-off, concentrated animal feeding

operations and landfill leachates (Benotti et al., 2009; Tian et al., 2021). The recent amendment of the REACH regulation, which makes the declaration of endocrine disrupting properties mandatory, reveals the EU concern about this problematic.

Another well described health effect is the ability of some compounds to trigger a dioxin-like response by activating the Aryl hydrocarbon receptor (AhR), also known as the "dioxin receptor" (Tuomisto, 2019). The AhR is a ligand-activated transcription factor that functions primarily as a sensor of exogenous chemicals and as a regulator of enzymes (i.e cytochrome P450s) in charge of their metabolism. The AhR belongs to the family of basic Helix–Loop–Helix-PAS (bHLH/PAS) proteins, which have important roles in i.e. regulation of neural development, generation and maintenance of circadian rhythms, cellular environment sensing and as transcriptional partners and co-activators. In this way, AhR activation can integrate environmental, dietary, microbial and metabolic cues to control complex transcriptional programs in a ligand-specific, cell-type-specific and context-specific manner (Tuomisto, 2019). The AhR-mediated effects can translate in neurologic, immunologic and reproductive impairments. Multiple species of birds, fish, reptiles and mammal exhibit developmental toxicity, reproductive impairment, compromised immunologic function, and other adverse effects after the exposure to dioxin-like compounds, and humans appear to be susceptible to these effects in a similar way (White & Birnbaum, 2009). Dioxin-like compounds can be generated as unwanted side products of burning processes or as impurities generated in different industrial synthesis processes. For instance, polychlorinated dibenzo-p-dioxins and furans (PCDD/F) can be produced either during the synthesis of polychlorinated biphenyls (PCBs), chlorophenol fungicides and phenoxy acid herbicide, or during the burning of materials containing these compounds. Poor burning conditions, like accidental dumpsite fires and backyard waste burning, represent big sources of PCDD/Fs (Tuomisto, 2019). Many legislations have taken place over the years around dioxins and dioxin-like compounds emissions regulation, being one example their introduction in the Priority List (**Table 2**).

The potential to alter the endocrine system and/or trigger a dioxin-like response have been considered as risk factors in the regulation of several compounds and could be also used in evaluating the risk associated to CECs exposure. Nonetheless, these risk factors are usually evaluated by individual chemical exposure, which is far from the current trends, that consider a exposure scenario to complex toxic mixtures (Meade et al., 2022). The EU aimed to regulate CECs spreading into ground/surface waters by writing a proposal this past October 26th 2022 for the introduction of 24 CECs in the Priority List[1]. These compounds include Per- and Polyfluorinated Substances (PFAS), a range of pesticides, diverse pharmaceuticals, anticonvulsants, and antibiotics (**Table 4**).

Aquatic environments and aquifers pollution by CECs

As aforementioned, WWTPs appear unable to fully degrade CECs since they were initially designed to handle organic matter in the mg/L range (Patel et al., 2019). Due to this fact, their activated sludges and effluent discharges are one of the major sources of CECs in aquatic environments (Petrie et al., 2015). Depending on CECs chemical and physical characteristics, then may "travel" unaltered through WWTPs and remain active at very low (ng/L–µg/L) concentrations. This is particularly true for pharmaceuticals like carbamazepine, atenolol, acetylsalicylic acid, diclofenac, mefenamic acid, propranolol, atenolol, clofibric acid and lincomycin which experience removal rates of less than 10% after WWTP (Patel et al., 2019). The failure of WWTPs to

[1] https://environment.ec.europa.eu/publications proposal-amending-water-directives_en

Table 4. The 24 CECs selected for regulation in the proposal[1] for a directive amending the Water Framework Directive, the Groundwater Directive and the Environmental Quality Standards Directive.

Water body	New substances	Substances to more stringent	Substances to less stringent
Surface water	17β-estradiol (E2), Acetamiprid, Azithromycin, Bifenthrin, Bisphenol A, Carbamazepine, Clarithromycin, Clothianidin, Deltamethrin, Diclofenac, Erythromycin, Esfenvalerate, Estrone (E1), Ethinylestradiol (EE2), Glyphosate, Ibuprofen, Imidacloprid, Nicosulfuron, Permethrin, Thiacloprid, Thiamethoxam, Triclosan, Silver, PFAS	Chlorpyrifos, Cypermethrin, Dicofol, Dioxins, Diuron, Fluoranthene, Hexabromocyclododecane (HBCDD), Hexachlorobutadiene, Mercury, Nickel, Nonyl Phenol, PAHs, PBDEs, Tributyltin	Heptachlor/heptachlor epoxide, Hexachlorobenzene
Groundwater	Carbamazepine, Sulfamethoxazole, PFAS	Not stated	Not stated

completely remove a wide range of CECs has been highlighted with the development of advanced analytical techniques (such as GC-MS/MS, LC-MS/MS, UPLC/MS). Modern technologies allow the determination and quantification of almost 3,000 CECs in the aquatic environment at µg/L and ng/L concentration ranges. These values have been proven to be high enough to generate acute and chronic toxicity in aquatic organisms (Kasonga et al., 2021; Patel et al., 2019). In fact, many CECs show effective concentration (EC50) of less than 1 mg/L when tested in different animal models, including crustaceans, algae and fish, which classifies them as potentially very toxic to aquatic organisms under the EU-Directive 93/67/EEC (Patel et al., 2019).

While some CECs have high persistence rates in aquatic environments like naproxen, sulfamethoxazole and erythromycin which can persist for almost one year or clofibric acid that can remain unchanged for multiple years, others are considered as pseudopersistent, as they are generated at a faster rate than they are degraded (Vidal-Dorsch et al., 2012). In general, aquifers are less likely to get contaminated with CECs mixtures than surface aquatic environments due to the chemical and biological attenuation that occurs in the subsurface (Stefano et al., 2022). However, plenty of studies have regularly detected these compounds in groundwater (Acayaba et al., 2021; Lee et al., 2019; Marsala et al., 2020; Stefano et al., 2022). The presence of these contaminants in groundwater may pose risks to human health when used as potable water source (Stefano et al., 2022), as happens with the two and a half billion people who depend solely on groundwater to satisfy their daily drinking water needs. Controversially, a big source of groundwater pollution is groundwater abstraction itself, since it induces hydrochemical changes in confined aquifers potentially mobilizing CECs (Qian et al., 2020). The persistence of a high number of potentially toxic CECs in the aquatic environment underlines the necessity of a better understanding of their occurrence, fate, and ecological impact (Petrie et al., 2015). Establishing a guideline for the rate of decline of water quality decline related to the presence of CECs in different hydrogeological settings is a difficult task. CECs are hard to monitor in groundwater due to the complex interplay of the geological setting, pollution pathways, CEC properties and biogeochemical processes, which compromises risk pollution evaluation and a sustainable managing of groundwater resources (Qian et al., 2020).

Antibiotic Resistant Bacteria (ARB) and Antibiotic Resistant Genes (ARG)

Antibiotics (ABs) are natural, semi-synthetic or synthetic substances that inhibit the growth or cause the death of bacteria at low concentrations. ABs exert selective toxicity on bacterial cells through different modes of action that allow their

[1] https://environment.ec.europa.eu/publications/proposal-amending-water-directives_en

classification into different groups (**Figure 8**) (Kapoor et al., 2017):

– Inhibitors of cell wall formation: Several classes of antibacterials are capable to block the biosynthesis of peptidoglycans that conform the bacterial cell walls, making them more susceptible to osmotic lysis. For instance, the β-lactam antibiotics (penicillins, cephalosporins, monobactams and carbapenems) act by binding to penicillin-binding proteins (PBPs) and disrupting peptidoglycan cross-linking during cell wall synthesis, resulting in bacterial lysis and cell death.

- Inhibitors of protein biosynthesis: Protein synthesis is a complex, multi-step process involving many enzymes and a conformational alignment. Some antimicrobials inhibit protein biosynthesis by targeting the 30S or 50S subunit of the bacterial ribosome. For instance, tetracyclines and macrolides target the conserved sequences of the 16S ribosomal RNA (rRNA) of the 30S and the 23S rRNA of the 50S disabling transfer RNA (tRNA) binding and resulting in a premature detachment of incomplete peptide chains.

- Inhibitors of nucleic acid synthesis: Some antibiotics are capable to inhibit replication and transcription in bacteria. For example, quinolones can interfere with DNA synthesis by inhibiting the DNA gyrase, an enzyme involved in DNA replication. Other antibiotics, like actinomycin, interfere with RNA synthesis by inhibiting RNA polymerases.

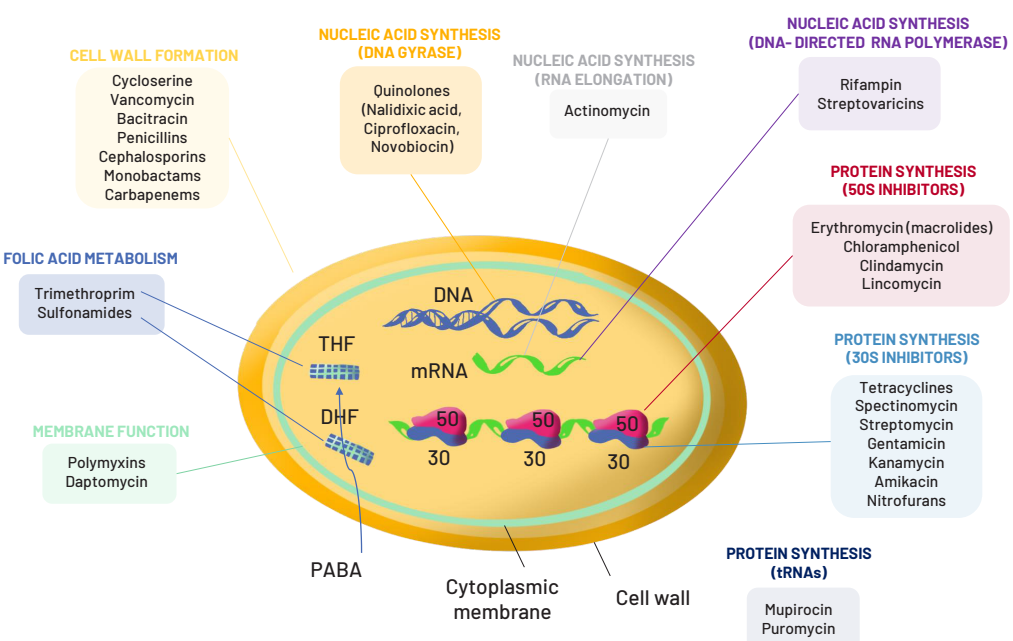

Figure 8. Antibiotics classification by groups according to their mechanism of action. THF stands for Tetrahydrofolic acid; DHF stands for dihydrofolate: PABA stands for para-aminobenzoic acid. Adapted from Madigan et al., (2006).

– Inhibitors of folate metabolism: Some ABs can inhibit folic acid biosynthesis in bacteria due to their structural similarity with the para-aminobenzoic acid (PABA), a crucial precursor in the folic acid metabolism. Others like sulfonamides can bind to the dihydropteroate synthase (DHPS) enzyme, instead of PABA, preventing the folate synthesis from occurring.

- Inhibitors of Membrane Function: The bacterial membrane provides selective permeability for cellular homeostasis and metabolic energy-transduction purposes. Several antimicrobial agents like Daptomycin or Polymyxins interfere with multiple targets through the lipophilic moiety of the bacterial membrane leading to functional and structural impairments.

Subinhibitory antibiotic concentrations can effectively select for bacteria able to counteract these modes of action through diverse antibiotic resistance mechanisms, enabling in this way their survival and transmission. Antibiotic resistance (AR) can be classified as either intrinsic or acquired depending on whether or not the resistance mechanism involves a genetic change. Intrinsic resistance refers to a generalizable trait that does not change regardless of antibiotic selective pressure (Culyba et al., 2015). By contrast, the acquired resistance develops when a new trait is expressed due to a genetic change selected by antibiotics exposure (Van Hoek et al., 2011).

The different strategies followed by resistant bacteria can be grouped into four main categories: (1) limiting drug uptake, (2) modification of drug targets, (3) drug inactivation and (4) drug efflux (Reygaert, 2018).

The ability of bacteria to limit the uptake of ABs is compromised by the structure of their outer membrane. For instance, mycobacteria have an outer membrane that has a high lipid content enabling an easier access to hydrophobic drugs such as rifampicin and fluoroquinolones but a limited access to hydrophilic drugs like aminoglycosides or β-lactams (A. Kumar & Schweizer, 2005; Lambert, 2002). Bacteria that lack a cell wall, such as *Mycoplasma* and related species, are therefore intrinsically resistant to all drugs that target the cell wall including β-lactams and glycopeptides. On the other hand, gram positive bacteria do not possess an outer membrane, and restricting drug access is not as prevalent (Bébéar & Pereyre, 2005). In those bacteria with large outer membranes, substances often enter the cell through porin channels. There are two main ways in which porin changes can limit drug uptake: a decrease in the number of porins present, and mutations that change the selectivity of the porin channel (A. Kumar & Schweizer, 2005). Members of the Enterobacteriaceae are known to become resistant to carbapenems by reducing the number of porins. Mutations that cause changes within the porin channel have been seen in *Neisseria gonorrhoeae* resistant to β-lactams and tetracycline (Gill et al., 1998; Thiolas et al., 2004). Another phenomenon that limits drug uptake is the formation of biofilms by the bacterial communities. The thick, sticky consistency of the biofilm matrix, which contains polysaccharides, proteins and DNA from the resident bacteria, prevents ABs from reaching bacteria (Mah, 2012).

Regarding the modification of drug targets, there are multiple components in the bacterial cell, that may be ABs' targets, that can be modified by bacteria to gain resistance. For instance, one mechanism of resistance to the β-lactam drugs is via alterations in the structure and/or number of penicillin-binding proteins (PBPs). PBPs are transpeptidases involved in the construction of peptidoglycan in the cell wall. A change in the number of PBPs impacts the amount of drug that can bind to that target. A change in structure may decrease the ability of the drug to bind, or totally inhibit drug binding (Beceiro et al., 2013; Reygaert, 2009). Another example of drug target modification is the mechanism to gain resistance to drugs that target ribosomal subunits. This type of resistance may

occur via ribosomal mutation (aminoglycosides, oxazolidinones), ribosomal subunit methylation (aminoglycosides, macrolides), or ribosomal protection (tetracyclines). These mechanisms interfere with the ability of the drug to bind to the ribosome (Eliopoulos et al., 2003; S. Kumar et al., 2013).

There are two main ways in which bacteria can inactivate ABs; by actual degradation (i.e hydrolysis) of the molecule, or by transfer of a chemical group to the drug. The β-lactamases are a very large group of drug hydrolyzing enzymes that inactivate β-lactam drugs by hydrolyzing a specific site in the β-lactam ring structure, causing the ring to open. The production of β-lactamases is the most common resistance mechanism used by gram negative bacteria against β-lactam drugs, and the most important resistance mechanism against penicillin and cephalosporin drugs (Bush & Jacoby, 2010; S. Kumar et al., 2013). Drug inactivation by transfer of a chemical group to the drug most commonly uses transfer of acetyl, phosphoryl, and adenyl groups. Acetylation is the most diversely used mechanism, and is known to be used against the aminoglycosides, chloramphenicol, the streptogramins, and the fluoroquinolones. (Ramirez & Tolmasky, 2010).

Lastly, bacteria possess chromosomally encoded genes for efflux pumps. Some are expressed constitutively, and others are induced/overexpressed under certain environmental stimuli or when a suitable substrate is present. Efflux-pumps are membrane proteins that export ABs out of the cell maintaining their intracellular concentrations low (Du et al., 2018). These pumps are present in the cytoplasmic membrane and most of them are multidrug transporters capable to pump a wide range of unrelated ABs (macrolides, tetracyclines and quinolones) contributing, in this way, to multidrug resistance (Du et al., 2018; Kapoor et al., 2017). However, their resistance capability is influenced by what carbon source is available (Villagra et al., 2012).

The transmission of genes that provide bacteria with a battery of different resistance mechanisms can occur vertically, from parent to daughter bacterial cell, or horizontally by horizontal gene transfer (HGT). HGT is a category of evolutionary mechanisms that facilitate the transmission of genetic elements from one bacterial cell to another, even between taxonomically distant groups, and is largely responsible for AR spreading by three main processes: conjugation, transformation or transduction (**Figure 9**). Conjugation occurs when there is a transference of genes through conjugative plasmids (Ryan et al., 2008) by direct cell-to-cell contact between two bacteria. The conjugative process involves a donor and a recipient cell. The donor bacterium needs to possess the conjugative plasmids and both donor and recipient need to have specific structures like the F-like pili, the P-like pili or the type IV secretion apparatus for the transference to take place (Hong et al., 2017; Norman et al., 2009). Transformation is a process where DNA fragments, usually coming from the lysis of other bacteria, are taken up by bacteria from the environment. The uptake of DNA, its integration and its expression require bacteria to be in a regulated physiological state of competence. DNA uptake needs protein components also utilized in type IV secretion and twitching mobility (Zaneveld et al., 2008). This type of HGT is widely spread among diverse bacterial taxonomic groups having an important environmental role (Thomas & Nielsen, 2005). Transduction occurs when bacteria-specific viruses (called bacteriophages or, simply, phages) transfer DNA between two bacteria, acting as DNA vectors. Phages gain entry to their microbial host cell by binding to extracellular receptors on the cell surface (Smith et al., 2013). Interestingly, the life cycle of the phage that infect the donor bacterium may have an extra impact on HGT apart from their role as DNA vectors. For instance, lytic bacteriophages may release a considerable quantity of plasmid and chromosomal DNA after

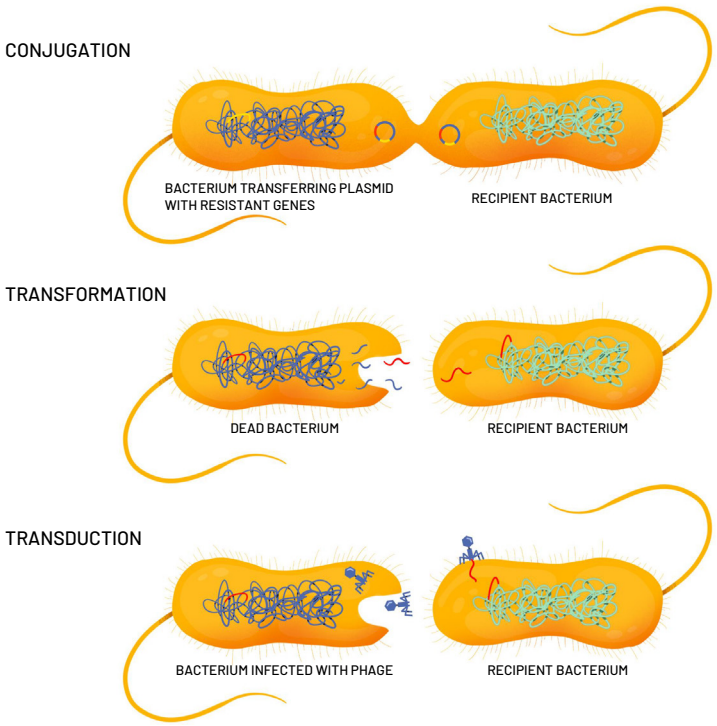

Figure 9. Main mechanisms of HGT in bacteria. Conjugation is the transfer of plasmid DNA from a donor to recipient via direct contact between cells. Transformation occurs when naked DNA from the environment is absorbed by a recipient bacterium. In transduction, genes are transferred from a donor to a recipient bacterium via bacteriophages (phage). Adapted from Furuya and Lowy, (2006).

provoking bacterial lysis, increasing the chances for transformation processes to occur (Keen et al., 2017).

HGT requires enzymes and proteins that mediate the transfer of DNA between bacterial cells. The segments of DNA that encode for these biomolecules are the Mobile Genetic Elements (MGEs) with plasmids and transposons as relevant members. A plasmid is a collection of functional genetic modules organized into a stable, self-replicating extrachromosomal entity. Plasmids usually encompass genes that give bacteria phenotypic advantages in response to selective pressures, like ARGs or heavy metal resistance genes (Li et al., 2015; Seiler & Berendonk, 2012). Plasmids can successfully spread resistance traits to co-occurring phylogenetically diverse bacteria (Li et al., 2015). IncP-1 plasmids are worth highlighting due to their broad host range derived from their highly efficient conjugative transfer activity in Gram-negative bacteria (Popowska & Krawczyk-Balska, 2013). They are potential AB resistance vectors and they may carry *int*I1, *sul*1, *tet*, bla_{OXA} and bla_{TEM}, all of them genetic elements relevant in the context of this thesis (Sen et al., 2013). Transposons contain one or multiple functional genes that confer a given phenotype to the bacterial host, such as resistance to a specific antibiotic in addition to those required for transposition (Bennet, 2004). Transposons have been found in plasmids and as a part of integrons (Bennet, 2004), genetic elements that allow bacteria to acquire exogenous genes in the form of mobile gene cassettes. The complete integron is not considered to be a mobile element by itself, since it lacks functions for self-mobility, whereas the gene cassettes present in integrons are considered mobile (Domingues et al., 2012). All integrons share three core features: the integron integrase gene, *int*I, encoding a site-specific recombinase; a recombination site attI, where the integrase catalyzes the insertion of

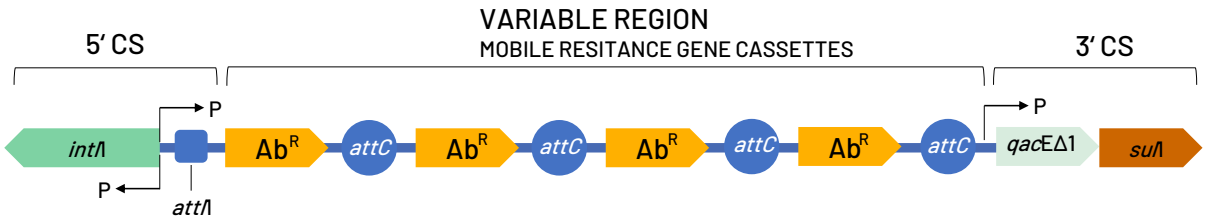

Figure 10. General structure of class 1 integrons. They consist of the integrase gene (*int*I1) and a recombination site (*att*I1) into which new genes (here conferring antibiotic resistance) harboring the recombination site attC are inserted through site-specific recombination. The gene cassettes constitute the most variable region between different integrative constructs. Adapted from Rajpara et al., (2015).

new genes as part of the genes cassette; and one or two promoters that drive the expression of an inserted gene cassette (Gillings et al., 2015, **Figure 10**). Class 1 integrons are of special interest since they have been widely reported in pathogens from clinical settings, carrying gene cassettes associated with antibiotic resistance. Most Class 1 integrons share common features i) the three core features described above and ii) the carriage of the *qac*E and *sul*1 genes cassettes encoding resistance to disinfectants and sulfonamides (**Figure 10**), although there is also increasing evidence of them carrying additional gene cassettes (Gaze et al., 2011). Class 1 integrons have also been detected in microbial species from various environments, including wastewater, river water and soil, suggesting that their dissemination may be a general problem of environmental contamination and public health (Gillings et al., 2015). Therefore, they have been proposed as a proxy for anthropogenic impact due their vastly increased abundance in natural environments impacted by anthropogenic activities (Gillings et al., 2015).

The simultaneous presence of ABs and ARBs in biosolids and wastewaters, along with the rest of regulated and unregulated compounds, contributes to the impact associated with their reuse. The life-threatening consequences derived from their presence underlines the relevance of including ARB and Antibiotic Resistance Genes (ARGs) screening in any reuse scheme in order to monitor any potential transmission and properly evaluate AR risk (Spielmeyer et al., 2017).

6. Environmental toxicology as a tool for risk assessment

Any risk evaluation needs to be framed under an Environmental Toxicology context. This science arose out of the necessity of identifying, studying and describing the dose, nature, incidence, reversibility and mechanisms of the adverse effects derived from the exposure to "environmental hazards". A environmental hazard can be defined as any hazard that compromises the integrity of environments' physical and biological components altering normal environmental processes (Cockerham & Shane, 2019; Suzuki et al., 2020). Environmental Toxicology has to be understood as a multi-disciplinary science that feeds from different fields like Environmental Sciences, Biology, classic Toxicology, Computer & Math science, and Chemistry (**Figure 11**) in order to fully comprehend, assess, prevent and predict the relevance of the effects exerted by the environmental hazards. Ecotoxicology is a subdiscipline of Environmental Toxicology that goes a step further and puts these effects at population and ecosystem levels, enabling risk evaluation (Suzuki et al., 2020). Environmental Toxicology along with Ecotoxicology represent the base of the environmental risk analysis.

The Adverse Outcome Pathway (AOP) framework is a widely used tool in Environmental Toxicology for a better understanding of the effects posed by environmental hazards to living organisms. The objective of AOPs is to explain in a structured way

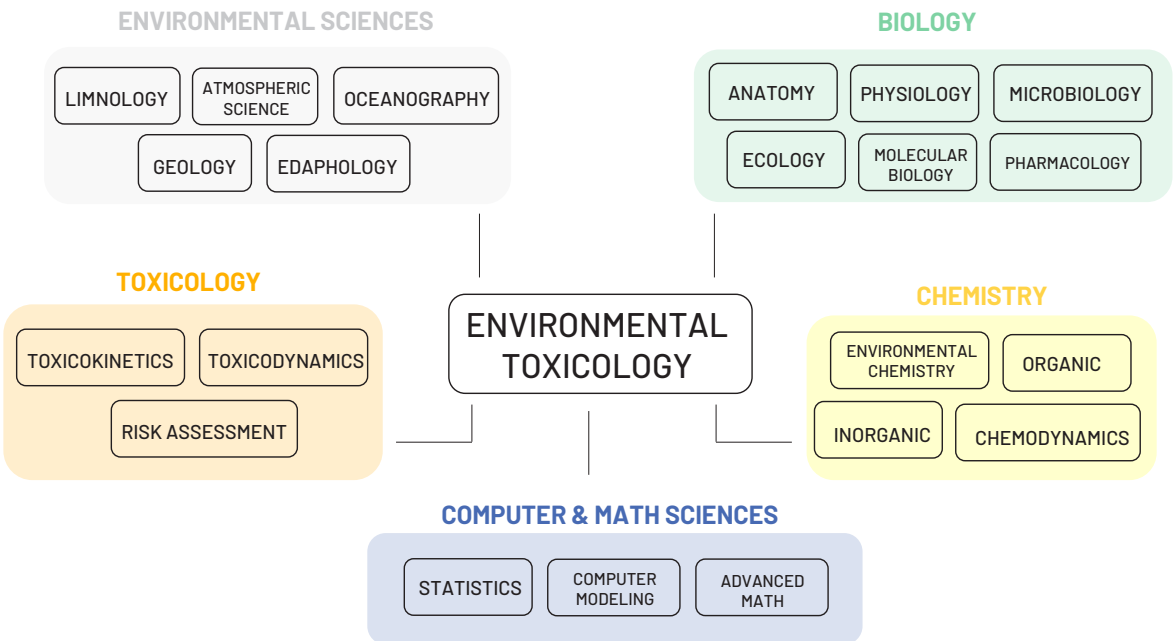

Figure 11. Environmental Toxicology as a multi-disciplinary science.

causal relationships linking the initial perturbation of a biological system after a chemical interaction with molecular biological targets (molecular initiating event, MIE) to an adverse outcome (AO) through a sequential series of key events (KE) that reflect changes at different biological levels (Sachana, 2019). A general scheme of this AOP framework is represented in **Figure 12**.

After a MIE, different signaling cascades and alterations at several biological levels (key events or KEs) are triggered, ultimately leading to an observable specific adverse outcome (Allen et al., 2016). Once the key events and their relationships are understanded and supported by several evidence, an AOP framework can be described. The final aim of an AOP is to explain the mechanism of action of a given hazard, including all the different MIEs, the subsequent propagation of the signaling cascades across the affected pathways, up to all adverse outcomes across the different organization levels (Allen et al., 2014, 2016). General toxicity assays usually focus on qualitative and quantitative observations of impaired phenotypes including lethality, weight, length, reproductive impairment or morphological deformations (Knöbel et al., 2012; Suter et al., 1987). Alternatively, novel tools for hazard monitoring focus on initiating or key events with the aim to better understand the modes of action of environmental hazards, searching for fingerprints at the molecular level as markers of exposure. These novel tools are provided by the so called "omic" technologies which development was considered a milestone in environmental toxicology, since they represent excellent methodologies to study different KEs and gain insight on adverse outcomes in exposed organisms (Piña et al., 2018). Among the different omic sciences we find: genomics, for the study of variations in DNA sequences; transcriptomics, for the characterization of gene expression using the measurement of messenger RNA (mRNA); proteomics, for the measurement of the levels and expression of proteins; and metabolomics, for the global evaluation of the metabolites present in a given biological system (Piña et al., 2018).

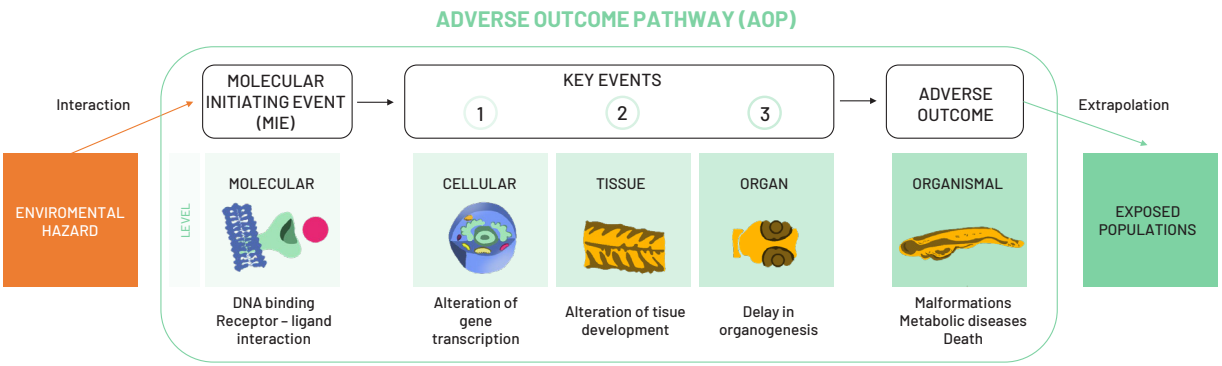

Figure 12. General scheme of an AOP framework. After the interaction with a given environmental hazard, a MIE triggers signaling cascades that cause alterations at several biological levels (key events or KEs) ultimately leading to an observable specific adverse outcome. The observed effects could be extrapolated in further risk evaluations to potential exposed populations.

The standing omic techniques cover all the steps in the flux of genomic information from genomes to gene and metabolic products. They allow to connect molecular events and adverse outcomes with biological levels of organization, improving the knowledge and understanding of the potential risks posed by environmental hazards on exposed ecosystems and thus relevant in risk assessment schemes (Simmons et al., 2015).

In the context of modelling the effects derived from ARB exposure, genomic studies are essential in order to retrieve phylogenetic information and monitor potential bacterial shifts. HGT between different bacterial taxa may happen more often than previously thought, meaning that broad-host range plasmids can be hosted by diverse types of bacteria and can also be received by bacteria distantly related to the donor. Moreover, in open systems, incoming bacterial species may not be able to outcompete and colonize the ecological niche, but, if they persist in the recipient environment, intra-taxon genetic exchange will occur more often than inter-taxon. In this context, phylogenetic information becomes relevant in the modelling of resistance between and inside bacterial communities from different microbiomes (Forsberg et al., 2014).

On the other hand, when monitoring the effects exerted by complex mixtures of CECs, transcriptomic studies enable a detailed exploration of exposed organism responses by detecting changes in gene expression, being suitable tools for assessing toxicity. Gene expression can be altered by the direct and/or indirect interaction with a given pollutant, which results in changes (activation or repression) in the transcription of target or related genes (Piña et al., 2018). Thus, an altered transcriptomic profile reflects a perturbation on normal mRNA abundances since they respond quickly after stressor exposures (López-Maury et al., 2008; Orsini et al., 2018).

6.1 Detoxification mechanisms after toxic exposure

The first set of reactions that take place in exposed organisms after their contact with exogenous toxic molecules are those related with detoxification. Once inside the organism, exogenous molecules undergo multiple metabolic transformations with the ultimate goal of an easier excretion (**Figure 13**, Iyanagi, 2007). This process (called biotransformation) not only promotes drug elimination but also often results in an inactivation of its pharmacological activity, thereby changing the overall biological properties of the drug (Iyanagi, 2007). Most biotransformation reactions are carried out in liver hepatocytes by enzymes

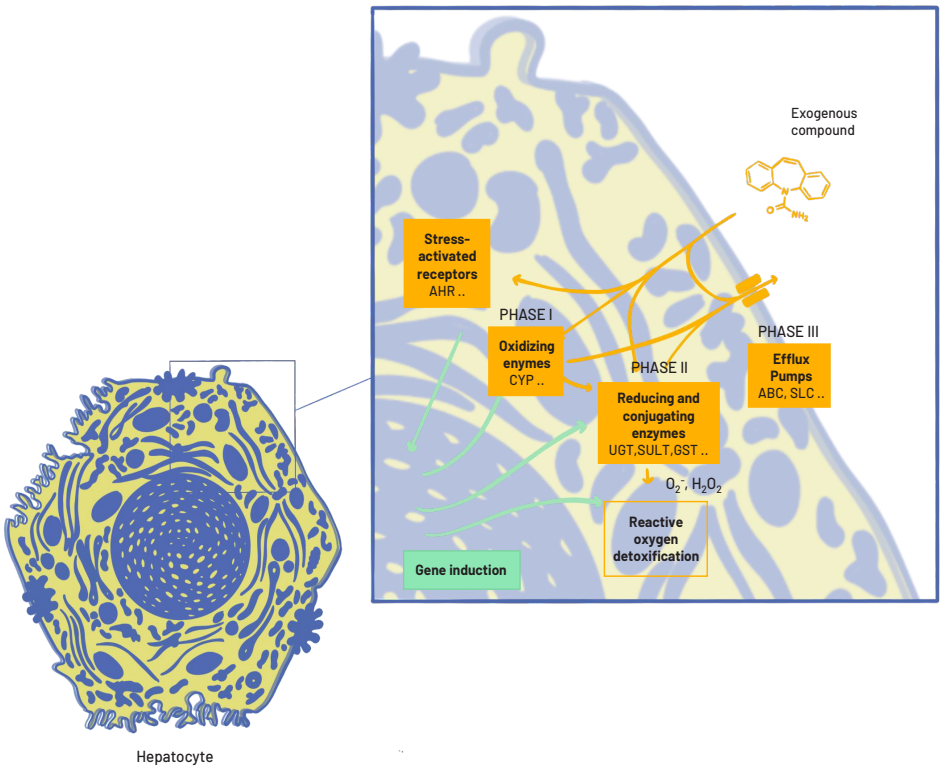

Figure 13. The chemical defensome. This generalized scheme shows the complex integration of pathways involved in oxidation, reduction, conjugation, and excretion of toxic compounds. Endogenous toxicants are metabolized and/or excreted by members of the gene families detailed here and in the text. Abbreviations noted in the text. Adapted from Stegeman et al., (2010).

found primally at the cytoplasm, endoplasmic reticulum, and mitochondria (Iyanagi, 2007; Renton, 1986). However, some of these reactions can also occur in extrahepatic tissues, such as adipose or intestinal tissues. The enzymes that catalyze this process are commonly refer to as drug-metabolizing enzymes (DMEs) and are usually classified as Phase I, Phase II and Phase III enzymes.

Phase I enzymes (functionalization reactions), which mediate oxidation, reduction, or hydrolysis reactions, introduce a functional group (-OH, -SH, $-NH_2$, or -COOH) into the drug molecule. These reactions serve to convert lipophilic drugs into more polar molecules by adding or exposing a polar functional group such as amino or hydroxyl groups and are mainly catalyzed by the cytochrome P450 system. This system is a family of membrane-bound enzymes found within the endoplasmic reticulum of hepatocytes that catalyze the metabolism of a wide range of exogenous substances and are involved in many biological functions including steroid metabolism, drug and procarcinogen deactivation, fatty acid metabolism, and catabolism of exogenous compounds (Iyanagi, 2007; Stavropoulou et al., 2018).

Drugs that already have -OH, $-NH_2$ or COOH groups can bypass Phase I and enter Phase II directly to become conjugated. Phase II reactions allow the addition of hydrophilic groups to the original molecule, a toxic intermediate or a nontoxic metabolite formed in Phase I, that requires further transformation to increase its polarity. These reactions include conjugation, glucuronidation, acetylation and sulfation reactions catalyzed

by enzymes like UDP-glucuronosyltransferases (UGTs, addition of glucuronate), sulfotransferases (SULTs, addition of sulfate), or glutathione S-transferases (GSTs, addition of glutathione). NAD(P)H: quinone:oxidoreductase (also called DT-diaphorase), methyltransferase and acetyltransferase are also classed as phase II enzymes (Iyanagi, 2007). The metabolites generated by Phase I and II reactions are finally excreted from the organism thanks to Phase III ATP-binding cassette (ABC) and solute carrier (SLC) transporters (Almazroo et al., 2017).

The expression of these enzymes is regulated by the activation of stress-activated receptors, like the AhR, the Constitutive Androstane Receptor (CAR), the Pregnane X Receptor (PXR) amongst others. Recent analysis suggest that AhR could also play a role in determining the hydrophobicity of metabolites and perhaps their transporter-mediated movement into and out of tissues (Granados et al., 2022).

The main purpose of Phase I, II and III reactions is to deactivate substances by facilitating their excretion. However, they may also bioactivate some compounds by transforming them from nontoxic/inactive to toxic/active forms. If the detoxification process produces a toxic intermediate, its effect on the organism will depend on different factors. Some of these factors could include how rapidly the intermediate can undergo further metabolism to a less toxic metabolite, the amount of toxic byproduct that is produced and accumulated, the type and amount of damage caused and the additional factors that could prolong its excretion (Iyanagi, 2007). For example, BaPyr toxicity is mostly linked to the production of radical species by *cyp1a* (Phase I Reaction, Shimizu et al., 2000).

6.2 Zebrafish as a model organism in transcriptomic studies

The choice of an appropriate model organism represents a crucial step in transcriptomic studies. This is mainly due to the fact that a comprehensive interpretation of the experiment's results requires previous knowledge of biological information regarding the chosen organism. For instance, obtaining information regarding the molecular function and biological role(s) of the genes which transcription has been altered after exposure is much easier if the reference genome is adequately annotated (Campos et al., 2018).. Moreover, the use of a well-characterized model will allow a better extrapolation of the observed effects to other species, enabling a better risk evaluation. The zebrafish (*Danio rerio*) fully meets this requirements, being a suitable widely-used model organism in transcriptomic studies worldwide (Shehwana & Konu, 2019).

D. rerio was first described by Francis Hamilton in 1822 (Hamilton, 1822) and is a freshwater teleost fish, natural from South Asia, that has been used in research since the middle 80s and represents one of the most studied vertebrate models. Its use in environmental toxicology (as well as in other fields as medical research) has highly popularized due to:

1. the fact that its genome has been sequenced, published and is well-annotated, being widely used in genomics (Whiteley et al., 2011) and transcriptomics (Hermsen & Piersma, 2014; Shehwana & Konu, 2019) studies.

2. the similarity between its genome and the human genome, with 70% of human genes having at least one obvious zebrafish orthologue (Howe et al., 2013), allowing a better extrapolation of the results.

3. the ability to accelerate genetic studies by gene knockdown or overexpression (Varshney et al., 2013). This technique has been applied in the study of many pathologies in clinical research and in the determination of the modes of action of different compounds.

4. their suitability for lab-scale experiments. Their effortless rearing and manipulation conditions due to their small size along with their large offspring (usually in the range of 150-250 eggs per female, (Skinner & Watt, 2007; Spence & Smith, 2006) and relatively short life cycle (**Figure 14**) allow to obtain high number of replicates and to perform inter/transgenerational studies in a relatively easy way. Moreover, the transparency of their larvae allows the non-invasive live observation of the internal organs and following their development during and after the exposure period (Cavalieri & Spinelli, 2017).

Zebrafish is becoming the preferred model for animal toxicity and drug discovery. An average of 3500 annual publications in environmental toxicology used zebrafish as their model organism in the last five years, amply surpassing the number of articles based on *Daphnia magna* or other key fish species proposed by the OECD (Scholz et al., 2008; Tanguay, 2018). Moreover, the Zebrafish Information Network (ZFIN; https://zfin.org/) has been stablished as a "central repository for zebrafish genetic, genomic, phenotypic and developmental data" and can be used to complement and gain insight in zebrafish transcriptomic studies (Bradford et al., 2010).

7. Thesis objectives in the context of biosolids and wastewater reuse

The reuse of agricultural biosolids and treated wastewaters are optimal alternatives to the use of chemical fertilizers and water over abstraction. Although these solutions contribute to the settling of circularity, they are highly

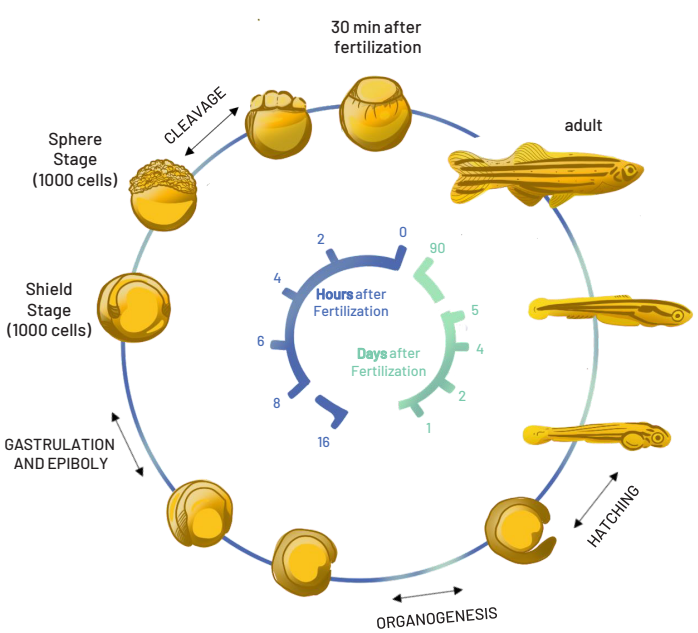

Figure 14. Life cycle of *Danio rerio*.

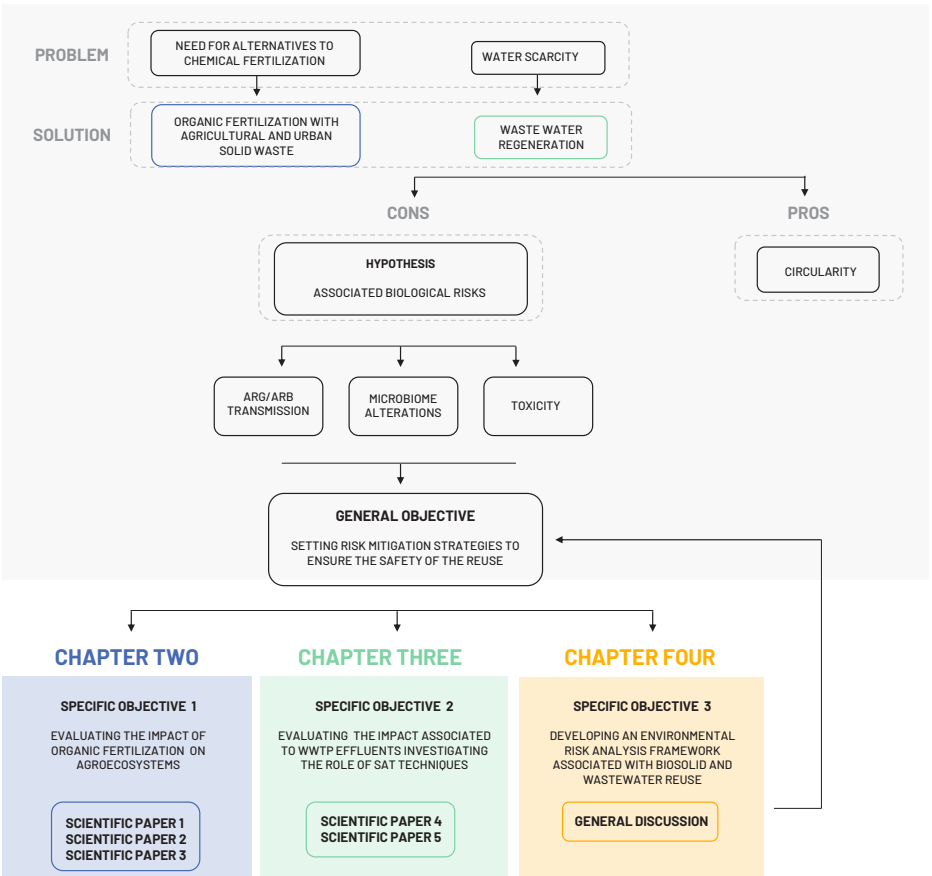

Figure 15. Thesis outline.

compromised by the concerns about its safety. Thus, our general working hypothesis is that there are several biological risks associated to biosolids and wastewaters that prevent their safe reuse. Among these risks, three main endpoints have been targeted in this thesis: ARB and ARGs transmission, microbiome alterations, and toxicity by CECs (**Figure 15**). Through the screening of these endpoints, we aimed to achieve the general objective of setting a series of risk mitigation strategies in order to reduce the risk posed to the exposed environmental compartments and humans.

In order to accomplish this goal, three specific objectives were defined:

1. The evaluation of the impact of organic fertilization on agroecosystems through ABs, ARGs and ARBs transmission and microbiome modulations monitoring in fertilizers and target soils and crops (**Chapter Two**).

2. The evaluation of the impact associated to WWTP effluents through ARGs and ARBs and associated toxic responses screening along with microbiome alterations monitoring simultaneously investigating the role of SAT technologies in their removal (**Chapter Three**).

3. The development of an environmental risk analysis framework associated to biosolids and wastewater reuse considering the occurrence of the monitored hazards and their potential impacts on exposed environments (**Chapter Four**).

8. Methodology

8.1 Untargeted and targeted approaches used in genomic studies

The workflow followed in the genomic studies of ARBs and ARGs dissemination and potential microbiome alterations included in Chapter Two and Three (Scientific Papers I, II, III and IV) is summarized in **Figure 16** and the two techniques used for this purpose will be further explained below.

Microbiome analysis by 16S rDNA amplicon sequencing

Using genomic tools to study ribosomal DNA is a common practice to retrieve microbiomes' phylogenetic information in order to monitor any potential shift under selective pressure. Specifically, the sequencing of the 16S rDNA gene is the main tool used for microbiome analysis. This gene, that codes for the ribosomal RNA associated to the prokaryotic small subunit, is present in every bacterial cell and contains both highly conserved and hypervariable regions. The 16S rDNA gene is about 1542 base-pairs and it is constituted by 9 hypervariable regions V1 to V9 (**Figure 17**). Each phylogenetic group has unique oligonucleotide sequences in the variable regions, surrounded by conserved regions, allowing the design of 'universal' primers. These primers allow DNA amplification of conserved regions and hyper-

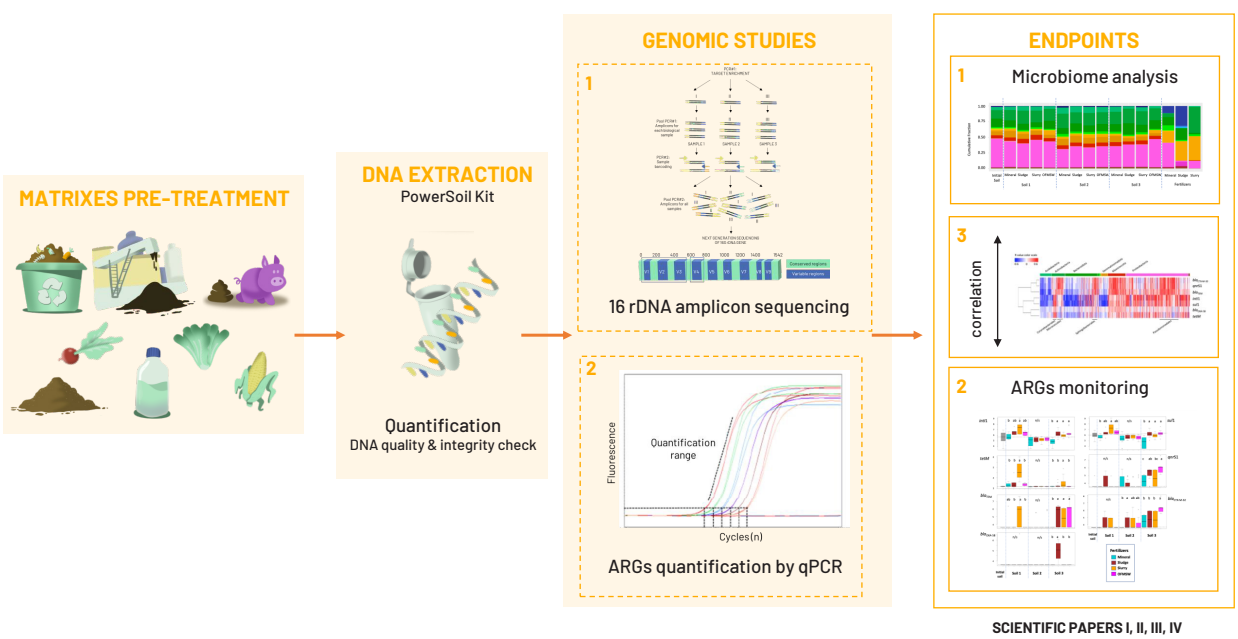

Figure 16. Workflow followed for ARGs dissemination and microbiome analysis in Scientific Papers I, II, III and IV. After matrixes pre-treatment and DNA extraction, genomic studies based on 16S rDNA amplicon sequencing coupled with ARGs quantification allowed microbiome analysis and its further correlation with quantified ARG profiles.

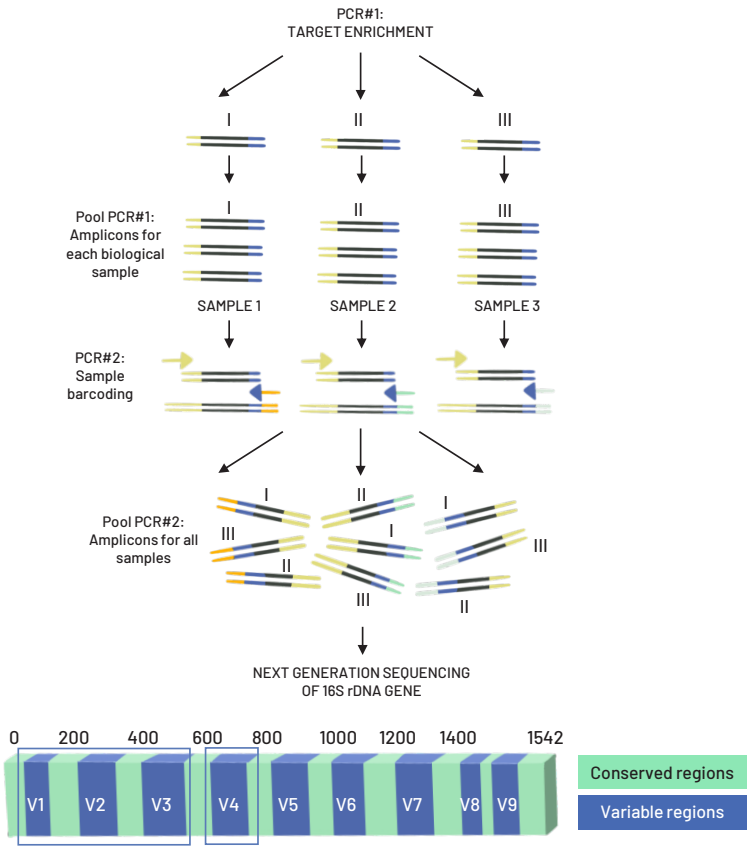

Figure 17. Steps for preparing the 16S rDNA library allowing pooling of different samples, in two sequential PCRs. Firstly, to add the overhangs to the target sequences. Secondly, to add the DNA barcodes to allow sample multiplexing. Adapted from Bernstein et al., (2015).

variable regions and the subsequent identification of bacteria (Patwardhan et al., 2014).

While sequencing the entire 16s gene is difficult due to read length restrictions of many Next Generation Sequencing (NGS) platforms, sequencing one or more hypervariable regions is relatively quick and affordable. Specifically, the 27F-519R (V1-V3 region) and 515F-806R (V4 region) are the most commonly sequenced. To perform 16S rDNA amplicon sequencing, total DNA is isolated from the samples and subjected to targeted enrichment of the 16S rDNA regions of interest by PCR. This produces amplicon libraries that are then subjected to two additional PCR cycles. The purpose of the first PCR is to add unpaired nucleotides at 5' of both sense and anti-sense sequences. The subsequent PCR will add a specific sequence of nucleotides (multiplexing indexes) per sample, allowing either single or double indexation (https://www.illumina.com/). Following this, the samples are pooled and a single NGS run is performed (**Figure 17**).

16S rDNA sequencing has its limitations, particularly concerning sensitivity and resolution. Short amplified sequencing from NGS results in a narrow choice of sets of primers for certain hypervariable regions. The short size of these sequences, added to the fact that many bacteria may share the same sequences, may lead to the uneven amplification of certain taxa with a posterior erroneous taxonomy attribution and under- or over- estimation of their abundance, reducing considerably the sensitivity of this technique (Yang et al., 2016). Therefore, 16S

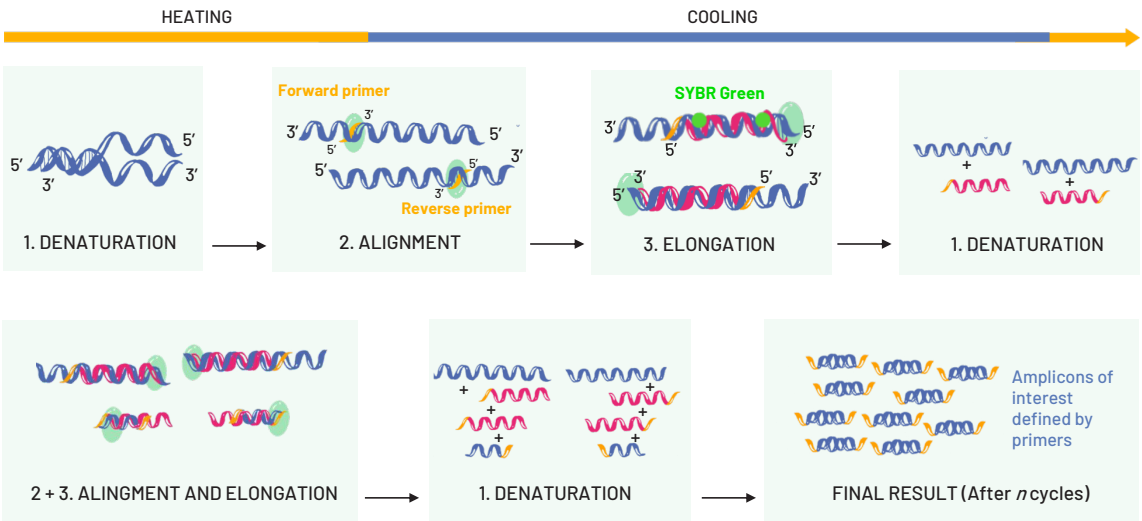

Figure 18. General scheme of qPCR basics.

rDNA sequencing is not a perfect technique but it can be considered a good approximation to the taxonomic profiles.

ARGs quantification by quantitative polymerase chain reaction (qPCR)

One of the most widely used methods for monitoring ARGs in environmental samples is their quantification by Quantitative Polymerase Chain Reaction (qPCR). This is a very sensitive tool that provides quantitative information about the DNA sequences of interest in a relatively short period of time (1-2h) (Waseem et al., 2019). This technique is based on the Polymerase Chain Reaction (PCR), first introduced in the middle 80's (see Bartlett and Stirling (2003) for a historical perspective of PCR development). A PCR reaction requires the template DNA, two short nucleic acid sequences complementary to both strands of the target DNA region (primers), the four deoxyrribonucleotides, and a heat-stable DNA polymerase, usually the Taq polymerase.(**Figure 18**, Chien et al., 1976). By applying repeated thermal cycles of heating and cooling, DNA amplification takes place in three steps: denaturation, annealing and elongation. In the denaturation step, the solution with DNA template and reagents is heated above the melting point of the double strand of the target sequence, allowing the two strands of DNA to separate one from each other. Then, the temperature is lowered slightly below the primers melting temperature to allow them to anneal to the target DNA sequences. Finally, temperature is raised allowing the heat-stable DNA polymerase to synthesize a new DNA strand complementary to the target DNA region (Garibyan & Avashia, 2013). The number of copies of the DNA template is duplicated after each PCR cycle, following the equation:

$$N = N_0 \cdot (1+E)^n$$

being N the number of cDNA strand copies after n number of thermal cycles, N_0 the original number of copies and E the efficiency of the amplification.

qPCR goes a step further than basic PCR enabling the quantification of the concentration of the template DNA. qPCR uses a fluorophore, either in solution (as the SYBR Green) or attached to specific primers (as the TaqMan probes) to monitor the amplification of the template DNA at each thermal cycle (Zhang et al., 2011). By this mechanism, the fluorescence exponentially increases in each thermal cycle, which can be measured to calculate the template DNA amount. This measurement

needs to be performed in the exponential phase of the amplification curve since it is the only range in which the fluorescence is directly proportional to the original input of transcript. The quantification cycle (Cq) of each sample is indicative of its DNA amount and could be used for further comparisons (Bustin et al., 2009). qPCR is normally used for the amplification of specific short regions of the DNA, the so-called "amplicons". The use of a specific pair of primers (one forward and one reverse), purposely designed to be complementary to each DNA strand, allows to selectively amplify this specific region. In qPCR, each amplicon usually covers between 70 and 200 bp (nucleotide base pairs), although longer amplicons (up to 400-500 bp) can be also used (Menezes, 2016). The specific and optimal amplification of the desired amplicon can be qualitatively assessed in qPCR by the efficiency of the amplification and the melting peak. On the one hand, the efficiency needs to be between 90-110% to ensure a good precision of the quantification. On the other hand, a melting curve is performed at the end of the process to ensure the specificity of the amplification. During this step the temperature increases gradually provoking the denaturation of the double strand. Since each amplicon has a specific melting point (single peak), the observation of several melting peaks could indicate the amplification of undesired amplicons (Bustin et al., 2009). Results from qPCR can be dependent on DNA extraction, which may differ in efficiency among matrices (water, soil, crop tissue). Also, resulting DNA extracts may contain inhibitors, such as humic acids or organic salts, that interfere in the amplification reaction and may lead to either false negatives or underestimated copy counts. Thus, it is important to be consistent in applying quality control measures, such as internal amplification controls and a proper DNA dilution in order to avoid false negatives (Luby et al., 2016).

The levels of expressed ARGs can be measured by absolute quantification. This quantification relates the PCR signal to a given copy number using a calibration curve with known concentrations of the amplified gene of interest. For this purpose, we used the pNORM1 or specific pUC19 plasmids that contained the ARGs of interest (**Figure 19**)

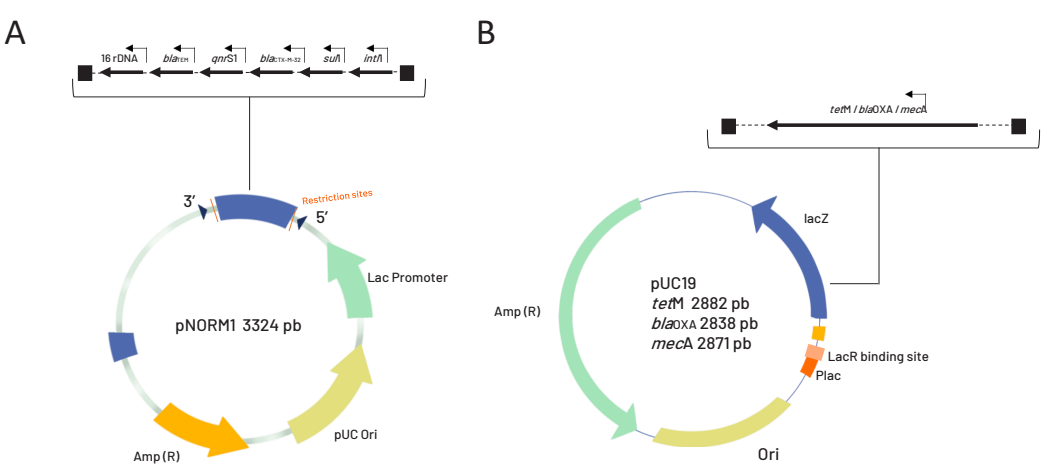

Figure 19. Plasmids used as standards in ARGs absolute quantification. **A)** Plasmid pNORM1, with multiple cloning site under the control of the Lac promoter with 16S, *intI1*, *sul1*, *qnrS1*, bla_{TEM}, $bla_{CTX\text{-}M\text{-}32}$ introduced genes and an ampicillin resistance gene to allow recombinant selection. **B)** Plasmid pUC19, with ORI, Amp resistance, an under the Lac promoter a gene of interest (*mec*A, or *tet*M, or $bla_{OXA\text{-}58}$).

carried by transformed *Escherichia coli*. The plasmids were extracted, purified and stored in stocks with known concentrations of the target genes. Several dilutions of these stocks were used to create a standard curve from which final ARGs copies number was extrapolated.

The ARGs selected for qPCR in the works from Chapter Two were *bla*$_{TEM}$, *bla*$_{CTX\text{-}M\text{-}32}$, *bla*$_{OXA\text{-}58}$, *mec*A, *qnr*S1, *sul*1 and *tet*M due to their relevance in the assessment of the antibiotic resistance status in environmental settings, on their clinical relevance (described below) and association with MGEs (Berendonk et al., 2015). In addition, integron class 1 (*int*I1) was chosen as a proxy for anthropogenic impact and marker of HGT activity (Gillings et al., 2015).

The main characteristics of the chosen genes appear below:

- *bla*$_{TEM}$ gene encodes for TEM β-lactamases that confer resistance to betalactamic ABs (Muhammad et al., 2014). They have a high prevalence and distribution in the environment (Lachmayr et al., 2009) and require just few specific single nucleotide polymorphisms (SNPs) to turn from specific to extended-spectrum β-lactamase (ESBL) genes (Muhammad et al., 2014).

- *bla*$_{CTX\text{-}M\text{-}32}$ encodes an extended-spectrum β-lactamase (ESBL) found mostly in the Enterobacteriaceae family members, including *E. coli* (Cartelle et al., 2004; Mugnaioli et al., 2006).

- *bla*$_{OXA\text{-}58}$ confers resistance to carbapenems and is commonly found in *Acinetobacter* species. Several of those species are important nosocomial (frequent in clinical settings) pathogens (Bertini et al., 2007).

- *mec*A confers resistance to methicillin and it is present in *Staphylococcus* MRSA species (methicilin resistant *Staphylococcus aureus*), also responsible for a number of nosocomial infections (Wielders et al., 2002).

- *qnr*S1 confers resistance to quinolones and it is found in Enterobacteriaceae clinical isolates (Tamang et al., 2008).

- *tet*M (tetracycline resistance) and *sul*1 (sulfonamide resistance) have been shown to co-occur in plasmids found in environmental samples with anthropogenic impact, sometimes linked to *int*I1 (Gillings et al., 2015; Hu et al., 2008; Nonaka et al., 2012).

- *int*I1 encodes the site-specific recombinase IntI1, responsible for the insertion and excision of exogenous gene cassettes at the integron-class 1 associated recombination site *att*I1 (Mendes et al., 2007).

8.2 Untargeted and targeted approaches used in transcriptomic studies

The workflow followed in the toxicogenomic study carried in Scientific Paper V is summarized in **Figure 20** and the two main techniques used are explained below.

Untargeted transcriptomics by RNA-Seq

The analysis of the whole transcriptome can be achieved through NGS of the RNA (RNA-Seq). RNA-Seq technologies allow detection of transcriptomic changes derived from CECs exposure and are based on a wide spectrum of methods that present many advantages: 1) Non target detection of essentially all transcripts from a given sample above the statistical threshold; 2) a high dynamic range, as it allows quantification of transcripts whose expression levels differs in 3 to 4 orders of magnitude. 3) the identification and quantification of rare transcripts, alternative splicing, mutations, etc. is allowed, 4) low amount of total RNA is needed (Lowe et al., 2017). Amongst all the different RNA-Seq technologies, Illumina sequencing has been the most predominant

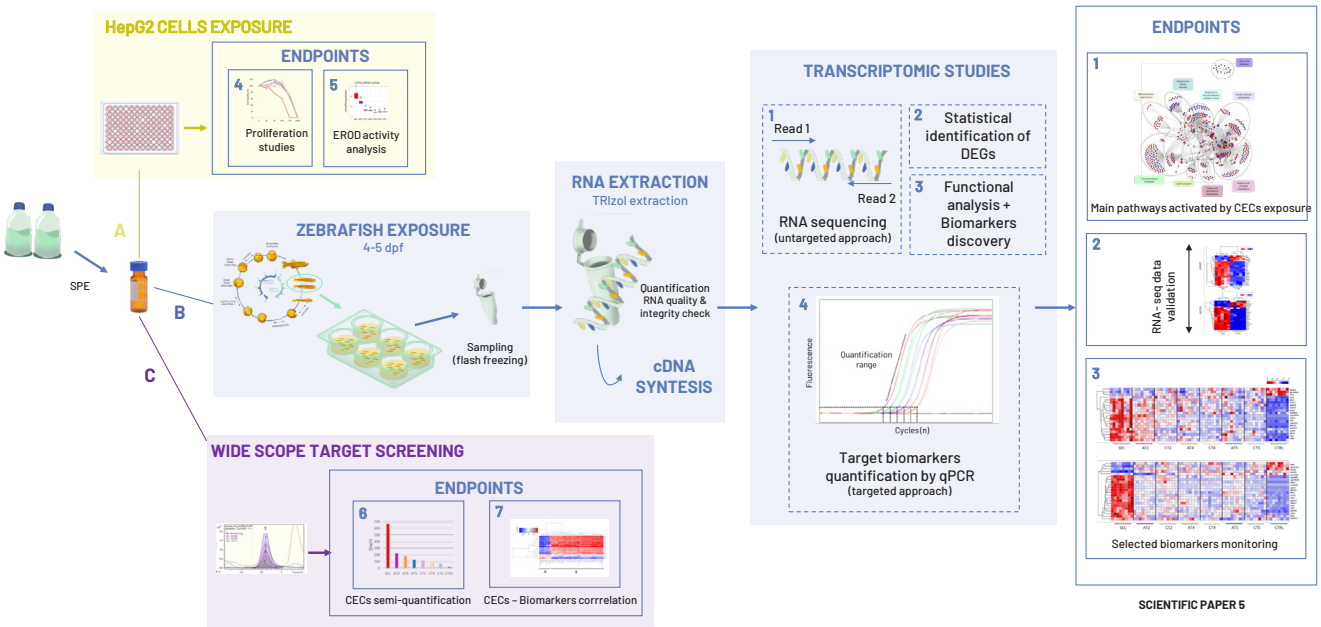

Figure 20. Workflow followed for toxicity monitoring in Scientific Paper V. After samples' Solid Phase Extraction, three studies were run in parallel using the same resultant extract. **A)** HepG2 cells and **B)** Zebrafish larvae were used as model organisms for toxicity studies along with a **C)** wide scope target screening for an untargeted semi-quantification of CECs. In zebrafish assays, four days post fertilization larvae were exposed for 24h to the obtained extracts. Paired-end sequencing of the extracted RNA allowed the identification of DEGs followed by the comprehension of their biological role and relevance through funtional analysis. The obtained information allowed the selection of molecular markers further targeted by qPCR.

method in the last years and thus the chosen one for our study. Different characteristics as the type of transcript enrichment (amplification), fragmentation and library preparation, sequencing reads (long or short, single o paired) and others can slightly vary between the different sequencing methods. In this thesis, paired-end RNA-seq was applied. At the same sequencing depth, the paired-end RNA-seq increases the sensitivity and specificity of the detection and mapping of the reads in comparison with the single-end sequencing. Therefore, paired-end sequencing is a more efficient strategy for characterizing and quantifying the transcriptome (Fang & Cui, 2011). As introduced earlier, thanks to the development of genomic databases, is it possible to correlate differentially expressed genes (DEGs) identified to be affected by environmental stressors with specific biological functions. Bioinformatic platforms and databases like the Gene Ontology (GO) Database[1] and the Kyoto Encyclopedia of Genes and Genomes[2] (KEGG) make possible to link genes with metabolic and signaling pathways. The GO Database has more than 6.6 million annotations corresponding to more than 100 species, although 1.5 million correspond to only three species (*Homo sapiens, Mus musculus* and *Rattus norvegicus*). GO annotations are organized in hierarchical GO categories (i.e, "molecular function", "biological process", "cellular component") that include information about subcellular localization, metabolic activity or roles in cell division or development, among others. KEGG integrates smaller databases, classified according to whether they offer system information, genomic information, chemical information and biomedical information. Since genes within the same pathway or under the same control mechanism would change their transcription in a coordinated manner (Ihmels et al., 2004) the functional analysis of DEGs helped us better understand the pathways and functions

[1] http://geneontology.org/
[2] https://www.genome.jp/kegg/

affected by CECs exposure, characterizing specific gene expression patterns and therefore selecting specific molecular makers of exposure subsequently quantified by qPCR.

Target transcriptomics by qPCR

The complexity of the data obtained by RNA-seq requires a highly-extensive computational processing although it allows to detect both known and unknown molecules. These studies are usually expensive what translates in a few number of samples being analyzed in each experiment. On the contrary, the quantification of pre-selected molecular markers by qPCR can be done simultaneously in a big number of samples at a much lower cost. However, this pre-selection depends on previous information retrieved by RNA-seq and/or specified in existing bibliography. Thus, the combination of both approaches extremely facilitates the multi-scale assessment of the impacts derived from CECs exposure. While RNA-seq offers the opportunity of screening thousands of genes at once, providing a complete picture of the transcriptome, qPCR analyses allow the monitoring of pre-selected molecular markers with high resolution in a quantitative way (Martyniuk & Simmons, 2016).

In the case of target markers quantification, only a relative quantification of the selected mRNA amplicons can be made. For this purpose, different normalization methods that rely on the measurement of a reference gene (transcript with a constant level not affected by experimental factors) are available (Obolenskaya et al., 2016). The normalization method carried out in this thesis was the ΔΔCp method (Livak & Schmittgen, 2001; Pfaffl, 2001). In this method, at a given quantification cycle, the number of copies are:

$$\mathrm{N}_{target} = \mathrm{N0}_{target} \cdot (1 + \mathrm{E}_{target})^{Cp_{target}}$$

$$N_{ref} = \mathrm{N0}_{ref} \cdot (1 + \mathrm{E}_{ref})^{Cp_{ref}}$$

Thereby, the relationship between the copies of target and reference genes is:

$$\frac{\mathrm{N}_{target}}{N_{ref}} = \frac{\mathrm{N0}_{target} \cdot (1 + \mathrm{E}_{target})^{Cp_{target}}}{\mathrm{N0}_{ref} \cdot (1 + \mathrm{E}_{ref})^{Cp_{ref}}} = K$$

And normalized copies (NC) regarding the reference gene:

$$NC = \frac{\mathrm{N0}_{target}}{\mathrm{N0}_{ref}} = \frac{\mathrm{N}_{target} \cdot (1 + \mathrm{E}_{ref})^{Cp_{ref}}}{\mathrm{N}_{ref} \cdot (1 + \mathrm{E}_{target})^{Cp_{target}}} = K \cdot \frac{(1 + \mathrm{E}_{ref})^{Cp_{ref}}}{(1 + \mathrm{E}_{target})^{Cp_{target}}}$$

If the efficiencies of the amplification of both genes are similar between them and close to 1 (100 %), then 1 + E ≈ 2, and:

$$NC = K \cdot \frac{2^{Cp_{ref}}}{2^{Cp_{target}}} = K \cdot 2^{Cp_{ref} - Cp_{target}} = K \cdot 2^{\Delta Cp}$$

where ΔCp = Cpref – Cptarget

Then, the calculation of the relationship (fold-change; FC) between the mRNAs abundance of two experimental groups (usually performed for control versus treated), assuming a uniform PCR amplification efficiency across all samples (K1≈ K2), is performed as follows:

$$FC = \frac{NC_{treated}}{NC_{control}} = \frac{K_1 \cdot 2^{\Delta Cp_{treated}}}{K_2 \cdot 2^{\Delta Cp_{control}}} = 2^{\Delta Cp_{treated} - \Delta Cp_{control}} = 2^{\Delta\Delta Cp}$$

where ΔΔCp = ΔCptreated – ΔCpcontrol

Bibliography

Abdullahi, Y. A., Akunna, J. C., White, N. A., Hallett, P. D., & Wheatley, R. (2008). Investigating the effects of anaerobic and aerobic post-treatment on quality and stability of organic fraction of municipal solid waste as soil amendment. Bioresource Technology, 99(18), 8631–8636. https://doi.org/10.1016/j.biortech.2008.04.027

Acayaba, R. D., de Albuquerque, A. F., Ribessi, R. L., Umbuzeiro, G. de A., & Montagner, C. C. (2021). Occurrence of pesticides in waters from the largest sugar cane plantation region in the world. Environmental Science and Pollution Research, 28(8), 9824–9835.

Alam, S., Borthakur, A., Ravi, S., Gebremichael, M., & Mohanty, S. K. (2021). Managed aquifer recharge implementation criteria to achieve water sustainability. Science of The Total Environment, 768, 144992.

Allen, T. E. H., Goodman, J. M., Gutsell, S., & Russell, P. J. (2014). Defining molecular initiating events in the adverse outcome pathway framework for risk assessment. Chemical Research in Toxicology, 27(12), 2100–2112.

Allen, T. E. H., Goodman, J. M., Gutsell, S., & Russell, P. J. (2016). A history of the molecular initiating event. Chemical Research in Toxicology, 29(12), 2060–2070.

Almazroo, O. A., Miah, M. K., & Venkataramanan, R. (2017). Drug metabolism in the liver. Clinics in Liver Disease, 21(1), 1–20.

Bartlett, J., & Stirling, D. (2003). A short history of the polymerase chain reaction. In PCR protocols (pp. 3–6). Springer.

Bébéar, C. M., & Pereyre, S. (2005). Mechanisms of drug resistance in Mycoplasma pneumoniae. Current Drug Targets-Infectious Disorders, 5(3), 263–271.

Beceiro, A., Tomás, M., & Bou, G. (2013). Antimicrobial resistance and virulence: a successful or deleterious association in the bacterial world? Clinical Microbiology Reviews, 26(2), 185–230.

Bender, S. F., & van der Heijden, M. G. A. (2015). Soil biota enhance agricultural sustainability by improving crop yield, nutrient uptake and reducing nitrogen leaching losses. Journal of Applied Ecology, 52(1), 228–239.

Bennet, P. M. (2004). Genome Plasticity: Insertion sequence elements, transposons and integrons and DNA rearrangements. Methods in Molecular Biology, 266, 71–113.

Benotti, M. J., Trenholm, R. A., Vanderford, B. J., Holady, J. C., Stanford, B. D., & Snyder, S. A. (2009). Pharmaceuticals and endocrine disrupting compounds in US drinking water. Environmental Science & Technology, 43(3), 597–603.

Berendonk, T. U., Manaia, C. M., Merlin, C., Fatta-Kassinos, D., Cytryn, E., Walsh, F., Bürgmann, H., Sørum, H., Norström, M., Pons, M.-N., Kreuzinger, N., Huovinen, P., Stefani, S., Schwartz, T., Kisand, V., Baquero, F., & Martinez, J. L. (2015). Tackling antibiotic resistance: the environmental framework. Nature Reviews Microbiology, 13(5), 310–317. https://doi.org/10.1038/nrmicro3439

Bernstein, D. L., Kameswaran, V., Le Lay, J. E., Sheaffer, K. L., & Kaestner, K. H. (2015). The BisPCR2 method for targeted bisulfite sequencing. Epigenetics & Chromatin, 8(1), 1–9.

Bertini, A., Poirel, L., Bernabeu, S., Fortini, D., Villa, L., Nordmann, P., & Carattoli, A. (2007). Multicopy bla OXA-58 gene as a source of high-level resistance to carbapenems in Acinetobacter baumannii. Antimicrobial Agents and Chemotherapy, 51(7), 2324–2328.

Boretti, A., & Rosa, L. (2019). Reassessing the projections of the World Water Development Report. Npj Clean Water, 2(1). https://doi.org/10.1038/s41545-019-0039-9

Bradford, Y., Conlin, T., Dunn, N., Fashena, D., Frazer, K., Howe, D. G., Knight, J., Mani, P., Martin, R., & Moxon, S. A. T. (2010). ZFIN: enhancements and updates to the Zebrafish Model Organism Database. Nucleic Acids Research, 39(suppl_1), D822–D829.

Breukelman, H., Krikke, H., & Löhr, A. (2019). Failing services on urban waste management in developing countries: A review on symptoms, diagnoses, and interventions. Sustainability (Switzerland), 11(24). https://doi.org/10.3390/su11246977

Bush, K., & Jacoby, G. A. (2010). Updated functional classification of β-lactamases. Antimicrobial Agents and Chemotherapy, 54(3), 969–976.

Bustin, S. A., Benes, V., Garson, J. A., Hellemans, J., Huggett, J., Kubista, M., Mueller, R., Nolan, T., Pfaffl, M. W., & Shipley, G. L. (2009). The MIQE Guidelines: M inimum I nformation for Publication of Q uantitative Real-Time PCR E xperiments. Oxford University Press.

Campos, B., Fletcher, D., Piña, B., Tauler, R., & Barata, C. (2018). Differential gene transcription across the life cycle in Daphnia magna using a new all genome custom-made microarray. BMC Genomics, 19(1), 1–13.

Cartelle, M., del Mar Tomas, M., Molina, F., Moure, R., Villanueva, R., & Bou, G. (2004). High-level resistance to ceftazidime conferred by a novel enzyme, CTX-M-32, derived from CTX-M-1 through a single Asp240-Gly substitution. Antimicrobial Agents and Chemotherapy, 48(6), 2308–2313.

Cavalieri, V., & Spinelli, G. (2017). Environmental epigenetics in zebrafish. Epigenetics & Chromatin, 10(1), 1–11.

Cerqueira, F., Matamoros, V., Bayona, J., Elsinga, G., Hornstra, L. M., & Piña, B. (2019). Distribution of antibiotic resistance genes in soils and crops. A field study in legume plants (Vicia faba L.) grown under different watering regimes. Environmental Research, 170, 16–25.

Chien, A., Edgar, D. B., & Trela, J. M. (1976). Deoxyribonucleic acid polymerase from the extreme thermophile Thermus aquaticus. Journal of Bacteriology, 127(3), 1550–1557.

Cockerham, L. G., & Shane, B. S. (2019). Basic environmental toxicology. Routledge.

Cohen, B. (2006). Urbanization in developing countries: Current trends, future projections, and key challenges for sustainability. Technology in Society, 28(1–2), 63–80. https://doi.org/10.1016/j.techsoc.2005.10.005

Culyba, M. J., Mo, C. Y., & Kohli, R. M. (2015). Targets for combating the evolution of acquired antibiotic resistance. Biochemistry, 54(23), 3573–3582.

Dillon, P., Stuyfzand, P., Grischek, T., Lluria, M., Pyne, R. D. G., Jain, R. C., Bear, J., Schwarz, J., Wang, W., Fernandez, E., Stefan, C., Pettenati, M., van der Gun, J., Sprenger, C., Massmann, G., Scanlon, B. R., Xanke, J., Jokela, P., Zheng, Y., … Sapiano, M. (2019). Sixty years of global progress in managed aquifer recharge. Hydrogeology Journal, 27(1), 1–30. https://doi.org/10.1007/s10040-018-1841-z

Domingues, S., da Silva, G. J., & Nielsen, K. M. (2012). Integrons: vehicles and pathways for horizontal dissemination in bacteria. Mobile Genetic Elements, 2(5), 211–223.

Du, D., Wang-Kan, X., Neuberger, A., Van Veen, H. W., Pos, K. M., Piddock, L. J. V, & Luisi, B. F. (2018). Multidrug efflux pumps: structure, function and regulation. Nature Reviews Microbiology, 16(9), 523–539.

Eliopoulos, G. M., Eliopoulos, G. M., & Roberts, M. C. (2003). Tetracycline therapy: update. Clinical Infectious Diseases, 36(4), 462–467.

Fang, Z., & Cui, X. (2011). Design and validation issues in RNA-seq experiments. Briefings in Bioinformatics, 12(3), 280–287.

Fereja, W. M., & Chemeda, D. D. (2022). Status, characterization, and quantification of municipal solid waste as a measure towards effective solid waste management: The case of Dilla Town, Southern Ethiopia. Journal of the Air and Waste Management Association, 72(2), 187–201. https://doi.org/10.1080/10962247.2021.1923585

Forsberg, K. J., Patel, S., Gibson, M. K., Lauber, C. L., Knight, R., Fierer, N., & Dantas, G. (2014). Bacterial phylogeny structures soil resistomes across habitats. Nature, 509(7502), 612–616. https://doi.org/10.1038/nature13377

Furuya, E. Y., & Lowy, F. D. (2006). Antimicrobial-resistant bacteria in the community setting. Nature Reviews Microbiology, 4(1), 36–45. https://doi.org/10.1038/nrmicro1325

Garibyan, L., & Avashia, N. (2013). Research techniques made simple: polymerase chain reaction (PCR). The Journal of Investigative Dermatology, 133(3), e6.

Gaze, W. H., Zhang, L., Abdouslam, N. A., Hawkey, P. M., Calvo-Bado, L., Royle, J., Brown, H., Davis, S., Kay, P., & Boxall, A. (2011). Impacts of anthropogenic activity on the ecology of class 1 integrons and integron-associated genes in the environment. The ISME Journal, 5(8), 1253–1261.

Gill, M. J., Simjee, S., Al-Hattawi, K., Robertson, B. D., Easmon, C. S. F., & Ison, C. A. (1998). Gonococcal resistance to β-lactams and tetracycline involves mutation in loop 3 of the porin encoded at the penB locus. Antimicrobial Agents and Chemotherapy, 42(11), 2799–2803.

Gillings, M. R., Gaze, W. H., Pruden, A., Smalla, K., Tiedje, J. M., & Zhu, Y. G. (2015). Using the class 1 integron-integrase gene as a proxy for anthropogenic pollution. ISME Journal, 9(6), 1269–1279. https://doi.org/10.1038/ismej.2014.226

Granados, J. C., Falah, K., Koo, I., Morgan, E. W., Perdew, G. H., Patterson, A. D., Jamshidi, N., & Nigam, S. K. (2022). AHR is a master regulator of diverse pathways in endogenous metabolism. Scientific Reports, 12(1), 1–16.

Gruetzmacher, G., & Kumar, P. J. S. (2012). Introduction to Managed Aquifer Recharge (MAR)–Overview of schemes and settings world wide. Conference on Managed Aquifer Recharge: Methods, Hydrogeological Requirements, Post and Pre-Treatment Systems.

Hamilton, F. (1822). An account of the fishes found in the river Ganges and its branches (Vol. 1). Archibald Constable.

Hermsen, S. A. B., & Piersma, A. H. (2014). Implementation of transcriptomics in the zebrafish embryotoxicity test. In Toxicogenomics-Based Cellular Models (pp. 127–141). Elsevier.

Hong, T. P., Carter, M. Q., Struffi, P., Casonato, S., Hao, Y., Lam, J. S., Lory, S., & Jousson, O. (2017). Conjugative type IVb pilus recognizes lipopolysaccharide of recipient cells to initiate PAPI-1 pathogenicity island transfer in Pseudomonas aeruginosa. BMC Microbiology, 17(1), 1–11.

Howe, K., Clark, M. D., Torroja, C. F., Torrance, J., Berthelot, C., Muffato, M., Collins, J. E., Humphray, S., McLaren, K., & Matthews, L. (2013). The zebrafish reference genome sequence and its relationship to the human genome. Nature, 496(7446), 498–503.

Hu, J., Shi, J., Chang, H., Li, D., Yang, M., & Kamagata, Y. (2008). Phenotyping and genotyping of antibiotic-resistant Escherichia coli isolated from a natural river basin. Environmental Science & Technology, 42(9), 3415–3420.

Ihmels, J., Levy, R., & Barkai, N. (2004). Principles of transcriptional control in the metabolic network of Saccharomyces cerevisiae. Nature Biotechnology, 22(1), 86–92.

Iyanagi, T. (2007). Molecular Mechanism of Phase I and Phase II Drug-Metabolizing Enzymes: Implications for Detoxification. International Review of Cytology, 260(06), 35–112. https://doi.org/10.1016/S0074-7696(06)60002-8

Kapoor, G., Saigal, S., & Elongavan, A. (2017). Action and resistance mechanisms of antibiotics: A guide for clinicians. Journal of Anaesthesiology, Clinical Pharmacology, 33(3), 300.

Kasonga, T. K., Coetzee, M. A. A., Kamika, I., Ngole-Jeme, V. M., & Momba, M. N. B. (2021). Endocrine-disruptive chemicals as contaminants of emerging concern in wastewater and surface water: A review. Journal of Environmental Management, 277, 111485.

Keen, E. C., Bliskovsky, V. V, Malagon, F., Baker, J. D., Prince, J. S., Klaus, J. S., & Adhya, S. L. (2017). Novel "superspreader" bacteriophages promote horizontal gene transfer by transformation. MBio, 8(1), e02115-16.

Knöbel, M., Busser, F. J. M., Rico-Rico, A., Kramer, N. I., Hermens, J. L. M., Hafner, C., Tanneberger, K., Schirmer, K., & Scholz, S. (2012). Predicting adult fish acute lethality with the zebrafish embryo: relevance of test duration, endpoints, compound properties, and exposure concentration analysis. Environmental Science & Technology, 46(17), 9690–9700.

Kubanza, N. S., & Simatele, D. (2016). Social and environmental injustices in solid waste management in sub-Saharan Africa: a study of Kinshasa, the Democratic Republic of Congo. Local Environment, 21(7), 866–882. https://doi.org/10.1080/13549839.2015.1038985

Kumar, A., & Schweizer, H. P. (2005). Bacterial resistance to antibiotics: active efflux and reduced uptake. Advanced Drug Delivery Reviews, 57(10), 1486–1513.

Kumar, S., Mukherjee, M. M., & Varela, M. F. (2013). Modulation of bacterial multidrug resistance efflux pumps of the major facilitator superfamily. International Journal of Bacteriology, 2013.

Lambert, P. A. (2002). Cellular impermeability and uptake of biocides and antibiotics in Gram-positive bacteria and mycobacteria. Journal of Applied Microbiology, 92(s1), 46S-54S.

Lee, H.-J., Kim, K. Y., Hamm, S.-Y., Kim, M., Kim, H. K., & Oh, J.-E. (2019). Occurrence and distribution of pharmaceutical and personal care products, artificial sweeteners, and pesticides in groundwater from an agricultural area in Korea. Science of the Total Environment, 659, 168–176.

Li, A.-D., Li, L.-G., & Zhang, T. (2015). Exploring antibiotic resistance genes and metal resistance genes in plasmid metagenomes from wastewater treatment plants. Frontiers in Microbiology, 6, 1025.

Liu, J., Yang, H., Gosling, S. N., Kummu, M., Flörke, M., Pfister, S., Hanasaki, N., Wada, Y., Zhang, X., Zheng, C., Alcamo, J., & Oki, T. (2017). Water scarcity assessments in the past, present, and future. Earth's Future, 5(6), 545–559. https://doi.org/10.1002/2016EF000518

Liu, Q., Li, L., Zhang, X., Saini, A., Li, W., Hung, H., Hao, C., Li, K., Lee, P., & Wentzell, J. J. B. (2021). Uncovering global-scale risks from commercial chemicals in air. Nature, 600(7889), 456–461.

Livak, K. J., & Schmittgen, T. D. (2001). Analysis of relative gene expression data using real-time quantitative PCR and the 2− ΔΔCT method. Methods, 25(4), 402–408.

López-Maury, L., Marguerat, S., & Bähler, J. (2008). Tuning gene expression to changing environments: from rapid responses to evolutionary adaptation. Nature Reviews Genetics, 9(8), 583–593.

Lowe, R., Shirley, N., Bleackley, M., Dolan, S., & Shafee, T. (2017). Transcriptomics technologies. PLoS Computational Biology, 13(5), e1005457.

Luby, E., Ibekwe, A. M., Zilles, J., & Pruden, A. (2016). Molecular methods for assessment of antibiotic resistance in agricultural ecosystems: prospects and challenges. Journal of Environmental Quality, 45(2), 441–453.

Madigan, M. T., Martinko, J. M., & Parker, J. (2006). Brock biology of microorganisms (Vol. 11). Pearson Prentice Hall Upper Saddle River, NJ.

Mah, T.-F. (2012). Biofilm-specific antibiotic resistance. Future Microbiology, 7(9), 1061–1072.

Marsala, R. Z., Capri, E., Russo, E., Bisagni, M., Colla, R., Lucini, L., Gallo, A., & Suciu, N. A. (2020). First evaluation of pesticides occurrence in groundwater of Tidone Valley, an area with intensive viticulture. Science of The Total Environment, 736, 139730.

Martyniuk, C. J., & Simmons, D. B. (2016). Spotlight on environmental omics and toxicology: a long way in a short time. In Comparative Biochemistry and Physiology Part D: Genomics and Proteomics (Vol. 19, pp. 97–101). Elsevier.

Meade, E. B., Iwanowicz, L. R., Neureuther, N., LeFevre, G. H., Kolpin, D. W., Zhi, H., Meppelink, S. M., Lane, R. F., Schmoldt, A., Mohaimani, A., Mueller, O., & Klaper, R. D. (2022). Transcriptome signatures of wastewater effluent exposure in larval zebrafish vary with seasonal mixture composition in an effluent-dominated stream. Science of The Total Environment, 856(September 2022), 159069. https://doi.org/10.1016/j.scitotenv.2022.159069

Meena, R. S. (2021). Input Use Efficiency for Food and Environmental Security. In Input Use Efficiency for Food and Environmental Security. https://doi.org/10.1007/978-981-16-5199-1

Mendes, R. E., Castanheira, M., Toleman, M. A., Sader, H. S., Jones, R. N., & Walsh, T. R. (2007). Characterization of an integron carrying bla IMP-1 and a new aminoglycoside resistance gene, aac (6′)-31, and its dissemination among genetically unrelated clinical isolates in a Brazilian hospital. Antimicrobial Agents and Chemotherapy, 51(7), 2611–2614.

Menezes, A. (2016). Steps for a successful qPCR experiment. Integrated DNA Technologies. https://www. idtdna. com/pages/education ….

Möller, K., & Schultheiß, U. (2015). Chemical characterization of commercial organic fertilizers. Archives of Agronomy and Soil Science, 61(7), 989–1012.

Mugnaioli, C., Luzzaro, F., De Luca, F., Brigante, G., Perilli, M., Amicosante, G., Stefani, S., Toniolo, A., & Rossolini, G. M. (2006). CTX-M-type extended-spectrum β-lactamases in Italy: molecular epidemiology of an emerging countrywide problem. Antimicrobial Agents and Chemotherapy, 50(8), 2700–2706.

Muhammad, I., Golparian, D., Dillon, J.-A. R., Johansson, Å., Ohnishi, M., Sethi, S., Chen, S., Nakayama, S., Sundqvist, M., & Bala, M. (2014). Characterisation of bla TEM genes and types of β-lactamase plasmids in Neisseria gonorrhoeae–the prevalent and conserved bla TEM-135 has not recently evolved and existed in the Toronto plasmid from the origin. BMC Infectious Diseases, 14(1), 1–7.

Nonaka, L., Maruyama, F., Miyamoto, M., Miyakoshi, M., Kurokawa, K., & Masuda, M. (2012). Novel conjugative transferable multiple drug resistance plasmid pAQU1 from Photobacterium damselae subsp. damselae isolated from marine aquaculture environment. Microbes and Environments, 27(3), 263–272.

Noor, T., Javid, A., Hussain, A., Bukhari, S. M., Ali, W., Akmal, M., & Hussain, S. M. (2020). Types, sources and management of urban wastes. In Urban Ecology. Elsevier Inc. https://doi.org/10.1016/b978-0-12-820730-7.00014-8

Norman, A., Hansen, L. H., & Sørensen, S. J. (2009). Conjugative plasmids:

vessels of the communal gene pool. Philosophical Transactions of the Royal Society B: Biological Sciences, 364(1527), 2275–2289.

Obolenskaya, M. Y., Kuklin, A. V, Rodrigez, R. R., Martsenyuk, O. P., Korneyeva, K. L., Docenko, V. A., & Draguschenko, O. O. (2016). Practical approach to quantification of mRNA abundance using RT-qPCR, normalization of experimental data and MIQE. Biopolymers and Cell.

Oelkers, K. (2021). Is the objective of the Water Framework Directive to deal with pollutant emissions at source coherently implemented by the EU's substance-specific legal acts? A comparison of the environmental risk control of pharmaceutical legislation with the REACH-, Bi. Sustainable Chemistry and Pharmacy, 20, 100386.

Orsini, L., Brown, J. B., Shams Solari, O., Li, D., He, S., Podicheti, R., Stoiber, M. H., Spanier, K. I., Gilbert, D., & Jansen, M. (2018). Early transcriptional response pathways in Daphnia magna are coordinated in networks of crustacean-specific genes. Molecular Ecology, 27(4), 886–897.

Paramashivam, D., Dickinson, N. M., Clough, T. J., Horswell, J., & Robinson, B. H. (2017). Potential environmental benefits from blending biosolids with other organic amendments before application to land. Journal of Environmental Quality, 46(3), 481–489.

Patel, M., Kumar, R., Kishor, K., Mlsna, T., Pittman Jr, C. U., & Mohan, D. (2019). Pharmaceuticals of emerging concern in aquatic systems: chemistry, occurrence, effects, and removal methods. Chemical Reviews, 119(6), 3510–3673.

Patwardhan, A., Ray, S., & Roy, A. (2014). Molecular markers in phylogenetic studies-a review. Journal of Phylogenetics & Evolutionary Biology, 2014.

Peck, D., Kandachar, P., & Tempelman, E. (2015). Critical materials from a product design perspective. Materials and Design, 65, 147–159. https://doi.org/10.1016/j.matdes.2014.08.042

Petrie, B., Barden, R., & Kasprzyk-Hordern, B. (2015). A review on emerging contaminants in wastewaters and the environment: Current knowledge, understudied areas and recommendations for future monitoring. Water Research, 72, 3–27. https://doi.org/https://doi.org/10.1016/j.watres.2014.08.053

Pfaffl, M. (2001). Development and validation of an externally standardised quantitative insulin-like growth factor-1 RT-PCR using LightCycler SYBR Green I technology. Rapid Cycle Real-Time PCR: Methods and Applications, 281–291.

Piña, B., Raldúa, D., Barata, C., Portugal, J., Navarro-Martín, L., Martínez, R., Fuertes, I., & Casado, M. (2018). Chapter Twenty - Functional Data Analysis: Omics for Environmental Risk Assessment. In J. Jaumot, C. Bedia, & R. B. T.-C. A. C. Tauler (Eds.), Data Analysis for Omic Sciences: Methods and Applications (Vol. 82, pp. 583–611). Elsevier. https://doi.org/https://doi.org/10.1016/bs.coac.2018.07.007

Popowska, M., & Krawczyk-Balska, A. (2013). Broad-host-range IncP-1 plasmids and their resistance potential. Frontiers in Microbiology, 4, 44.

Qian, H., Chen, J., & Howard, K. W. F. (2020). Assessing groundwater pollution and potential remediation processes in a multi-layer aquifer system. Environmental Pollution, 263, 114669. https://doi.org/https://doi.org/10.1016/j.envpol.2020.114669

Rajpara, N., Kutar, B. M., Sinha, R., Nag, D., Koley, H., Ramamurthy, T., & Bhardwaj, A. K. (2015). Role of integrons, plasmids and SXT elements in multidrug resistance of Vibrio cholerae and Providencia vermicola obtained from a clinical isolate of diarrhea. Frontiers in Microbiology, 6, 57.

Ramirez, M. S., & Tolmasky, M. E. (2010). Aminoglycoside modifying enzymes. Drug Resistance Updates, 13(6), 151–171.

Renton, K. W. (1986). Factors affecting drug biotransformation. Clinical Biochemistry, 19(2), 72–75.

Reygaert, W. (2009). Methicillin-resistant Staphylococcus aureus (MRSA): molecular aspects of antimicrobial resistance and virulence. Clinical Laboratory Science, 22(2), 115.

Reygaert, W. C. (2018). An overview of the antimicrobial resistance mechanisms of bacteria. AIMS Microbiology, 4(3), 482.

Ribeiro, C., Ribeiro, A. R., & Tiritan, M. E. (2016). Priority substances and emerging organic pollutants in Portuguese aquatic environment: a review. Reviews of Environmental Contamination and Toxicology, 1–44.

Robitaille, J., Denslow, N. D., Escher, B. I., Kurita-Oyamada, H. G., Marlatt, V., Martyniuk, C. J., Navarro-Martín, L., Prosser, R., Sanderson, T., & Yargeau, V. (2022). Towards regulation of Endocrine Disrupting chemicals (EDCs) in water resources using bioassays-A guide to developing a testing strategy. Environmental Research, 205, 112483.

Ryan, R. P., Germaine, K., Franks, A., Ryan, D. J., & Dowling, D. N. (2008). Bacterial endophytes: recent developments and applications. FEMS Microbiology Letters, 278(1), 1–9.

Sachana, M. (2019). Adverse outcome pathways and their role in revealing biomarkers. In Biomarkers in Toxicology (pp. 163–170). Elsevier.

Sakai, S. ichi, Yoshida, H., Hirai, Y., Asari, M., Takigami, H., Takahashi, S., Tomoda, K., Peeler, M. V., Wejchert, J., Schmid-Unterseh, T., Douvan, A. R., Hathaway, R., Hylander, L. D., Fischer, C., Oh, G. J., Jinhui, L., & Chi, N. K. (2011). International comparative study of 3R and waste management policy developments. Journal of Material Cycles and Waste Management, 13(2), 86–102. https://doi.org/10.1007/s10163-011-0009-x

Salimi, M., Esrafili, A., Gholami, M., Jonidi Jafari, A., Rezaei Kalantary, R., Farzadkia, M., Kermani, M., & Sobhi, H. R. (2017). Contaminants of emerging concern: a review of new approach in AOP technologies. Environmental Monitoring and Assessment, 189(8), 1–22.

Sariatli, F. (2017). Linear Economy Versus Circular Economy: A Comparative and Analyzer Study for Optimization of Economy for Sustainability. Visegrad Journal on Bioeconomy and Sustainable Development, 6(1), 31–34. https://doi.org/10.1515/vjbsd-2017-0005

Scholz, S., Fischer, S., Gündel, U., Küster, E., Luckenbach, T., & Voelker, D. (2008). The zebrafish embryo model in environmental risk assessment—applications beyond acute toxicity testing. Environmental Science and

Pollution Research, 15(5), 394–404.

Seiler, C., & Berendonk, T. U. (2012). Heavy metal driven co-selection of antibiotic resistance in soil and water bodies impacted by agriculture and aquaculture. Frontiers in Microbiology, 3, 399.

Sen, D., Brown, C. J., Top, E. M., & Sullivan, J. (2013). Inferring the evolutionary history of IncP-1 plasmids despite incongruence among backbone gene trees. Molecular Biology and Evolution, 30(1), 154–166.

Shehwana, H., & Konu, O. (2019). Comparative transcriptomics between zebrafish and mammals: a roadmap for discovery of conserved and unique signaling pathways in physiology and disease. Frontiers in Cell and Developmental Biology, 7, 5.

Shimizu, Y., Nakatsuru, Y., Ichinose, M., Takahashi, Y., Kume, H., Mimura, J., Fujii-Kuriyama, Y., & Ishikawa, T. (2000). Benzo [a] pyrene carcinogenicity is lost in mice lacking the aryl hydrocarbon receptor. Proceedings of the National Academy of Sciences, 97(2), 779–782.

Shroder, J. F. (2015). Biological and environmental hazards, risks, and disasters. Elsevier.

Simmons, D. B. D., Benskin, J. P., Cosgrove, J. R., Duncker, B. P., Ekman, D. R., Martyniuk, C. J., & Sherry, J. P. (2015). Omics for aquatic ecotoxicology: Control of extraneous variability to enhance the analysis of environmental effects. Environmental Toxicology and Chemistry, 34(8), 1693–1704.

Skinner, A. M. J., & Watt, P. J. (2007). Strategic egg allocation in the zebra fish, Danio rerio. Behavioral Ecology, 18(5), 905–909.

Smith, M. C. M., Hendrix, R. W., Dedrick, R., Mitchell, K., Ko, C.-C., Russell, D., Bell, E., Gregory, M., Bibb, M. J., & Pethick, F. (2013). Evolutionary relationships among actinophages and a putative adaptation for growth in Streptomyces spp. Journal of Bacteriology, 195(21), 4924–4935.

Spence, R., & Smith, C. (2006). Mating preference of female zebrafish, Danio rerio, in relation to male dominance. Behavioral Ecology, 17(5), 779–783.

Spielmeyer, A., Höper, H., & Hamscher, G. (2017). Long-term monitoring of sulfonamide leaching from manure amended soil into groundwater. Chemosphere. https://doi.org/10.1016/j.chemosphere.2017.03.020

Stavropoulou, E., Pircalabioru, G. G., & Bezirtzoglou, E. (2018). The role of cytochromes P450 in infection. Frontiers in Immunology, 9, 89.

Stefano, P. H. P., Roisenberg, A., Santos, M. R., Dias, M. A., & Montagner, C. C. (2022). Unraveling the occurrence of contaminants of emerging concern in groundwater from urban setting: A combined multidisciplinary approach and self-organizing maps. Chemosphere, 299, 134395. https://doi.org/https://doi.org/10.1016/j.chemosphere.2022.134395

Stegeman, J. J., Goldstone, J. V, & Hahn, M. E. (2010). 10 - Perspectives on zebrafish as a model in environmental toxicology. In S. F. Perry, M. Ekker, A. P. Farrell, & C. J. B. T.-F. P. Brauner (Eds.), Zebrafish (Vol. 29, pp. 367–439). Academic Press. https://doi.org/https://doi.org/10.1016/S1546-5098(10)02910-9

Stjepanović, M., Velić, N., Lončarić, A., Gašo-Sokač, D., Bušić, V., & Habuda-Stanić, M. (2019). Adsorptive removal of nitrate from wastewater using modified lignocellulosic waste material. Journal of Molecular Liquids, 285, 535–544.

Sumpter, J. P. (2005). Endocrine disrupters in the aquatic environment: an overview. Acta Hydrochimica et Hydrobiologica, 33(1), 9–16.

Suter, G. W., Rosen, A. E., Linder, E., & Parkhurst, D. F. (1987). Endpoints for responses of fish to chronic toxic exposures. Environmental Toxicology and Chemistry, 6(10), 793–809.

Suzuki, T., Hidaka, T., Kumagai, Y., & Yamamoto, M. (2020). Environmental pollutants and the immune response. Nature Immunology, 21(12), 1486–1495.

Tadić, Đ., Bleda Hernandez, M. J., Cerqueira, F., Matamoros, V., Piña, B., & Bayona, J. M. (2021). Occurrence and human health risk assessment of antibiotics and their metabolites in vegetables grown in field-scale agricultural systems. Journal of Hazardous Materials, 401(April 2020), 123424. https://doi.org/10.1016/j.jhazmat.2020.123424

Tamang, M. D., Seol, S. Y., Oh, J.-Y., Kang, H. Y., Lee, J. C., Lee, Y. C., Cho, D. T., & Kim, J. (2008). Plasmid-mediated quinolone resistance determinants qnrA, qnrB, and qnrS among clinical isolates of Enterobacteriaceae in a Korean hospital. Antimicrobial Agents and Chemotherapy, 52(11), 4159–4162.

Tanguay, R. L. (2018). The rise of zebrafish as a model for toxicology. Toxicological Sciences, 163(1), 3–4.

Thiolas, A., Bornet, C., Davin-Régli, A., Pagès, J.-M., & Bollet, C. (2004). Resistance to imipenem, cefepime, and cefpirome associated with mutation in Omp36 osmoporin of Enterobacter aerogenes. Biochemical and Biophysical Research Communications, 317(3), 851–856.

Thomas, C. M., & Nielsen, K. M. (2005). Mechanisms of, and barriers to, horizontal gene transfer between bacteria. Nature Reviews Microbiology, 3(9), 711–721.

Tian, Z., Wark, D. A., Bogue, K., & James, C. A. (2021). Suspect and non-target screening of contaminants of emerging concern in streams in agricultural watersheds. Science of The Total Environment, 795, 148826.

Tran, H. N., Lee, C.-K., Vu, M. T., & Chao, H.-P. (2017). Removal of copper, lead, methylene green 5, and acid red 1 by saccharide-derived spherical biochar prepared at low calcination temperatures: adsorption kinetics, isotherms, and thermodynamics. Water, Air, & Soil Pollution, 228(10), 1–16.

Tuomisto, J. (2019). Dioxins and dioxin-like compounds: toxicity in humans and animals, sources, and behaviour in the environment. WikiJournal of Medicine, 6(1), 1–26.

Urben, P. (2017). Bretherick's handbook of reactive chemical hazards. Elsevier.

Valhondo, C., Martínez-Landa, L., Carrera, J., Díaz-Cruz, S. M., Amalfitano, S., & Levantesi, C. (2020). Six artificial recharge pilot replicates to gain insight into water quality enhancement processes. Chemosphere, 240. https://doi.org/10.1016/j.chemosphere.2019.124826

Van Hoek, A. H. A. M., Mevius, D., Guerra, B., Mullany, P., Roberts, A. P., & Aarts, H. J. M. (2011). Acquired antibiotic resistance genes: an overview. Frontiers in Microbiology, 2, 203.

Varshney, G. K., Lu, J., Gildea, D. E., Huang, H., Pei, W., Yang, Z., Huang, S. C., Schoenfeld, D., Pho, N. H., & Casero, D. (2013). A large-scale zebrafish gene knockout resource for the genome-wide study of gene function. Genome Research, 23(4), 727–735.

Villagra, N. A., Fuentes, J. A., Jofré, M. R., Hidalgo, A. A., García, P., & Mora, G. C. (2012). The carbon source influences the efflux pump-mediated antimicrobial resistance in clinically important Gram-negative bacteria. Journal of Antimicrobial Chemotherapy, 67(4), 921–927.

Wang, H., Hashimoto, S., Moriguchi, Y., Yue, Q., & Lu, Z. (2012). Resource use in growing China: Past trends, influence factors, and future demand. Journal of Industrial Ecology, 16(4), 481–492. https://doi.org/10.1111/j.1530-9290.2012.00484.x

Wang, H., Xu, J., Yu, H., Liu, X., Yin, W., Liu, Y., Liu, Z., & Zhang, T. (2015). Study of the application and methods for the comprehensive treatment of municipal solid waste in northeastern China. Renewable and Sustainable Energy Reviews, 52, 1881–1889. https://doi.org/10.1016/j.rser.2015.08.038

Waseem, H., Jameel, S., Ali, J., Saleem Ur Rehman, H., Tauseef, I., Farooq, U., Jamal, A., & Ali, M. I. (2019). Contributions and challenges of high throughput qPCR for determining antimicrobial resistance in the environment: a critical review. Molecules, 24(1), 163.

White, S. S., & Birnbaum, L. S. (2009). An overview of the effects of dioxins and dioxin-like compounds on vertebrates, as documented in human and ecological epidemiology. Journal of Environmental Science and Health, Part C, 27(4), 197–211.

Whiteley, A. R., Bhat, A., Martins, E. P., Mayden, R. L., Arunachalam, M., UUSI-HEIKKILÄ, S., Ahmed, A. T. A., Shrestha, J., Clark, M., & Stemple, D. (2011). Population genomics of wild and laboratory zebrafish (Danio rerio). Molecular Ecology, 20(20), 4259–4276.

Wielders, C. L. C., Fluit, A. C., Brisse, S., Verhoef, J., & Schmitz, F. (2002). mecA gene is widely disseminated in Staphylococcus aureus population. Journal of Clinical Microbiology, 40(11), 3970–3975.

Winans, K., Kendall, A., & Deng, H. (2017). The history and current applications of the circular economy concept. Renewable and Sustainable Energy Reviews, 68(September 2016), 825–833. https://doi.org/10.1016/j.rser.2016.09.123

Wuttke, W., Jarry, H., & Seidlova-Wuttke, D. (2010). Definition, classification and mechanism of action of endocrine disrupting chemicals. Hormones, 9(1), 9–15.

Yadav, D., Rangabhashiyam, S., Verma, P., Singh, P., Devi, P., Kumar, P., Hussain, C. M., Gaurav, G. K., & Kumar, K. S. (2021). Environmental and health impacts of contaminants of emerging concerns: Recent treatment challenges and approaches. Chemosphere, 272, 129492.

Yang, B., Wang, Y., & Qian, P.-Y. (2016). Sensitivity and correlation of hypervariable regions in 16S rRNA genes in phylogenetic analysis. BMC Bioinformatics, 17(1), 1–8.

You, R., Margenat, A., Lanzas, C. S., Cañameras, N., Carazo, N., Navarro-Martín, L., Matamoros, V., Bayona, J. M., & Díez, S. (2020). Dose effect of Zn and Cu in sludge-amended soils on vegetable uptake of trace elements, antibiotics, and antibiotic resistance genes: Human health implications. Environmental Research, 191, 109879. https://doi.org/10.1016/j.envres.2020.109879

Zaneveld, J. R., Nemergut, D. R., & Knight, R. (2008). Are all horizontal gene transfers created equal? Prospects for mechanism-based studies of HGT patterns. Microbiology, 154(1), 1–15.

Zeller, V., Towa, E., Degrez, M., & Achten, W. M. J. (2019). Urban waste flows and their potential for a circular economy model at city-region level. Waste Management, 83, 83–94. https://doi.org/https://doi.org/10.1016/j.wasman.2018.10.034

Zhang, G., Brown, E. W., & González-Escalona, N. (2011). Comparison of real-time PCR, reverse transcriptase real-time PCR, loop-mediated isothermal amplification, and the FDA conventional microbiological method for the detection of Salmonella spp. in produce. Applied and Environmental Microbiology, 77(18), 6495–6501.

Zhang, W., Efstathiadis, H., Li, L., & Liang, Y. (2020). Environmental factors affecting degradation of perfluorooctanoic acid (PFOA) by In2O3 nanoparticles. Journal of Environmental Sciences, 93, 48–56.

Zhang, X. Q. (2016). The trends, promises and challenges of urbanisation in the world. Habitat International, 54(13), 241–252. https://doi.org/10.1016/j.habitatint.2015.11.018

CHAPTER TWO.

BIOLOGICAL RISKS ASSOCIATED TO BIOSOLIDS REUSE IN AGRICULTURE

Antibiotic and antibiotic-resistant gene loads in swine slurries and their digestates: implications for their use as fertilizers in agriculture

Sanz, Claudia[1]; Casado, Marta[1]; Navarro-Martin, Laia[1]; Tadić, Đorđe[1]; Parera, Joan[2]; Tugues, Jordi[2]; Bayona, Josep M[1]; Piña, Benjamin[1]

1) IDAEA-CSIC, Jordi Girona, 18. E-08034, Barcelona, Spain

2) DARP Catalunya Central, GENCAT, Carrer de la Llotja, s/n (Recinte Firal El Sucre) 08500, Vic, Spain

Environmental Research, 194 (2021)

Available in https://doi.org/10.1016/j.envres.2020.110513)

Abstract

The spread of antibiotic resistance in bacteria is a matter of global concern, and the identification of possible sources of the associated genetic elements (antibiotic resistance genes -ARGs, components of the horizontal gene transfer mechanism), is becoming an urgent need. While the transmission of ARGs in medical settings have been adequately characterized, ARG propagation in agroecosystems remains insufficiently studied. Particularly crucial is the determination of potential risks associated to the use of swine slurries and related products as component of organic fertilizers, an increasingly used farming practice. We determined ARGs and antibiotic loads analyzed from swine slurries and digestates from eight farms from Catalonia (NE Spain), and compared the results with their microbiome composition. Both ARGs and antibiotic were conspicuous in farm organic wastes, and the levels of some antibiotics exceeded currently accepted minimum inhibitory concentrations. Particularly, the presence of high loads of fluoroquinolones was directly correlated to the prevalence of the related *qnr*S1 ARG in the slurry. We also found evidence that ARG loads were directly correlated to the prevalence of determined bacterial taxa (Actinobacteria, Proteobacteria, Spirochaeta), a parameter that could be potentially modulated by the processing of the raw slurry prior to their use as fertilizer.

Funding sources

This work was supported by a grant from the Spanish Ministry of Science, Innovation and University (RTI2018-096175-B-I00) and from the LIFE Program of the European Union (LIFE17 ENV/ES/000439). CSL was supported by an FI predoctoral fellowship from the Generalitat de Catalunya.

1. Introduction

The use of manure and of its digestates for soil fertilization represents a sustainable option to first valorise residues and, second, to provide farmers with an important supply of macro and micronutrient that should be otherwise obtained from mineral fertilization. In this regard, using organic fertilizers in agriculture is included in the schemes of circular economy to optimize sources and reduce residues. Furthermore, soil fertilization with manure and related products could improve the amount and quality of the soil organic matter, which is essential for soil functionality. In fact, soil organic matter is particularly depleted in the southern European countries (Zdruli et al., 2004).

However, the use of farm-originated manure for food production has some potential hazards, being its impact in animal and human health perhaps the most important one. Farm wastes may contain viral and bacterial pathogens and toxicants (veterinarian drugs and heavy metals) that could represent an occupational risk for the exposed farmers, livestock secondarily exposed, and, if used for food production, for the general public (Goss et al., 2013; Tadić et al., 2021). Recently, a new matter of concern has appeared in the form of their role as facilitators of the ever-increasing phenomenon of antibiotic resistance, a major menace for the human health worldwide.

The occurrence of pathogenic bacterial strains increasingly recalcitrant to medical treatment with the existing antibiotics is becoming a worldwide concern (WHO, 2014). Antibiotic resistance (AR) is associated to increased hospitalization and mortality rates of humans and with AR-resistant zoonotics, two serious concerns for the health and welfare of both humans and animals (Berendonk et al., 2015; Koch et al., 2017). Health authorities from the United States of America[1] and the European Union[2] estimate that 35.000 and 33.000 premature deaths, respectively, occur annually due to Antibiotic Resistant Bacteria (ARB).

AR is basically mediated by two types of genetic elements. First, antibiotic-resistant genes (ARGs) confer resistance to one or more antibiotics to the harbouring bacteria, by a series of molecular mechanisms (excretion, degradation, competition, modification of cellular targets) that determine their spectrum of substances against which they confer resistance (Berendonk et al., 2015; Forsberg et al., 2014; Shi et al., 2020). Secondly, elements of different horizontal gene transfer (HGT) mechanisms (phages, transposons, plasmids) contribute to spread ARGs among bacterial lineages, crossing environmental and taxonomic barriers (Nesme and Simonet, 2015; Von Wintersdorff et al., 2016). In the worst cases, HGT processes may allow the natural genetic engineering of elements carrying resistance to multiple antibiotic from different families and modes of action, leading to the emergence of multi-antibiotic-resistant microbes, against which most current medical treatments are inefficient (Johnning et al., 2013; Tennstedt et al., 2003).

In this work, we present a survey of the abundance of seven ARGs of clinical relevance (*sul*1, *tet*M, *qnr*S1, *mec*A, *bla*$_{TEM}$, bla$_{CTX-M-32}$, bla$_{OXA-58)}$ (Bertini et al., 2007; Hembach et al., 2017; Tamang et al., 2008; Wielders et al., 2002), plus the integrase gene intI1 (Gillings et al., 2008), in swine slurries

[1] https://www.cdc.gov/drugresistance/
[2] https://ec.europa.eu/health/amr/antimicrobial-resistance_en

Table 1. Sample and sampling site characteristics.

Sample Code	Region	Site code	Description	Sampling point
A	Osona	1	pregnant sow (slurry)	Tank
B	Osona	1	pregnant sow + nursy sow (slurry)	Lagoon
C	Osona	2	transition piglet (slurry)	Tank
D	Osona	2	transition piglet (slurry)	Lagoon
E	Osona	3	fatting pigglet (slurry)	Tank
F	Osona	3	fatting pigglet (slurry)	Lagoon
G	Osona	4	digested sow slurry + slaughter sludge + waste cake industry + barley waste	Digestor
H	Osona	5	liquid fraction sows	Liquid/Solid separator
J	Osona	5	solid fraction sows	Liquid/Solid separator
K	Urgell	6	liquid fraction sows	Liquid/Solid separator
L	Urgell	7	fatting pigglet (slurry)	Lagoon
M	Urgell	8	digested solid pig fraction+ WTT sludge+ poultry waste	Digestor

and their digestates from different operating pig farms from Catalonia (NE Spain). Furthermore, a targeted screening of 17 antibiotics in samples from the same sites was performed in parallel and their concentrations were compared to minimum selective concentration (MSC) to estimate their potential risk. Culture-independent, quantitative real-time PCR (qRT-PCR) methods to quantify their incidence among the different samples, and high throughput 16S rDNA sequencing to correlate their prevalence to the abundance of particular bacterial taxonomic groups (Beckers et al., 2016) were applied. Our main objective was the assessment of the potential risk of using these nutrient-rich materials for fertilizing soils in extensive agriculture.

2. Materials and Methods

2.1. Sampling and sample preparation

Different potential fertilizers were sampled from tanks and lagoons from six pig farms and two composting facilities (**Table 1**). In total, twelve samples were taken, including six samples of swine slurry from different stages of the pig production cycle (pregnancy, nursery, transition to adult feed, and piglet fatting, samples A-F), solid (sample J) and liquid (samples H, K, and L) slurry fractions, and two digestate mixtures specifically formulated for their application on fields (samples G and M). These samples are residues of biogas-producing plants, in which pig slurry is mixed with other substrates with a higher organic load (slaughter sludge, cake industry wastes, and barley waste for sample G, chicken waste and sludge from a wastewater treatment plant for sample M). This mixture is used to produce biogas (CH_4 + CO_2) by mesophile, methanogenic fermentation (http://www.ecobiogas.es; https://www.kriegfischer.de/biogasanlagen/). These digestated were formulated to have basic nutrient composition similar to the non-digested fertilizers (**Supplementary Table ST1**).

All samples were collected in sterile 100 mL glass bottles and transported refrigerated to the laboratory as fast as possible. Given the liquid nature of swine slurry and the different origin of samples, the amount of suspended solids was visibly different among them. Therefore, once at the laboratory, samples were vortexed until homogeneity and aliquoted in 2mL Eppendorf tubes. Three subsamples were taken from each original sample (labelled as A1, A2, A3, etc...) and were processed and analysed independently.

In order to harvest the total amount of bacteria present in the matrixes, samples were centrifuged during 10 min at 4ºC at 4000 rpm, discarding the supernatant and using the solid residue for DNA extraction.

2.2 Antibiotic determination in pig slurries and its derivatives

The analytical procedure for antibiotic determination is based on a previously published method (Berendsen et al., 2015). Briefly, 500 mg of sample was submitted to ultrasound assisted extraction with McIlvain-EDTA buffer (pH=4) and acetonitrile followed by protein precipitation with lead acetate, centrifugation (3500 g) and solid-phase extraction (Strata X-RP, 200 mg / 6 mL, Phenomenex, Torrance CA, USA) cleanup. Final determination was performed by Waters Acquity Ultra-Performance Liquid Chromatography™ System (Milford, MA, USA) coupled with Waters TQ-Detector (Manchester, UK) in the multiple reaction mode with two transitions per compound by using a core-shell Ascentis® Express RP-Amide column (10 cm × 2.1 mm, 2.7 µm particle size) (Supelco, Bellefonte, PA, USA). Chromatographic and mass spectrometry conditions are slightly modified from the method described elsewhere ((Tadić et al., 2019)). For procedural reasons, only one sample from each of the sites 1, 2, and 3 was analyzed (samples B, D, and F). The following antibiotics were assessed: azithromycin, ciprofloxacin, clindamycin, chlortetracycline, doxycycline, enrofloxacin, tetracycline, ofloxacin, oxytetracycline, sulfadiazine, sulfamethoxazole, sulfathiazole, sulfapyridine, sulfacetamide, sulfamethazine, sulfamethizole, and trimethoprim. Antibiotic concentrations are expressed in dry or fresh weigh weight basis and are corrected by deuterated surrogate standards (sulfamethoxazole-d4, enrofloxacin-d3, ofloxacin-d3 and clindamycin-d3) spiked to the initial sample. Recoveries were compound and matrix dependant but ranged from 14% for chlortetracycline up to 83% for azithromycin. Limits of detection and quantification ranged from 0.07 and 0.18 ng of azithromycin up to 2.44 and 5.53 ng of lincomycin per g of sample (fresh weight) respectively. The relative standard deviations were below 25% (N=3). Reported results were corrected for surrogate recoveries, and their concentrations were compared to minimum selective concentration (MSC) to estimate their potential risk (Bengtsson-Palme and Larsson, 2016), using the calculated humidity contain of the samples.

2.3 Molecular methods

DNA extraction was performed employing the QIAamp Power Fecal Pro DNA kit (Qiagen, Hilden, Germany) using a maximum of 0.25g of sample solid residue, after centrifugation. Total DNA was eluted in 100 µl and concentration and quality was determined in a NanoDrop Spectrophotometer 8000 (Thermo Fisher Scientific, Inc). Extracted DNA samples were stored at −20 °C.

Primers for *int*I1, *sul*1, *tet*M, *qnr*S1, *mec*A, bla_{TEM}, $bla_{CTX\text{-}M\text{-}32}$, $bla_{OXA\text{-}58}$ and bacterial 16S rDNA sequences are listed in **Supplementary Table ST2.** Their quantification was performed by qPCR reactions in a LightCycler 480 II (A F. Hoffmann–La Roche AG, Inc) on 96-well plates using 20 µL reactions. Optimal primer concentration was 200 nM for bla_{TEM} and 300 nM for the rest of genes. A fixed dilution of 5 ng/µl of raw DNA extract was used. All qPCR assays were run as technical duplicates along with the quantification curve to reduce potential variability between assays. Melting curves were programmed to confirm amplification specificity. Dynamo ColorFlash SYBR Green (Thermo Scientific, Inc.) chemistry was used for *tet*M, *mec*A, and $bla_{OXA\text{-}58}$ qPCR quantifications, while all the other genes were

quantified with LightCycler 480 SYBR Green I Master (A F. Hoffmann–La Roche AG, Inc). The amplification protocol was performed following the manufacturer guidelines, and different annealing temperatures were used as indicated in **Supplementary Table ST2.**

2.4 Quantification and normalization methods

Absolute quantification of all qRT-PCR amplicons was carried out with four plasmid vectors used as standards. Purified DNA samples from the plasmid pNORM1 were used as standards for the quantification of 16S rDNA gene, *int*I1, *sul*1, *qnr*S1, *bla*$_{TEM}$ and *bla*$_{CTX-M-32}$ (Rocha et al., 2020)(Gat et al., 2017), while three different pUC19 plasmids were used for *tet*M, *mec*A and *bla*$_{OXA-58}$ (Laht et al., 2014; Szczepanowski et al., 2009; Tamminen et al., 2011) (**Supplementary Table ST2**). DNA plasmid purification was performed using the kit QIAprep Spin Miniprep Kit (Qiagen) Total DNA concentration was measured in a NanoDrop Spectrophotometer 8000 (Thermofisher Scientific, Inc). Gene copy number per µL of each standard was determined by combining the plasmid size and the DNA concentration, in the DNA Copy Number and Dilution Calculator algorithm from Thermo Fisher Scientific, Inc (https://www.thermofisher.com/us). Quantification curves for all genes were generated in each run, from 10-fold serial dilutions of the corresponding initial standards, amplified by triplicate. Negative controls using nuclease free water instead of template were also included. ARGs copy numbers per µL for each sample were calculated by extrapolating their Ct value from the standard curves and normalized in relation to the processed fresh weight of swine slurry (ARGs copies/g). Quantification limits (LOQs) for each gene were set as the minimum concentration of plasmid (copies/µL) that can be detected without interference from the negative control. LOQs are collected on **Supplementary Table ST2.**

2.5 16S library preparation and sequencing

Bacterial communities present in the swine slurry samples were determined by 16S sequencing analysis. An aliquot of each extracted sample (36 samples) was sent to Novogene Europe (Cambridge, UK) where concentration and purity were monitored on 1% agarose gels. After passing this first quality control, DNA was diluted to 1ng/µL using sterile water, and 16S rRNA genes of distinct regions (16SV4/16SV3/16SV3-V4/16SV4-V5, 18S V4/18S V9, ITS1/ITS2, Arc V4) were amplified using specific primers (e.g. 16S V4: 515F-806R) with a barcode for amplicon generation. All PCR reactions were carried out with Phusion® High-Fidelity PCR Master Mix (New England Biolabs). Quality of PCR products was checked by electrophoresis on 2% agarose gels, and those samples with a clear band between 400-450bp were selected for the following steps. PCR products were mixed at equal density ratios and purified by Qiagen Gel Extraction Kit (Qiagen, Germany). Sequencing libraries were generated using NEBNext Ultra DNA Library Pre ®Kit for Illumina, following manufacturer's recommendations, and index codes were added. Library quality was assessed on the Qubit@ 2.0 Fluorometer (Thermo Scientific) and Agilent Bioanalyzer 2100 system. Sequencing was carried out on an Illumina platform and 250 bp paired-end reads were generated. Quality control parameters appear in **Supplementary Table ST3**.

2.6 Analysis of bacterial communities and relationship with ARGs

Sequences were analysed with the Uparse software (Uparse v7.0.1001, http://drive5.com/uparse/) and assigned to the same Operational Taxonomic Units (OTUs) if they had a ≥ 97% similarity. To annotate the taxonomic information the GreenGene Database (http://greengenes.

lbl.gov/cgi-bin/nph-index.cgi) was used based on the RDP classifier algorithm (Version 2.2, http://sourceforge.net/projects/rdp-classifier/). Phylogenetic OTUs study was conducted in MUSCLE (Version 3.8.31, http://www.drive5.com/muscle/)). OTUs abundance was normalized using the sequence number of the sample with the least sequences. Analyses for α-diversity and β-diversity analysis were performed with QIIME (Version 1.7.0). The significance of difference amongst the structure of microbial communities was analysed by a non-metric multi-dimensional scaling (NMDS) with the Bray–Curtis dissimilarity index (Bray and Curtis, 1957). Correlations between bacteria composition and AB resistance were analysed by Spearman's correlations between OTUs counts and genetic elements (ARGs and *int*I1). The false positive discovery rate (FDR) correction was set at $p<0.05$ (Benjamini and Hochberg, 1995), using the psych R package. The global results from the taxonomic analysis are shown in **Supplementary Table ST4**.

2.7 Data analysis for ARGs and *int*I1

The analysis of the absolute abundance of ARGs was performed in the R environment (version 3.6.1; http://www.rproject.org/). Normality and homogeneity of the variances were checked using the Shapiro-Wilk and Levene tests, respectively. Since it was possible to assume a normal distribution, a one-way ANOVA plus Tukey' HSD post-hoc correction for multiple tests was performed with the car R package. Significance levels were set at $p \leq 0.05$. Heatmap and hierarchical clustering were performed using the function *heatmap2*, from the *ggplot2* R package[1].

3. Results

3.1 ARG distribution

All analysed sequences were detected in all samples, although in some cases values were under the limit of quantification, LOQ (**Figure 1,** data in **Supplementary table ST5**; values below the LOQ are marked with red asterisks). Abundance values (in copies per g of sample) typically varied around one order of magnitude among samples, in a pattern essentially reflecting the 16S rDNA abundance data. This suggests that most of the observed variation was related to the total bacterial abundance present in each sample (**Figure 1**). The most abundant sequences corresponded to *tet*M, *int*I1, and *sul*1, whose levels were above LOQ for all samples and that reached values of 10^{10}-10^{11} copies per gram of some samples (**Figure 1**). These values were comparable to the total amount of 16S rDNA copies calculated for many samples, suggesting that a large fraction of bacterial cells harboured at least one of these genetic elements.

Analysis of ARG prevalence, that is, the ratio between ARG and 16S rDNA copy abundance data, suggest that more than 90% of bacterial cells were positive for *tet*M (and, presumably, tetracycline resistant) in some samples, and around 1 % of them were positive for *int*I1 and *sul*1 (magenta and red sectors in **Figure 2**). Note also the very similar distribution of *int*I1 and *sul*1 among samples, a phenomenon already observed in comparable analyses of soil and plant samples from the same region, but with no direct relation to the type of fertilizers analysed here (Cerqueira et al., 2019b). The rest of sequences were found at much lower prevalence values, bellow 0.1%), including ARGs from the ß-lactamase group (bla_{TEM}, $bla_{CTX\text{-}M\text{-}32}$, and $bla_{OXA\text{-}58}$, by decreasing order of prevalence), and the quinolone- and metillicine resistance genes *qnr*S1 and *mec*A.

Hierarchical clustering grouped samples from a

[1] https://CRAN.R-project.org/package=gplots

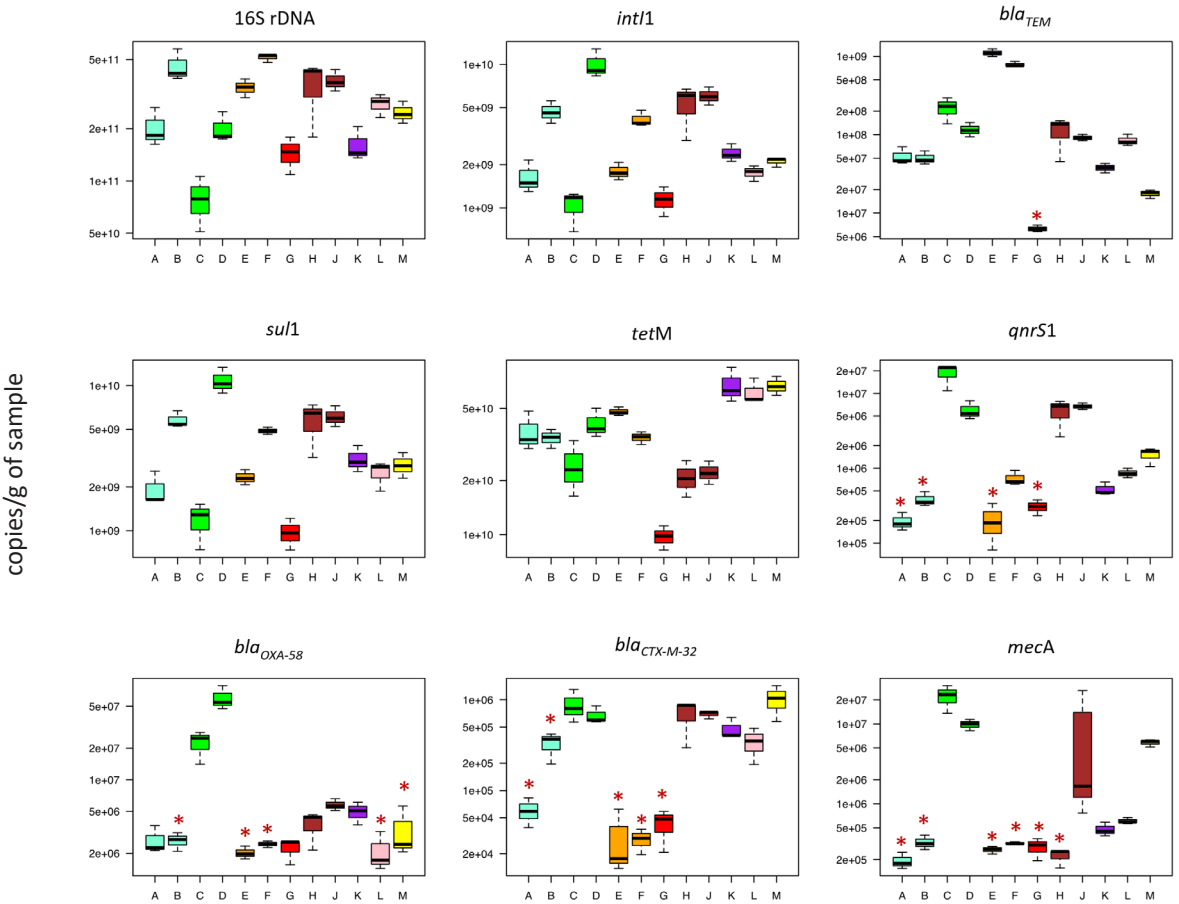

Figure 1. Absolute abundance of the different genetic elements in all samples. Boxes are color-coded by their origin (see *Table 1*). Data are expressed as copies of each sequence per g of sample. Thick black line, boxes and whiskers represent average, first-to third percentiles and total distribution of samples, respectively. Red asterisks correspond to distributions that include estimates from values under the limit of quantitation. Original data in *Supplementary Table ST6*.

same facility in most cases (colours in the column sidebar in **Figure 2,** see **Table 1**). In general terms, sites 2 (samples C y D) and 3 (Samples E and F, green and orange sidebar colours in **Figure 2**) appeared as divergent from the rest. These data suggest that the prevalence of different ARGs (and, presumably, the selective pressure imposed on the respective microbiomes) varied from one facility to another.

3.2 Correlations between ARG prevalence and AB levels in pig slurry samples and digestates

Fluoroquinolones, tetracyclines and sulfonamides were detected at concentrations ranging from <LOD up to 21,048 ng/g of fresh weight (**Supplementary Table ST6**). These values are consistent with the veterinary antibiotic usage in Spain (European Medicines Agency, 2019) and similar to the ones previously reported characteristics for pig slurries with medium to low antibiotic content (Wohde et al., 2016). Concentrations were dependent on the farm management and the production cycle being fatting and transition piglets, the samples that exhibited the highest concentrations (see **Table 1**). Fluoroquinolones (enrofloxacin or ciprofloxacin) and tetracyclines (tetracycline and oxytetracycline) were the most abundant ABs (**Supplementary Table ST6**). When these absolute concentration values were compared to the corresponding MSC values, enrofloxacin and/or

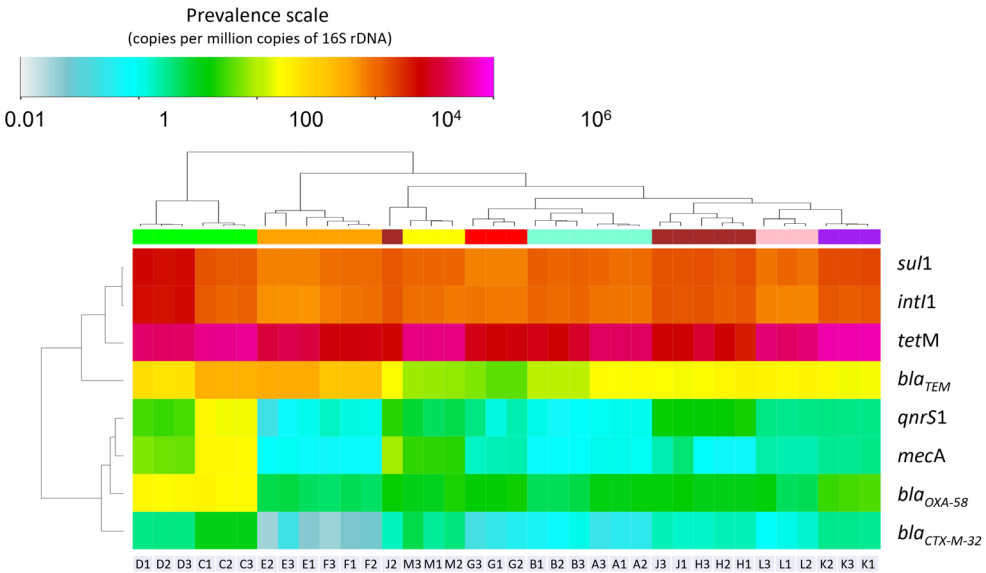

Figure 2. Heatmap of the relative prevalence of genetic elements among samples, expressed as copies of each ARG per million copies of 16S rDNA (color scale on top of the figure), and log transformed for clustering. Colors in the column sidebar correspond to sample origin, as in *Figure 1*.

ciprofloxacin showed concentrations (expressed as µg/L values) more than 1000 times higher than the reported MSC in 5 out of the 10 analyzed samples (Samples A and E were not analyzed, **Figure 3A**, salmon sectors), whereas tetracycline and oxytetracycline concentrations surpassed 100 times their MSC values in one and two samples, respectively (**Figure 3A**). We concluded that fluoroquinolones and, to a lesser extend, tetracyclines, may exert a significant selective pressure for AB resistance bacteria.

Fluoroquinolone concentration and the prevalence of the quinolone-resistance *qnr*S1 gene showed a significant correlation (**Figure 3B**, p=0.04, Spearman correlation). Note that in this graph, *qnr*S1 is expressed as copies per million of 16S rDNA copies, a measure of the potential selective pressure. Note that samples from Sites 2 (C, D) and 5 (H, J) showed the highest Fluoroquinolone and *qnr*S1 loads, whereas sample L was the only case in which the two parameters did not correlate (**Figure 3B**). No correlation was observed between total tetracycline concentrations and *tet*M levels (not shown), likely due to the very high prevalence of the ARG in all samples (not shown, see **Figure 1**).

3.3 Bacterial taxa distribution

Analysis of the bacterial taxa composition of the different samples revealed a relatively uniform composition, at least at the Phylum/Class levels (**Figure 4**, **Supplementary Table ST7**). Firmicutes appeared as the prevalent bacterial Class in all samples, totalling more than 50% of total reads in many of them. Almost 50% of the OTUs classified in this class belonged to the Clostridiae Family, being Ruminococcaceae the second Firmicutes Family in order of importance (**Supplementary Table ST7**). Other bacterial Families with strong representation in the dataset were Corynebacteriaceae (Actinobacteria), Porphyromonadaceae (Bacteroidetes), and Spirochaetaceae (Spirochaetes), all of them with more than 100,000 reads in the total dataset (**Supplementary Table ST7**). Three groups of Archea were also detected, corresponding to the

A

Antibiotic	Samples									
	B	C	D	F	G	H	J	K	L	M
Azithromycin	3	<1	<1	<1	19	<1	<1	<1	<1	<1
Enrofloxacin	<1	3744	10594	<1	<1	2234	5159	<1	20390	94
Ciprofloxacin	18	670	4188	22	163	218	378	<1	593	31
Tetracyline	8	<1	4	<1	9	182	95	<1	<1	<1
Doxyciline	<1	<1	<1	<1	<1	<1	<1	<1	<1	<1
Oxytetracycline	<1	<1	927	<1	353	3	8	<1	<1	<1
Sulfadiazine	<1	<1	<1	<1	<1	<1	<1	<1	<1	<1
Sulfametoxazole	<1	<1	<1	<1	<1	<1	<1	<1	<1	<1
Lincomycin	<1	<1	<1	61	81	<1	<1	10	87	97

B

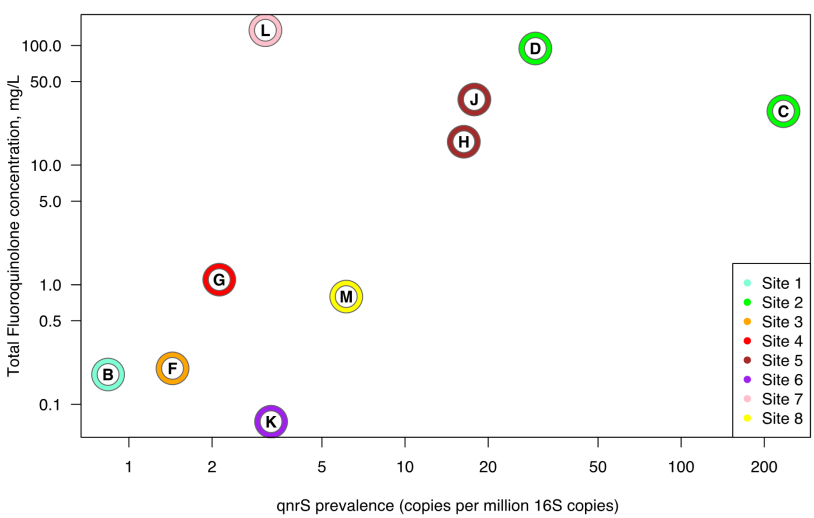

Figure 3. A) Antibiotic loads, expressed as fold minimum selective concentration (MSC) equivalents. Non-detected or below MSC values are expressed as "<1" sign. Colors indicate the relative concentration of each given antibiotic in each particular sample, from pale green (low concentration) to salmon (high concentration). B) Double-log plot of qnrS prevalence values (expressed as copies per million 16S rDNA sequences) and fluoroquinolones total loads (expressed as the sum of Ciprofloxatin and Enrofloxacin, in µg/L). Samples are labelled and color-coded as in *Figure 2*.

Classes Methanomicrobia, Methanobacteria, and Thermoplasmata, all of them belonging to the Phylum Euryarchaeota (**Supplementary Table ST7**).

The distribution of the different OTUs among samples analysed by NMDS showed a clear separation between taxonomic groups, and of the sites of origin (**Figure 5**). At the OTU level ("species" in the NMDS terminology), note the accumulation of Clostridia groups at the center of distribution (**Figure 5**, golden dots), whereas other groups (Euryarchaeota, Spirochaetes, Bacteroidetes, Cloacimonetes) appeared relegated to the periphery of the plot, indicating their uneven distribution among samples (**Figure 5**). Samples C and D (Site 2) and E and F (Site 3) appeared separated one each other and both from the rest of samples, which constitute a relatively loose cluster (**Figure 5**). This distribution reminds the clustering of samples defined by their relative content in ARG genes in **Figure 2**. We interpret these similarities in distribution as an indication

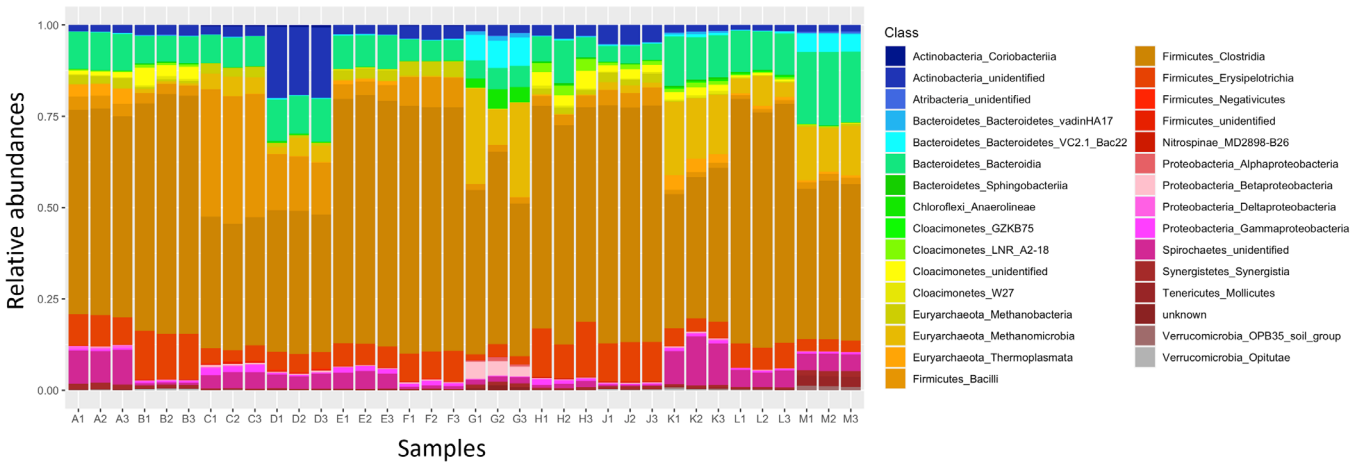

Figure 4. Bacterial composition of the different samples, aggregated at the Class level. Data are expressed as percentages of the total number of reads obtained for each sample. Note that Euryarcheota groups belong to the Archea Kingdom.

of the influence of the taxonomic composition in the relative prevalence of ARGs.

A more detailed image of the relative distribution of significant taxa among samples is provided by the comparison of taxa (species or genera, if the species was unknown) classified as "top 10" (that is, among the 10 most abundant taxa) in at least one of the samples (**Figure 6**). Hierarchical clustering of this data defines several groups similar to the ones observed in the previous analyses, as the grouping of samples C and D on one side and K and M on the other one. However, it is characteristic of this analysis the specific differentiation of G samples (**Figure 6**). In general, the graph confirms the high prevalence of Firmicutes species, but divided in several subgroups. A Clostridia group, constituted by the genera Clostridium, Fastidiosipila, Terrisporobacter, and Turicibacter appear at the bottom of the graph as very prevalent in most samples. In contrast, members of the Bacillus group (Lactobacillus, Enterococcus, Trichococcus) appear as much less evenly distributed among samples, as well as other Clostridia, like Alkaliphilus, Tissierella, the species *Clostridium butyricum* and an unidentified member of the Christensenellaceae family (**Figure 6**). The archaeal Phylum Euryarchaeota appears forming a clear cluster with high prevalence in samples K and M, and which includes the genera Methanoculleus, Methanospirillum, Methanosaeta, and a Methanoplasma candidate (**Figure 6**).

3.4 Correlation between ARG prevalence and bacterial taxa composition

Bivariate analyses identified 515 taxonomic entities whose relative abundances were significantly correlated to the prevalence of at least one of the analysed ARGs, 139 from them identified at least at the Species level and 248 only at the Genus level (**Supplementary Figure SF1**). Taxonomic analysis of the 309 species (including those entities identified only at the genus level) with positive correlations with the prevalence of at least one of the different ARG revealed taxon profiles compositions very different among them and clearly differentiated the general taxon composition of the whole samples (**Figure 7A**, compare to **Figure 4**). For example, prevalence values of *int*I1, *sul*1, *bla*$_{OXA-58}$, *qnr*S1, and *mec*A correlated with a large fraction of Actinobacteria and Bacteriodetes group at the upper part of

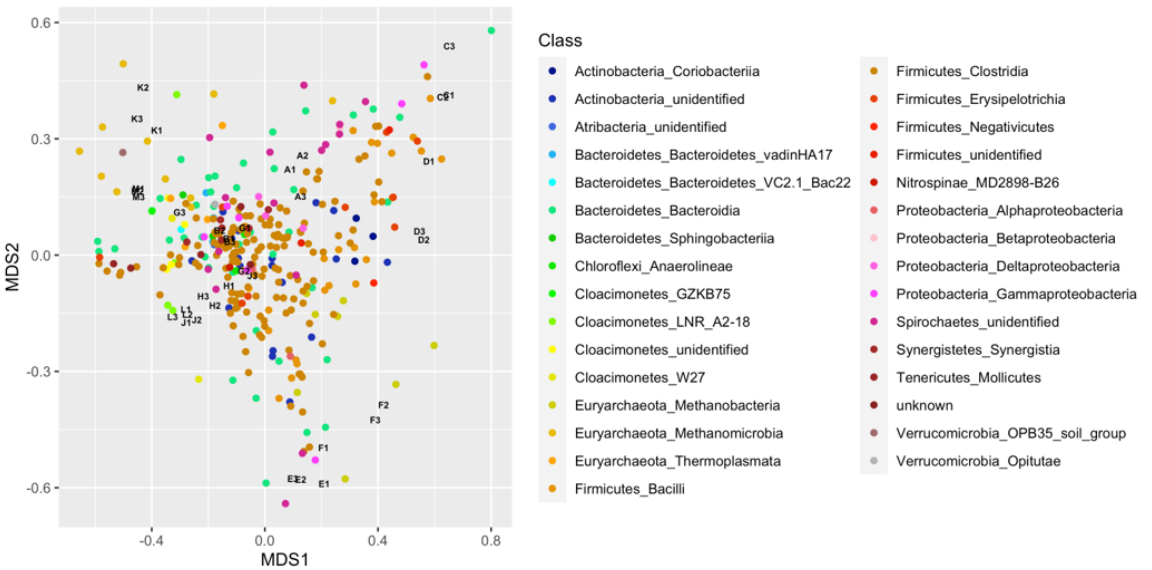

Figure 5. NMDS (non-metric dimensional scaling) analysis of the distribution of bacterial taxa, aggregated at the Class level. Only Classes with more than 1000 reads in the whole dataset (334 Classes in total) were included in the analysis. The relative position of the samples are indicated by their corresponding label. Note that the Euryarcheota groups belong to the Archea Kingdom.

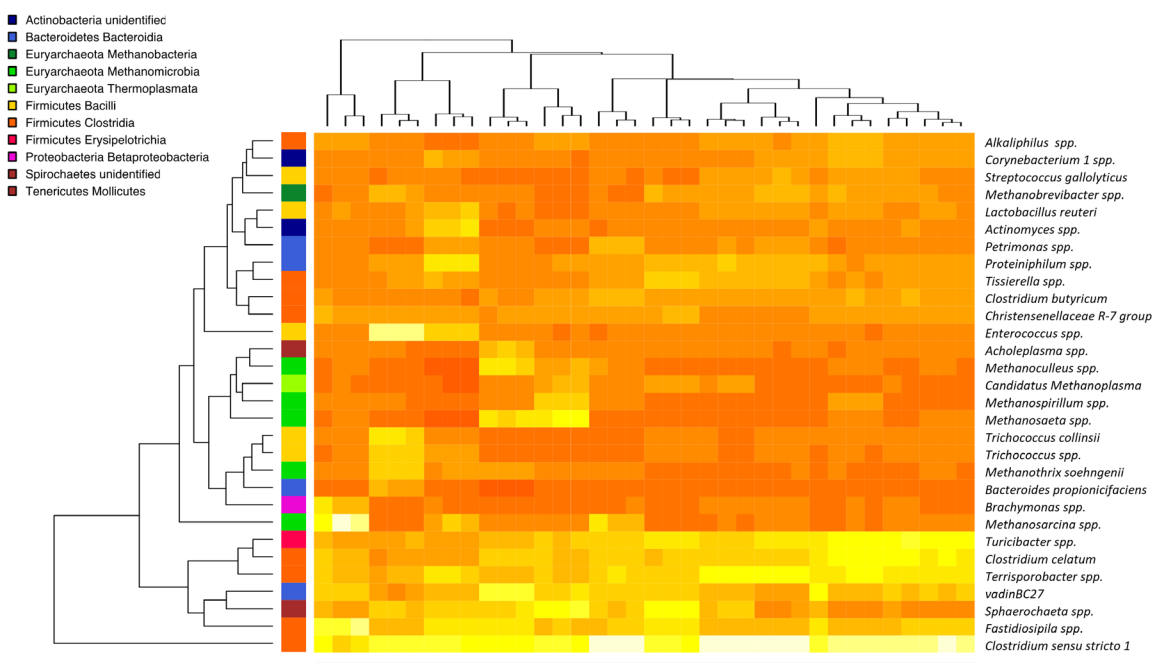

Figure 6. Relative abundances of microbial species among samples. Only species (or genera aggregates when no species was identified) in the top 10 list for at least one samples are included. Colors in the sidebar on the left indicate the corresponding Phyla. Note that one of the groups (Euryarcheota) belongs to the Archea Kingdom.

A

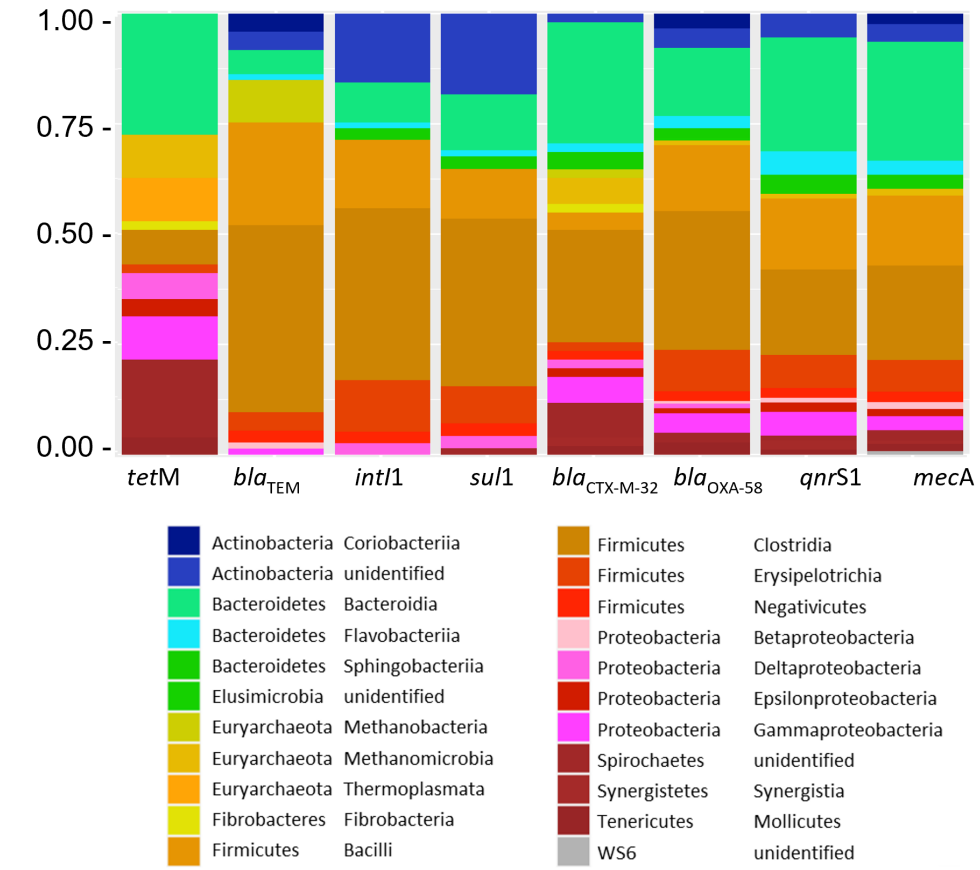

the graph, whereas high prevalence of *tet*M and, in a lesser extent, *bla*$_{OXA-58}$, showed, in addition, positive correlations with different Proteobacteria and Spirochaetes groups. Only bacterial groups positively correlated to *bla*$_{TEM}$ showed a Class distribution similar to that of the whole dataset, with a predominance of Clostridia and Bacilli (**Figure 7A**).

A suitable interpretation of the difference on taxon profiles among bacterial groups associated to high prevalence of the different ARGs is that they actually correspond to specific subpopulations of bacteria found at different proportions among samples. The network in **Figure 7B**, which shows the correlations at the single species level, supports that interpretation. The figure shows a close cluster that includes *int*I1, *sul*1, *bla*$_{OXA-58}$, *qnr*S1, and *mec*A, probably indicating their correlation to a common subset of bacterial species, whereas *bla*$_{TEM}$ and *tet*M appeared as substantially differentiated from the rest. This clustering strongly resembles the one observed in **Figure 2**, suggesting that the differences in ARG loads were related to the bacterial profile of the samples. Note that this similarity extends to some specific details, like the close clustering between *int*I1 and *sul*1, and the relatively differentiated position of *bla*$_{OXA-58}$ (compare **Figures 2** and **7B**).

4. Discussion

According to the last UN Global Environmental

B

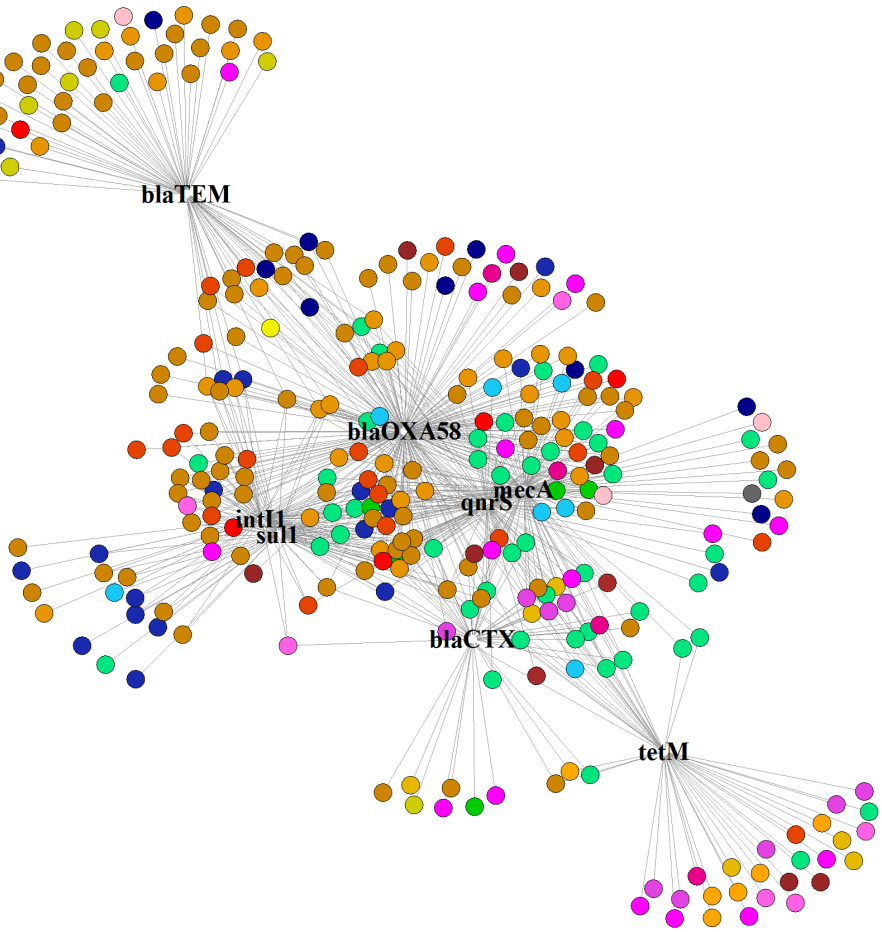

Figure 7. Correlation between bacterial population and ARG prevalence. **A)** Taxon composition, at the Class level, of the 307 bacterial species with significant positive correlations with the different ARG abundances. **B)** Network constructed from a contingency matrix between ARGs and the bacterial species with positive correlations to them. Each dot corresponds to a bacterial species, colored-coded according their adscription to bacterial Classes .

Outlook, "Human illnesses and deaths due to antibiotic- and antimicrobial-resistant infections are increasing rapidly and are projected to become a main cause of death worldwide by 2050" (Glob. Environ. Outlook – GEO-6 Heal. Planet, Heal. People, 2019). This grim prediction points to ARB and ARGs as main pollutants for water sources, and call for the application of effective policies for its control in water bodies worldwide (Glob. Environ. Outlook – GEO-6 Heal. Planet, Heal. People, 2019). The main concern is the capacity of the released on ARB and ARGs reach the human food and water supplies, therefore contributing to the widespread onset of pathogenic bacterial strains increasingly recalcitrant to medical treatment with the existing antibiotics (WHO, 2014). In previous works, we have found evidence that AB and ARGs can move from agricultural soils to edible parts of commercial crops, and that their presence and concentration is soils and plants depends upon farming practices (Cerqueira et al., 2019b, 2019a; Manaia et al., 2018). Among these practices, organic fertilizers are particularly relevant, due to the high bacterial loads they carry. This work was intended to assess the potential contributions of using as fertilizers actual swine slurries and of their digestates from commercial pig farms.

Our results show high loads of particular ARGs (notably, *sul*1 and *tet*M) in essentially all samples analysed. These two ARGs provide resistance against two of the antibiotic families found in the same samples, sulfonamides and tetracyclines. There is therefore little doubt that their prevalence in the swine slurry is related to their veterinary use. Whether or not the use of

antibiotics favoured the observed high prevalence of the integron *int*I1 (and, presumably, of other components of HGT mechanisms) is unclear, but it is at least presumable. The fact that the ARG profiles in the different samples varied from one facility to another also supports the conclusion that the handling of the animals and/or of their wastes influenced ARG loads that may end into the agricultural soils when these farm residues are used for fertilization after different levels of processing.

The total bacterial loads (or its proxy, abundance of 16S rDNA sequences) appeared as a relatively minor factor on ARG loads among the different samples. Controlling by the different bacterial loads, ARGs with the highest prevalence, understood as the ratio between their copy number to the total 16S rDNA copies, differed substantially among farms. Sites 1,4, and 5 showed a general lower ARG prevalence than the rest, whereas Site 3 only showed a significant prevalence of *bla*$_{TEM}$, an ARG already widespread in agricultural soils from the area and elsewhere (Cerqueira et al., 2019c). Site 2 showed high loads of all ARGs, although the highest levels of *tet*M corresponded to Sites 6 and 7. The fact that all samples come from operating, commercial facilities prevent us to control, or even having a perfectly defined picture of, the veterinarian and animal handling procedures applied in each of them. However, the data reinforces the hypothesis that animal handling and, perhaps, farm conditions, may have a fundamental role in determining the load of ARGs being released from the farm, either by the use of the slurry as fertilizers, or when disposed as waste or runoffs. This also suggests that the potential selective pressure associated to the fertilizers may be enough to favor the soil colonization by antibiotic-resistant bacteria, either from the same fertilizers or from the pre-existing soil microbial community.

While *sul*1 and *tet*M appeared as generally widespread among slurry microbiomes, the relatively minor *qnr*S1 gene showed the strongest evidence for selective pressure. Fluoroquinolones were by far the antibiotic family with higher loads compared to their MSC values, and, with a single exception, sites with higher fluoroquinolone loads presented higher *qnr*S1 prevalence and vice versa. It is tempting to speculate that the past use and abuse of more "classical" ABs, like tetracyclines and sulfonamides, lead to the presence of their corresponding resistance gene in pigs' guts, even in the absence of the AB themselves. For example, sul1 and *bla*$_{TEM}$ have been observed in microbiomes from agricultural and forest soils, even in those that have not been amended for decades (Cerqueira et al., 2019c). However, genes conferring resistance to a relative new antibiotic family, like fluoroquinolones, may not be so widespread yet, and their prevalence may still depend on continuous selective pressure. The unescapable conclusion is that, should fluoroquinolones become more and more usual in farm animal treatment, the corresponding resistance genes would also become part of the "general" resistome of the gut microbiomes, and therefore independent from the actual presence of the antibiotic. This has great implications for the spread of prescription AB-related ARGs in the microbiome of the agricultural soils, eventually reaching crops and consumers.

Bacterial composition of the different samples revealed the expected predominance of anaerobic bacterial taxa, with a strong contribution of the Clostridia group. This analysis has been performed at Phyla, Family and Genus/species level, and all three levels revealed a very consistent picture of a major core taxa, present in all samples, and mainly composed by Clostridia, with minor contributions from Bacteroidetes and Spirochaetes groups. The relative contributions from rest of major taxa configured a sample distribution resembling to the one observed for the ARG loads, with samples from Sites 2, 3, and, partially, 6 and 7, appearing as clearly separated from the rest. Samples from Site

2 show significantly high levels of Actinobacteria and Bacilli groups. Another taxonomic group contributing to the separation between samples is the archaeal Euryarchaeota Phylum, basically due to the presence of methanogenic species. Although these differences are difficult to interpret, we propose that they may reflect the state of "maturation" of the initial swine slurry, being the loss of typical enterobacteria (Proteobacteria, Lactobacillus, Actinobacteria) and the increase on the levels of methanogenic taxa indicative for more processed samples. The Taxon distribution we observed in our samples is similar to previously described swine fecal microbiomes, dominated by Firmicutes and Bacteriodetes groups (Lamendella et al., 2011; Zhang et al., 2019). It is also similar to the distribution observed for wastewater lagoons in Chinese farms, in which methanogenic Archea also appear (He et al., 2019). The same study in Chinese farms also shows the modulation of the microbiome profile from farm wastes after different treatment procedures (He et al., 2019). Similar results, albeit showing significantly different microbiome profiles, have been reported in dairy farms (Pandey et al., 2018; Zhang et al., 2020). We consider these data as demonstrating that the handling of farm wastes is instrumental in modulating their microbiome profile and, consequently, their potential to represent a risk for exposed environments and human populations (Zhang et al., 2020).

Correlation analyses showed a close interdependence between the loads in different ARGs and the prevalence of some particular bacterial taxonomical groups. This was more evident for the ARGs found at higher loads and that represent a higher potential risk of contamination for the receiving soils. For example, *tet*M relative abundance values showed strong correlations with bacterial species from the Phyla Spirochaetes and Proteobacteria, whereas the prevalence of *sul*1 (and of *int*I1) correlated with different Actinobacteria group. These taxa constituted a relatively small fraction of the microbiome for most samples, and they are not particularly relevant in the swine gut microbiome composition (Lamendella et al., 2011). It is interesting to note that Proteobacteria and Actinobacteria are more abundant in human gut than in swine's, a circumstance that can influence the transferability of these ARGs to the gut of potential human consumers (Lamendella et al., 2011).

Assessment of the risk associated to the spread of ARGs into agricultural products is hampered by a number of uncertainties. There are several steps between the ARG input into the soil, via fertilization or fertigation procedures, and the guts of the final human or animal consumers. Analysis of the transmission from soils and irrigation water to edible part showed that from 1 to 0.01% of the ARG loads present in the soil may be ultimately found in edible plant parts (Cerqueira, Victor Matamoros, et al., 2019; Cerqueira, Víctor Matamoros, J. Bayona, et al., 2019; Cerqueira, Víctor Matamoros, J. M. Bayona, et al., 2019). These values depend on the type of plant, the particular part of the plant being used in food products (leaves, fruits, seeds, roots), and, very likely, on the agricultural practices used in each plot (organic, extensive, fertigation, etc.) The rate of transmission of ARGs from food to the consumer's gut, the ability of these ARGs to propagate in it, either by propagation of intake bacteria or by HGT, and the actual health risk posed by the existence of this external source of ARGs is much less known, and most likely depends on the selective pressure posed by the use of antibiotics by the consumer, either human or animal. Independently of the intervening rates of transmission, the ARG loads is soil appear as the seminal parameter from which the rest of calculations should be made. Therefore, it is important to decide whether or not a particular agricultural practice may represent a significant increase in soil ARGs loads. Our results suggest that application of realistic amounts of organic fertilizers from farm wastes may result

in significant amounts of ARGs loads for the receiving soils, increasing the basal ARG levels by several orders of magnitude. Our data also provides some directions to reduce this excessive loads.

The most important action to reduce ARG loads in organic fertilizers is to do so from the origin. This implies a very careful control of the use of antibiotics in the farm. Should our conclusion that the amount of AB present in the slurry is enough to add selective pressure to the receiving soils prove to be correct, the limitation of AB usage would become a most pressing issue. This may be especially crucial for antibiotics of recent incorporation, to prevent the corresponding resistance genes from entering in the gut's and soil's core resistomes.

A second possible level of ARG load control is to reduce the total loads of bacteria in the final fertilizer composition. In our samples, the handling of the initial slurries affected very little the total bacterial loads, and procedural systems (temperature treatments, filtrations, etc.) able to reduce them should be explored and incorporated to the routine processing of organic fertilizers.

Finally, farm wastes may likely be processed in conditions that do not favour the persistence of typical gut microbes. For example, high prevalence in Clostridia and in methanogenic bacteria appear to be negatively correlated to ARG loads, suggesting that controlling the temperature and oxygen levels of the digestates may have a significant influence on the final ARG levels.

While reducing the inputs of ARG and AB arriving in the soils is likely to be beneficial for the whole process, there is still a missing factor, which is the probability of the input ARG to actually colonize the soils. This is a main aspect that has to be addressed in future studies.

5. Conclusions

The use of manure as fertilizer, after its due processing, has many economic and environmental benefits. However, the practice should not result in a significant contamination of receiving soils by potentially harmful biological or chemical agents, in the form of ARGs/ARB, pharmaceuticals or pathogens. Our results indicate that the control of AB use in the farms is the most straightforward measure to limit the arrival of ARGs (and presumably, ARB) and ABs in agricultural fields, being the processing of the original slurry a subsequent, valuable aspect to consider. The development of these strategies is becoming an urgent need that has to be addressed before widespread adverse economic and health consequences of the presence of ABs, ARGs and ARB in agricultural products may appear.

Acknowledgements

This work was supported by a grant from the Spanish Ministry of Science, Innovation and University (RTI2018-096175-B-I00) and from the LIFE Program of the European Union (LIFE17 ENV/ES/000439). CSL was supported by an FI predoctoral fellowship from the Generalitat de Catalunya.

Bibliography

Beckers, B., Op De Beeck, M., Thijs, S., Truyens, S., Weyens, N., Boerjan, W., Vangronsveld, J., 2016. Performance of 16s rDNA primer pairs in the study of rhizosphere and endosphere bacterial microbiomes in metabarcoding studies. Front. Microbiol. 7, 650. https://doi.org/10.3389/fmicb.2016.00650

Bengtsson-Palme, J., Larsson, D.G.J., 2016. Concentrations of antibiotics predicted to select for resistant bacteria: Proposed limits for environmental regulation. Environ. Int. 86, 140–149. https://doi.org/10.1016/j.envint.2015.10.015

Berendonk, T.U., Manaia, C.M., Merlin, C., Fatta-Kassinos, D., Cytryn, E., Walsh, F., Buergmann, H., Sorum, H., Norstrom, M., Pons, M.-N., Kreuzinger, N., Huovinen, P., Stefani, S., Schwartz, T., Kisand, V., Baquero, F., Luis Martinez, J., 2015. Tackling antibiotic resistance: the environmental framework. Nat. Rev. Microbiol. 13, 310–317. https://doi.org/10.1038/nrmicro3439

Berendsen, B.J.A., Wegh, R.S., Memelink, J., Zuidema, T., Stolker, L.A.M., 2015. The analysis of animal faeces as a tool to monitor antibiotic usage. Talanta 132, 258–268. https://doi.org/10.1016/j.talanta.2014.09.022

Bertini, A., Poirel, L., Bernabeu, S., Fortini, D., Villa, L., Nordmann, P., Carattoli, A., 2007. Multicopy bla(OXA-58) gene as a source of high-Level resistance to carbapenems in Acinetobacter baumannii. Antimicrob. Agents Chemother. 51, 2324–2328. https://doi.org/10.1128/aac.01502-06

Cerqueira, F., Matamoros, V., Bayona, J., Elsinga, G., Hornstra, L.M., Pina, B., 2019a. Distribution of antibiotic resistance genes in soils and crops. A field study in legume plants (Vicia faba L.) grown under different watering regimes. Environ. Res. 170, 16–25. https://doi.org/10.1016/j.envres.2018.12.007

Cerqueira, F., Matamoros, V., Bayona, J., Piña, B., 2019b. Antibiotic resistance genes distribution in microbiomes from the soil-plant-fruit continuum in commercial Lycopersicon esculentum fields under different agricultural practices. Sci. Total Environ. 652, 660–670. https://doi.org/10.1016/j.scitotenv.2018.10.268

Cerqueira, F., Matamoros, V., Bayona, J.M., Berendonk, T.U., Elsinga, G., Hornstra, L.M., Piña, B., 2019c. Antibiotic resistance gene distribution in agricultural fields and crops. A soil-to-food analysis. Environ. Res. 177, 108608. https://doi.org/10.1016/j.envres.2019.108608

European Medicines Agency, 2019. Sales of veterinary antimicrobial agents in 31 European countries in 2017 (EMA/294674/2019).

Forsberg, K.J., Patel, S., Gibson, M.K., Lauber, C.L., Knight, R., Fierer, N., Dantas, G., 2014. Bacterial phylogeny structures soil resistomes across habitats. Nature 509, 612–616. https://doi.org/10.1038/nature13377

Gillings, M.R., Krishnan, S., Worden, P.J., Hardwick, S.A., 2008. Recovery of diverse genes for class 1 integron-integrases from environmental DNA samples. FEMS Microbiol Lett 287, 56–62. https://doi.org/10.1111/j.1574-6968.2008.01291.x

Global Environment Outlook – GEO-6: Healthy Planet, Healthy People, 2019. , Global Environment Outlook – GEO-6: Healthy Planet, Healthy People. Cambridge University Press, Nairobi. https://doi.org/10.1017/9781108627146

Goss, M.J., Tubeileh, A., Goorahoo, D., 2013. A Review of the Use of Organic Amendments and the Risk to Human Health, in: Advances in Agronomy. Academic Press Inc., pp. 275–379. https://doi.org/10.1016/B978-0-12-407686-0.00005-1

He, L.Y., He, L.K., Liu, Y.S., Zhang, M., Zhao, J.L., Zhang, Q.Q., Ying, G.G., 2019. Microbial diversity and antibiotic resistome in swine farm environments. Sci. Total Environ. 685, 197–207. https://doi.org/10.1016/j.scitotenv.2019.05.369

Hembach, N., Schmid, F., Alexander, J., Hiller, C., Rogall, E.T., Schwartz, T., 2017. Occurrence of the mcr-1 Colistin Resistance Gene and other Clinically Relevant Antibiotic Resistance Genes in Microbial Populations at Different Municipal Wastewater Treatment Plants in Germany. Front. Microbiol. 8, 1282. https://doi.org/10.3389/fmicb.2017.01282

Johnning, A., Moore, E.R.B., Svensson-Stadler, L., Shouche, Y.S., Larsson, D.G.J., Kristiansson, E., 2013. Acquired Genetic Mechanisms of a Multiresistant Bacterium Isolated from a Treatment Plant Receiving Wastewater from Antibiotic Production. Appl. Environ. Microbiol. 79, 7256–7263. https://doi.org/10.1128/aem.02141-13

Koch, B.J., Hungate, B.A., Price, L.B., 2017. Food-animal production and the spread of antibiotic resistance: the role of ecology. Front. Ecol. Environ. 15, 309–318. https://doi.org/10.1002/fee.1505

Lamendella, R., Santo Domingo, J.W., Ghosh, S., Martinson, J., Oerther, D.B., 2011. Comparative fecal metagenomics unveils unique functional capacity of the swine gut. BMC Microbiol. 11, 103. https://doi.org/10.1186/1471-2180-11-103

Manaia, C.M., Rocha, J., Scaccia, N., Marano, R., Radu, E., Biancullo, F., Cerqueira, F., Fortunato, G., Iakovides, I.C., Zammit, I., Kampouris, I., Vaz-Moreira, I., Nunes, O.C., 2018. Antibiotic resistance in wastewater treatment plants: Tackling the black box. Env. Int 115, 312–324. https://doi.org/10.1016/j.envint.2018.03.044

Nesme, J., Simonet, P., 2015. The soil resistome: a critical review on antibiotic resistance origins, ecology and dissemination potential in telluric bacteria. Environ. Microbiol. 17, 913–930. https://doi.org/10.1111/1462-2920.12631

Pandey, P., Chiu, C., Miao, M., Wang, Y., Settles, M., Del Rio, N.S., Castillo, A., Souza, A., Pereira, R., Jeannotte, R., 2018. 16S rRNA analysis of diversity of manure microbial community in dairy farm environment. PLoS One 13, e0190126. https://doi.org/10.1371/journal.pone.0190126

Rocha, J., Cacace, D., Kampouris, I., Guilloteau, H., Jäger, T., Marano, R.B.M., Karaolia, P., Manaia, C.M., Merlin, C., Fatta-Kassinos, D., Cytryn, E., Berendonk, T.U., Schwartz, T., 2020. Inter-laboratory calibration of quantitative analyses of antibiotic resistance genes. J. Environ. Chem. Eng. 8, 102214. https://doi.org/10.1016/j.jece.2018.02.022

Shi, W., Liu, Y., Li, J., Zhang, H., Shi, R., Chen, J., Li, H., 2020. Distribution pattern of antibiotic resistance genes and bacterial community in

agricultural soil samples of Wuliangsuhai watershed. China. Agric. Ecosyst. Environ. 295, 106884. https://doi.org/10.1016/j.agee.2020.106884

Tadić, Bleda Hernandez, M.J., Cerqueira, F., Matamoros, V., Piña, B., Bayona, J.M., 2021. Occurrence and human health risk assessment of antibiotics and their metabolites in vegetables grown in field-scale agricultural systems. J. Hazard. Mater. 401, 123424. https://doi.org/10.1016/j.jhazmat.2020.123424

Tadić, Đ., Matamoros, V., Bayona, J.M., 2019. Simultaneous determination of multiclass antibiotics and their metabolites in four types of field-grown vegetables. Anal. Bioanal. Chem. 411, 5209–5222. https://doi.org/10.1007/s00216-019-01895-y

Tamang, M.D., Seol, S.Y., Oh, J.Y., Kang, H.Y., Lee, J.C., Lee, Y.C., Cho, D.T., Kim, J., 2008. Plasmid-Mediated Quinolone Resistance Determinants qnrA, qnrB, and qnrS among Clinical Isolates of Enterobacteriaceae in a Korean Hospital. Antimicrob. Agents Chemother. 52, 4159–4162. https://doi.org/10.1128/aac.01633-07

Tennstedt, T., Szczepanowski, R., Braun, S., Puhler, A., Schluter, A., 2003. Occurrence of integron-associated resistance gene cassettes located on antibiotic resistance plasmids isolated from a wastewater treatment plant. FEMS Microbiol Ecol 45, 239–252. https://doi.org/10.1016/S0168-6496(03)00164-8

Von Wintersdorff, C.J.H., Penders, J., Van Niekerk, J.M., Mills, N.D., Majumder, S., Van Alphen, L.B., Savelkoul, P.H.M., Wolffs, P.F.G., 2016. Dissemination of antimicrobial resistance in microbial ecosystems through horizontal gene transfer. Front. Microbiol. 7, 1–10. https://doi.org/10.3389/fmicb.2016.00173

WHO, 2014. Antimicrobial resistance. Global report on surveillance. World Heal. Organ. 61, 12–28. https://doi.org/10.1007/s13312-014-0374-3

Wielders, C.L.C., Fluit, A.C., Brisse, S., Verhoef, J., Schmitz, F.J., 2002. mecA gene is widely disseminated in Staphylococcus aureus population. J. Clin. Microbiol. 40, 3970–3975. https://doi.org/10.1128/jcm.40.11.3970-3975.2002

Wohde, M., Berkner, S., Junker, T., Konradi, S., Schwarz, L., Düring, R.A., 2016. Occurrence and transformation of veterinary pharmaceuticals and biocides in manure: a literature review. Environ. Sci. Eur. 28, 23. https://doi.org/10.1186/s12302-016-0091-8

Zdruli, P., Jones, R., Montanarella, L., 2004. Organic Matter in the Soils in Southern Europe, European Soil Bureau Technical Report, EUR 21083 EN. https://doi.org/eusoils.jrc.ec.europa.eu/esdb_archive/eusoils_docs/esb

Zhang, D., Liu, H., Wang, S., Zhang, W., Wang, J., Tian, H., Wang, Y., Ji, H., 2019. Fecal microbiota and its correlation with fatty acids and free amino acids metabolism in piglets after a Lactobacillus strain oral administration. Front. Microbiol. 10, 1–13. https://doi.org/10.3389/fmicb.2019.00785

Zhang, L., Li, L., Sha, G., Liu, C., Wang, Z., Wang, L., 2020. Aerobic composting as an effective cow manure management strategy for reducing the dissemination of antibiotic resistance genes: An integrated meta-omics study. J. Hazard. Mater. 386, 121895. https://doi.org/10.1016/j.jhazmat.2019.121895

Implications of the use of organic fertilizers for Antibiotic Resistance Gene distribution in agricultural soils and fresh food products. A plot-scale study

Claudia Sanz[1], Marta Casado[1], Laia Navarro-Martin[1], Núria Cañameras[2], Núria Carazo[2], Victor Matamoros[1], Josep Maria Bayona[1], Benjamin Piña[1]

1) IDAEA-CSIC, Jordi Girona, 18. E-08034, Barcelona, Spain

2) Department of Agri-Food Engineering and Biotechnology DEAB-UPC, Esteve Terrades 8, Building 4, Castelldefels, 08860, Spain

Science of the Total Environment, 815, (2022) *Available in https://doi.org/10.1016/j.scitotenv.2021.151973*

Abstract

The spread of antibiotic resistance genes (ARG) into agricultural soils, products, and foods severely limits the use of organic fertilizers in agriculture. In order to help designing agricultural practices that minimize the spread of ARG, we fertilized, sown, and harvested lettuces and radish plants in experimental land plots for two consecutive agricultural cycles using four types of fertilizers: mineral fertilization, sewage sludge, pig slurry, or composted organic fraction of municipal solid waste. The analysis of the relative abundances of more than 200,000 ASV (Amplicon Sequence Variants) identified a small, but significant overlap (<10%) between soil's and fertilizer microbiomes. Clinically relevant ARG were found in higher loads (up to 100 fold) in fertilized soils than in the initial soil, particularly in those treated with organic fertilizers, and their loads grossly correlated to the amount of antibiotic residues found in the corresponding fertilizer. Similarly, low, but measurable ARG loads were found in lettuce (*tet*M, *sul*1) and radish (*sul*1), corresponding the lowest values to samples collected from minerally fertilized fields. Comparison of soil samples collected along the total period of the experiment indicated a relatively year-round stability of soil microbiomes in amended soils, whereas ARG loads appeared as unstable and transient. The results indicate that ARG loads in soils and foodstuffs were likely linked to the contribution of bacteria from organic fertilizer to the soil microbiomes, suggesting that an adequate waste management and good pharmacological and veterinarian practices may significantly reduce the presence of these ARGs in agricultural soils and plant products.

1. Introduction

The use of organic wastes as agricultural fertilizers, allows a better management of the finite resources we dispose for soil fertilization and food production. Amongst all the different types of organic wastes that are generated annually, wastewater treatment plants' sludge and animal slurry represent the most abundant ones, making them usual candidates for organic fertilization (Bosch-Serra et al., 2020; Fernández et al., 2009; Pascual et al., 2018; Terrero et al., 2018). The use of sludge from municipal wastewater treatment operations is usually a subject under strict regulatory control (Alvarenga et al., 2015; Murray et al., 2019). There are different types of sludge depending on the level of thermal treatment and drying, alkaline stabilization, digestion or composting, which lead to liquid or cake-like sewage biosolids while animal manure is a combination of feces, urine and animal bedding that depending on the level of "turning" can result on solid, semi-solid or liquid manure (slurry) (Qian et al., 2016). The most common treatment used to stabilize the N and improve handling characteristics in this type of organic waste is composting. The product of composting is a material that has a much smaller C:N ratio than the original mixture and may result in a decrease of the concentration of some contaminants including antibiotics (ABs) (Dolliver and Gupta, 2008; Goss et al., 2013). However, there is a potential tendency of increasing of Cu, Zn, K and P concentration during this process (Tejada et al., 2001).

While organic fertilizers can provide macro- and micronutrients to the soil, they may also contain components that can be harmful for animal, plant, and human health (Chen et al., 2018; Urra et al., 2019; Zhou et al., 2019). The presence of pathogens represents an obvious threat, but other pollutants, like pharmaceuticals, hormones and ABs may also represent a potential risk. The presence of these last ones, may promote the increase of bacteria resistant to multiple antimicrobial and antibiotic drugs. The acquisition of Antibiotic Resistance (AR) is a natural phenomenon, but the application of organic fertilizers may step up its dissemination and evolution in the soil. Therefore, the potential transmission of AR from amended soils to crops and, ultimately, to consumers is a matter of major concern, particularly for plants that are usually consumed raw (Berendonk et al., 2015; Chen et al., 2016; Freitag et al., 2018; Koch et al., 2017; Yang et al., 2018). Antibiotic Resistance Genes (ARGs) may spread from the organic fertilizer to the soil-plant continuum via endophytes or by adhering to plant surfaces or soil particles, nonetheless few studies have deepened in this topic (Cerqueira et al., 2019a; Marano et al., 2019). Considering those facts and under the actual climate change scenario, there is an urgent need to consider organic sources of nutrients as key factors to a sustainable food production chain. The main question remains in finding the right source that finds balance between the benefits in support of the plant growth and the potential threats and risks (Goss et al., 2013).

The concentration of some antibiotics and other molecules in sludge and slurry may vary depending on the origin and nature of the waste and the different composting processes (Berendsen et al., 2018; Bondarczuk et al., 2016; Ezzariai et al., 2018; Gros et al., 2019; Liu et al., 2015; Qian et al., 2016; Widyasari-Mehta et al., 2016). The potential long-term presence of ABs in the soil under organic fertilization may exert selective pressure over soil microbiomes, leading to changes in its composition (Cerqueira et al., 2019b; Pan and Chu, 2016; Zhang et al., 2014). This usually happens at sub-inhibitory concentrations favoring antibiotic resistant (AR) bacterial strains over sensitive ones, thus turning soil into hotspots for ARGs (Andersson and Hughes, 2011; Cerqueira et al., 2019b).

While it is generally known that organic fertilizers may alter microbiomes and transcriptomes from

the receiving soils and, ultimately, from crops, there are only few studies specifically focused in comparing these effects between different types of organic fertilizers in different crops (Buta et al., 2021; Cerqueira et al., 2019a; Muhammad et al., 2020; Radu et al., 2021; Tadić et al., 2021; Xie et al., 2018). Yet, the development of agricultural practices minimizing the potential risk of their use is a requirement for many world regions in which, like in the Mediterranean region, intensive pork farming co-exists with limiting water availability and strong organic fertilization needs, since soils are almost depleted of organic matter (Noya et al., 2017; Palma-Heredia et al., 2020). In this work, we intend to investigate three key aspects that have been seldomly addressed in an integrated way: 1) The influence of the type of organic fertilizer in the final ARG loads in soils and crops; 2) The contribution of bacteria from fertilizers to the changes observed in the receiving soils' microbiome and how stable this contribution is; and 3) The origin of ARGs found in foodstuffs and particularly whether they come from the fertilizer or from the original soil resistomes. To address these questions, we used an integrated setup in which experimental plots located in an agricultural environment (the Llobregat River Delta, South of Barcelona, Spain), using three different organic fertilizers: sewage sludge, piglet slurry and the organic fraction from municipal waste (OFMSW), in addition to a conventional chemical fertilizer (Mineral), and two crops of agronomic interest that are commonly eaten raw, lettuce and radish (*L. sativa* and *R. sativus*). We completed two agricultural cycles, to obtain temporal information, and performed molecular analyses of microbiomes and ARG loads from the different compartments. The microbial population present in the fertilizers and soil samples was studied using high throughput 16S rDNA sequencing techniques at the ASV (Amplicon Sequence Variant) level, which provides an extremely detailed identification of the bacterial and archaea strains present in the samples that allows tracking the transmission of these strains from fertilizers to soils and from soil to plants. In addition, seven ARGs of clinical relevance (*sul*1, *tet*M, *qnr*S1, *mec*A, bla_{TEM}, $bla_{CTX\text{-}M\text{-}32}$, $bla_{OXA\text{-}58}$,) were analyzed using quantitative real-time PCR methods (RT-PCR) in samples of biosolids, soil, and harvest products. The integron class 1 (*int*I1) was added to the analysis as it is considered a marker of anthropogenic pollution and Horizontal Gene Transfer activity (HGT) (Agerso and Sandvang, 2005; Forsberg et al., 2014; Gillings et al., 2015; Marano et al., 2019; Zheng et al., 2020). It has been found closely associated to *sul*1 (Poey et al., 2019) and to several genes encoding extended-spectrum β-lactamases and resistance for tetracycline and quinolones (Agerso and Sandvang, 2005; Chen et al., 2010; Gillings et al., 2008; Quiroga et al., 2013).

This work integrates different approaches to provide a global picture of the effect of organic fertilization in the presence of clinically relevant ARGs in soils and crops, linking their levels to the composition of the corresponding fertilizers in terms of microbiome profiles, ARG loads and antibiotic residue levels. The final goal of this project is to help devising agricultural practices that minimize the spread of ARG from organic fertilizers to agricultural soils, foodstuffs and, eventually, consumers.

2. Materials and methods

2.1 Experimental site and conditions

The present study was developed along two productive cycles (1st cycle: March 2019-May 2019; 2nd cycle: November 2019 – March 2020) at the scientific-technical unit of Polytechnic University of Catalonia (UPC) ("Agrópolis", Viladecans (Barcelona), 41°17'19,1"N, 2°02'43,4"E). **Figure**

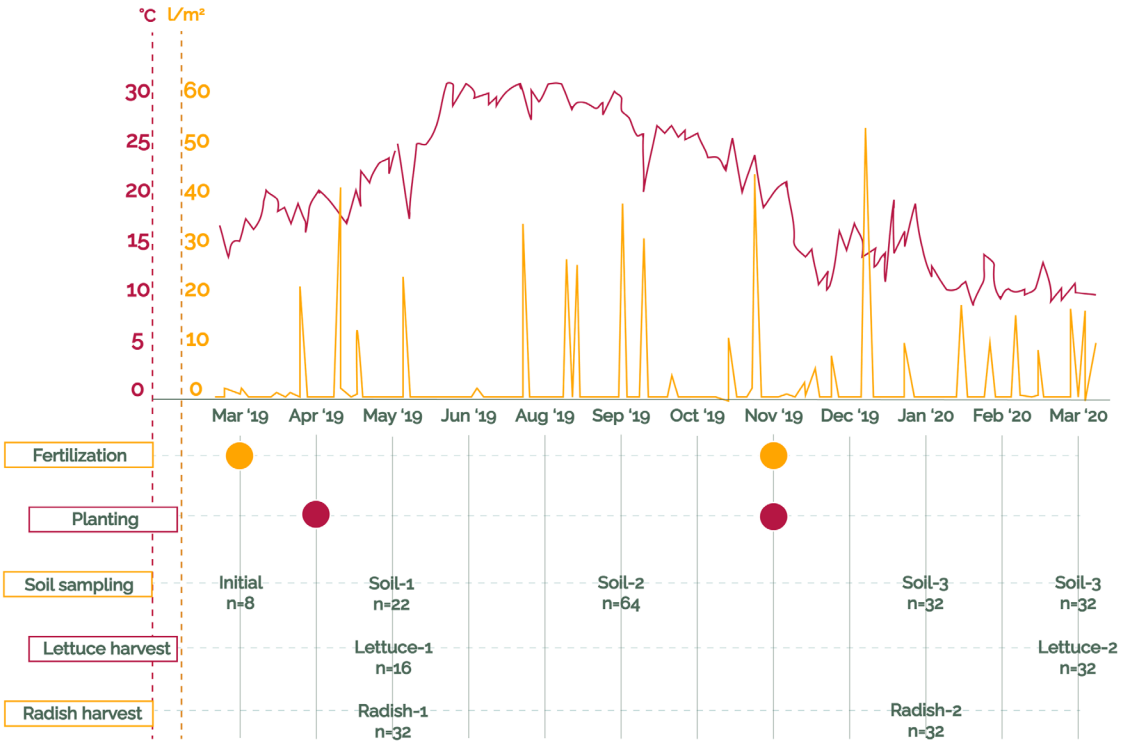

Figure 1. Average temperatures, daily accumulated precipitation, organic fertilizers application, sow and harvest dates along the experimental period. Note the different sampling times for lettuce and radish, as well as for the corresponding soil samples, imposed by weather conditions and plant growth.

1 shows weather conditions and the schedule of fertilization, planting, soil sampling and harvesting along the two cycles. The sandy-clay (sand 40%, silt 35.2% and clay 24.8%) soil used in this experiment did not have any history of agriculture prior to this date. Thirty-two experimental plots were cultivated, with half destined for lettuce cropping (*L. sativa* cv "Maravilla", 16 plots of 10 m^2) and radishes (Raphanus sativus cv "Redondo rojo", 16 plots of 3 m^2). Twelve lettuce seedlings were planted in each of three rows spaced at 30 cm and 200 radish seeds per row spaced at 7-8 cm. Each plot received one of the three tested biosolids (sludge, slurry, OFMSW) or a mineral fertilizer (n=4, per treatment) and were randomly distributed in the field. The sludge-based fertilizer consisted in anaerobically-digested sludge from Gavà-Viladecans (Barcelona, Spain) wastewater treatment plant (WWTP), the slurry came from a piglet farm in Osona (Barcelona, Spain) and the OFMSW-derived compost was made of urban waste composted with wood residues for 3-4 months. Main physico-chemical properties of the studied organic fertilizers are shown in **Supplementary Table S1**. In each cycle, OFMSW was spread along its respective plots, sludge was applied as small moist aggregates and the slurry was applied as a liquid (dry matter content below 5%) using a watering can. All the amendments were incorporated manually to a depth of 5 cm immediately after application. The amount of organic fertilizer added per plot was calculated to ensure the same amount of ammoniacal nitrogen in all treatments (100 kg of N per ha for lettuce and 80 kg of N per ha for radish), corresponding to the average extractions of the crops (Ramos and Pomares, 2010). Specifically, the application rate for OFMSW, sludge and slurry was 4.5 kg/m^2, 3 kg/m^2 and 4 l/m^2 for lettuces and 2.8 kg/m^2, 2.3 kg/m^2 and 3 l/m^2 for radishes, respectively.

For the inorganic fertilization group, ammonium nitrate (34% N) was added to provide the same amount of N as in the organic treatments (100 kg N/ha for lettuce and 80 kg N/ha for radish), and superphosphate (43.6% P_2O_5) and potassium sulphate (54% K_2O) were added to adjust potassium (40 kg P_2O_5/ha in lettuce and 30 kg P_2O_5/ha in radish) and phosphate levels 185 kg K_2O/ha in lettuce and 90 kg K_2O/ha in radish) to meet Spanish agronomical guidelines (Ramos and Pomares, 2010). Main physico-chemical properties of the studied soils are shown in **Supplementary Table S2**.

2.2 Biosolids, soil and vegetable sampling, characterization and processing

In each production cycle, organic fertilizers were collected just prior to their application. Moreover, before the experiment and between the first and the second fertilization cycle, soil samples (Initial soil and Soil 2, respectively) were taken at a 10 cm depth with 50 ml sterile polypropylene tubes to characterize the soil along the experimental period, using each tube as a biological replicate. At harvest, eight heads of lettuce and eight handfuls of radishes were randomly sampled per treatment plot respectively and taken refrigerated (4ºC) to the laboratory in Ziploc bags for their processing, treating each head or handful as a biological replicate. Immediately after harvest, 3 x 11.5 cm lettuce soil and radish soil cores were sampled, at a 10 cm depth with 50 ml sterile tubes (Soil 1 for the first fertilization cycle, Soil 3 for the second fertilization cycle). Note that Soil 3 (post harvest) samples were taken at two different time points, as lettuces and radish had different harvesting times at this particular campaign. As the two sets of data (n=32 each) were statistically identical for the analyzed parameters, we opted to treat them as a single set of samples (not shown). Once at the laboratory, excess soil was removed from the plants using a sterile gauze to achieve the visual cleanliness desired by consumers. About 90g of product per biological replicate were processed in a grinder (Retsch GRINDOMIX GM200). The crushed material was transferred to a beaker along with 50 ml of sterile PBS, mixed thoroughly with a hand blender, and then filtered through a gauze to remove the pulp. This procedure was repeated twice to ensure a proper bacterial rinse. The flow through was then transferred to 50 ml sterile polypropylene tubes through a 100 µm mesh nylon Cell strainer (Corning® Cell Strainer), centrifuged at 4500 rpm for 15 min, and the pellets stored at -20°C until further bacterial DNA extraction. For further clarification, an scheme of the procedure is shown in **Supplementary Figure S1.**

2.3 Bacterial DNA extraction and genetic elements quantification

DNA from soil, organic fertilizers, and from pellets from vegetal matrices (250 mg each), was extracted using the DNeasy PowerSoil Kit (Qiagen Laboratories, Inc.), to a final elution volume of 100 µl. The concentration and the quality of the DNA were tested using a NanoDrop Spectrophotometer 8000 (Thermofisher Scientific, Inc). Extracted DNA samples were stored at −20 °C.

Absolute abundance values (copies/g of sample) were calculated for 16S rDNA, *int*I1 and the following ARGs: *sul*1 (Encodes for the enzyme dihydropteroate synthetase, that confers resistance to sulfonamide), *qnr*S1 (a protein from the Pentapeptide Repeat Protein (PRP) family, which contains a tandem of five amino acid repeats, that inhibits the effect of quinolones), *tet*M (a ribosomal protection protein, which confers tetracycline resistance by binding to the ribosome and chasing the drug from its binding site), *mec*A (penicillin-binding protein 2A (PBP2a), which enables transpeptidase activity in

the presence of β-lactams, preventing them from inhibiting cell wall synthesis), *bla*$_{TEM}$, *bla*$_{CTX-M-32}$, *bla*$_{OXA-58}$, (β-lactamases conferring resistance to beta-lactamic antibiotics such as cephalosporins, monobactams, and carbapenems). The seven selected ARGs confer bacterial resistance against five types of antibiotics widely used both in clinical and veterinary practices. They often associate to mobile genetic elements and they are considered highly relevant in environmental settings (Berendonk et al., 2015). They have been intensively studied in our laboratory for the past four years as robust indicators of the presence of antibiotic resistance genes in the samples (Cerqueira et al., 2019c, 2019b, 2019a). Quantification was performed by real time PCR reactions in a LightCycler 480 II (A F. Hoffmann–La Roche AG, Inc), using the primer sequences listed in **Supplementary Table S3**. Reactions were conducted in 20 µl volumes on 96-well plates, using primer concentrations of 200 nM for *bla*$_{TEM}$ and of 300 nM for the rest of genes. Dynamo ColorFlash SYBR Green (Thermo Scientific, Inc.) was used for *mec*A, *tet*M and *bla*$_{OXA-58}$ qPCR quantifications; all the other genes were quantified with LightCycler 480 SYBR Green I Master (A F. Hoffmann–La Roche AG, Inc). Amplification protocol was adapted following manufacturers guidelines and different annealing temperatures were used as indicated in **Supplementary Table S3**. All samples were run as technical duplicates along with the standard curve to reduce variability between assays. Plasmids used for the quantification curves were pNORM1 conjugative plasmid (Gat et al., 2017) for *int*I1, *sul*1, *qnr*S1, *tet*M, *bla*$_{TEM}$, *bla*$_{CTX-M-32}$, *bla*$_{OXA-58}$ and individual pUC19 plasmids for *mec*A, *tet*M and *bla*$_{OXA-58}$ (Laht et al., 2014; Szczepanowski et al., 2009; Tamminen et al., 2011). Quantification limits (LOQ) were established as the minimum amount of plasmid that could be detected without interference from the negative control, the corresponding values are reported in **Supplementary Table S3**. The quality criteria within the standard curve was a R^2> 0.99, and a slope between −3.1 and −3.4. The accepted efficiency of the reactions ranged from 97% to 100%. Melting curves were obtained to confirm amplification specificity.

Copy numbers per gene were calculated by extrapolation from the standard curves, and expressed in relation to the processed grams of fresh weight. Prevalence values, understood as the fraction of the bacterial population harbouring a given genetic element, was estimated as copies of the genetic element per million 16S rDNA copies (**Supplementary Figure S2** for absolute values). Statistical analysis and plots were performed in the R environment (version 3.6.1; http://www.rproject.org/). Normality and homogeneity of the variances were checked using the Shapiro-Wilk and Levene tests, respectively. Since data followed a normal distribution, an Analysis of Variance (ANOVA) followed by Tukey's B post-hoc correction for multiple tests was performed with the multcomp R package (Hothorn et al., 2016). Significance levels were set at $p \leq 0.05$.

2. 4 Microbial population analysis by 16S rDNA sequencing

Bacterial communities present in the samples were examined by 16S sequencing analysis. Fertilizers and soil samples from all treatments were sent to Novogene Europe (Cambridge, UK). 16S rRNA genes of distinct regions (16SV4/16SV3/16SV3-V4/16SV4-V5) were amplified using specific primers barcoding for amplicon generation. All PCR reactions were carried out with Phusion® High-Fidelity PCR Master Mix (New England Biolabs). Quality-checked PCR products were mixed at equal density ratios and purified by Qiagen Gel Extraction Kit (Qiagen, Germany). Sequencing libraries were generated using NEBNext Ultra DNA Library Pre ®Kit for Illumina, following manufacturer's recommendations, and index codes were added. Sequencing was carried

out on an Illumina platform and 400 bp paired-end reads were generated (https://www.ncbi.nlm.nih.gov/geo/query/acc.cgi?acc=GSE179685). Total reads per sample and other DNA sequencing quality parameters appear in **Supplementary Table S4**.

Clean Sequences were analysed and associated to 201,182 ASVs (Amplicon Sequence Variants) using the DADA2 R package (Callahan et al., 2016). The SILVA database v128, formatted for DADA2, was used to provide taxonomic annotation (Quast et al., 2013). The number of taxa identified and the percentage of taxon coverage (fraction of ASVs annotated to each particular taxonomic level) are shown in **Supplementary Table S5**. β-diversity analysis were performed with QIIME (Version 1.7.0). The significance of difference amongst the structure of microbial communities was analysed by a non-metric multi-dimensional scaling (NMDS) with the Bray–Curtis dissimilarity index (Bray and Curtis, 1957), using the vegan R package. Contributions of fertilizers to soil microbiomes were characterized using the FEAST (fast expectation-maximization for microbial source tracking) R package (Shenhav et al., 2019). Correlations between bacteria composition and AB resistance were tested by Spearman's correlations between ASV counts and ARGs and intl1 abundance. The false positive discovery rate (FDR) correction was set at $p<0.05$ (Benjamini and Hochberg, 1995), using the psych R package (Revelle, 2013).

2.5 Antibiotic determination in organic fertilizers

Antibiotic determination in the organic fertilizers used in both campaigns was performed as previously described (Berendsen et al., 2015; Sanz et al., 2021), using 500 mg of sample extracted by ultrasound assisted sonication (35 kHz) in McIlvain-EDTA buffer (pH=4) and acetonitrile, followed by protein precipitation with lead acetate, centrifugation (3500 g) and solid-phase extraction (Strata X-RP, 200 mg / 6 ml, Phenomenex, Torrance CA, USA) clean-up. Chemical species determination was performed by Waters Acquity Ultra-Performance Liquid Chromatography™ System (Milford, MA, USA) coupled with Waters TQ-Detector (Manchester, UK), as described (Tadić et al., 2019). Only aggregated values for sulfonamides (sulfadiazine, sulfamethoxazole, sulfathiazole, sulfapyridine, sulfacetamide, sulfamethazine, sulfamethizole), tetracyclines (chlortetracycline, doxycycline, tetracycline, oxytetracycline) and fluoroquinolones (ciprofloxacin, enrofloxacin, ofloxacin) are presented here. Antibiotic concentrations are expressed in dry or fresh weigh weight basis and are corrected by deuterated surrogate standards (sulfamethoxazole-d4, enrofloxacin-d3, ofloxacin-d3) spiked to the initial sample. A detailed description of antibiotic content in these samples will be published elsewhere (Matamoros et al., submitted).

3. Results

1. Soil microbiome changes associated to fertilization procedures

Ribosomal 16S rDNA sequencing analysis of soil and amendment samples identified 201,031 amplicon sequence variants (ASV), 83.6% of which were assigned at the level of Family and 59.5% at the level of Genus (**Supplementary Table S5**). **Figure 2** shows ASV relative compositions of the different samples, averaged by sampling and treatment, and color-labeled at the Phylum level.

The analysis showed a general common microbiome pattern for all soils, with a clear predominance of Proteobacteria, Actinobacteria, Bacteroidetes, and Gemmatimonadota, as well

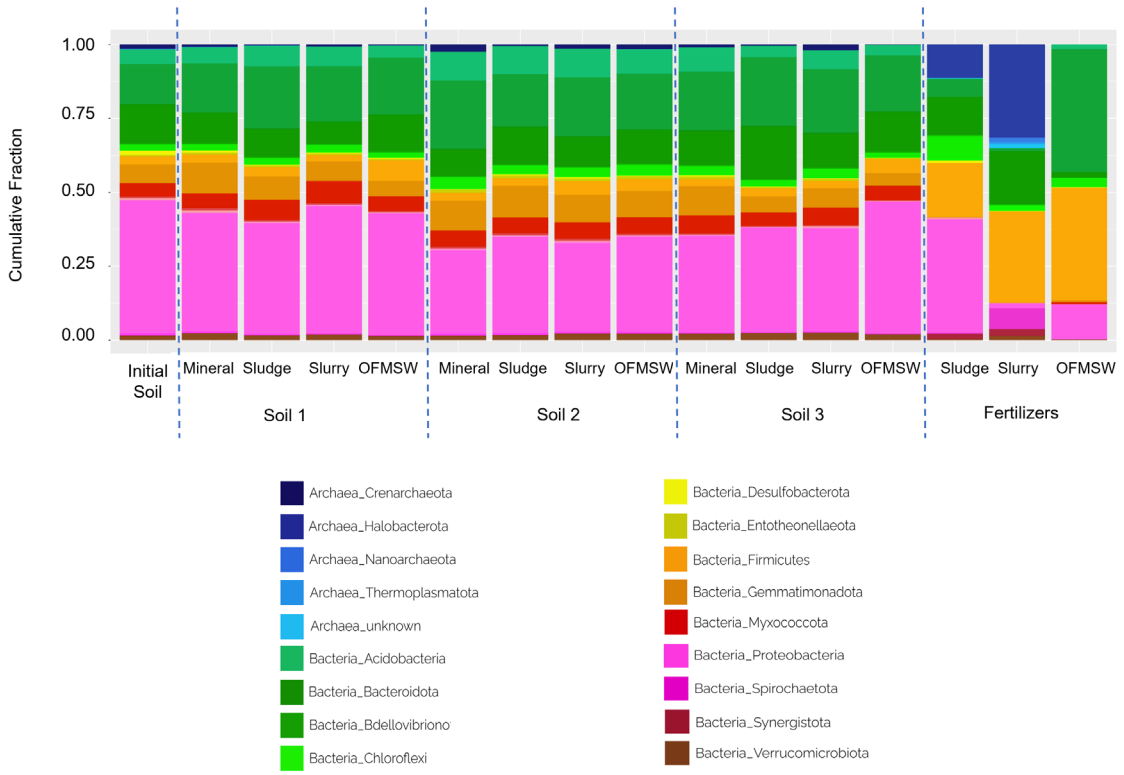

Figure 2. Bacterial and Archaeal Taxon distribution among soil and amendment samples. Sectors correspond to the different Phyla identified in the samples. For sake of simplicity, assignation of the different color codes only includes predominant Phyla.

as a significant contribution of Firmicutes in some samples. In contrast, the three types of organic fertilizers showed very different Phyla distributions, both among them and between them and the soil samples. A significant fraction of Archaea appeared in sludge and slurry fertilizers, whereas Firmicutes predominate in OFMSW compost and slurry samples. Finally, Proteobacteria were only predominant in the sludge microbiome, the structure of which was the most similar one to the soil microbiome (**Figure 2**). Giving the disparate taxonomic composition between soil and fertilizer samples, subsequent analyses of taxonomic diversity and distribution were restricted to soil samples.

ASV distribution among soil samples varied by both sampling time and the fertilizer used in each plot, with a strong interaction between the two factors (two-way ADONIS, **Supplementary Table S6**). Sub-setting the data by both factors (sampling and fertilizer used) further confirmed the relevance of both of them (one-way ADONIS, **Supplementary Table S6**). The analysis showed that mineral fertilization (which in principle did not represent any external addition of bacteria) altered ASV distribution significantly in all samplings, and that the effect of the different treatments was significant both for the pre-amendment Soil 2 and for the post-harvest Soils 1 and 3.

ASV distribution among samples was further analyzed using Non-Metric Dimensional Scaling (NMDS). The analysis only included ASVs representing at least 0.1% of reads in at least one of the soil samples (696 ASVs in total, Figure 3). Most ASV grouped in the center of the NMDS plot, indicating their relatively uniform presence in most samples (**Figure 3A**). When the loadings of the different samples were plotted at the same scale

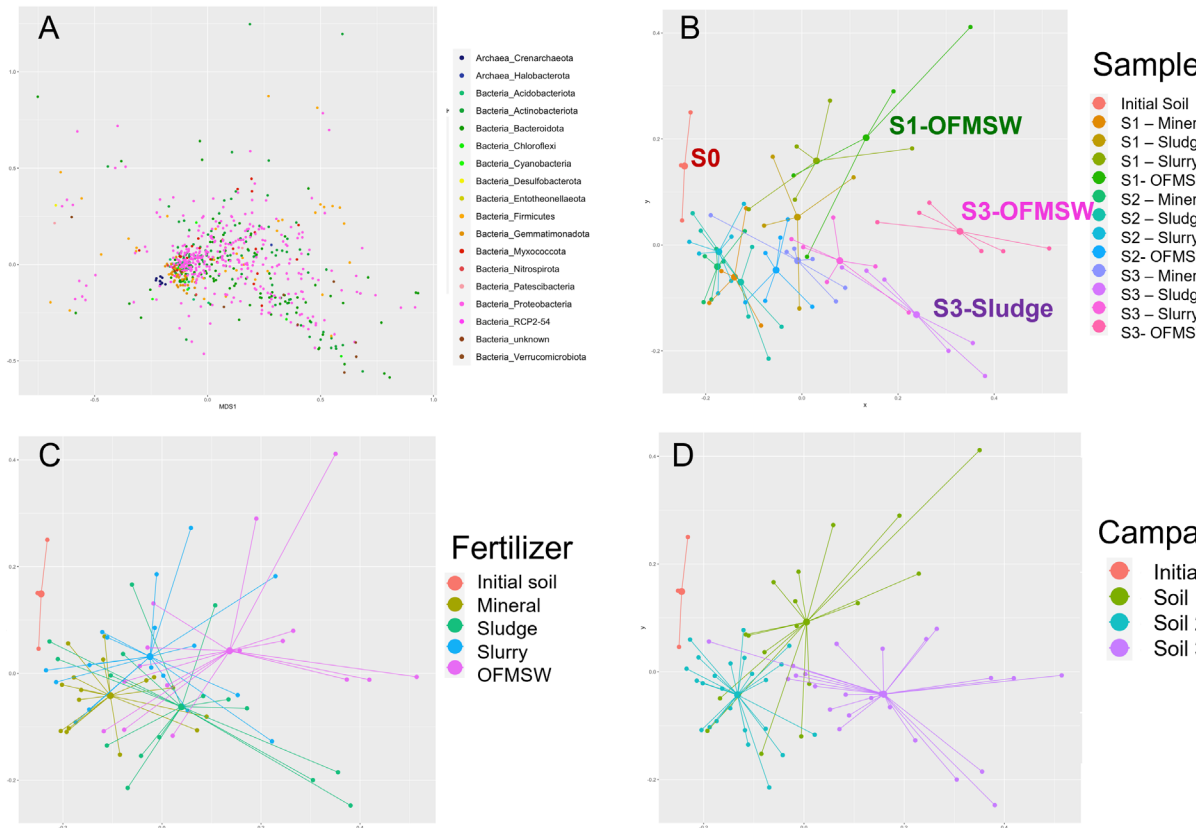

Figure 3. Analysis of ASV distribution among soil samples. ***A)*** NMDS (non-metric dimensional scaling) analysis of the distribution of bacterial OTUs. Only OTUs with more than 100 reads in the total sequence effort were consider in the analysis. ***B-D)*** Site distribution in the NMDS analysis. Samples were color-coded by sample (***B***), sampling campaign (***C***) or type of fertilizer used in the amendment (***D***). Centroids for each group are indicated as thicker dots.

(plot B), only the initial, untreated soil samples (red dots), the OFMSW-fertilized samples from Soil 1 and two groups from Soil 3 (OFMSW- and sludge-fertilized samples) appeared separated from the rest, indicating their differential ASV composition. To facilitate further discussion, these four groups have been labelled in **Figure 3B** as S0, S1-OFMSW, S3-OFMSW, and S3-Sludge, respectively. Grouping samples from the same treatment resulted in a very poor separation of the groups, except for the initial soil samples (red dots, **Figure 3C**). Finally, grouping samples by the sampling time resulted in relatively separated groups, particularly for the initial soil and the second post-harvest sampling (Soil 3, **Figure 3D)**. Taken together, these results indicate that the time of sampling (pre- versus post-harvest, fertilized versus non-fertilized soils), and not the type of fertilizer applied, appeared as the main driver of the soil microbiome composition.

3.2. Contribution of fertilizers to soil microbiomes

Microbial source-tracking analysis by FEAST showed a very low (below 1%) background level of coincidence between soil and fertilizer microbiomes (**Figure 4)**, being this figure particularly low for the slurry fertilizer (0.1% or less, **Figure 4**). Both sludge and OFMSW fertilization increased the percentage of shared microbiomes to 1-3% in the receiving soils in both campaigns (**Figure 4**, pink and red sectors), whereas soils fertilized with slurry only showed a modest 0.2-0.4% of microbiome overlapping with the fertilizer (**Figure 4**). These increments

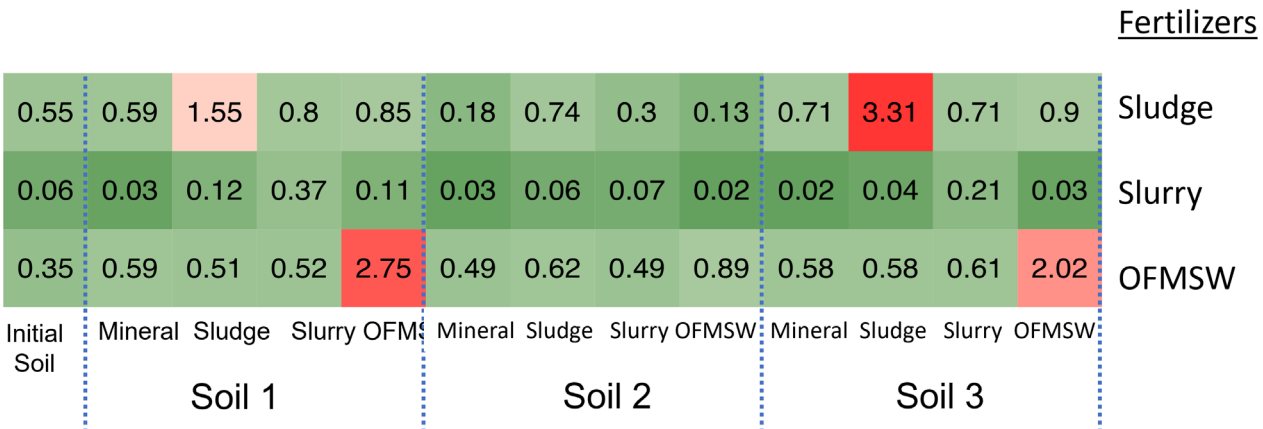

Figure 4. Microbial source-tracking analysis by FEAST. Figures in the graph correspond to the percentage of soil microbiomes (columns) attributable to each fertilizer (rows). Color scale from green to red indicates lower to higher contributions, respectively. Note that the algorithm makes no assumption about the fertilizer used in each soil, so most of the cells show background microbiome coincidence values.

appeared to be transient, as pre-amendment Soil 2 values were indistinguishable from those from the initial soil (**Figure 4**). These results are consistent with the beta-diversity analysis of soil samples in **Figure 3,** as all post-harvest samples shared a similar ASV composition, and that slurry-fertilized samples appeared as less differentiated from the initial soil than sludge- or OFMSW- fertilized ones. These results suggest that at least part of the observed differences in microbiome composition was indeed related to the direct contribution of fertilizer microbiome to the soils.

3.3. ARG loads in organic fertilizers, edible crop parts, and soils

Organic fertilizers showed very high bacterial content, with 16S rDNA levels between 10^{10} to 10^{12} copies per g of sample (blue squares in **Figure 5A**). The highest bacterial load corresponded to the pig slurry in both campaigns, whereas the OFMSW compost showed the lowest bacterial loads, one to two orders of magnitude below the values found for the other two organic fertilizers (**Figure 5A**). The levels of *int*I1 and of the targeted ARGs showed a similar trend, with highest values for the slurry fertilizer samples and the lowest ones for OFMSW. The most prevalent genetic elements were *int*I1, *sul*1 and *tet*M, whereas bla_{TEM} and bla_{OXA-48} showed high levels in some samples (bars in **Figure 5A**). The very high *tet*M loads in the slurry fertilizer was remarkable, although it is consistent with previous studies of ARG loads in different fertilizers derived from swine slurries (Sanz et al., 2021). The distribution of antibiotic concentrations in the different fertilizer samples was consistent with the corresponding ARG profiles, with non-detectable levels in OFMSW compost samples and maximum tetracycline levels in pig slurry samples (**Figure 5B**). Note that *sul*1, *tet*M and *qnr*S1 confer resistance against sulfonamides, tetracyclines and fluoroquinolones, respectively.

The initial soil showed very low levels of all targeted genes, as only intI1 and sul1 were found at levels above quantitation (**Figure 5C**, grey boxes). Addition of organic fertilizers significantly increased at least some ARG loads in Soil 1 and Soil 3 samples relative to the initial, unamended soil, whereas the effect was only marginal for Soil 2 (pre-amendment samples, **Figure 5C**).

Loads of the different genes varied according both the type of fertilizer used and the campaign.

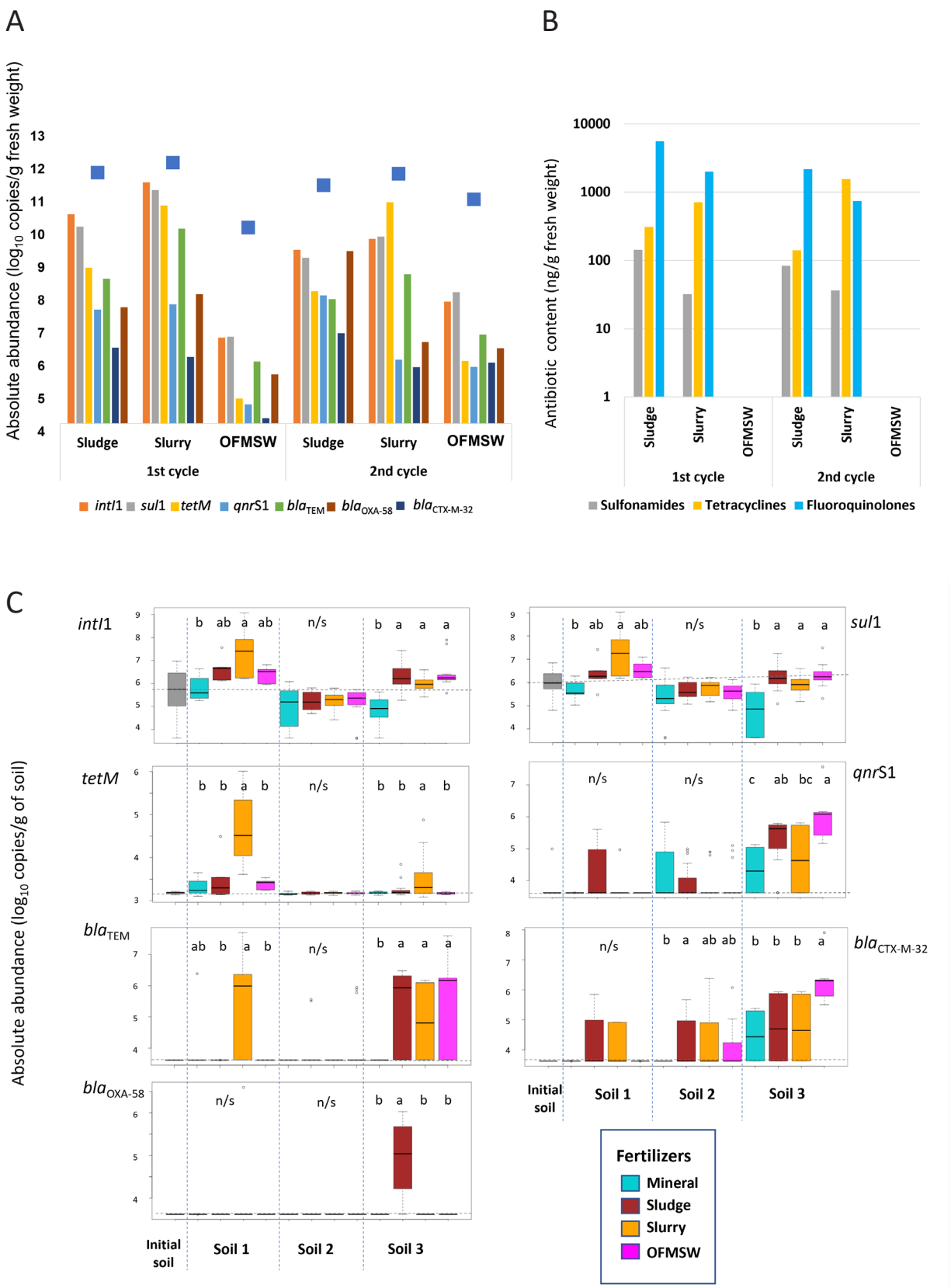
A
Absolute abundance (log10 copies/g fresh weight)
Sludge
Slurry
OFMSW
1st cycle
2nd cycle
intI1 sul1 tetM qnrS1 blaTEM blaOXA-58 blaCTX-M-32
B
Antibiotic content (ng/g fresh weight)
Sulfonamides
Tetracyclines
Fluoroquinolones
C
Absolute abundance (log10 copies/g of soil)
intI1
sul1
tetM
qnrS1
blaTEM
blaCTX-M-32
blaOXA-58
n/s
Initial soil
Soil 1
Soil 2
Soil 3
Fertilizers
Mineral
Sludge
Slurry
OFMSW

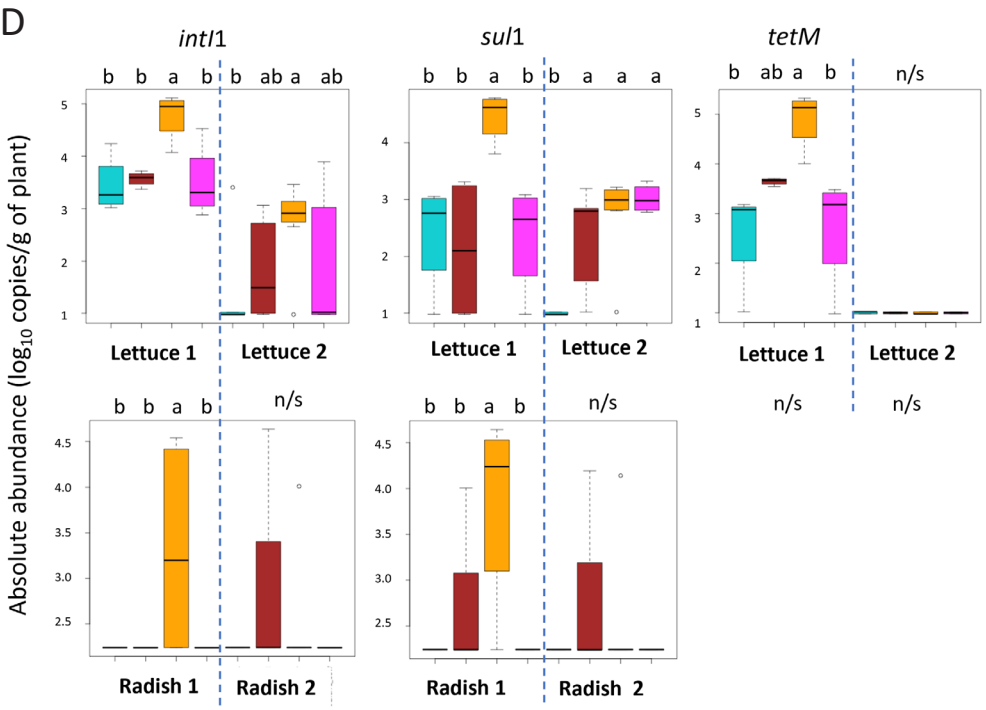

Figure 5. ARG distribution among soil, fertilizers and crop samples. **A)** Abundance of the targeted genes in fertilizers, expressed as copies per gram of fertilizer (logarithmic transformants). Blue squares indicate copies of 16S rDNA per gram of fertilizer, as indicative of the total bacterial abundance, and represented at the same scale. ; **B)** Antibiotic content of the different fertilizers used in this work, expressed in ng/g (fresh weight) of aggregated amounts for each antibiotic family (Sulfonamides, Tetracyclines and Fluoroquinolones). "bdl", below detection levels; **C)** Absolute loads for the different genetic elements in soil samples, expressed as copies per g of soil in logarithmic scale. Thick black lines, boxes and whiskers represent the median, first-to third percentiles and total distribution of samples, respectively. Grey, cyan, brown, orange, and magenta boxes represent the initial soil and soils fertilized with Mineral, Sludge, Slurry, or OFMSW-based fertilizers, respectively. Low-case letters at the top of the graph indicate statistically different distributions (ANOVA+Tukey's B test). Note that ANOVA was performed for each set of soil samples independently (vertical blue dotted lines). "n/s" indicates no statistical difference between genetic element distributions. ; **D)** Analysis of the distribution of the different genetic elements in lettuce (top) and radish (bottom). Color-codes and statistical analyses as in *Figure 5A*. Only genetic elements detected above LOQ in at least one of the sample groups are included in the graphs.

The pre-amendment Soil 2 showed essentially no effect of the type of fertilizer on ARG loads, except for *bla*$_{CTX-M-32}$ (**Figure 5C**, lowercase letters within each graph). In both post-harvest soils (Soils 1 and 3), the lowest ARG levels corresponded to the chemically-fertilized samples in all cases in which significant differences were observed (**Figure 5C**). The highest ARG loads corresponded to soils fertilized with slurry for Soil 1 samples, and to all three organic amendments for Soil 3 samples (**Figure 5C**). Although making a direct correlation of these data (**Figure 5C**) with the ARG loads present in the different organic fertilizers (**Figure 5A**) is not straightforward, the overall ARG profiles in post-harvest soils could be related to the profiles of the corresponding fertilizers. The highest ARG loads corresponded to slurry-fertilized soils in both campaigns, consistent with the high levels of antibiotic found in the slurry-based fertilizer (**Figure 5C**, orange boxes). In the case of *tet*M, its predominance in the slurry-fertilized soils reflected both the high prevalence of this ARG and the high levels of tetracycline in pig slurry (**Figures 5A-C**). Finally, the only soil sample in which the levels of *bla*$_{OXA-58}$ were found above quantification limits was the Soil 3 sample fertilized with sludge

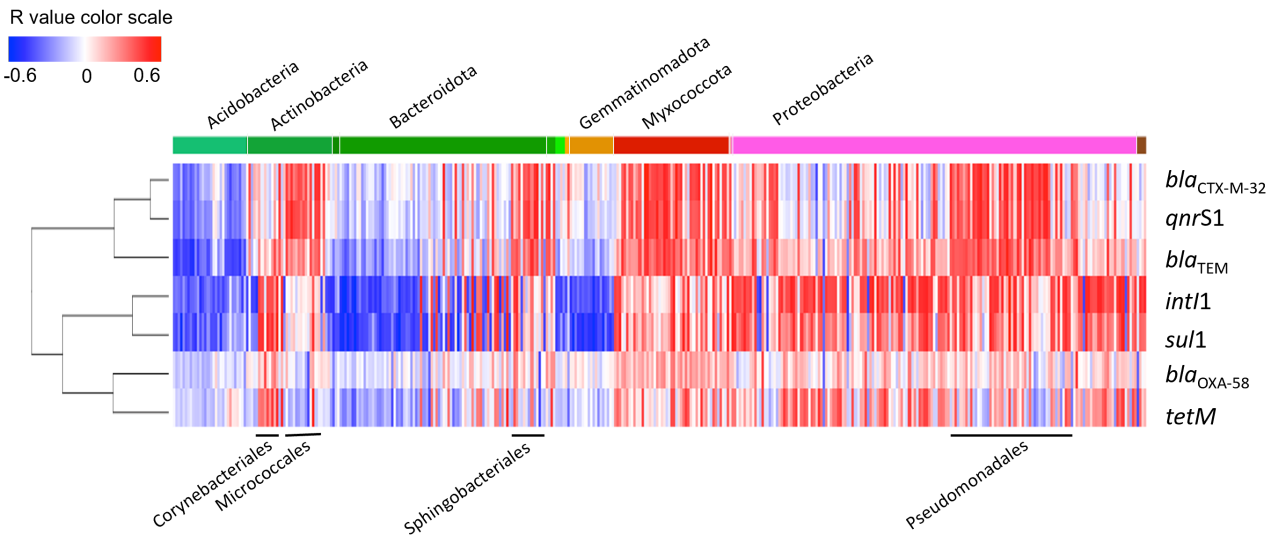

Figure 6. Correlation analysis (Pearson) between ASV abundance and genetic element prevalence (copies per 16S rDNA copy) among soil samples. Initial soil samples were excluded from the analysis. Only AVS with significative correlation with at least one genetic element are represented. Red and blue sectors correspond to positive and negative correlations, respectively (color scale on top). ASVs are ordered taxonomically, as indicated by the color bar at the top of the heatmap, which follows the same color-code as in *Figure 2*. Names of some relevant Phyla are indicated at the top; names of some bacterial families are also indicated at the bottom of the graph. Genetic elements were grouped by hierarchical clustering.

from the 2nd campaign, coinciding with the high levels of *bla*$_{OXA-58}$ found in this particular fertilizer sample (compare **Figures 5A** and **C**).

ARG analysis only detected *int*I1, *sul*1, and *tet*M in lettuce leaves, and only *int*I1 and *sul*1 in radish edible roots (**Figure 5D**). ARG loads were in general higher in the first sampling (corresponding to Soil 1 samples) than in the second one (Lettuce 1/ Radish 1 for Soil 1, Lettuce 2/Radish 2 for Soil 3, **Figure 5D**), a trend also observed in soil samples for these particular genes (compare **Figure 5C** and **D**). In fact, the distribution of *int*I1, *sul*1, and *tet*M among lettuce and, in a lesser extent, radish samples roughly reflected the ARG profiles of both soils and fertilizers, with highest levels corresponding to soils and plants fertilized with slurry, and the lowest levels, when significant, to mineral and OFMSW-fertilized ones (compare **Figures 5A**, **C**, and **D**).

3.4. Correlation between ARG loads and bacterial taxa distribution in soils

Correlation analysis identified 717 ASVs whose relative abundance strongly correlated (either positive or negatively) with the prevalence (copies relative to 16S rDNA copies) of *int*I1 or at least one of the analyzed ARGs (Pearson correlation, p≤0.01, fdr correction, **Figure 6**). Hierarchical clustering revealed a strong taxonomic dependence of the ARG distribution. Only three Phyla (Actinobacteria, Myxococcota and Proteobacteria), plus a single Bacteroidota Family (Sphingobacteriales) included most of the ASV showing positive correlation with ARGs, whereas Acidobacteria, most Bacteroidota, and Gemmatimonadota showed an equally strong negative correlation with ARG prevalence (**Figure 6**, top color bar). In addition to the case of Sphingobacteriales in the Bacteroidota Phylum, other bacterial Families showed specific correlation patterns differentiated from the other groups from the same Phylum, as Pseudomonadales in the Proteobacteria Phylum or Corynebacteriales and Micrococcales in the Actinobacteria Phylum (**Figure 6**, labels at the bottom of the heatmap). Clustering analysis

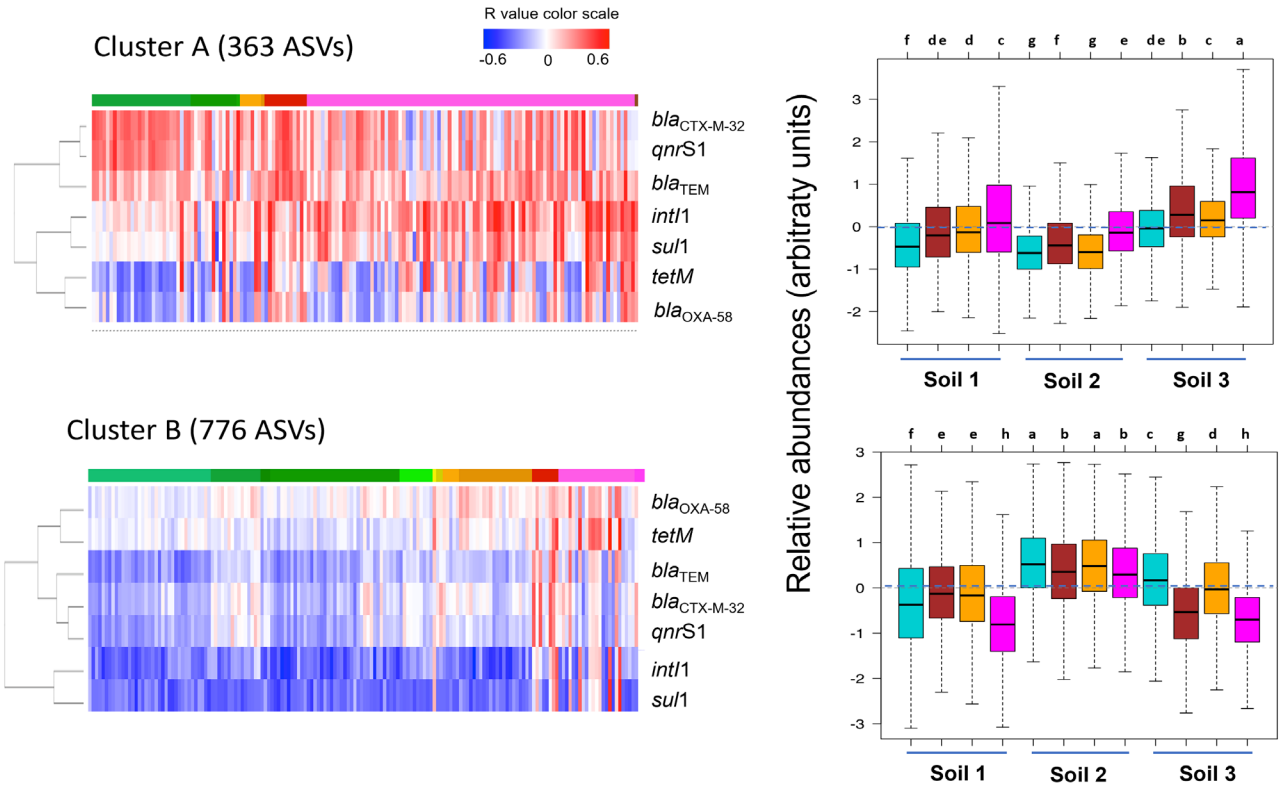

Figure 7. PAM clustering analysis of ASV distribution among soil samples (initial soil samples excluded). The correlation maps on the left show the correlations of the different ASVs in each cluster with the different genetic elements. As in *Figure 6*, ASVs were grouped taxonomically (color bar on the top, same code as in *Figure 2*). Positive and negative correlations are indicated by red and blue sectors, as in Figure 6. Boxplots on the right indicate distribution of ASVs included in each cluster (normalized values) in each sample set. Boxes are colored as in *Figure 5*. Low-case letters at the top of the graph indicate statistically different distributions (ANOVA+Tukey's B test), using the whole dataset.

showed a very similar distribution for *int*I1 and *sul*1 among the different taxonomic groups (**Figure 6**), suggesting a physical linkage between these two genes in a substantial fraction of bacterial cells. A similarly close distribution was observed for *qnr*S1, bla_{TEM}, and $bla_{CTX\text{-}M\text{-}32}$, on one side, and for *tet*M and $bla_{OXA\text{-}58}$ on the other (**Figure 6**), although in these cases their potential physical linkage is purely hypothetical and would require further analyses.

The relationship between ASV abundance and ARG prevalence can be better analyzed when classifying ASVs according their different distribution among samples. ANOVA analysis identified 1139 ASVs with differential distribution among fertilized soil samples, which could be classified into two clusters by PAM clustering: Cluster A (363 ASVs) and Cluster B (776 ASVs, **Figure 7**, left panels). Analysis of the distribution of the components of each of the two clusters revealed a strong dependency on both the sampling campaign and the fertilizer used in each case. Within each campaign, organically-fertilized soils showed higher proportion of ASVs from Cluster A than their chemically-fertilized counterparts, which were correlatively enriched in ASVs from Cluster B. This effect was much stronger in both post-harvest samples (Soil 1 and Soil 3) than in the pre-amendment Soil 2 samples (**Figure 7**). The three sample groups with the highest proportion of ASVs from Cluster A corresponded to OFMSW-fertilized Soil 1 and Soil 3 samples and to the sludge-fertilized Soil 3 samples, the same samples

identified as more diverse in ASV composition by NDMS (groups labelled as S0, S1-OFMSW, S3-OFMSW, and S3-Sludge in **Figure 3**).

Correlation analyses revealed that ASVs from Cluster A showed, in general, a positive correlation with prevalence values for different ARGs (red sectors in the left panels in **Figure 7**), whereas most (but not all) ASVs in Cluster B showed a negative correlation (blue sectors in the left panels in **Figure 7**). The color bars at the top of each heatmap indicate the different taxa composition of the two clusters: Cluster A was mainly integrated by Actinobacteroidota and Proteobacteria, with minor contributions of Firmicutes and Mixococcota, whereas Cluster B showed a much more complex mixture, including Acidobacteroidota, Actinobacteroidota, Bacteroidota, Gemmatimonadota, and different Alpha and Gamma Proteobacteria (**Figure 7**). We conclude that Cluster A included ASVs whose relative abundance in soil depended on the contribution of the fertilizer's microbiome, and that this contribution implicated higher ARG loads. Following the same reasoning, Cluster B included ASVs present in the soil and with a generally low prevalence of the studied ARGs.

4. Discussion

Urban solid waste, sewage sludge, and animal manure are among the most commonly used sources of organic amendments in agriculture (Urra et al., 2019). Our comparison between these three sources indicated that the nature of the fertilizer used in each was less important than the process itself, with the result that the final microbiome composition was very similar irrespectively of using mineral, anaerobically digested WWTP sludge, untreated slurry, or composted OFMSW. The results also suggest a relatively stability in the soil microbiome composition, irrespectively from seasonal variations (the whole experiment covered about a year) and from singular weather events, like stormy events or high temperature periods. This notwithstanding, the use of the highly sensitive ASV sequence identification allowed us to identify a small, but significant contribution of fertilizer microbiomes to the receiving soils, indicating a moderate persistence of fertilizer microbiome in soil conditions for relatively long periods of time (months, at least.)

Our data shows that ARG loads were generally higher in amended soils than in the initial sample, and that both ARG total loads and ARG profiles depended on the fertilized used and on the time of sampling. Pre-amended soil samples, either from the initial soil or from those taken immediately before starting the second agricultural cycle, showed relatively low ARG loads, and, in the case of Soil 2, essentially no influence from the type of fertilizer used in the previous campaign. Therefore, we concluded that, whereas soil microbiomes stayed relatively stable all through the year-round survey in amended soils, ARG loads in soils appeared as unstable and transient. ARG loads seemed to depend on a combination of the persistence of the fertilizer effect and the input of ARG-harboring bacteria from the different amendments. Soils amended with mineral fertilizer showed higher ARG loads than the original soil in some cases, probably indicating proliferation of ARG-harboring soil bacteria as a consequence of the process of amending itself, as previously reported (Nõlvak et al., 2016; Sun et al., 2019). However, this effect can probably explain only a minor fraction of the total increase in ARG loads, as their profiles varied according the type of amendment and the harvest cycle. In almost all cases, soils amended with inorganic fertilizer (and therefore, with no ARG added in the process) showed the minimal ARG loads within a given sampling campaign.

ARG loads in soils appeared linked to the relative

abundance of a small group of bacterial taxa, particularly Actinobacteriota, and Delta- and Gamma-Proteobacteria. These groups were also linked to higher ARG loads in fertilizers based on swine slurries and on their digestates (Sanz et al., 2021). In addition, different Gammaproteobacteria families (Xanthomonadales, Pseudomonadales, Enterobacteriales) appeared linked to a high ARG prevalence in commercial agricultural soils, plants, and fruits (Cerqueira et al., 2019c; Fogler et al., 2019). As most of these bacterial groups have representatives in both swine and human gut, as well as in soil microbiomes, they may represent significant vectors for the spread of antibiotic resistance from animal farms to human populations via fresh food products

ARG loads in crops were relatively low in all cases, particularly in radish samples, although both *int*I1 and *sul*1 in lettuces and radish, and *tet*M in lettuces showed significantly high loads when pig slurry was used as fertilizer, particularly in the first harvest. The differences in ARG profiles between the two species may be related to the particular ARGs we are analyzing in this work, which were chosen according their clinical relevance and the availability of robust analytical protocols to quantify the corresponding antibiotic families in the fertilizers. Previously published shot-gun analyses of resistomes from these two species revealed similar relative ARG loads, but showing different profiles (Fogler et al., 2019). However, the technique used for this particular study did not allow a precise absolute quantitation of ARG loads (sequences per gram of tissue) in the samples. In general terms, we observed a consistent pattern in ARG loads in the three compartments analyzed (fertilizers, soils and crops), in which *int*I1, *sul*1, and *tet*M reached their maximum loads in slurry or slurry-fertilized samples, and particularly in the first campaign. This suggests that pig slurry-based amendments have a strong potential for influencing ARG loads of soils and crops, consistently with previous data on manure fertilization (Sanz et al., 2021; Wan Ying Xie et al., 2018; X. Zhou et al., 2019), and despite the limited capacity of colonization of soils shown by the slurry microbiome. Our data is also consistent with previous results that ARG in soils can translocate to edible plant parts, and that lettuces are particularly prone to present comparatively high levels of both ARGs, antibiotics, and antibiotic transformation products (Cerqueira et al., 2019c; Christou et al., 2018; Domínguez et al., 2014; Gao et al., 2020; Margenat et al., 2017; Tadić et al., 2020).

There are many indications that soil resistomes are the main driving factors of ARG loads in food products, and that their composition may be affected by agricultural practices, particularly by the application of organic fertilizers (Cerqueira et al., 2019c; Muurinen et al., 2017; Piña et al., 2020). The results presented here are consistent with this interpretation, despite the relative minor fraction of fertilizer' ASVs found in the receiving soils' microbiomes. Furthermore, soil and food ARG loads appeared to be highly dependent on the fertilizer used in each case and on its ARG loads. Fertilizer's ASV contribution to soil microbiomes and ARG levels in soils showed strong and comparable temporal variations, suggesting a link between the two parameters. We propose that fertilizers, rather than the original soil microbiomes, were the main source of clinically-relevant ARGs found in foods. This implicates that a strict control on the ARG loads in the initial waste used to produce the fertilizer will be essential for the minimization of the risk of their spreading to soils and crops (Muurinen et al., 2017). We hope our results will be useful for developing more efficient and safer agricultural management frameworks to regulate the type, dose, and timing of application of the different organic fertilizers, and as a support for a general implementation of protocols limiting the use of antibiotics in pharmaceutical and veterinary practices (Muurinen et al., 2017; Sneeringer and

Clancy, 2020).

Credit author statement

Claudia Sanz and Marta Casado contributed to sampling, DNA extraction, qPCR, and sample management; Núria Cañameras, Núria Carazo, and Victor Matamoros participated in the experimental design, plot management and characterization of samples; Victor Matamoros, Claudia Sanz, Marta Casado, and Benjamin Piña participated in the data analysis; Claudia Sanz, Laia Navarro-Martin, and Benjamin Piña contributed to the elaboration of the manuscript; Victor Matamoros, Josep Maria Bayona and Benjamin Piña participated in the financing, conceptual design, and final revision of the manuscript.

Acknowledgments

This work was supported by grants from the Spanish Ministry of Science, Innovation and University (MCIN/AEI/10.13039/501100011033, grants RTI2018-096175-B-I00 and AGL2017-89518-R), and the Generalitat de Catalunya (2017SGR902). CSL was supported by a FI predoctoral fellowship from the Generalitat de Catalunya and the European Social Fund (2018 FI B 00368, ESF Investing in your future). IDAEA-CSIC is a Centre of Excellence Severo Ochoa (Spanish Ministry of Science and Innovation, Project CEX2018-000794-S, ERDF A way of making Europe).

Bibliography

Agerso, Y., Sandvang, D., 2005. Class 1 integrons and tetracycline resistance genes in alcaligenes, arthrobacter, and Pseudomonas spp. isolated from pigsties and manured soil. Appl Env. Microbiol 71, 7941–7947. https://doi.org/10.1128/AEM.71.12.7941-7947.2005

Alvarenga, P., Mourinha, C., Farto, M., Santos, T., Palma, P., Sengo, J., Morais, M.-C., Cunha-Queda, C., 2015. Sewage sludge, compost and other representative organic wastes as agricultural soil amendments: Benefits versus limiting factors. Waste Manag. 40, 44–52. https://doi.org/10.1016/j.wasman.2015.01.027

Andersson, D.I., Hughes, D., 2011. Persistence of antibiotic resistance in bacterial populations. Fems Microbiol. Rev. 35, 901–911. https://doi.org/10.1111/j.1574-6976.2011.00289.x

Benjamini, Y., Hochberg, Y., 1995. Controlling the false discovery rate: A practical approach to multiple testing. J R Stat Soc 57, 289–300.

Berendonk, T.U., Manaia, C.M., Merlin, C., Fatta-Kassinos, D., Cytryn, E., Walsh, F., Buergmann, H., Sorum, H., Norstrom, M., Pons, M.-N., Kreuzinger, N., Huovinen, P., Stefani, S., Schwartz, T., Kisand, V., Baquero, F., Luis Martinez, J., 2015. Tackling antibiotic resistance: the environmental framework. Nat. Rev. Microbiol. 13, 310–317. https://doi.org/10.1038/nrmicro3439

Berendsen, B.J.A., Lahr, J., Nibbeling, C., Jansen, L.J.M., Bongers, I.E.A., Wipfler, E.L., van de Schans, M.G.M., 2018. The persistence of a broad range of antibiotics during calve, pig and broiler manure storage. Chemosphere. https://doi.org/10.1016/j.chemosphere.2018.04.042

Berendsen, B.J.A., Wegh, R.S., Memelink, J., Zuidema, T., Stolker, L.A.M., 2015. The analysis of animal faeces as a tool to monitor antibiotic usage. Talanta 132, 258–268. https://doi.org/10.1016/j.talanta.2014.09.022

Bondarczuk, K., Markowicz, A., Piotrowska-Seget, Z., 2016. The urgent need for risk assessment on the antibiotic resistance spread via sewage sludge land application. Environ. Int. https://doi.org/10.1016/j.envint.2015.11.011

Bosch-Serra, A.D., Yagüe, M.R., Valdez, A.S., Domingo-Olivé, F., 2020. Dairy cattle slurry fertilization management in an intensive Mediterranean agricultural system to sustain soil quality while enhancing rapeseed nutritional value. J. Environ. Manage. 273, 111092. https://doi.org/10.1016/j.jenvman.2020.111092

Bray, J.R., Curtis, J.T., 1957. An Ordination of the Upland Forest Communities of Southern Wisconsin. Ecol. Monogr. 27, 325–349. https://doi.org/10.2307/1942268

Buta, M., Hubeny, J., Zieliński, W., Harnisz, M., Korzeniewska, E., 2021. Sewage sludge in agriculture – the effects of selected chemical pollutants and emerging genetic resistance determinants on the quality of soil and crops – a review. Ecotoxicol. Environ. Saf. 214. https://doi.org/10.1016/j.ecoenv.2021.112070

Callahan, B.J., McMurdie, P.J., Rosen, M.J., Han, A.W., Johnson, A.J.A., Holmes, S.P., 2016. DADA2: High-resolution sample inference from Illumina amplicon data. Nat. Methods 13, 581–+. https://doi.org/10.1038/nmeth.3869

Cerqueira, F., Matamoros, V., Bayona, J., Elsinga, G., Hornstra, L.M., Pina, B., 2019a. Distribution of antibiotic resistance genes in soils and crops. A field study in legume plants (Vicia faba L.) grown under different watering regimes. Environ. Res. 170, 16–25. https://doi.org/10.1016/j.envres.2018.12.007

Cerqueira, F., Matamoros, V., Bayona, J., Piña, B., 2019b. Antibiotic resistance genes distribution in microbiomes from the soil-plant-fruit continuum in commercial Lycopersicon esculentum fields under different agricultural practices. Sci. Total Environ. 652, 660–670. https://doi.org/10.1016/j.scitotenv.2018.10.268

Cerqueira, F., Matamoros, V., Bayona, J.M., Berendonk, T.U., Elsinga, G., Hornstra, L.M., Piña, B., 2019c. Antibiotic resistance gene distribution in agricultural fields and crops. A soil-to-food analysis. Environ. Res. 177, 108608. https://doi.org/10.1016/j.envres.2019.108608

Chen, H., Shu, W., Chang, X., Chen, J.A., Guo, Y., Tan, Y., 2010. The profile of antibiotics resistance and integrons of extended-spectrum beta-lactamase producing thermotolerant coliforms isolated from the Yangtze River basin in Chongqing. Environ. Pollut. 158, 2459–2464. https://doi.org/10.1016/j.envpol.2010.03.023

Chen, Q., An, X., Li, H., Su, J., Ma, Y., Zhu, Y.G., 2016. Long-term field application of sewage sludge increases the abundance of antibiotic resistance genes in soil. Environ. Int. 92–93, 1–10. https://doi.org/10.1016/j.envint.2016.03.026

Chen, Q.L., An, X.L., Zheng, B.X., Ma, Y.B., Su, J.Q., 2018. Long-term organic fertilization increased antibiotic resistome in phyllosphere of maize. Sci. Total Environ. https://doi.org/10.1016/j.scitotenv.2018.07.260

Christou, A., Papadavid, G., Dalias, P., Fotopoulos, V., Michael, C., Bayona, J.M., Piña, B., Fatta-Kassinos, D., 2018. Ranking of crop plants according to their potential to uptake and accumulate contaminants of emerging concern. Environ. Res. 170, 422–432. https://doi.org/10.1016/j.envres.2018.12.048

Dolliver, H., Gupta, S., 2008. Antibiotic Losses in Leaching and Surface Runoff from Manure-Amended Agricultural Land. J. Environ. Qual. 37, 1227–1237. https://doi.org/10.2134/jeq2007.0392

Domínguez, C., Flores, C., Caixach, J., Mita, L., Piña, B., Comas, J., Bayona, J.M., 2014. Evaluation of antibiotic mobility in soil associated with swine-slurry soil amendment under cropping conditions. Environ. Sci. Pollut. Res. 21. https://doi.org/10.1007/s11356-014-3174-3

Ezzariai, A., Hafidi, M., Khadra, A., Aemig, Q., El Fels, L., Barret, M., Merlina, G., Patureau, D., Pinelli, E., 2018. Human and veterinary antibiotics during composting of sludge or manure: Global perspectives on persistence, degradation, and resistance genes. J. Hazard. Mater. https://doi.org/10.1016/j.jhazmat.2018.07.092

Fernández, J.M., Plaza, C., García-Gil, J.C., Polo, A., 2009. Biochemical properties and barley yield in a semiarid Mediterranean soil amended with two kinds of sewage sludge. Appl. Soil Ecol. 42, 18–24. https://doi.org/https://doi.org/10.1016/j.apsoil.2009.01.006

Fogler, K., Guron, G.K.P., Wind, L.L., Keenum, I.M., Hession, W.C., Krometis, L.A., Strawn, L.K., Pruden, A., Ponder, M.A., 2019. Microbiota and Antibiotic Resistome of Lettuce Leaves and Radishes Grown in Soils Receiving Manure-Based Amendments Derived From Antibiotic-Treated Cows. Front. Sustain. Food Syst. 3, 1–17. https://doi.org/10.3389/fsufs.2019.00022

Forsberg, K.J., Patel, S., Gibson, M.K., Lauber, C.L., Knight, R., Fierer, N., Dantas, G., 2014. Bacterial phylogeny structures soil resistomes across habitats. Nature 509, 612–616. https://doi.org/10.1038/nature13377

Freitag, C., Michael, G.B., Li, J., Kadlec, K., Wang, Y., Hassel, M., Schwarz, S., 2018. Occurrence and characterisation of ESBL-encoding plasmids among Escherichia coli isolates from fresh vegetables. Vet. Microbiol. https://doi.org/10.1016/j.vetmic.2018.03.028

Gao, F.Z., He, L.Y., He, L.X., Zou, H.Y., Zhang, M., Wu, D.L., Liu, Y.S., Shi, Y.J., Bai, H., Ying, G.G., 2020. Untreated swine wastes changed antibiotic resistance and microbial community in the soils and impacted abundances of antibiotic resistance genes in the vegetables. Sci. Total Environ. 741. https://doi.org/10.1016/j.scitotenv.2020.140482

Gat, D., Mazar, Y., Cytryn, E., Rudich, Y., 2017. Origin-Dependent Variations in the Atmospheric Microbiome Community in Eastern Mediterranean Dust Storms. Environ. Sci. Technol. 51, 6709–6718. https://doi.org/10.1021/acs.est.7b00362

Gillings, M.R., Gaze, W.H., Pruden, A., Smalla, K., Tiedje, J.M., Zhu, Y.-G., 2015. Using the class 1 integron-integrase gene as a proxy for anthropogenic pollution. ISME J. 9, 1269–1279. https://doi.org/10.1038/ismej.2014.226

Gillings, M.R., Krishnan, S., Worden, P.J., Hardwick, S.A., 2008. Recovery of diverse genes for class 1 integron-integrases from environmental DNA samples. FEMS Microbiol Lett 287, 56–62. https://doi.org/10.1111/j.1574-6968.2008.01291.x

Goss, M.J., Tubeileh, A., Goorahoo, D., 2013. A Review of the Use of Organic Amendments and the Risk to Human Health, in: Advances in Agronomy. Academic Press Inc., pp. 275–379. https://doi.org/10.1016/B978-0-12-407686-0.00005-1

Gros, M., Mas-Pla, J., Boy-Roura, M., Geli, I., Domingo, F., Petrović, M., 2019. Veterinary pharmaceuticals and antibiotics in manure and slurry and their fate in amended agricultural soils: Findings from an experimental field site (Baix Empordà, NE Catalonia). Sci. Total Environ. https://doi.org/10.1016/j.scitotenv.2018.11.061

Hothorn, T., Bretz, F., Westfall, P., Heiberger, R.M., Schuetzenmeister, A., Scheibe, S., Hothorn, M.T., 2016. Package 'multcomp.'

Koch, B.J., Hungate, B.A., Price, L.B., 2017. Food-animal production and the spread of antibiotic resistance: the role of ecology. Front. Ecol. Environ. 15, 309–318. https://doi.org/10.1002/fee.1505

Laht, M., Karkman, A., Voolaid, V., Ritz, C., Tenson, T., Virta, M., Kisand,

V., 2014. Abundances of Tetracycline, Sulphonamide and Beta-Lactam Antibiotic Resistance Genes in Conventional Wastewater Treatment Plants (WWTPs) with Different Waste Load. PLoS One 9. https://doi.org/10.1371/journal.pone.0103705

Liu, B., Li, Y., Zhang, X., Feng, C., Gao, M., Shen, Q., 2015. Effects of composting process on the dissipation of extractable sulfonamides in swine manure. Bioresour. Technol. https://doi.org/10.1016/j.biortech.2014.10.098

Marano, R.B.M., Zolti, A., Jurkevitch, E., Cytryn, E., 2019. Antibiotic resistance and class 1 integron gene dynamics along effluent, reclaimed wastewater irrigated soil, crop continua: elucidating potential risks and ecological constraints. Water Res. https://doi.org/10.1016/j.watres.2019.114906

Margenat, A., Matamoros, V., Díez, S., Cañameras, N., Comas, J., Bayona, J.M., 2017. Occurrence of chemical contaminants in peri-urban agricultural irrigation waters and assessment of their phytotoxicity and crop productivity. Sci. Total Environ. 599–600, 1140–1148. https://doi.org/10.1016/j.scitotenv.2017.05.025

Muhammad, J., Khan, S., Su, J.Q., Hesham, A.E.L., Ditta, A., Nawab, J., Ali, A., 2020. Antibiotics in poultry manure and their associated health issues: a systematic review. J. Soils Sediments 20, 486–497. https://doi.org/10.1007/s11368-019-02360-0

Murray, R., Tien, Y.C., Scott, A., Topp, E., 2019. The impact of municipal sewage sludge stabilization processes on the abundance, field persistence, and transmission of antibiotic resistant bacteria and antibiotic resistance genes to vegetables at harvest. Sci. Total Environ. 651, 1680–1687. https://doi.org/10.1016/j.scitotenv.2018.10.030

Muurinen, J., Stedtfeld, R., Karkman, A., Pärnänen, K., Tiedje, J., Virta, M., 2017. Influence of Manure Application on the Environmental Resistome under Finnish Agricultural Practice with Restricted Antibiotic Use. Environ. Sci. Technol. 51, 5989–5999. https://doi.org/10.1021/acs.est.7b00551

Nõlvak, H., Truu, M., Kanger, K., Tampere, M., Espenberg, M., Loit, E., Raave, H., Truu, J., 2016. Inorganic and organic fertilizers impact the abundance and proportion of antibiotic resistance and integron-integrase genes in agricultural grassland soil. Sci. Total Environ. 562, 678–689. https://doi.org/10.1016/j.scitotenv.2016.04.035

Noya, I., Aldea, X., González-García, S., M. Gasol, C., Moreira, M.T., Amores, M.J., Marín, D., Boschmonart-Rives, J., 2017. Environmental assessment of the entire pork value chain in Catalonia – A strategy to work towards Circular Economy. Sci. Total Environ. 589, 122–129. https://doi.org/10.1016/j.scitotenv.2017.02.186

Palma-Heredia, D., Poch, M., Cugueró-Escofet, M., 2020. Implementation of a decision support system for sewage sludge management. Sustain. 12, 1–18. https://doi.org/10.3390/su12219089

Pan, M., Chu, L.M., 2016. Phytotoxicity of veterinary antibiotics to seed germination and root elongation of crops. Ecotoxicol. Environ. Saf. 126, 228–237. https://doi.org/10.1016/j.ecoenv.2015.12.027

Pascual, J.A., Morales, A.B., Ayuso, L.M., Segura, P., Ros, M., 2018. Characterisation of sludge produced by the agri-food industry and recycling options for its agricultural uses in a typical Mediterranean area, the Segura River basin (Spain). Waste Manag. 82, 118–128. https://doi.org/https://doi.org/10.1016/j.wasman.2018.10.020

Piña, B., Bayona, J.M., Christou, A., Fatta-Kassinos, D., Guillon, E., Lambropoulou, D., Michael, C., Polesel, F., Sayen, S., 2020. On the contribution of reclaimed wastewater irrigation to the potential exposure of humans to antibiotics, antibiotic resistant bacteria and antibiotic resistance genes - NEREUS COST Action ES1403 position paper. J. Environ. Chem. Eng. 8. https://doi.org/10.1016/j.jece.2018.01.011

Poey, M.E., Azpiroz, M.F., Laviña, M., 2019. On sulfonamide resistance, sul genes, class 1 integrons and their horizontal transfer in Escherichia coli. Microb. Pathog. 135. https://doi.org/10.1016/j.micpath.2019.103611

Qian, M., Wu, H., Wang, J., Zhang, H., Zhang, Z., Zhang, Y., Lin, H., Ma, J., 2016. Occurrence of trace elements and antibiotics in manure-based fertilizers from the Zhejiang Province of China. Sci. Total Environ. https://doi.org/10.1016/j.scitotenv.2016.03.123

Quast, C., Pruesse, E., Yilmaz, P., Gerken, J., Schweer, T., Yarza, P., Peplies, J., Glöckner, F.O., 2013. The SILVA ribosomal RNA gene database project: Improved data processing and web-based tools. Nucleic Acids Res. 41, 590–596. https://doi.org/10.1093/nar/gks1219

Quiroga, M.P., Arduino, S.M., Merkier, A.K., Quiroga, C., Petroni, A., Roy, P.H., Centrón, D., 2013. "Distribution and functional identification of complex class 1 integrons." Infect. Genet. Evol. 19, 88–96. https://doi.org/10.1016/j.meegid.2013.06.029

Radu, E., Woegerbauer, M., Rab, G., Oismüller, M., Strauss, P., Hufnagl, P., Gottsberger, R.A., Krampe, J., Weyermair, K., Kreuzinger, N., 2021. Resilience of agricultural soils to antibiotic resistance genes introduced by agricultural management practices. Sci. Total Environ. 756, 143699. https://doi.org/10.1016/j.scitotenv.2020.143699

Ramos, C., Pomares, F., 2010. Abonado de los cultivos hortícolas, in: Guía Práctica de La Fertilización Racional de Los Cultivos En España. Secretaría General Técnica, Centro de Publicaciones, Madrid (Spain), pp. 181–192.

Revelle, W., 2013. psych: Procedures for Psychological, Psychometric, and Personality Research. R Package Version 1.0–95. Evanston, Illinois.

Sanz, C., Casado, M., Navarro-Martin, L., Tadić, Đ., Parera, J., Tugues, J., Bayona, J.M., Piña, B., 2021. Antibiotic and antibiotic-resistant gene loads in swine slurries and their digestates: Implications for their use as fertilizers in agriculture. Environ. Res. 194. https://doi.org/10.1016/j.envres.2020.110513

Shenhav, L., Thompson, M., Joseph, T.A., Briscoe, L., Furman, O., Bogumil, D., Mizrahi, I., Pe'er, I., Halperin, E., 2019. FEAST: fast expectation-maximization for microbial source tracking. Nat. Methods 16, 627–632. https://doi.org/10.1038/s41592-019-0431-x

Sneeringer, S., Clancy, M., 2020. Incentivizing New Veterinary

Pharmaceutical Products to Combat Antibiotic Resistance. Appl. Econ. Perspect. Policy 42, 653–673. https://doi.org/10.1093/aepp/ppz022

Sun, Y., Qiu, T., Gao, M., Shi, M., Zhang, H., Wang, X., 2019. Inorganic and organic fertilizers application enhanced antibiotic resistome in greenhouse soils growing vegetables. Ecotoxicol. Environ. Saf. 179, 24–30. https://doi.org/10.1016/j.ecoenv.2019.04.039

Szczepanowski, R., Linke, B., Krahn, I., Gartemann, K.-H., Gützkow, T., Eichler, W., Pühler, A., Schlüter, A., 2009. Detection of 140 clinically relevant antibiotic-resistance genes in the plasmid metagenome of wastewater treatment plant bacteria showing reduced susceptibility to selected antibiotics. Microbiology 155, 2306–2319. https://doi.org/https://doi.org/10.1099/mic.0.028233-0

Tadić, Đ., Bleda Hernandez, M.J., Cerqueira, F., Matamoros, V., Piña, B., Bayona, J.M., 2021. Occurrence and human health risk assessment of antibiotics and their metabolites in vegetables grown in field-scale agricultural systems. J. Hazard. Mater. 401, 123424. https://doi.org/https://doi.org/10.1016/j.jhazmat.2020.123424

Tadić, Đ., Gramblicka, M., Mistrik, R., Flores, C., Piña, B., Bayona, J.M., 2020. Elucidating biotransformation pathways of ofloxacin in lettuce (Lactuca sativa L). Environ. Pollut. 260, 114002. https://doi.org/10.1016/j.envpol.2020.114002

Tadić, Đ., Matamoros, V., Bayona, J.M., 2019. Simultaneous determination of multiclass antibiotics and their metabolites in four types of field-grown vegetables. Anal. Bioanal. Chem. 411, 5209–5222. https://doi.org/10.1007/s00216-019-01895-y

Tamminen, M., Karkman, A., Lohmus, A., Muziasari, W.I., Takasu, H., Wada, S., Suzuki, S., Virta, M., 2011. Tetracycline Resistance Genes Persist at Aquaculture Farms in the Absence of Selection Pressure. Environ. Sci. Technol. 45, 386–391. https://doi.org/10.1021/es102725n

Tejada, M., Dobao, M.M., Benitez, C., Gonzalez, J.L., 2001. Study of composting of cotton residues. Bioresour. Technol. https://doi.org/10.1016/S0960-8524(01)00059-1

Terrero, M.A., Faz, Á., Ondoño, S., Muñoz, M.Á., 2018. Chapter 14 - Impacts of Raw and Purified Pig Slurry on Carbon and Nitrogen Contents in Mediterranean Agricultural Soil, in: Muñoz, M.Á., Zornoza, R. (Eds.), Soil Management and Climate Change. Academic Press, pp. 207–219. https://doi.org/10.1016/B978-0-12-812128-3.00014-8

Urra, J., Alkorta, I., Garbisu, C., 2019. Potential benefits and risks for soil health derived from the use of organic amendments in agriculture. Agronomy 9, 1–23. https://doi.org/10.3390/agronomy9090542

Widyasari-Mehta, A., Hartung, S., Kreuzig, R., 2016. From the application of antibiotics to antibiotic residues in liquid manures and digestates: A screening study in one European center of conventional pig husbandry. J. Environ. Manage. https://doi.org/10.1016/j.jenvman.2016.04.012

Xie, W. Y., Shen, Q., Zhao, F.J., 2018. Antibiotics and antibiotic resistance from animal manures to soil: a review. Eur. J. Soil Sci. 69, 181–195. https://doi.org/10.1111/ejss.12494

Xie, Wan Ying, Yuan, S.T., Xu, M.G., Yang, X.P., Shen, Q.R., Zhang, W.W., Su, J.Q., Zhao, F.J., 2018. Long-term effects of manure and chemical fertilizers on soil antibiotic resistome. Soil Biol. Biochem. 122, 111–119. https://doi.org/10.1016/j.soilbio.2018.04.009

Yang, L., Liu, W., Zhu, D., Hou, J., Ma, T., Wu, L., Zhu, Y., Christie, P., 2018. Application of biosolids drives the diversity of antibiotic resistance genes in soil and lettuce at harvest. Soil Biol. Biochem. https://doi.org/10.1016/j.soilbio.2018.04.017

Zhang, Y., Zhong, X., Xiong, W., Sun, Y., Zeng, Z., Liang, W., Ding, X., 2014. Responses of plasmid-mediated quinolone resistance genes and bacterial taxa to (fluoro)quinolones-containing manure in arable soil. Chemosphere 119, 473–478. https://doi.org/10.1016/j.chemosphere.2014.07.040

Zheng, W., Huyan, J., Tian, Z., Zhang, Y., Wen, X., 2020. Clinical class 1 integron-integrase gene – A promising indicator to monitor the abundance and elimination of antibiotic resistance genes in an urban wastewater treatment plant. Environ. Int. https://doi.org/10.1016/j.envint.2019.105372

Zhou, S.Y.D., Zhu, D., Giles, M., Yang, X.R., Daniell, T., Neilson, R., Zhu, Y.G., 2019. Phyllosphere of staple crops under pig manure fertilization, a reservoir of antibiotic resistance genes. Environ. Pollut. https://doi.org/10.1016/j.envpol.2019.05.098

Zhou, X., Qiao, M., Su, J.Q., Zhu, Y.G., 2019. High-throughput characterization of antibiotic resistome in soil amended with commercial organic fertilizers. J. Soils Sediments 19, 641–651. https://doi.org/10.1007/s11368-018-2064-6

Impact of organic soil amendments in antibiotic levels, antibiotic resistance gene loads, and microbiome composition in corn fields and crops

Sanz, Claudia[1]; Casado, Marta[1]; Đorde Tadic[1]; Pastor-López, Edward J[1].; Navarro-Martin, Laia[1]; Parera, Joan[2]; Tugues, Jordi[2]; Ortiz, Carlos A.[2], Bayona, Josep M.[1]; Piña, Benjamin[1]

1) IDAEA-CSIC, Jordi Girona, 18. E-08034, Barcelona, Spain

2) DACC, Departament d'Acció Climàtica, Alimentació i Agenda Rural, Generalitat de Catalunya, Gran Via de les Corts Catalanes, 612-614, E-08007, Barcelona, Spain

Environmental Research, 214, (2022)

Available in https://doi.org/10.1016/j.envres.2022.113760

Abstract

The potential spreading of antibiotic resistance genes (ARG) into agricultural fields and crops represent a fundamental limitation on the use of organic fertilization in food production systems. We present here a study of the effect of spreading four types of organic soil amendments (raw pig slurry, liquid and solid fractions, and a digested derivative) on demonstrative plots in two consecutive productive cycles of corn harvest (*Zea mays*), using a mineral fertilizer as a control, following the application of organic amendments at 32-62 T per ha (150 kg total N/ha) and allowing 5 to 8 months between fertilization and harvest. A combination of qPCR and high-throughput 16S rDNA sequencing methods showed a small, but significant impact of the fertilizers in both ARG loads and microbiomes in soil samples, particularly after the second harvesting cycle. The slurry solid fraction showed the largest impact on both ARG loads and microbiome variation, whereas its digestion derivatives showed a much smaller impact. Soil samples with the highest ARG loads also presented increased levels of tetracyclines, indicating a potential dual hazard by ARG and antibiotic residues linked to some organic amendments. Unlike soils, no accumulation of ARG or antibiotics was observed in corn leaves (used as fodder) or grains, and no grain sample reached detection limits for neither parameter. These results support the use of organic soil amendments in corn crops, while proposing the reduction of the loads of ARGs and antibiotics from the fertilizers to greatly reduce their potential risk.

1. Introduction

The use of livestock manure as agricultural organic soil amendment has been proposed as a circular economy strategy. In this way, a potentially polluting waste is used to increase both plant growth and productivity. This strategy should allow a better management of the finite available resources for soil fertilization and food production. Manure from farms and sludge from wastewater treatment plants are amongst the most abundant types of organic wastes that are generated annually, making them the usual candidates for organic fertilization (Bosch-Serra et al., 2020; Terrero et al., 2018).

Organic fertilizers provide plenty of benefits for soils and plant production, since they constitute relevant sources of macro- and micronutrients, enhance soil carbon levels, increase soil microbial activity, improve soil permeability and water-holding capacity, and reduce erosion (Goss et al., 2013). However, they may also contain components that can be harmful for animal, plant, and human health (Chen et al., 2018; Zhou et al., 2019). The presence of pathogens represents an obvious threat, but other pollutants, like pharmaceuticals, hormones, and antibiotics (ABs) may also represent a potential risk (Margenat et al., 2019; Tadić et al., 2021; Urra et al., 2019). In addition, the presence of antibiotic (AB) and other biocidal residues may promote the proliferation of bacterial strains resistant to multiple antimicrobial and antibiotic drugs (Bengtsson-Palme et al., 2016). Antibiotic Resistance (AR) is a natural phenomenon, but the application of organic fertilizers may step up its dissemination and evolution in the soil (Kuppusamy et al., 2018). Therefore, the potential transmission of AR from amended soils to crops and, ultimately, to consumers is a matter of major concern (Berendonk et al., 2015; Chen et al., 2016; Koch et al., 2017). Antibiotic Resistance Genes (ARGs) may spread from the organic fertilizer to the soil-plant continuum via endophytes or by adhering to plant surfaces or soil particles, although comparatively few studies have deepened in this topic (Cerqueira et al., 2019a; Marano et al., 2019). Considering those facts, and under the actual climate change scenario, there is an urgent need to consider organic sources of nutrients as key factors to a sustainable food production chain. The main question remains in finding the right balance between the benefits in support of the plant growth and the potential threats and risks (Goss et al., 2013).

The present study aims to assess the impact of using different organic fertilizers from pig slurry (raw slurry, digestate slurry, and liquid and solid slurry fractions) in commercially operative corn plots (*Zea mays*), during two consecutive harvesting cycles, and using mineral fertilizer as control. Among them, veterinary ABs (tetracyclines, lincosamides, sulfonamides, fluoroquinolones), ARGs of clinical and/or veterinarian relevance (*sul*1, *tet*M, *qnr*S1, *mec*A, bla_{TEM}, $bla_{CTX\text{-}M\text{-}32}$, $bla_{OXA\text{-}58}$,), as well as the integron gene *int*I1 (a marker of potential horizontal gene transfer activity) (Marano et al., 2019; Zheng et al., 2020), were analyzed by quantitative real-time PCR methods (qPCR) in fertilizer, soil, corn leaves and grain samples. The microbial population of each sample was also studied using high throughput 16S rDNA sequencing techniques at the ASV (Amplicon Sequence Variant), sub-species level. By integrating both sets of data, we intend to provide a global picture of the effect of these particular type of organic fertilizers in soil microbiomes and ARG loads from both agricultural soils and edible plant parts.

2. Methods

2.1 Site description and Experimental setting

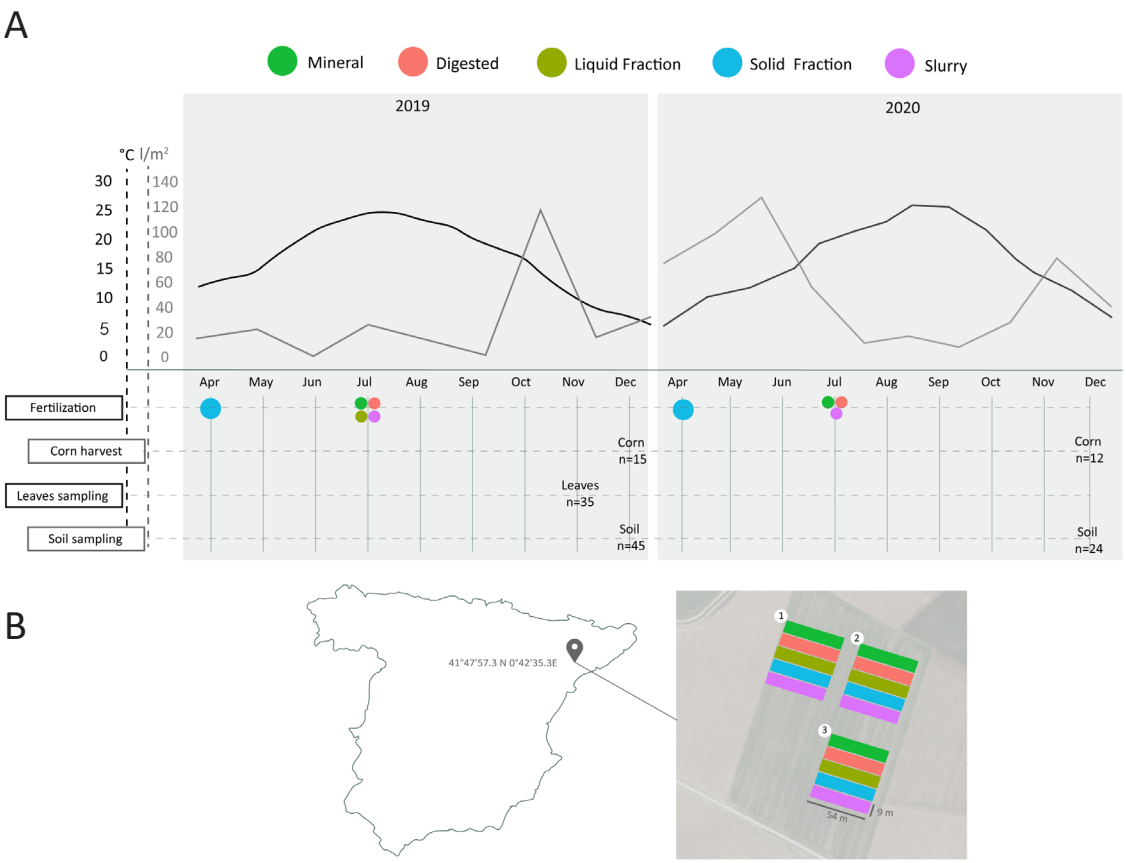

Figure 1. A) Average temperatures, daily accumulated precipitation, organic fertilizers application, harvest and sampling dates along the experimental period., **B)** Experimental plots location and setup.

The study was carried out along two harvest cycles, April 2019 – December 2019 and April 2020 – December 2020. The experimental plot covered a total of 1.8 ha and it was located at Castelló de Farfanya (Catalunya, Spain, **Figure 1**). This commercially operative corn plot included three subplots, subdivided in sections as shown in **Figure 1B**. Initial soil composition for each plot is shown in **Supplementary Table ST1**. The different sections of the plot were amended with either mineral fertilizers or with one of these four organic amendments: raw slurry from a fatting piglet farm at Castelló de Farfanya, a digested slurry derivative, based on anaerobic digestion and mixed with poultry manure) from another farm at Castelló de Farfanya, and liquid and solid fractions from a pregnant sow farm located at Soses (Catalonia, Spain), separated by sifting followed by screw pressing. The total amount of N per ha was set at 300 kg in all cases (150 kg from raw slurry, digested slurry, liquid fraction or solid fraction + 150 kg of mineral fertilizer, or 300kg of mineral fertilizer for controls). Digested, raw slurry and liquid fraction were applied using a tanker truck with a hose distributor, while solid fraction was applied using a spreader trailer; the mineral control was added manually. Irrigation was performed by sprinklers from water withdrawn from a non-polluted canal. The composition of soil amendments for sampling campaigns 2019 and 2020 is reported in **Supplementary Table ST2**. Weather conditions, schedule of fertilization, harvest and sampling and experimental setup along the two cycles are shown in **Figure 1**. The liquid fraction could not be applied at the second cycle due to COVID-19 restrictions.

2.2 Sampling and processing of organic fertilizers, soils, and vegetables

In each production cycle, organic fertilizers were sampled prior to their application. One month before harvest, one composite leave`s sample was taken from each experimental plot by cutting leaves from different heights of the corn plants and from random individuals, creating a composite sample from which five subsamples were taken. At harvest, all corn per plot was harvested using a combine harvester, forming a composite sample (five subsamples for the study). At the same time, 30 cm soil samples were taken randomly along the treatment plot with a core sampler and mixed. Samples were refrigerated (4ºC) and transported in Ziploc bags to the processing lab and treated as biological replicates. About 90g of leaves/ corn per biological replicate were processed in a grinder (Retsch GRINDOMIX GM200). The crushed material was transferred to a beaker along with 50 ml of sterile PBS, mixed thoroughly with a hand blender, and then filtered through a gauze to remove the pulp. This procedure was repeated twice to ensure a proper bacterial rinse. The flow through was then transferred to 50 ml sterile polypropylene tubes through a 100 µm mesh nylon Cell strainer (Corning® Cell Strainer), centrifuged at 4500 rpm for 15 min, and the pellets stored at -20°C until further bacterial DNA extraction.

2.3 Bacterial DNA extraction and genetic elements' quantitation

DNA from soil, organic fertilizers, and vegetal matrices (250 mg each) was extracted using the DNeasy PowerSoil Kit (Qiagen Laboratories, Inc.), to a final elution volume of 100 µl. The concentration and the quality of the DNA were tested using a NanoDrop Spectrophotometer 8000 (Thermofisher Scientific, Inc). Extracted DNA samples were stored at −20 °C. A total amount of 143 samples were extracted (n=12 for fertilisers of the first cycle, n= 35 for corn leaves of the first cycle, n=15 and n=12 for corn grains of the first and second cycle respectively, and n =45 and n=24 for soil of the first and second cycle respectively).

Absolute quantification was performed for 16S rDNA, *int*I1 and for the following set of ARGs: *sul*1 (dihydropteroate synthetase, conferring resistance to sulphonamide), *qnr*S1 (a Pentapeptide Repeat Protein family member that inhibits the effect of quinolones), *tet*M (a ribosomal protection protein, which confers tetracycline resistance by binding to the ribosome and preventing drug interaction with its binding site), *mec*A (penicillin-binding protein 2A that enables transpeptidase activity in the presence of beta-lactams, preventing them from inhibiting cell wall synthesis), and bla_{TEM}, $bla_{CTX\text{-}M\text{-}32}$, and $bla_{OXA\text{-}58}$, three β-lactamases conferring resistance to beta-lactamic antibiotics such as cephalosporins, monobactams, and carbapenems. The relevance of the chosen analysed ARGs, lies in the fact that they confer bacterial resistance to five types of antibiotics widely used in veterinary practices across Europe (EMA, 2021). It was also taken into consideration that tet and sul are generally the most abundant ARGs quantified in organic wastes specially in pig waste (He et al., 2020).

Primer sequences are listed in **Supplementary Table ST3**. A fixed dilution of 10 ng/µl of total DNA preparations was used for ARG quantification by real time qPCR in a LightCycler 480 II (A F. Hoffmann−La Roche AG, Inc), in 20 µL reaction volumes on 96-well plates. Optimal primer concentrations were 200 nM for bla_{TEM} and 300 nM for the rest of the genes. All samples were run as technical duplicates along with the quantification curve to reduce variability between assays. Plasmids used for the quantification curves were pNORM1 conjugative plasmid (Gat et al., 2017) for *int*I1, *sul*1, *qnr*S1, *tet*M, bla_{TEM}, $bla_{CTX\text{-}M\text{-}32}$, $bla_{OXA\text{-}58}$ and individual pUC19 plasmids for *mec*A, *tet*M and $bla_{OXA\text{-}58}$ (Laht et al., 2014; Szczepanowski et

al., 2009; Tamminen et al., 2011). Quantification limits (LOQ) were established as the minimum amount of plasmid that could be detected without interference from the negative control. LOQ values are reported in **Supplementary Table ST3**. The quality criteria within the standard curve was a $R^2 > 0.99$, and a slope between −3.1 and −3.4. The accepted efficiency of the reactions ranged from 97% to 100%. Melting curves were obtained to confirm amplification specificity. Dynamo ColorFlash SYBR Green (Thermo Scientific, Inc.) was used for *mec*A, *tet*M and bla_{OXA-58} qPCR quantifications; all the other genes were quantified with LightCycler 480 SYBR Green I Master (A F. Hoffmann–La Roche AG, Inc). Amplification protocol was adapted following manufacturers guidelines and different annealing temperatures were used as indicated in **Supplementary Table ST3**.

Copy numbers per gene were calculated by extrapolation from the standard curves, and expressed in relation to the processed grams of fresh weight. Prevalence values, understood as the fraction of the bacterial population harbouring a given genetic element, was estimated as copies of the genetic element per million 16S rDNA copies. Statistical analysis and plots were performed in the R environment (version 3.6.1; http://www.rproject.org/). Normality and homogeneity of the variances were checked using the Shapiro-Wilk and Levene tests, respectively. Since it was able to assume a normal distribution, an Analysis of Variance (ANOVA) followed by Tukey's B post-hoc correction for multiple tests was performed with the multcomp R package (Hothorn et al., 2016). Significance levels were set at $p \leq 0.05$.

2.4 Microbial population analysis by 16 rDNA sequencing

Bacterial communities present in fertilisers, corn, corn leaves and soil samples were analyzed by 16S sequencing analysis. Aliquots of each of the 72 extracted samples were sent to Novogene Europe (Cambridge, UK). Note that corn and corn leaves (slurry and mineral) samples were analysed as single pools for each condition. 16S rRNA genes of distinct regions (16SV4/16SV3/16SV3-V4/16SV4-V5, Arc V4) were amplified using the specific primers 515F and 806R (Caporaso et al., 2011). All PCR reactions were carried out with Phusion® High-Fidelity PCR Master Mix (New England Biolabs). Quality-checked PCR products were mixed at equal density ratios and purified by Qiagen Gel Extraction Kit (Qiagen, Germany). Sequencing libraries were generated using NEBNext Ultra DNA Library Pre ®Kit for Illumina, following manufacturer's recommendations, and index codes were added. Sequencing was carried out on an Illumina platform and 250 bp paired-end reads were generated. Quality control parameters appear in **Supplementary Table ST4**.

Clean Sequences were analysed and associated to 201,182 ASVs (Amplicon Sequence Variants) using the R package DADA2 (Callahan et al., 2016). The SILVA database v128, formatted for DADA2, was used to provide taxonomic annotation (Quast et al., 2013). The number of taxa identified and the percentage of taxon coverage (fraction of ASVs annotated to each particular taxonomic level) are shown in **Supplementary Table ST5**. Analyses for α-diversity and β-diversity analysis were performed with QIIME (Version 1.7.0). The significance of difference amongst the structure of microbial communities was analysed by a non-metric multi-dimensional scaling (NMDS) with the Bray–Curtis dissimilarity index (Bray and Curtis, 1957), using the *vegan* R package. Contributions of fertilizers to soil microbiomes were characterized using the FEAST (fast expectation-maximization for microbial source tracking) R package (Shenhav et al., 2019). Correlations between bacteria composition and AB resistance were tested by Spearman's correlations between ASV counts and genetic element abundances (ARGs and *intI*1). The

false positive discovery rate (FDR) correction was set at $p<0.05$ (Benjamini and Hochberg, 1995), using the psych R package (Revelle, 2013).

2.5 Antibiotic determination in fertilizers, soil and corn

Following the European Surveillance of Veterinary Antimicrobial Consumption analyses (EMA, 2021) and the veterinary information disclosed by the supplier farms, tetracycline, doxycycline, oxytetracycline and lincomycin were analysed in fertilizers, soil and corn grains from both harvest cycles. Detection and quantification limits, and absolute recoveries appear in **Supplementary Table ST6**. In the case of fertilizers, the analytical procedure for their determination was based on previously published method (Berendsen et al., 2015). Briefly, 500 mg of sample was subjected to ultrasound assisted extraction (UAE) with McIlvain-EDTA buffer (pH=4) and acetonitrile followed by protein precipitation, centrifugation (10min at 3500 g), solid-phase extraction (Strata X-RP, 200 mg/6 ml, Phenomenex, Torrance CA, USA) clean-up and determination by Waters Acquity Ultra-Performance Liquid Chromatography™ System (Milford, MA, USA). This system was coupled with Waters TQ-Detector (Manchester, UK) in the multiple reaction mode (MRM) with two transitions per compound,using a core-shell Kinetex® C18 column (5 cm × 2.1 mm, 2.6 µm particle size) (Phenomenex, Torrance CA, USA). Chromatographic and mass spectrometry conditions were slightly modified from the method described elsewhere (Tadić et al., 2019). Soil samples were lyophilized, sieved through a 2 mm and 0.5 g of sample was subjected to UAE with McIlvaine buffer pH = 4.0 / EDTA 0.1M (50/50, v/v). The obtained extracts were centrifuged for 15 min at 4000 rpm for two cycles. The supernatants were combined and diluted to 100 ml with H2O. Preconditioned SPE-cartridges (Strata X-RP, 200 mg/6 ml) were used for clean-up and the ABs were eluted with 4 ml methanol/ethyl acetate (50/50, v/v) evaporated to dryness, and reconstituted with 0.5 ml of the initial conditions of the mobile phase. The final determination was performed by the same instrument described above but using core-shell Ascentis® Express RP-Amide column (10 cm × 2.1 mm, 2.7 µm particle size) (Supelco, Bellefonte, PA, USA). Finally, corn grain samples were homogenized by freeze-mill using liquid N_2 and 1 g of the sample was subjected to UAE using the same extraction solvent as soil samples and centrifuged conditions. The clean-up step was performed by preconditioned Strata X-RP (100 mg/6 ml, Phenomenex, Torrance CA, USA) and the final determination by LC-MS/MS was performed as described. All antibiotic concentrations were expressed in fresh weight basis and were corrected by the specific deuterated surrogate standards.

3. Results

3.1 Occurrence of ARG and antibiotic loads in organic fertilizers, soils and corn

Organic fertilizers from both campaigns showed very high loads of all tested ARG, particularly of *sul*1 (and of its often-associated integron element *intI*1) and *tet*M, at levels exceeding the 10^9 copies per g of sample (**Figure 2**, top panel). Loads of bla_{TEM}, *qnr*S1 and $bla_{CTX\text{-}M\text{-}32}$ were relatively lower, but still significant, in all cases, ranging levels of 10^7, 10^6 and 10^5 copies per g of sample, respectively (**Figure 2**). The slurry solid fraction showed the highest ARG loads, with levels up to 3 to 5 times higher for *intI*1, *sul*1, and *qnr*S1 than the other organic fertilizers. No clear pattern in ARG content was observed for the other organic fertilizers, as their relative loads vary depending on the analyzed genetic element (**Figure 2**). On the other hand,

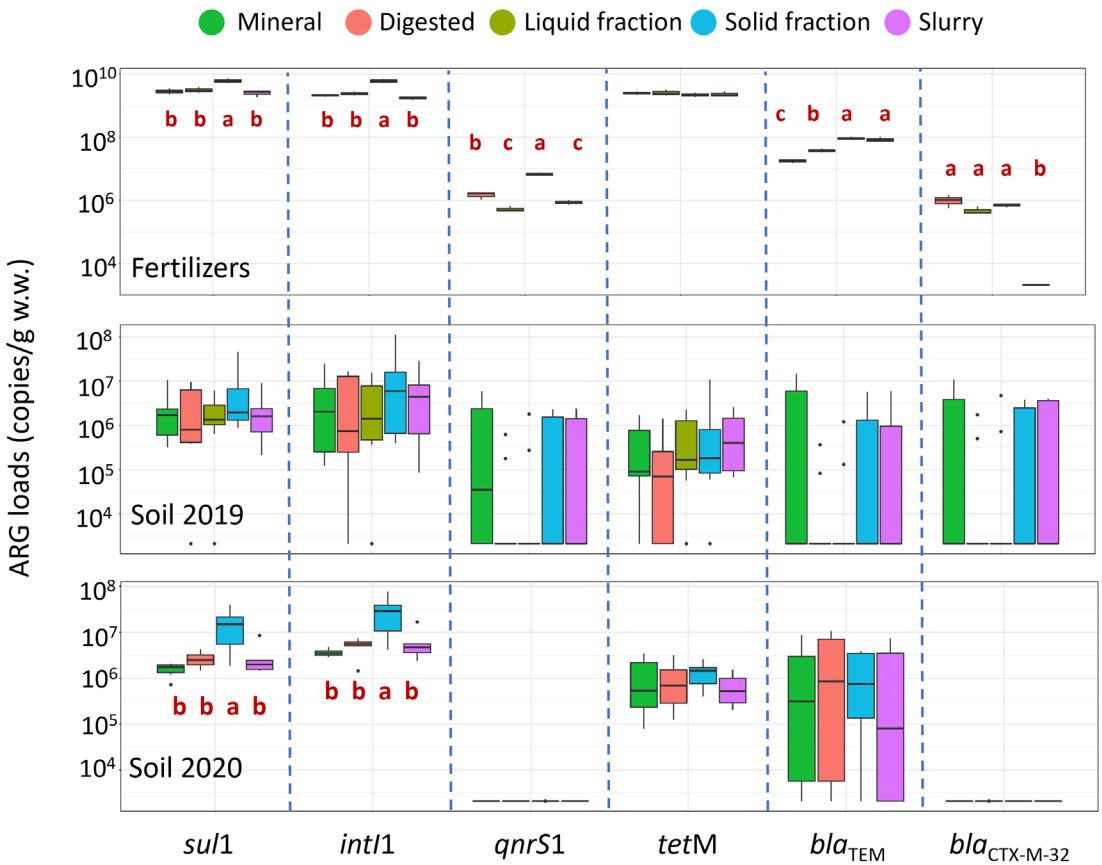

Figure 2. ARG loads in fertilizers' (top) and soil samples after the first (middle) and second (bottom) harvest. Low-case letters identify statistically different value distributions (ANOVA plus Tukey's B analyses, only significant variations are shown). Panels lacking this letter code correspond to data combinations for which no significative correlation was found. Note the logarithmic Y-scale in all plots. The liquid fraction could not be applied at the second harvest cycle due to COVID-19 restrictions.

residues of the Tetracycline AB family, Doxycycline and Oxitetracycline were only detected in the solid fraction, with remarkably high concentrations for the last two ones (11472.2 and 1217.8 ng/g fw respectively). Lincomycin was detected in all three fertilizers analyzed, finding again the highest concentration in the solid fraction, with a value of 259.9 ng/g fw (**Table 1**).

No effect of the type of fertilizer used was observed in ARG loads in soils after the first harvest (**Figure 2**, middle panel), with overall levels representing some 0.1% of the fertilizers' corresponding values. These loads increased slightly after the second harvest (**Figure 2**, bottom panel), with the difference that both *intI*1 and *sul*1 showed significant higher levels in soils fertilized with the solid fraction than the rest of soil samples (**Figure 2**). In terms of ABs, treated soil samples showed higher levels of tetracycline than the mineral group and solid fraction-fertilized soils showed the highest loads of oxytetracycline with a concentration of 351.9 ng/g fw (**Table 1**). Lincomycin showed levels below detection limit for all soils analyzed.

Corn grain samples showed no ARG loads above detection limits for any sample nor campaign (**Supplementary Table ST7**). Moreover, concentrations of antibiotics in corn grain were also below detection limits (**Table 1**) for all the experimental plots evaluated. Corn leaves showed ARG loads above detection limits for *intI*1, *sul*1, *qnr*S1 and *bla*$_{CTX-M-32}$ although the

Table 1. Range concentrations of antibiotics in fertiliser, corn and soil samples. Integrated values from 2019 to 2021. Values below the LOD are marked in italics.

		Range concentration [ng/g] fresh weight			
Matrix	Treatment	Lincomycin	Tetracycline	Doxycycline	Oxytetracycline
Fertiliser (n = 4)	Digested	95–181	*<2.0*	*<1.5* - 445	*<2.3* - 589
Fertiliser (n = 4)	Solid Fraction	220–269	21–24	1061–1192	1114–1325
Fertiliser (n = 4)	Slurry	174–1433	*<2.0*	*<1.5* - 2589	*<2.3* - 477
Fertiliser (n = 4)	Liquid Fraction	20–198	*<2.0*	*<1.5* - 636	*<2.3* - 589
Corn (n = 5)	Mineral	*<4.3*	*<5.3*	*<7.7*	*<4.3*
Corn (n = 5)	Digested	*<4.3*	*<5.3*	*<7.7*	*<4.3*
Corn (n = 5)	Solid Fraction	*<4.3*	*<5.3*	*<7.7*	*<4.3*
Corn (n = 5)	Slurry	*<4.3*	*<5.3*	*<7.7*	*<4.3*
Corn (n = 5)	Liquid Fraction	*<4.3*	*<5.3*	*<7.7*	*<4.3*
Soil (n = 9)*	Mineral	*<1.4*	*< 4.0*	*< 8.2* - 29	*< 2.6* - 44
Soil (n = 9)*	Digested	*<1.4*	18–20	59–76	33–34
Soil (n = 9)*	Solid Fraction	*<1.4*	21–25	9–60	105–335
Soil (n = 9)*	Slurry	*<1.4*	15–20	15–25	60–68
Soil (n = 9)*	Liquid Fraction	*<1.4*	n.a.	8–12	22–38

*Soil values were extrapolated from dry weight values using % Humidity of the samples (14 ± 3%).

levels were around 1% or less of those observed in soils (10^5 copies/g, **Supplementary Table ST7**). The highest average loads corresponded to intI1 and sul1 (**Supplementary Table ST7**). In any case, no significant effects of the fertilizer used was observed on the ARG loads in leaves (**Supplementary Table ST7**). Note that ABs leaves weren´t measured since they were deemed to be low due to long-term sunlight irradiation (Fiaz et al., 2021).

3.2 Microbiome analyses

Ribosomal 16S DNA sequence analysis of 72 samples of fertilizers, soils, and corn grains and leaves identified 164,858 amplicon sequence variants (ASV). Once plastid sequences were excluded (**Supplementary Table ST8**), 77.8% of the total ASV sequences were assigned to a given Family taxonomic level and 52.3% of them were identified at the Genus level (**Supplementary Table ST5**). **Figure 3** shows the ASV relative composition of the different samples, averaged by field, treatment, and harvest, labelled at the Phyla level.

Analysis of ASV distribution among the different samples revealed a very specific taxa composition for fertilizers, in which Euryarcheota (Archaea), Bacteroidota and Firmicutes were the predominant Phyla. In contrast, Proteobacteria was the dominant Phyla in the rest of samples, with variable representations of Acidobacteriota, Actinobacteriota, and Bacteroidota, among other taxa (**Figure 3**). Note that plastid sequences, not included in the figure, represented 85.38% of total grain sequences, but only 0.61% of leaves', 0.46% of soils' and 0.33% for fertilizer's microbiome sequences (**Supplementary Table ST8**).

Microbial source-tracking analysis by FEAST (Figure 4A), revealed that fertilizers' microbiome had a minor contribution to soils' microbiome (0 – 1.6%). This proportion was larger for the solid fraction (0. 5 – 1.6%), lower for the liquid fraction (0.3-0.4%) and the slurry (0.3-0.6%), and minimal for the digested slurry (0.01-0.06%). Estimations of fertilizers' contributions to corn grain and leaves microbiomes were similar to the ones observed for soils, being larger for the solid fraction (0.01– 2.9%), followed by a relatively high contribution of the slurry (0.5– 1.9%), with lower contributions of the liquid fraction (0-0.32%) and the digested slurry (0-1%). Although the presence of common ASV does not necessarily implicate cross-contamination, the results suggest that using solid fraction did increase the proportion of fertilizer's bacteria in the receiving soils, corn grain and corn leaves. Given the low fraction of soil microbiomes that could be sourced to fertilizers, it

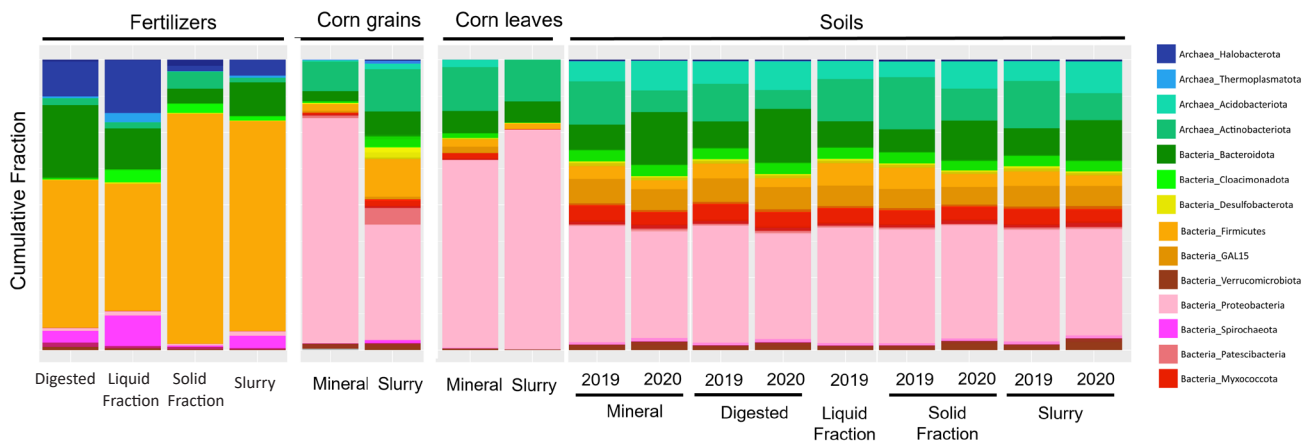

Figure 3. ASV relative distribution in fertilizers, soils and corn grains and leaves. Data correspond to the means of all replicates from each sampling and matrix. The fertilizer used in each case (or the type of fertilizer itself) is indicated at the bottom of the figure. The year of harvesting, when applicable, is also indicated at the bottom. Fertilizers, grains and leaves correspond to the 2019 campaign. ASV are labelled according to their assigned Phylum in the SILVA database (colors and taxa listed at the bottom). For simplicity, the assignation of the different color codes only includes predominant Phyla.

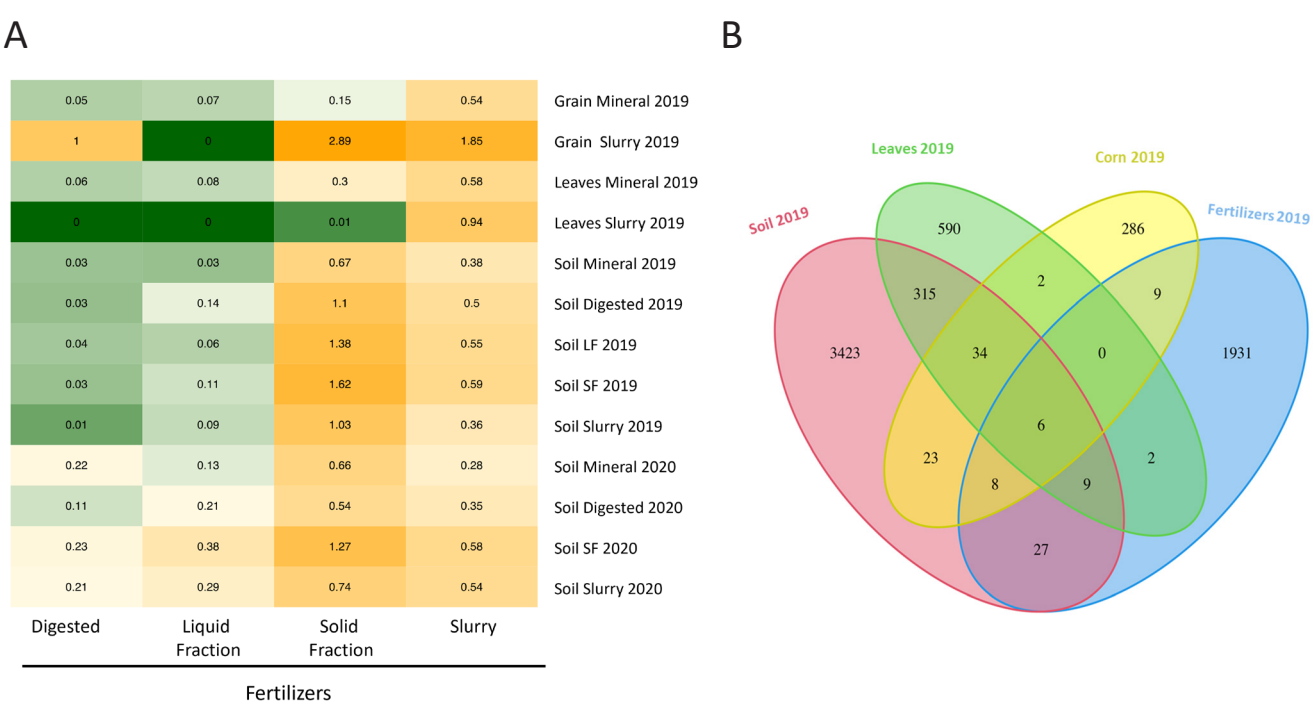

Figure 4. A) Microbial source-tracking analysis by FEAST. Figures in the graph correspond to the percentage of contribution of each "source" microbiome to each "sink" microbiome, following the FEAST nomenclature. Note that the algorithm makes no assumption about the fertilizer used in each soil, so most of the cells show background microbiome coincidence values. **B)** Venn diagram showing the distribution of individual ASVs in the different matrices. Data correspond to the 2019 campaign, and only ASV with at least 10 hits in at least one sample were considered.

is likely that most of the bacteria present in the treated soils were native from the original soil and did not come from the treatments. We observed a similar dynamyc for pathogens in which the two most abundant pathogen species in the fertiliers (*Streptococcus galloltycus* and *Corynebacterium diphtheriae*) did not appear in any of the other matrixes and the highest abundance of them two was found for the solid fraction. Note also that pathogens abundance was extremely reduced in corn, corn leaves and soil in comparison with fertilizers (**Supplementary Figure SF1**).

The distribution of common ASVs among different samples was further explored in the Venn plot in **Figure 4B** (only 2019 campaign and ASVs showing at least 10 hits in at least one sample). Most ASVs were unique for each matrix and, as seen on the FEAST analysis, it was remarkable the relatively low overlap between fertilizer samples and soil, corn and corn leaves samples, and the relative high overlap between soil and leaves samples and soil and corn samples. Therefore, the results indicate that bacteria present in the plant parts, irrespectively their relative amount, were more related to the soil microbiomes than to the fertilizer's.

Non-metric dimensional scaling (NMDS) analysis of soil microbiomes revealed a clear distinction

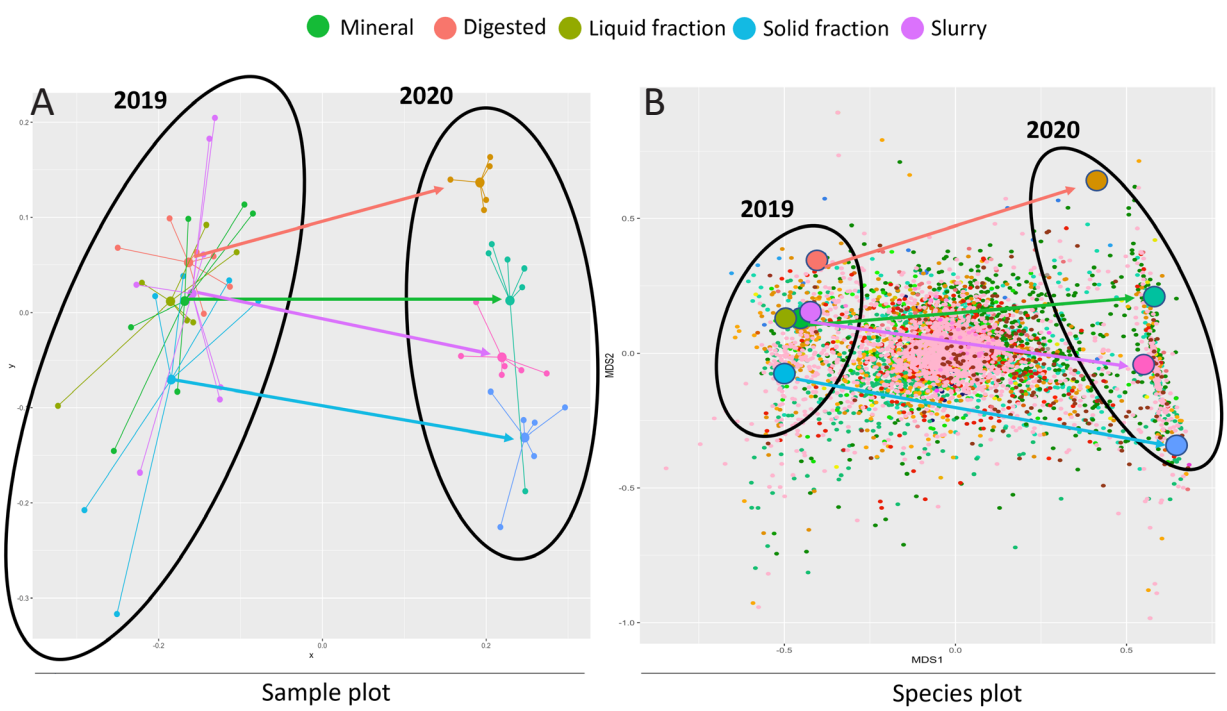

Figure 5. NDMS analysis of soil microbiomes. **A)** Sample plot", in which the different samples are placed according to their relative similarity in ASV ("Species", in NMDS terminology) content. Samples from the same campaign and treatment (small dots) are connected by lines to the resulting centroid values (large dots) and differentiated by colors (color codes on the right). Black ovals encircle 2019 and 2020 samples, arrows connect centroids corresponding to similar treatments in different campaigns. **B)** "Species plot", in which each individual ASV is placed according to their presence or absence in the different samples. For a better understanding, the relative position of centroids from the sample plots is also included in this plot as circles, using the same color code (legend on the right). Dots representing ASV are colored according their adscription to different Phyla, following the same color code as in *Figure 4*.

Table 2. PERMANOVA Adonis tests on ASV distributions among soil samples.

Two-way PERMANOVA, Treatment x Campaign				
	Df	F	*p*	
Treatment	4	1.4284	0.001	***
Campaign	1	5.0029	0.001	***
Treatment:Campaign	3	1.2098	0.023	*
One-way PERMANOVA, Treatment (2019)				
	Df	F	*p*	
Treatment	4	1.0049	0.412	
One-way PERMANOVA, Treatment (2020)				
	Df	F	*p*	
Treatment	3	1.6413	0.001	***

Significance levels: '***' 0.001 '**' 0.01 '*' 0.05.

between samples from both campaigns, whereas the type of fertilizer seemed only determinant in the ASV distribution for the 2020 samples (**Figure 5**, group on the right of both plots). Analysis of the distribution of individual ASVs ("Species plot", in NDMS terminology) showed that most of the microbiome was more or less evenly distributed in all soil samples (and therefore occupying the center of the plot). The analysis indicates that the repeated use of a same fertilizer in two consecutive agricultural campaigns increases the diversification of the microbiomes between the receiving fields, as indicated by the arrows in both plots (**Figure 5)**

Two-way PERMANOVA (Treatment x Campaign) revealed that both factors contributed to the observed variations, and a small, but significant interaction between them (**Table 2**). Parallel one-way PERMANOVA for each individual campaign indicate that soil microbiome composition was only significantly altered in the second campaign, consistent with the distribution observed in NMDS plots (**Figure 5**).

3.3 Correlation between ARG loads and bacterial taxa distribution in soils

Correlation analysis (Pearson correlation, $p \leq 0.01$, **Figure 6A**) showed strong correlations (either positives or negatives) between the relative abundance of the identified ASVs and the prevalence (copies relative to 16S rDNA copies) of the genes in soils (**Figure 6A**). Hierarchical clustering revealed that, in the case of soils from the first harvest cycle, only two Phyla (Actinobacteria and Firmicutes) composed mainly by two orders (Micrococcales and Bacillales respectively), included most of the ASV showing positive correlation with all 5 ARGs plus *int*I1, meanwhile the orders Blastocatellales, Nitrosphaerales, Gemmatimonadales, Polyangiales and Nitrospirales, showed an equally strong negative correlation with all ARG prevalence and Cytophagales correlated negatively with *int*I1 and *sul*1. On the other hand, for soils from the second harvest cycle, four orders Micromonosporales, Clostridiales, Polyangiales, Steroidobacterales and Pseudomonadales correlated positively with *int*I1 and *sul*1 and Gemmatimonadales correlated positively with *tet*M, bla_{TEM}, *qnr*S1 and $bla_{CTX\text{-}M\text{-}32}$. The different taxonomical composition of ASVs positively or negatively correlated to ARG abundance can be visualized in the relative abundance plots in **Figure 6B**, which groups ASVs showing Pearson's coefficients above 0.5 (top, 204 ASVs) or below 0.5 (bottom, 141 ASVs) in the correlations from **Figure 6A**. Analysis of fertilizer's microbiomes showed that the solid fractions presented the highest loads of ARG-positively correlated ASVs in the solid fraction,

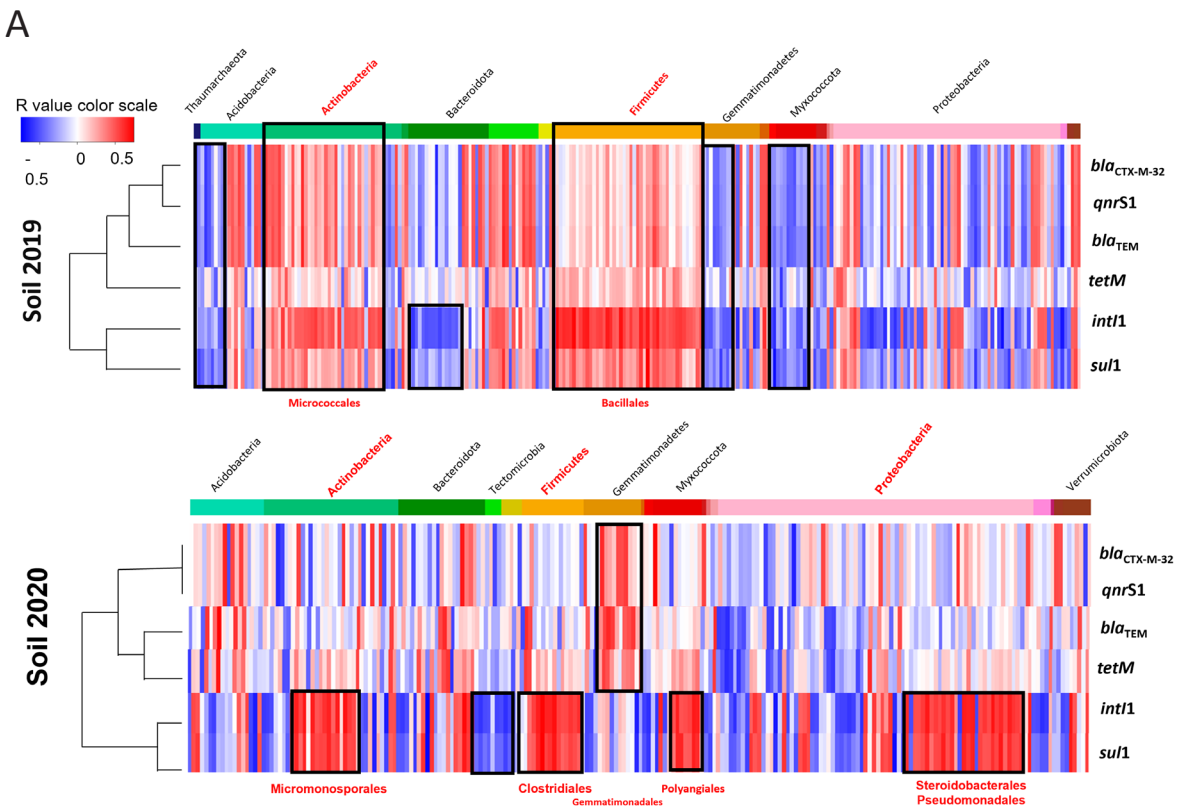

both in absolute (copies per gram of sample) and in relative (fraction of total ASVs), followed by the slurry fertilizer, whereas the liquid fraction and the digestate showed the lowest values (**Figure 6C**). Essentially all these ASVs corresponded to Firmicutes groups (data not shown), and represented almost 4% of the total bacterial load of the solid fraction (**Figure 6C**).

4. Discussion

The use of manure from intensive farming as fertilizers is a strategy that solves at the same time the disposal of a livestock waste and the need of nutrients for plant growth. However, the potential consequences of these procedures for the spreading of pharmaceuticals (including antibiotics), antibiotic resistant bacteria, ARGs, and other biological hazards may limit its widespread use. It is known that the simple action of fertilizing soils induces significant changes in the soil microbiome (Blau et al., 2019; Hartmann et al., 2015; Sun et al., 2019) and deeply alters the soil resistomes (Blau et al., 2019; Nõlvak et al., 2016; Udikovic-Kolic et al., 2014; Wolters et al., 2016; Yang et al., 2018; Zhang et al., 2017), even when using mineral fertilizers. While these alterations do not intrinsically represent any health hazard, the presence of chemical and biological contaminants in the original slurries makes necessary to control their potential translocation to the final products and, eventually, to the consumers.

There is abundant evidence on the migration of both pharmaceuticals and ARGs from fertilizers to soils and from soils to plants and crops (Cerqueira et al., 2019b; Christou et al., 2018; Rahube et al., 2014; Tadić et al., 2021). One of the conclusions of these studies is that the uptake of contaminants from soil strongly depends on the type of crop, and that the final potential risk for consumers

B

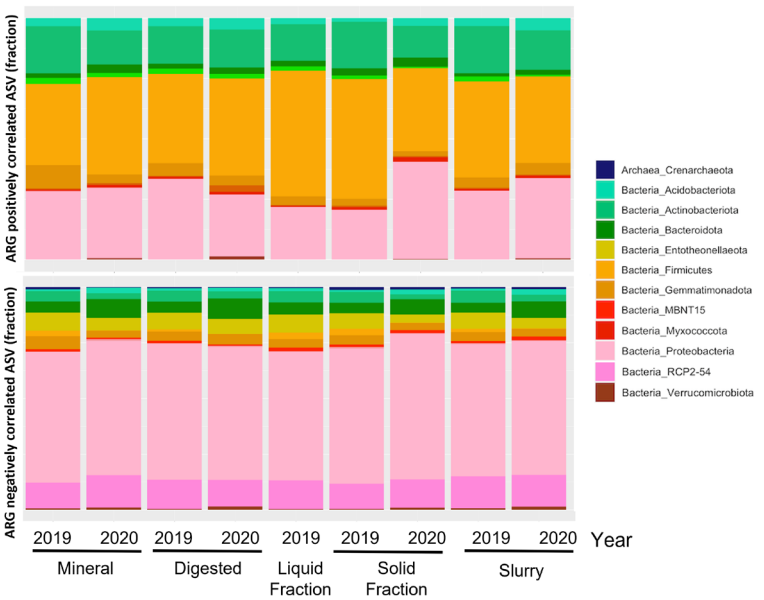

C

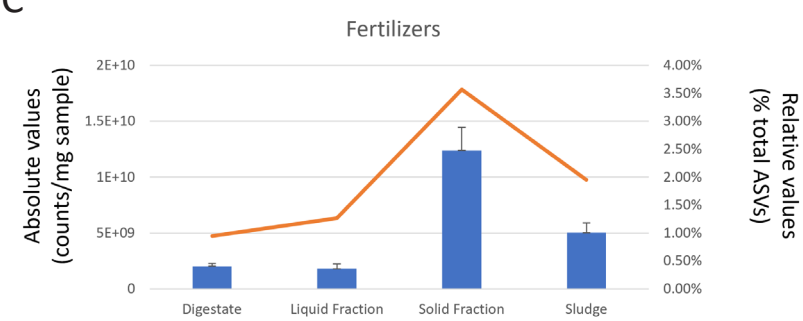

Figure 6. A) Correlation analysis (Pearson) between ASV abundance and genetic element prevalence (copies per 16S rDNA copy) among soil samples from both harvest cycles. Only AVS with significative correlation with at least one genetic element are represented. Red and blue sectors correspond to positive and negative correlations, respectively (color scale on top). Names of some relevant Phyla are indicated at the top; names of some bacterial orders are also indicated at the bottom of the graphs. Genetic elements were grouped by hierarchical clustering. ASVs are ordered taxonomically, as indicated by the color bar at the top of the heatmaps, which follows the same color-code as in Figure 3. **B)** Relative distribution in fertilizers of ASVs positively- (top) or negatively- (bottom) correlated to soil ARG loads, represented as in Figure 3. **C)** Integrated absolute loads (blue bars, counts per g of sample) as relative abundances (orange line, % of total ASVs) in fertilizers of ASVs positively correlated to soil ARG loads. Bars represent average values, whiskers correspond to standard deviation (n=3 for all fertilizers).

varies depending on the part of the plant used as food or fodder (Cerqueira et al., 2019b; Christou et al., 2018). Our results with corn are wholly consistent with these data, as cereals and grains are supposed to have a moderate to low uptake capacity and low ARG content than leafy crops or vegetables (Cerqueira et al., 2019b; Christou et al., 2018; Domínguez et al., 2014; Margenat et al., 2017; Tadić et al., 2020). Indeed, the virtual absence of ARG and ABs in grains and their moderate presence in corn leaves was predictable when considering these antecedents. This is an important conclusion of our study, as it identifies a global staple food crop, as it is corn, as potential recipient for animal slurry-based fertilizers with only a minor added hazard of contributing to the spread of ARG-harboring bacteria in consumers' guts. Although not specifically proven, it is likely that the same overall conclusion can be applied to other cereals and pseudo-cereal crops.

Organic fertilizers, and particularly those originated from animal farm slurry, present high levels of pharmaceuticals (including antibiotics), antibiotic resistant bacteria and ARGs, partially due to ill-controlled pharmaceutical treatments of animals (Sanz et al., 2021). This presence should be taken into consideration on the use of these potentially very advantageous source of nutrients in agriculture, and should promove the setting of legal requirements regarding the intensity and timing of their application. While our results support the use of organic fertilizer in corn

fields under the current legal limitations, they also represent a call for caution in several aspects. In the first place, we observed an increase on *int*I1 and sul1 levels in soils, as well as higher levels of tetracyclines, in samples fertilized with the slurry solid fraction. We also found higher contributions of the solid fraction´s microbiome into all samples' microbiomes than the rest of fertilizers. More than a direct cause-relationship between AB and ARG levels in soils, we consider these coincidences as an indicator of a higher impact of this fraction in soils relative to digested fertilizers, liquid fraction, or even to the raw slurry. Our current hypothesis is that these levels correspond to the selective pressure occurring either in the pig guts or, less likely, in the decantation ponds, as revealed by the very high loads of intI1, sul1, tetM, and Tetracyclines we find in fertilizers derived from pig slurry (Sanz et al., 2021), this paper).

ARG loads in soils appeared linked mostly to the orders Micrococcales and Bacillales for the first harvest cycle, and intI1 and sul1 to the orders Micromonosporales, Clostridiales, Polyangiales and to the Gamma-Proteobacteria orders Steroidobacterales and Pseudomonadales for the second harvest cycle. Some of these groups were also found linked to high ARGs loads in fertilizers (Sanz et al., 2021) and to high ARG prevalence in soils, plants, and fruits (Cerqueira et al., 2019b; Fogler et al., 2019). The data also showed higher levels of intI1 and sul1 and higher diversification of the microbiomes for the soils of the second cycle relatively to the first-cycle soils, and that the type of fertilizer was only determinant in the ASV distribution for the second cycle samples. We conclude from these two lines of evidence that there was an impact of a repeated use of fertilizers in two consecutive harvest cycles. A similar temporal trend was observed in experimental orchards fertilized with either organic or mineral fertilizers, as ARG total loads, ARG profiles and ASV distribution among soil samples depended on the time elapsed between fertilization and sampling (Sanz et al., 2021).

Our results suggest that, while the current directions on the application of swine fertilizers in agricultural soils are probably sufficient to minimize the potential risk associated the AB phenomenon, it is very likely that any relaxation on the rules of fertilizer intensity or timing of application may result in an increase of ARG levels in soils, the subsequent transmission to the plant and, ultimately, to leaves and grains. With the current data, it is difficult to identify which characteristics of the different fractions and derivatives are determinant for these effects, but in this case, it is clear that bacteria from the solid fraction reached a higher prevalence in the soil than those from other fertilizers. The solid fraction also showed the highest loads of ASVs identified as being positively correlated to ARG prevalence in soils, fact that could explain the increase on ARGs seen in soils treated with this fraction in the second cycle. In contrast, the liquid fraction and the digestate showed both the lowest capacity of altering the soils microbiome and the lowest proportion of ARG-positively correlated ASVs. We consider that this data indicates that the implementation of treatments (e.g., composting or digestion) to the initial slurry may reduce ARG loads and/or the alteration of soil microbiomes by the fertilizer. This notwithstanding, it is clear that the most straightforward measure to reduce the global risk associated to pharmaceuticals, antibiotics and ARGs should be the reduction of these elements by continuing to implement and optimise the actual animal-production practices on farms. (Muurinen et al., 2017; Sneeringer and Clancy, 2020).

Author contributions

Claudia Sanz, Marta Casado, Laia Navarro-Marin: Molecular methods development and analyses. Edward Pastor-López, Josep Ma Bayona: Antibiotic determination, risk analysis, Joan Parera, Carlos A Ortiz, Jordi Tugues: Field work, nutrient determination and assessment, Benjamin Piña: Statistical analyses, Jordi Tugues, Josep Ma Bayona, Benjamin Piña: Experimental design, team coordination, and manuscript organization and revision.

Declaration of competing interest

The authors declare that they have no known competing financial interests or personal relationships that could have appeared to influence the work reported in this paper.

Acknowledgements

This work was supported by grants from the LIFE Program of the European Union (LIFE17 ENV/ES/000439), the Spanish Ministry of Science, Innovation and University (MCIN/AEI/10.13039/501100011033, grant RTI2018-096175-B-I00), and the Generalitat de Catalunya (2017SGR902). CSL was supported by a FI predoctoral fellowship from the Generalitat de Catalunya and the European Social Fund (2018 FI B 00368, ESF Investing in your future). IDAEA-CSIC is a Centre of Excellence Severo Ochoa (Spanish Ministry of Science and Innovation, Project CEX2018-000794-S, ERDF A way of making Europe).

Bibliography

Bengtsson-Palme, J., Hammarén, R., Pal, C., Östman, M., Björlenius, B., Flach, C.F., Fick, J., Kristiansson, E., Tysklind, M., Larsson, D.G.J., 2016. Elucidating selection processes for antibiotic resistance in sewage treatment plants using metagenomics. Sci. Total Environ. 572, 697–712. https://doi.org/10.1016/j.scitotenv.2016.06.228

Benjamini, Y., Hochberg, Y., 1995. Controlling the false discovery rate: A practical approach to multiple testing. J R Stat Soc 57, 289–300.

Berendonk, T.U., Manaia, C.M., Merlin, C., Fatta-Kassinos, D., Cytryn, E., Walsh, F., Buergmann, H., Sorum, H., Norstrom, M., Pons, M.-N., Kreuzinger, N., Huovinen, P., Stefani, S., Schwartz, T., Kisand, V., Baquero, F., Luis Martinez, J., 2015. Tackling antibiotic resistance: the environmental framework. Nat. Rev. Microbiol. 13, 310–317. https://doi.org/10.1038/nrmicro3439

Berendsen, B.J.A., Wegh, R.S., Memelink, J., Zuidema, T., Stolker, L.A.M., 2015. The analysis of animal faeces as a tool to monitor antibiotic usage. Talanta 132, 258–268. https://doi.org/10.1016/j.talanta.2014.09.022

Blau, K., Jacquiod, S., Sorensen, S.J., Su, J.Q., Zhu, Y.G., Smalla, K., Jechalke, S., 2019. Manure and Doxycycline Affect the Bacterial Community and Its Resistome in Lettuce Rhizosphere and Bulk Soil. Front Microbiol 10, 725. https://doi.org/10.3389/fmicb.2019.00725

Bosch-Serra, A.D., Yagüe, M.R., Valdez, A.S., Domingo-Olivé, F., 2020. Dairy cattle slurry fertilization management in an intensive Mediterranean agricultural system to sustain soil quality while enhancing rapeseed nutritional value. J. Environ. Manage. 273, 111092. https://doi.org/10.1016/j.jenvman.2020.111092

Bray, J.R., Curtis, J.T., 1957. An Ordination of the Upland Forest Communities of Southern Wisconsin. Ecol. Monogr. 27, 325–349. https://doi.org/10.2307/1942268

Callahan, B.J., McMurdie, P.J., Rosen, M.J., Han, A.W., Johnson, A.J.A., Holmes, S.P., 2016. DADA2: High-resolution sample inference from Illumina amplicon data. Nat. Methods 13, 581-+. https://doi.org/10.1038/nmeth.3869

Caporaso, J.G., Lauber, C.L., Walters, W.A., Berg-Lyons, D., Lozupone, C.A., Turnbaugh, P.J., Fierer, N., Knight, R., 2011. Global patterns of 16S rRNA diversity at a depth of millions of sequences per sample. Proc. Natl. Acad. Sci. U. S. A. 108, 4516–4522. https://doi.org/10.1073/PNAS.1000080107

Cerqueira, F., Matamoros, V., Bayona, J., Piña, B., 2019a. Antibiotic resistance genes distribution in microbiomes from the soil-plant-fruit continuum in commercial Lycopersicon esculentum fields under different agricultural practices. Sci. Total Environ. 652, 660–670. https://doi.org/10.1016/j.scitotenv.2018.10.268

Cerqueira, F., Matamoros, V., Bayona, J.M., Berendonk, T.U., Elsinga, G., Hornstra, L.M., Piña, B., 2019b. Antibiotic resistance gene distribution in agricultural fields and crops. A soil-to-food analysis. Environ. Res. 177, 108608. https://doi.org/10.1016/j.envres.2019.108608

Chen, Q., An, X., Li, H., Su, J., Ma, Y., Zhu, Y.G., 2016. Long-term field application of sewage sludge increases the abundance of antibiotic resistance genes in soil. Environ. Int. 92–93, 1–10. https://doi.org/10.1016/j.envint.2016.03.026

Chen, Q.L., An, X.L., Zheng, B.X., Ma, Y.B., Su, J.Q., 2018. Long-term organic fertilization increased antibiotic resistome in phyllosphere of maize. Sci. Total Environ. https://doi.org/10.1016/j.scitotenv.2018.07.260

Christou, A., Papadavid, G., Dalias, P., Fotopoulos, V., Michael, C., Bayona, J.M., Piña, B., Fatta-Kassinos, D., 2018. Ranking of crop plants according to their potential to uptake and accumulate contaminants of emerging concern. Environ. Res. 170, 422–432. https://doi.org/10.1016/j.envres.2018.12.048

Domínguez, C., Flores, C., Caixach, J., Mita, L., Piña, B., Comas, J., Bayona, J.M., 2014. Evaluation of antibiotic mobility in soil associated with swine-slurry soil amendment under cropping conditions. Environ. Sci. Pollut. Res. 21. https://doi.org/10.1007/s11356-014-3174-3

Fogler, K., Guron, G.K.P., Wind, L.L., Keenum, I.M., Hession, W.C., Krometis, L.A., Strawn, L.K., Pruden, A., Ponder, M.A., 2019. Microbiota and Antibiotic Resistome of Lettuce Leaves and Radishes Grown in Soils Receiving Manure-Based Amendments Derived From Antibiotic-Treated Cows. Front. Sustain. Food Syst. 3, 1–17. https://doi.org/10.3389/fsufs.2019.00022

Gat, D., Mazar, Y., Cytryn, E., Rudich, Y., 2017. Origin-Dependent Variations in the Atmospheric Microbiome Community in Eastern Mediterranean Dust Storms. Environ. Sci. Technol. 51, 6709–6718. https://doi.org/10.1021/acs.est.7b00362

Goss, M.J., Tubeileh, A., Goorahoo, D., 2013. A Review of the Use of Organic Amendments and the Risk to Human Health, in: Advances in Agronomy. Academic Press Inc., pp. 275–379. https://doi.org/10.1016/B978-0-12-407686-0.00005-1

Hartmann, M., Frey, B., Mayer, J., Mader, P., Widmer, F., 2015. Distinct soil microbial diversity under long-term organic and conventional farming. ISME J 9, 1177–1194. https://doi.org/10.1038/ismej.2014.210

Hothorn, T., Bretz, F., Westfall, P., Heiberger, R.M., Schuetzenmeister, A., Scheibe, S., Hothorn, M.T., 2016. Package 'multcomp.'

Koch, B.J., Hungate, B.A., Price, L.B., 2017. Food-animal production and the spread of antibiotic resistance: the role of ecology. Front. Ecol. Environ. 15, 309–318. https://doi.org/10.1002/fee.1505

Kuppusamy, S., Kakarla, D., Venkateswarlu, K., Megharaj, M., Yoon, Y.E., Lee, Y.B., 2018. Veterinary antibiotics (VAs) contamination as a global agro-ecological issue: A critical view. Agric. Ecosyst. Environ. 257, 47–59. https://doi.org/10.1016/j.agee.2018.01.026

Laht, M., Karkman, A., Voolaid, V., Ritz, C., Tenson, T., Virta, M., Kisand, V., 2014. Abundances of Tetracycline, Sulphonamide and Beta-Lactam Antibiotic Resistance Genes in Conventional Wastewater Treatment Plants (WWTPs) with Different Waste Load. PLoS One 9. https://doi.org/10.1371/journal.pone.0103705

Marano, R.B.M., Zolti, A., Jurkevitch, E., Cytryn, E., 2019. Antibiotic resistance and class 1 integron gene dynamics along effluent, reclaimed wastewater irrigated soil, crop continua: elucidating potential risks and ecological constraints. Water Res. https://doi.org/10.1016/j.watres.2019.114906

Margenat, A., Matamoros, V., Díez, S., Cañameras, N., Comas, J., Bayona, J.M., 2019. Occurrence and human health implications of chemical contaminants in vegetables grown in peri-urban agriculture. Environ. Int. 124, 49–57. https://doi.org/10.1016/j.envint.2018.12.013

Margenat, A., Matamoros, V., Díez, S., Cañameras, N., Comas, J., Bayona, J.M., 2017. Occurrence of chemical contaminants in peri-urban agricultural irrigation waters and assessment of their phytotoxicity and crop productivity. Sci. Total Environ. 599–600, 1140–1148. https://doi.org/10.1016/j.scitotenv.2017.05.025

Muurinen, J., Stedtfeld, R., Karkman, A., Pärnänen, K., Tiedje, J., Virta, M., 2017. Influence of Manure Application on the Environmental Resistome under Finnish Agricultural Practice with Restricted Antibiotic Use. Environ. Sci. Technol. 51, 5989–5999. https://doi.org/10.1021/acs.est.7b00551

Nõlvak, H., Truu, M., Kanger, K., Tampere, M., Espenberg, M., Loit, E., Raave, H., Truu, J., 2016. Inorganic and organic fertilizers impact the abundance and proportion of antibiotic resistance and integron-integrase genes in agricultural grassland soil. Sci. Total Environ. 562, 678–689. https://doi.org/10.1016/j.scitotenv.2016.04.035

Quast, C., Pruesse, E., Yilmaz, P., Gerken, J., Schweer, T., Yarza, P., Peplies, J., Glöckner, F.O., 2013. The SILVA ribosomal RNA gene database project: Improved data processing and web-based tools. Nucleic Acids Res. 41, 590–596. https://doi.org/10.1093/nar/gks1219

Rahube, T.O., Marti, R., Scott, A., Tien, Y.C., Murray, R., Sabourin, L., Zhang, Y., Duenk, P., Lapen, D.R., Topp, E., 2014. Impact of Fertilizing with Raw or Anaerobically Digested Sewage Sludge on the Abundance of Antibiotic-Resistant Coliforms, Antibiotic Resistance Genes, and Pathogenic Bacteria in Soil and on Vegetables at Harvest. Appl. Environ. Microbiol. 80, 6898–6907. https://doi.org/10.1128/aem.02389-14

Revelle, W., 2013. psych: Procedures for Psychological, Psychometric, and Personality Research. R Package Version 1.0-95. Evanston, Illinois.

Sanz, C., Casado, M., Navarro-Martin, L., Tadić, Đ., Parera, J., Tugues, J., Bayona, J.M., Piña, B., 2021. Antibiotic and antibiotic-resistant gene loads in swine slurries and their digestates: Implications for their use as fertilizers in agriculture. Environ. Res. 194. https://doi.org/10.1016/j.envres.2020.110513

Shenhav, L., Thompson, M., Joseph, T.A., Briscoe, L., Furman, O., Bogumil, D., Mizrahi, I., Pe'er, I., Halperin, E., 2019. FEAST: fast expectation-maximization for microbial source tracking. Nat. Methods 16, 627–632. https://doi.org/10.1038/s41592-019-0431-x

Sneeringer, S., Clancy, M., 2020. Incentivizing New Veterinary Pharmaceutical Products to Combat Antibiotic Resistance. Appl. Econ. Perspect. Policy 42, 653–673. https://doi.org/10.1093/aepp/ppz022

Sun, Y., Qiu, T., Gao, M., Shi, M., Zhang, H., Wang, X., 2019. Inorganic and organic fertilizers application enhanced antibiotic resistome in greenhouse soils growing vegetables. Ecotoxicol. Environ. Saf. 179, 24–30. https://doi.org/10.1016/j.ecoenv.2019.04.039

Szczepanowski, R., Linke, B., Krahn, I., Gartemann, K.-H., Gützkow, T., Eichler, W., Pühler, A., Schlüter, A., 2009. Detection of 140 clinically relevant antibiotic-resistance genes in the plasmid metagenome of wastewater treatment plant bacteria showing reduced susceptibility to selected antibiotics. Microbiology 155, 2306–2319. https://doi.org/https://doi.org/10.1099/mic.0.028233-0

Tadić, Đ., Bleda Hernandez, M.J., Cerqueira, F., Matamoros, V., Piña, B., Bayona, J.M., 2021. Occurrence and human health risk assessment of antibiotics and their metabolites in vegetables grown in field-scale agricultural systems. J. Hazard. Mater. 401, 123424. https://doi.org/https://doi.org/10.1016/j.jhazmat.2020.123424

Tadić, Đ., Gramblicka, M., Mistrik, R., Flores, C., Piña, B., Bayona, J.M., 2020. Elucidating biotransformation pathways of ofloxacin in lettuce (Lactuca sativa L). Environ. Pollut. 260. https://doi.org/10.1016/j.envpol.2020.114002

Tadić, Đ., Matamoros, V., Bayona, J.M., 2019. Simultaneous determination of multiclass antibiotics and their metabolites in four types of field-grown vegetables. Anal. Bioanal. Chem. 411, 5209–5222. https://doi.org/10.1007/s00216-019-01895-y

Tamminen, M., Karkman, A., Lohmus, A., Muziasari, W.I., Takasu, H., Wada, S., Suzuki, S., Virta, M., 2011. Tetracycline Resistance Genes Persist at Aquaculture Farms in the Absence of Selection Pressure. Environ. Sci. Technol. 45, 386–391. https://doi.org/10.1021/es102725n

Terrero, M.A., Faz, Á., Ondoño, S., Muñoz, M.Á., 2018. Chapter 14 - Impacts of Raw and Purified Pig Slurry on Carbon and Nitrogen Contents in Mediterranean Agricultural Soil, in: Muñoz, M.Á., Zornoza, R. (Eds.), Soil Management and Climate Change. Academic Press, pp. 207–219. https://doi.org/10.1016/B978-0-12-812128-3.00014-8

Udikovic-Kolic, N., Wichmann, F., Broderick, N.A., Handelsman, J., 2014. Bloom of resident antibiotic-resistant bacteria in soil following manure fertilization. Proc. Natl. Acad. Sci. U. S. A. 111, 15202–15207. https://doi.org/10.1073/pnas.1409836111

Urra, J., Alkorta, I., Garbisu, C., 2019. Potential benefits and risks for soil health derived from the use of organic amendments in agriculture. Agronomy 9, 1–23. https://doi.org/10.3390/agronomy9090542

Wolters, B., Widyasari-Mehta, A., Kreuzig, R., Smalla, K., 2016. Contaminations of organic fertilizers with antibiotic residues, resistance genes, and mobile genetic elements mirroring antibiotic use in livestock? Appl. Microbiol. Biotechnol. 100, 9343–9353. https://doi.org/10.1007/s00253-016-7742-y

Yang, L., Liu, W., Zhu, D., Hou, J., Ma, T., Wu, L., Zhu, Y., Christie, P., 2018. Application of biosolids drives the diversity of antibiotic resistance genes in soil and lettuce at harvest. Soil Biol. Biochem. https://doi.org/10.1016/j.soilbio.2018.04.017

Zhang, Y.J., Hu, H.W., Gou, M., Wang, J.T., Chen, D., He, J.Z., 2017. Temporal succession of soil antibiotic resistance genes following application of swine, cattle and poultry manures spiked with or without antibiotics. Environ. Pollut. 231, 1621–1632. https://doi.org/10.1016/j.envpol.2017.09.074

Zheng, W., Huyan, J., Tian, Z., Zhang, Y., Wen, X., 2020. Clinical class 1 integron-integrase gene – A promising indicator to monitor the abundance and elimination of antibiotic resistance genes in an urban wastewater treatment plant. Environ. Int. https://doi.org/10.1016/j.envint.2019.105372

Zhou, S.Y.D., Zhu, D., Giles, M., Yang, X.R., Daniell, T., Neilson, R., Zhu, Y.G., 2019. Phyllosphere of staple crops under pig manure fertilization, a reservoir of antibiotic resistance genes. Environ. Pollut. https://doi.org/10.1016/j.envpol.2019.05.098

CHAPTER THREE.

BIOLOGICAL RISKS ASSOCIATED TO WASTEWATER EFFLUENTS. ROLE OF SAT TECHNOLOGIES

Use of soil-aquifer treatment to efficiently remove microbial pathogens and antibiotic resistance genes from treated wastewaters

Claudia Sanz[1], Marta Casado[1], Lurdes Martinez-Landa[2,3], Cristina Valhondo[1,2,4], Stefano Amalfitano[5], Francesca Di Pippo[5], Caterina Levantesi[5], Jesús Carrera[1,2], Benjamin Piña[1]

1) IDAEA-CSIC, Jordi Girona, 18. E-08034, Barcelona, Spain

2) Associated Unit: Hydrogeology Group (UPC-CSIC)

3) Dept. of Civil and Environmental Engineering. Universitat Politècnica de Catalunya, Barcelona, Spain

4) Geosciences Montpellier, Université de Montpellier, CNRS, Montpellier, France

5) Water Research Institute, National Research Council of Italy (IRSA-CNR), Monterotondo, Rome, 00015, Italy

To be submitted

Abstract

Soil Aquifer Treatment (SAT) is a robust technology to increase groundwater recharge and to enhance reclaimed water quality. SAT is known to reduce Dissolved Organic Carbon, contaminants of emerging concern, nutrients and colloidal matter, including pathogen indicators, but much less is known about its effect on the loads of antibiotic resistance genes (ARGs) present in reclaimed waters. We tested six pilot SAT systems, five of them enhanced with reactive barriers, for their capacity to remove ARGs, pathogens, and wastewater bacterial groups from a wastewater treatment plant (WWTP) secondary effluent. Water samples were taken during three recharge episodes (June 2020, October 2020, and September 2021) with different SAT operations (continuous or pulsed recharge). Using flow cytometry, PCR, and 16S rRNA gene amplicon sequencing methods, we determined that all six SAT systems reduced total loads of bacteria by more than 90% and of clinically relevant ARG by more than 95%. These efficiencies are similar to those of UV/oxidation or membrane-based tertiary treatments, which require much more energy and resources. Variations in reactive barrier composition, season, or flow regime did not affect significantly ARG removal, although they did alter significantly the microbial community composition, which suggests that further improvements can be obtained by an adequate design of the SAT reactive barriers. We observed an ecological succession of bacterial groups, linked to the changing physical-chemical conditions along the SAT, and likely correlated to the removal of ARGs. Overall results present SAT as cost-efficient technologies able to dramatically reduce ARG loads and other biological hazards from WWTP secondary effluents.

1. Introduction

According to the Food and Agriculture Organization ofthe United Nations (FAO), the world population will reach 9,000 million inhabitants by 2050, which will lead to an increase in water demand for domestic, agricultural production and industrial purposes. This demand is often supplied by increasing groundwater pumping (Konikow and Kendy, 2005). This strategy, coupled with climate change, is causing groundwater levels to decrease globally, regionally, and locally (Aeschbach-Hertig and Gleeson, 2012; Gurdak, 2017; Wada et al., 2010). Depressed groundwater levels favor seawater intrusion and limit groundwater discharge to springs, streams and wetlands, which lose part of their ecological services (Konikow and Kendy, 2005; Valhondo and Carrera, 2019; Wada et al., 2010).

A strategy to revert this situation is to increase groundwater recharge by infiltrating reclaimed water through Managed Aquifer Recharge (MAR) technologies (Dillon, 2005; Valhondo and Carrera, 2019; Dillon et al., 2020). Soil Aquifer Treatment (SAT) is a form of MAR that consists of infiltrating reclaimed water into the aquifer through the soil and the vadose zone, thus increasing groundwater resources while improving the quality of the recharged wastewater and benefiting groundwater-dependent ecosystems. The main concern about SAT is that effluents from waste water treatment plants (WWTPs) contain variable concentrations of Contaminants of Emerging Concern (CECs) such as many biologically active compounds, including antibiotics (ABs), pharmaceutical and personal care products (PPCPs), and endocrine disruptors (EDs), both natural and synthetic. Many of these are particularly refractory to the conventional WWTP treatment technologies (Kumar et al., 2022).

The efficiency of SAT in regenerating water free of CECs and pathogens can be boosted by the installation of reactive barriers (RBs). RBs include sorptive materials in order to increase the residence time of pollutants, thus facilitating their degradation. RBs also induce the development of a broad range of redox conditions (e.g., iron and manganese reducing) and a potential diversification of bacterial communities. The resulting diversity of microbial communities contributes to, first, facilitate biological degradation of compounds that are refractory to the comparatively more uniform digestions occurring at WWTPs, and, second, to limit or preclude growth of enteric bacteria, due to unfavorable environmental conditions. In fact, RB have been proven to contribute to the removal of both CECs and pathogen indicators (*E. coli* and Enterococci, Valhondo et al., 2020a, 2020b).

These redox states might be enhanced via water infiltration through a pulsating recharge. In this type of recharge, oxygen is pushed into the soil as the water level drops during the dry period and pushed out by the flowing water during the next wet period resulting in a much more oxidizing redox state when compared with a continuous recharge (Arad et al., 2022). This oxygen boost might also help reduce the high ammonium content of the WWTP effluent enabling higher nitrification rates.

WWTP effluents represent a substantial biological hazard beyond chemical pollutants. They may contain pathogens, parasites, viruses, antibiotic resistant bacteria (ARB) and antibiotic-resistance genes (ARGs). It is precisely the simultaneous presence of ABs, ARB and ARGs what makes WWTP effluents dangerous hotspots for antibiotic-resistance growth and dissemination in the environment (Pazda et al 2019). Antimicrobial resistance among human pathogens produces more 20,000 deaths annually in both the United States of America and the European Union (CDC, 2021), which makes it a severe problem. But it is this wide spread what makes it a maximum global challenge for which no short-term solutions exist (WHO, 2014). Research and public efforts appear

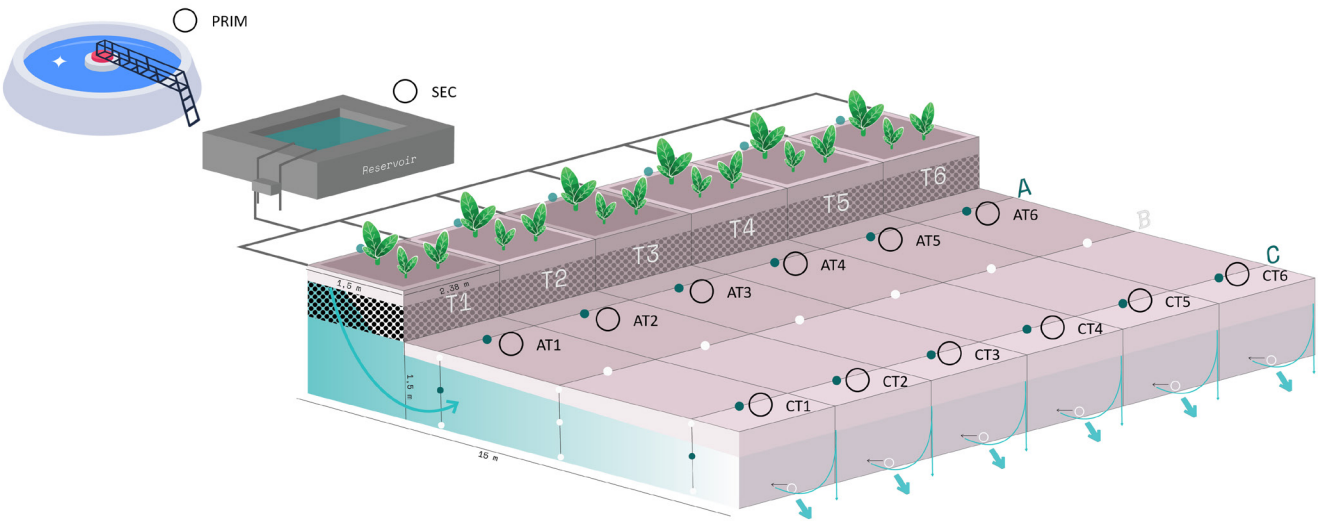

Figure 1. Graphic scheme of the six pilot SAT systems (T1 to T6) fed with WWTP effluent, and location of sampling points (A and C piezometers). Water reaches the recharge areas, infiltrates vertically through narrow unsaturated zones, and flows horizontally through the aquifer. Blue arrows indicate water flow.

to concentrate on monitoring this spread and seeking alternative antimicrobial pharmaceuticals (Larsson and Flach, 2022). We conjecture that the efficiency of SAT in removing organic pollutants and pathogens from reclaimed water may also contribute in reducing ARB and ARGs. But there are only a few studies addressing the behavior of ARGs in conventional SAT systems (Pei et al., 2019; Elkayam et al., 2018), and none in the case of SAT enhanced with RBs.

In this context, the aim of this study was to assess the efficiency of SAT systems to regenerate WWTP effluents by lowering the ARG and microbial pathogen load, and to evaluate the role of the reactive barrier composition and operational parameters, such as and recharge regime (continuous vs pulsating) in reducing the biological hazard of reusing reclaimed water for aquifer recovery.

2. Methods

2.1 Description of the pilot SAT systems and their operation

Six pilot SAT systems (named T1 to T6) were built in a WWTP facility to study the role of reactive barriers in recharged water quality enhancement (**Figure 1**). The WWTPs is located in the Nord-East Mediterranean Spanish coast and collects wastewater from several municipalities with seasonally varying population, reaching its maximum capacity in summer. Thus, the quality of its effluent may vary considerably throughout the year (see **Supplementary Table ST1** and (Valhondo et al., 2020b). The plant integrates a pre-treatment, primary treatment, biologic secondary treatment (activated sludge), and secondary settlers.

The effluent of the secondary treatment of the WWTP was stored in a reservoir (10 m^3 with a residence time around 24 h, continuously re-filled from the base with the effluent water) and pumped from there to the recharge areas of the SATs using PRIUS dosing pumps (EMEC, Rieti, Italy) and continuously monitored by ISOIL MS600 electromagnetic flowmeters (ISOIL Industria, Milan, Italy). The pumps allowed us to allocate the inflow continuously or in pulses (controlled by a programmable digital timer). The water level of the outflow of the systems was controlled by the elevation of the discharge pipe. The discharge

Table 1. Detailed composition of Reactive Barriers BR17 and BR20 for the six SAT systems, note that the Reference system, T2, is composed only of sand. Symbol % refers to the percentage in volume of each material over the 100% of reactive barrier volume (1.5 x 2.34 x 1 m^3) at each system. The composition of the reactive barriers of the systems that sere sampled for this work are in bold.

Set of SATs	T1	T2	T3	T4	T5	T6
"BR17"	Not sampled	**Sand (100%)**	Not sampled	**Sand (49%) Compost (49%) Clay (2%)**	**Sand (49%) Woodchips (49%) Clay (2%)**	Not sampled
"BR20"	**Sand (50%) Woodchips + compost (50%)**	**Sand (100%)**	**Sand (50%) Woodchips + Compost (30%) Biochar (10%) Zeolites (8%) Clay (2%)**	Not sampled	Not sampled	**Sand (49%) Woodchips + Compost (49%) Biochar (10%)**

flow rate was monitored by ETWD 110mm DN15 volumetric water meters (ZENNER, Saarbrücken, Germany). All systems were fed with similar average inflows during the recharge episodes (0.37 m/d) and kept the same water level. Therefore, all systems exhibited similar residence times (**Supplementary Table ST2**).

Each SAT system had a recharge area (1.5 m wide x 2.38 m long) characterized by vertical flow, connected with an aquifer (2.38 m wide x 15 m long x 1.5 m high) filled with sand of 0.1- 0.5 mm grain size, and characterized by horizontal flow (**Figure 1**). The reference system, T2, operated in a conventional way without reactive barrier, while the other five systems operated with a reactive barrier. In essence, all RBs consisted of a mixture of sand, to provide strength, organic matter (woodchips, vegetable compost), to promote the absorption of neutral organic compounds, and other minor components to increase the types of sorption sites (Valhondo et al.,2014). Moreover, we let plants grow in all systems, to increase the range of local environments visited by the recharged water and to delay clogging. A first set of reactive barriers, referred hereafter as "BR17", were installed in December, 2017. The SAT systems started to operate in January 2018 and went through nine recharge periods of several months until November 2020 when the BR17 were withdrawn. A second set of RBs, referred hereafter as "BR20", were installed in December 2020. The BR20 SAT systems have operated since February 2021. The actual composition of BR17 and BR20 is detailed in **Table 1**. A complete information on the reactive barriers installation has been published elsewhere (Valhondo et al., 2020b).

We used three sets of data to assess how the efficiency of SAT in removing ARG and microbial pathogen load is affected by the RBs composition and the recharge regime. For the RB composition, we examined several systems of the "BR17" and "BR20" (**Table 1**). For the recharge regime, we tested continuous and pulsating recharge (JUN20 and SEP21 continuous recharge, OCT20 pulsating). The composition of the water feeding the systems varied seasonally (slightly larger organic carbon and ammonium content during the summer) but, overall, it displayed average values of 44 mg/L of NH_4, 2617,5 µS/cm conductivity and a negligible concentration of NO^{2-} and NO^{3-} (see **Supplementary Table ST1**).

2.2 Water sampling

Monitoring points were installed in each SAT system for water sampling along the flow path. Piezometers A and C, screened between 60-70 cm from the aquifer bottom, were located 1.5 m and 12.5 m away from the recharge area, so recharged

water could be sampled immediately after passing through the vadose zone (A piezometers) and at the end of each system (C piezometers, **Figure 1**).

Three sampling campaigns took place in order to address the efficiency of different RBs and recharge operations. The first campaign took place in June 2020 (referred hereafter as JUN20 sampling) with the BR17 barriers and a continuous inflow. The following one was carried in October 2020 (OCT20), still with the BR17 barriers, but after pulsating recharge throughout the preceding summer. The third campaign took place in September 2021 (SEP21) with the BR20 barriers and after a continuous inflow. Recharge period lengths and samplings are shown in **Supplementary Figure SF1** and the specifications of the recharge conditions for the three periods and samplings appear on **Supplementary Table ST2**.

Samples were collected from the WWTP inflow (referred hereafter as PRIM), from the secondary treatment effluent (referred hereafter as SEC), which was the source water for the SAT systems, and from monitoring points A and C (referred hereafter with the name of the SAT system followed by the name of the monitoring point, see **Figure 1**). Sampling schedules were adjusted for the different sampling points while taking into account the hydraulic residence time in the WWTP and along the SAT systems, so as to sample the same bulk water as it flowed through the whole system (see **Supplementary Table ST3**). In order to cover the most different reactive barriers, we sampled T4 and T5 for BR17 and T1, T3 and T6 for BR20, always including the sand barrier control (T2).

Samples for flow cytometry analysis were fixed in formaldehyde (2%) and frozen until further analysis. Samples for ARG quantification (5L) were collected in amber bottles (thoroughly washed, rinsed with ethanol 70% and dried at room temperature the day before the sampling) and transported to the lab in a 4ºC portable fridge.

2.3 Flow cytometry

Formaldehyde-fixed water samples (2%, final concentration) were stained for 10 min in the dark at room temperature by SYBR Green I (1:10000 dilution; Life Technologies, code S7563). The Total Cell Counts (TCC) were assessed by using the flow cytometer A50-Micro (Apogee Flow Systems, Hertfordshire, UK), equipped with a solid state laser set at 20 mV and tuned to an excitation wave length of 488 nm. Forward and side scatter, green fluorescence (530/30 nm), and red fluorescence (>610 nm) signals were acquired and plotted on log-scales for the identification and characterization of cytometric events. Thresholding was set on the green channel and voltages were adjusted to move the background and instrumental noise below the first decade of the green fluorescence. Samples were run at low flow rates to keep the number of events below 1000 events/s. TCC were determined in SYBR-stained samples by the signatures of the prokaryotic cells in the density plots of the forward and side scatter vs the green fluorescence signals. The intensity of green fluorescence emitted by SYBR-positive prokaryotic cells allowed for the discrimination among cell groups exhibiting Low and High Nucleic Acid content (hereafter named LNA and HNA cells, respectively) (Amalfitano et al., 2018).

2.4 Sample processing and DNA extraction for 16S rDNA amplicon sequencing and ARGs quantification

The 5L samples were stored in a 4ºC chamber overnight to allow coarse particle aggregates to sediment. The decanted liquid was centrifuged at 3000 rpm during 15 min to form a pellet with the centrifuged solids in suspension. Both, the initially sedimented material and the pellet were stored in

50 ml sterile polypropylene tubes. The centrifuged water was filtered sequentially through 3µm and 0.2µm filters (Isopore and Omnipore respectively, Merck KGaA, Darmstadt, Germany). Three size fractions were obtained from each sample: coarse fraction (Co), from the combination of sedimented material plus the centrifuged pellet; and fine (F) and ultrafine (UF) fractions, which come from materials retained by the 3µm and the 0.2 µm filters, respectively. These fractions were analyzed separately, although the DNA yield of some of them was not enough for DNA sequencing analysis. In total, we processed and analyzed 69 subsamples (**Supplementary Table ST4**).

Total DNA from the Co, F and UF fractions was extracted using the PowerSoil DNA isolation kit (Qiagen). The Co fraction was treated following manufacturer indications, while DNA isolation from F and UF fractions, had some minor modifications. Briefly, filters were cut into small pieces using a sterile scalpel onto a glass surface previously rinsed with ethanol at 70%, and those introduced into the bead tube using sterilized tweezers. Bead beating time for filter samples was increased to 20 min. The final elution volume of all extracted samples was 100 µl. The concentration and the quality of the DNA were tested using a NanoDrop Spectrophotometer 8000 (Thermofisher Scientific, Inc) and extracted DNA samples were stored at −20 °C until further analysis.

2.5. Loop-Mediated Isothermal Amplification (LAMP)-PCR

LAMP-PCR was used to evaluate the presence/absence of pathogenic enterobacteria (*Salmonella* spp) and opportunistic pathogens (*Legionella* spp, *Legionella pneumophila* and *Pseudomonas aeruginosa*) along the sampling net. Each analysis was performed by using 3 µl of extracted DNA and the AVANTECH LAMP-PCR pathogens detection kits (EBT-615 Salmonella screen GLOW; EBT-629 Legionella screen GLOW. EBT-621 *Legionella pneumophila* GLOW; EBT 626-*Pseudomonas aeruginosa* GLOW) by following literature protocols (Hara-Kudo et al., 2005).

2.6 Quantification of genetic elements by qPCR

Absolute quantification was performed for 16S rDNA (marker of absolute bacterial abundance), *int*I1 (marker of horizontal gene transfer (HGT)) and for the following set of ARGs: *sul*1 (dihydropteroate synthetase, conferring resistance to sulphonamide), *qnr*S1 (a Pentapeptide Repeat Protein family member that inhibits the effect of quinolones), *tet*M (a ribosomal protection protein, which confers tetracycline resistance by binding to the ribosome and preventing drug interaction with its binding site), *mec*A (penicillin-binding protein 2A that enables transpeptidase activity in the presence of beta-lactams, preventing them from inhibiting cell wall synthesis), and bla_{TEM}, $bla_{\text{CTX-M-32}}$, and $bla_{\text{OXA-58}}$, three β-lactamases conferring resistance to beta-lactamic antibiotics such as cephalosporins, monobactams, and carbapenems (Cerqueira et al., 2019) (primer sequences listed in **Supplementary Table ST5**). Optimal primer concentrations were 300 nM for all genes. qPCR reactions were carried on 96-well plates in a final reaction volume of 20µl in a LightCycler 480 II (A F. Hoffmann−La Roche AG, Inc). Plasmids used for the quantification curves were pNORM1 conjugative plasmid (Gat et al., 2017) for *int*I1, *sul*1, *qnr*S1, *tet*M, bla_{TEM}, $bla_{\text{CTX-M-32}}$, $bla_{\text{OXA-58}}$ and individual pUC19 plasmids for *mec*A, *tet*M and $bla_{\text{OXA-58}}$ (Laht et al., 2014; Szczepanowski et al., 2009; Tamminen et al., 2011). All samples were run as technical duplicates along with the quantification curve to reduce variability between assays. We established as quantification limit (LOQ) the minimum amount of plasmid that could be detected without interference from the negative control (**Supplementary Table ST5**).

The quality criteria within the standard curve was a $R^2 > 0.99$, and a slope between −3.1 and −3.4, corresponding to an efficiency of the reaction from 97% to 100%. The specificity of the amplification was assessed by analysis of the corresponding melting curves. Dynamo ColorFlash SYBR Green (Thermo Scientific, Inc.) was used for *mec*A, *tet*M and *bla*$_{OXA-58}$ qPCR quantifications; all the other genes were quantified with LightCycler 480 SYBR Green I Master (A F. Hoffmann–La Roche AG, Inc)(Cerqueira et al., 2019). Amplification protocol was adapted following manufacturers guidelines and different annealing temperatures were used as indicated in **Supplementary Table ST5**. Copy numbers per gene were calculated by extrapolation from the standard curves, and expressed in relation to the total filtered volume of each sample in ml (copies/ml). Prevalence values, understood as the fraction of the bacterial population harboring a given genetic element, was estimated as copies of the genetic element per million 16S rDNA copies. Statistical analysis and plots were performed in the R environment (version 3.6.1; http://www.rproject.org/).

2.7 Microbial community composition by 16S rRNA gene sequencing

The 69 extracted samples were sent to Novogene Europe (Cambridge, UK) for high throughput sequencing. Different regions of the 16S rRNA gene (16SV4/16SV3/16SV3-V4/16SV4-V5) were amplified using specific primers barcoding for amplicon generation. All PCR reactions were carried out with Phusion® High-Fidelity PCR Master Mix (New England Biolabs). Quality-checked PCR products were mixed at equal density ratios and purified by Qiagen Gel Extraction Kit (Qiagen, Germany). Sequencing libraries were generated using NEBNext Ultra DNA Library Pre ®Kit for Illumina, following manufacturer's recommendations, and index codes were added. Sequencing was carried out on an Illumina platform and 250 bp paired- end reads were generated. Total reads per sample and other DNA sequencing quality control parameters appear in **Supplementary Table ST6**. Note that composite Amplicon Sequence Variant (ASV) relative abundances for a given sample were calculated, when necessary, as the sum of frequencies of the corresponding subsamples (Co, F and UF), weighted by their relative amount of 16s rDNA. Clean Sequences were analysed and associated to 189,336 ASVs (Amplicon Sequence Variants) using the R package DADA2 (Callahan et al., 2016). The SILVA database v128, formatted for DADA2, was used to provide taxonomic annotation (Quast et al., 2013). The total count distribution appears in **Supplementary Table ST7**. The number of bacterial taxa identified and the percentage of taxon coverage (fraction of ASVs annotated to each particular taxonomic level) are shown in **Supplementary Table ST8**. The significance of difference amongst the structure of microbial communities was analysed by a non-metric multi-dimensional scaling (NMDS) with the Bray–Curtis dissimilarity index (Bray and Curtis, 1957), using the *vegan* R package. The functional assignment was carried out using the FAPROTAX Metabolic DataBase (Louca et al., 2016).

3. Results

3.1. Microbial load and pathogen removal

Figure 2 summarizes the total cell counts (TCC) in samples of SEC, A and C of JUN20, OCT20 and SEP21 (top panel), and which of these were LNA or HNA cells (% of TCC, bottom panel). We observe how the water microbial load decreased consistently when WWTP effluents passed through the reactive barriers with no significant differences between either sampling periods or treatments (p

> 0.05). Overall, TCC was reduced by one order of magnitude. The percentage of LNA cells increased notably, passing from 59% in the effluent waters to 82% of total cells at the exit of the aquifer.

Supplementary Table ST9 summarizes the presence(+)/absence(-) of pathogenic enterobacteria (Salmonella spp) and opportunistic pathogens (*Legionella spp* and *Pseudomonas aeruginosa)* measured in samples of SEC, A and C monitoring point of T2, T4, and T5 during JUN20 and OCT20 recharge periods. LAMP-PCR showed that *Salmonella* spp. was not retrieved from any of the collected water samples, including SEC, whereas *Legionella* spp. was found in all samples. The occurrence of *Pseudomonas aeruginosa* was sporadic and lacked a clear retrieval pattern.

3.2. ARG removal

All tested ARG were detected in all samples, although their prevalence was too low for an adequate quantification in some cases, so only *int*I1, *sul*1, *qnr*S1, bla_{TEM}, $bla_{CTX\text{-}M\text{-}32}$ and *tet*M were plotted (**Figure 3**). The estimated total bacterial loads (absolute abundance), measured as 16S rDNA copies per ml, exhibited a maximum in PRIM, a discrete decrease from PRIM to SEC and a drop from SEC to SAT samples in all three recharge periods (**Figure 3**, top panel). ARG prevalence values were maximal in the PRIM and SEC samples in all three sampling campaigns, and the comparison between their respective values indicated that the WWTP treatment reduced their loads only by a relatively minor fraction, if any (**Figure 3**, middle panel). Integron *int*I1 had the

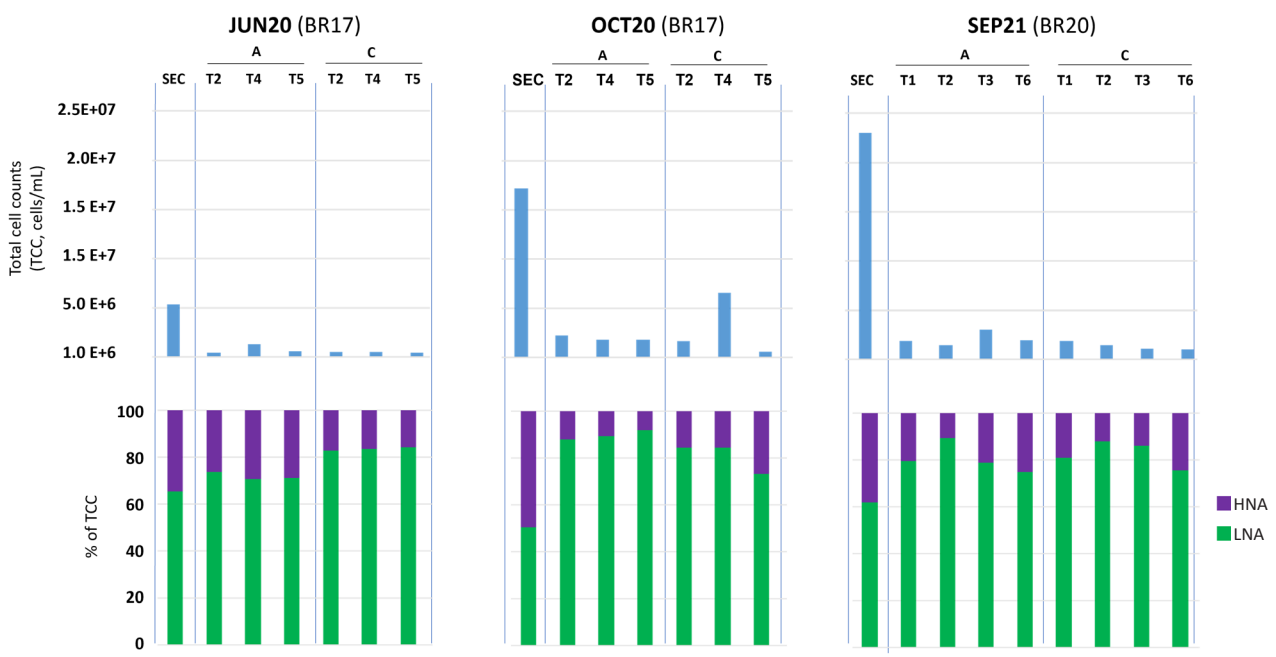

Figure 2. Flow cytometry results showing the microbial load removal by SAT systems. Top panel shows the total cell counts (TCC) in samples of SEC, A and C of JUN20, OCT20 and SEP21. Bottom panel shows the percentage of TCC that were HNA or LNA cells respectively.

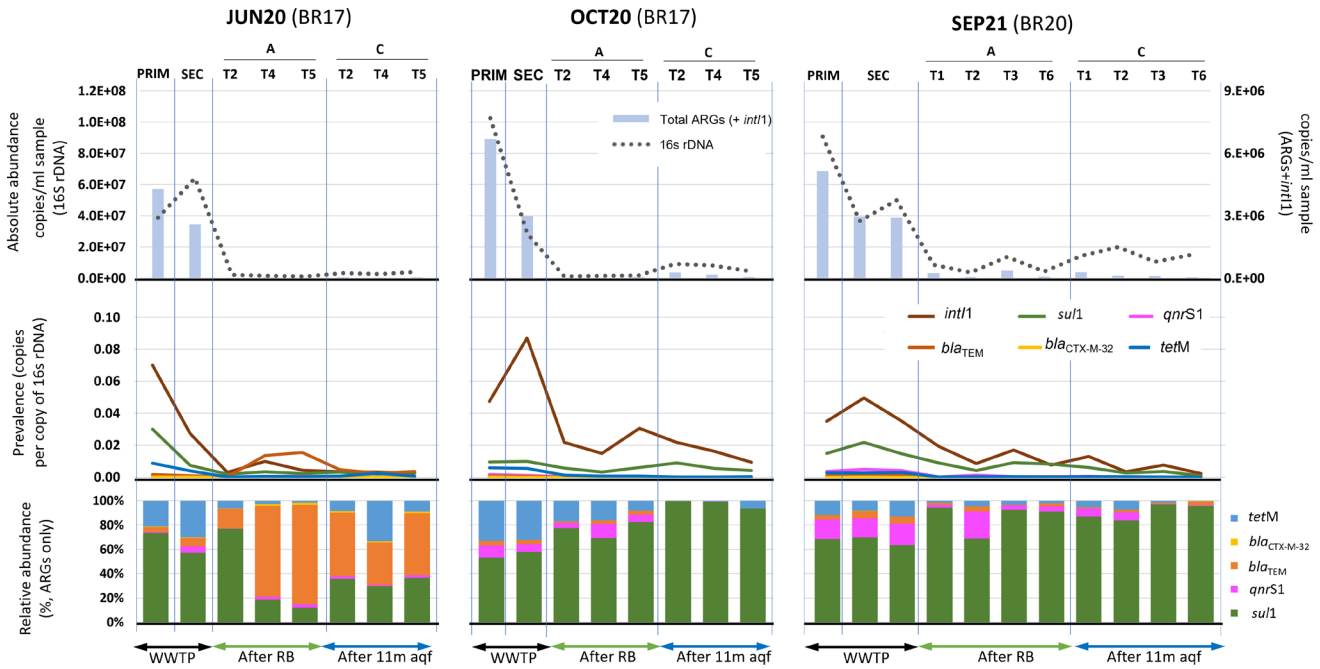

Figure 3. Graphic representation of ARG removal in pilot SAT systems operated with and without (T2) reactive barriers and fed with continuous or in pulses (OCT20) flow. Top panel: Absolute abundances, in copies per ml of sample, of 16s ribosomal DNA (discontinuous black line, left scale) and of the sum of the tested ARGs (including *intI*1, blue bars, right scale) for the different sampling points in all three campaigns. Vertical lines separate the three sampling areas: WWTP primary (PRIM) and secondary (SEC) effluents, A and C piezometers. The names of the SAT systems are indicated at the top of the graph. Middle panel: Prevalence values, in copies per copy of 16s DNA copies, of the different ARG and intI1 tested (colors indicated in the inset on the right graph). Color codes on the right. Bottom panel: Relative abundance of only ARGs.

highest prevalence in PRIM and SEC samples for all campaigns (3 and 8% of the total bacteria loads, expressed as 16S rDNA counts). Their similar values indicates again that the reduction in ARG load is due to the reduction in TCCs, rather to a reduction in prevalence, which is increased for some ARGs (**Figure 3**, middle panel). In all three recharge periods, *sul*1 showed the highest relative abundance followed by *tet*M, *qnr*S1 and bla_{TEM}, whereas $bla_{CTX\text{-}M\text{-}32}$ loads remained relatively low in all cases (**Figure 3**, bottom panel)

The SAT systems reduced considerably the total amount of bacteria (estimated as 16S rDNA copies and ARG loads in all aquifers in all campaigns (**Figure 3**, top panel), as well as the corresponding prevalence values (**Figure 3**, middle panel). Reduction ratios (**Supplementary Figure SF2**) depended on the system (nature of RB), recharge operation, and on the ARG. Loads of *tet*M and *qnr*S1 were reduced by 98 to 99.9% (values referred to the PRIM values) in the OCT20 and SEPT21 recharge periods, and to 95% in the JUN20 period; bla_{TEM} and $bla_{CTX\text{-}M\text{-}32}$ showed a similar reduction, above (98 to 99.9%) in the OCT20 and SEPT21 periods, but only a much poorer one (75 to 90%) in the JUN20 period; *intI*1 and *sul*1 showed a reversed pattern, with better removal ratios in the JUN20 period (97.5-99% for both) than in the OCT20 or SEP21 periods (90-98% and 73-98%, respectively,(see **Supplementary Figure SF2**). As a consequence, *sul*1 was the most predominant ARG in the outflows of the SAT systems for OCT20 or SEP21 periods, whereas during JUN20 period the outflow of the SAT systems showed a combination of *sul*1, bla_{TEM} and *tet*M sequences (**Figure 3**, bottom panel). We observed slight differences among the systems that could be related to the presence or the composition of

the different reactive barriers, with T4, T5 and T6 retrieving the highest reduction percentages at the C section samples for JUN20, OCT20 and SEP21 campaigns respectively (**Supplementary Figure SF2**).

The presence of ARG at the outflow of the SAT systems could, in principle, be related to either ARG-bearing strains from the SEC input, or to bacterial populations resident in the aquifer itself, or a combination of both. To test this, **Supplementary Figure SF3** shows the distribution of ASV in the three recharge periods in SEC and SAT samples identified by their positive correlation with either *bla*$_{TEM}$ (JUN20) or *sul*1 loads (OCT20, SEP21) in A and C piezometers samples in the corresponding SAT system. As shown in the figure, only a minor fraction of these ASVs were already present in the SEC samples (black sectors in the graph indicate undetected ASVs). This might indicate that most of the ARG loads found in the C piezometers correspond to bacteria grown in the aquifer, whereas the ones coming from the SEC only represent a minor fraction, particularly for the *bla*$_{TEM}$ bearing bacteria from JUN20 (see also bottom panel in **Figure 3**).

3.3. Phylogenetic profiles of the microbial community

Taxonomic classification showed a clear distinction between recharge periods, as well as substantial differences between PRIM and SEC samples and the rest (**Figure 4**). Proteobacteria and Campylobacterota predominated in PRIM and SEC, whereas SAT samples showed increasing proportion of Archaea, Patescibacteria and, for the SEP21 period, Desulfobacteria (**Figure 4**). We did not observe evident differences between the SAT systems in neither recharge period, nor between the different size fractions of a same sample (Co, F and UF, **Figure 4**). Non-metric multidimensional scaling (NMDS) analysis of ASV distribution among samples and recharge periods showed a separated ASV distribution for samples from all three periods, and an even stronger separation between PRIM and SEC samples and SAT samples (**Figure 5**), suggesting a stable composition of the microbiome along the WWTP process, and a radical change of bacterial groups in SATs. For JUN20 and OCT20 periods, A piezometers samples clustered between C piezometers and PRIM+SEC samples, meanwhile for SEP21, A and C samples appeared overlapped and separated from its respective PRIM+SEC samples (**Figure 5**).

The changes in ASV taxonomic profiles from PRIM and SEC samples to SAT ones also implicated a shift in the metabolic capacity of these bacterial populations. **Figure 6** shows the relative abundances of different metabolic categories (determined from the FAPROTAX Metabolic DataBase, note that a given ASV can, and most of them do, belong to more than one category). A shift between the metabolic profiles from the SEC samples to the SAT samples is clear (**Figure 6**). Aerobic chemoheterotrophs, nitrate reducers and human pathogens were most predominant in SEC samples in the three recharge periods, whereas bacterial groups able to perform iron, manganese, arsenate, sulfur compound (including thiosulfates), and nitrogen respiration were predominant at the SAT samples (see **Figure 7** and **Supplementary Table ST10**) which is consistent with the high values of Mn, Fe and As seen at zone C samples in all campaigns (see **Supplementary Figure SF4**).

Data also shows similarities between the T2, T4, and T5 SAT systems in JUN20 and OCT20 recharge periods, as well as the much large diversification in taxonomic and functional profiles among the four aquifers (T1, T2, T5, and T6) in SEP21 period (**Figure 4** and **Figure 6**). The presence of taxonomically different microbial populations in PRIM and SEC samples compared to SAT samples suggests that the decrease in ARGs loads was linked to the removal of the corresponding

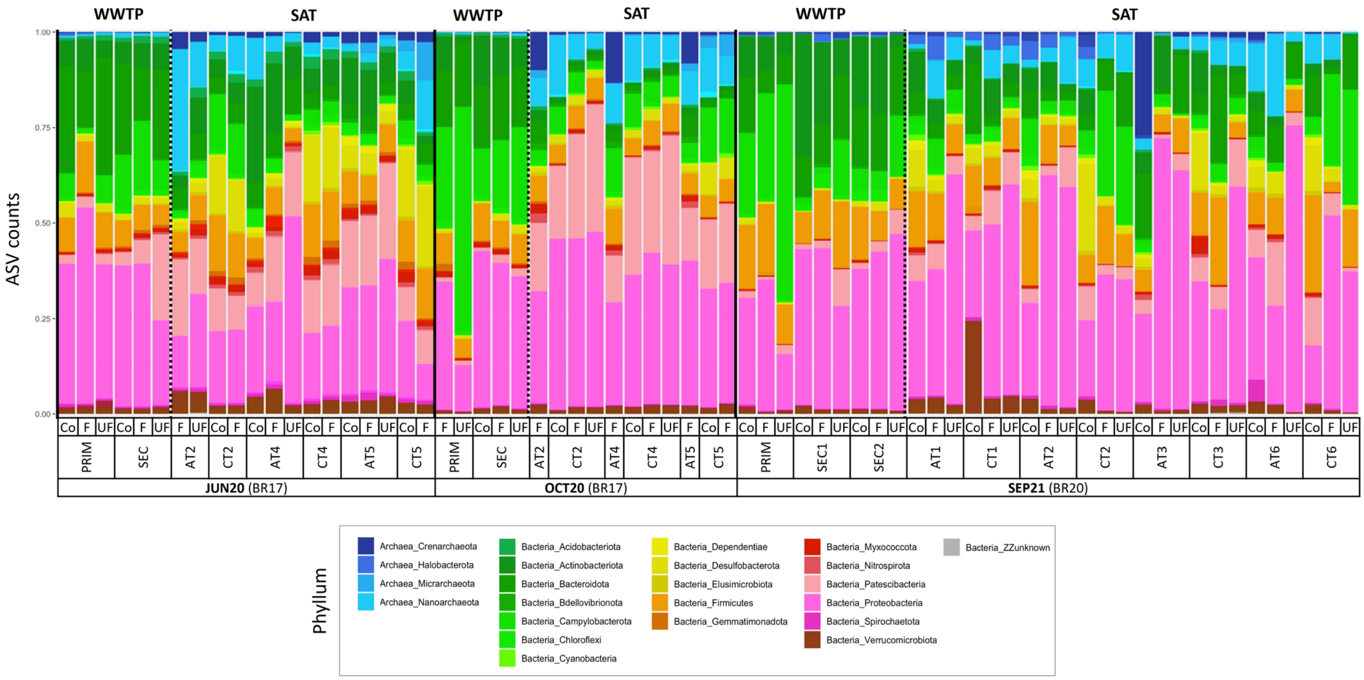

Figure 4. Taxonomic composition of the different samples. Relative abundances (%) of ASVs for the different samples is represented grouped at the Phylum level (color codes at the bottom on the right, only most abundant Phyla indicated). "Co", "F" and "UF" correspond to the different size fractions obtained for each sample (see the text). Sample denomination is shown at the bottom of the graph. As in *Figure 1*, vertical bars separate samples from the WWTP from those from the SAT systems.

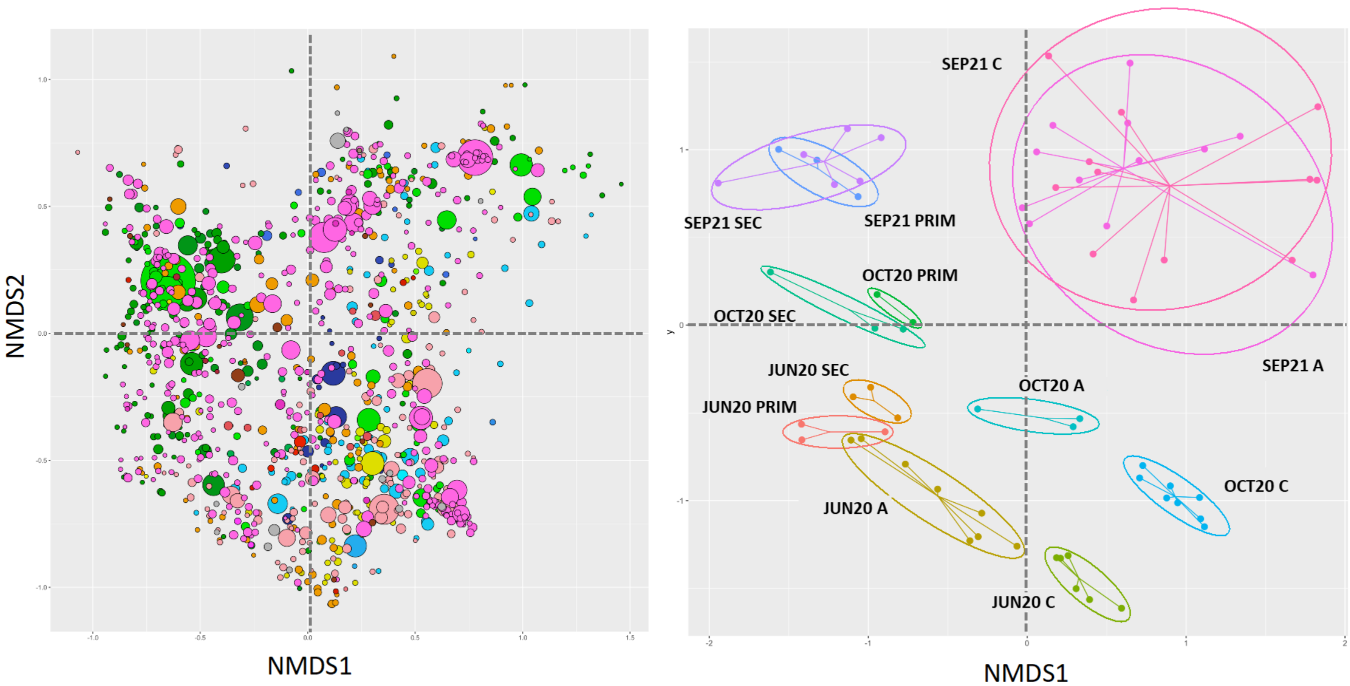

Figure 5. NMDS analysis. The score plot (left) shows the distribution of individual ASVs among subsamples (only ASVs with more than 1000 hits are included), with taxonomic (colors as in *Figure 3*) and relative abundance (circle size, log scale) information. The loadings plot (right) indicates the relative position of the samples; subfractions of a same sample are joined by lines intersecting at the medioid value. Values corresponding to each sample are further indicated by an oval; color codes are indicated on the right of the figure. In addition, the abbreviated codes for each sample is indicated.

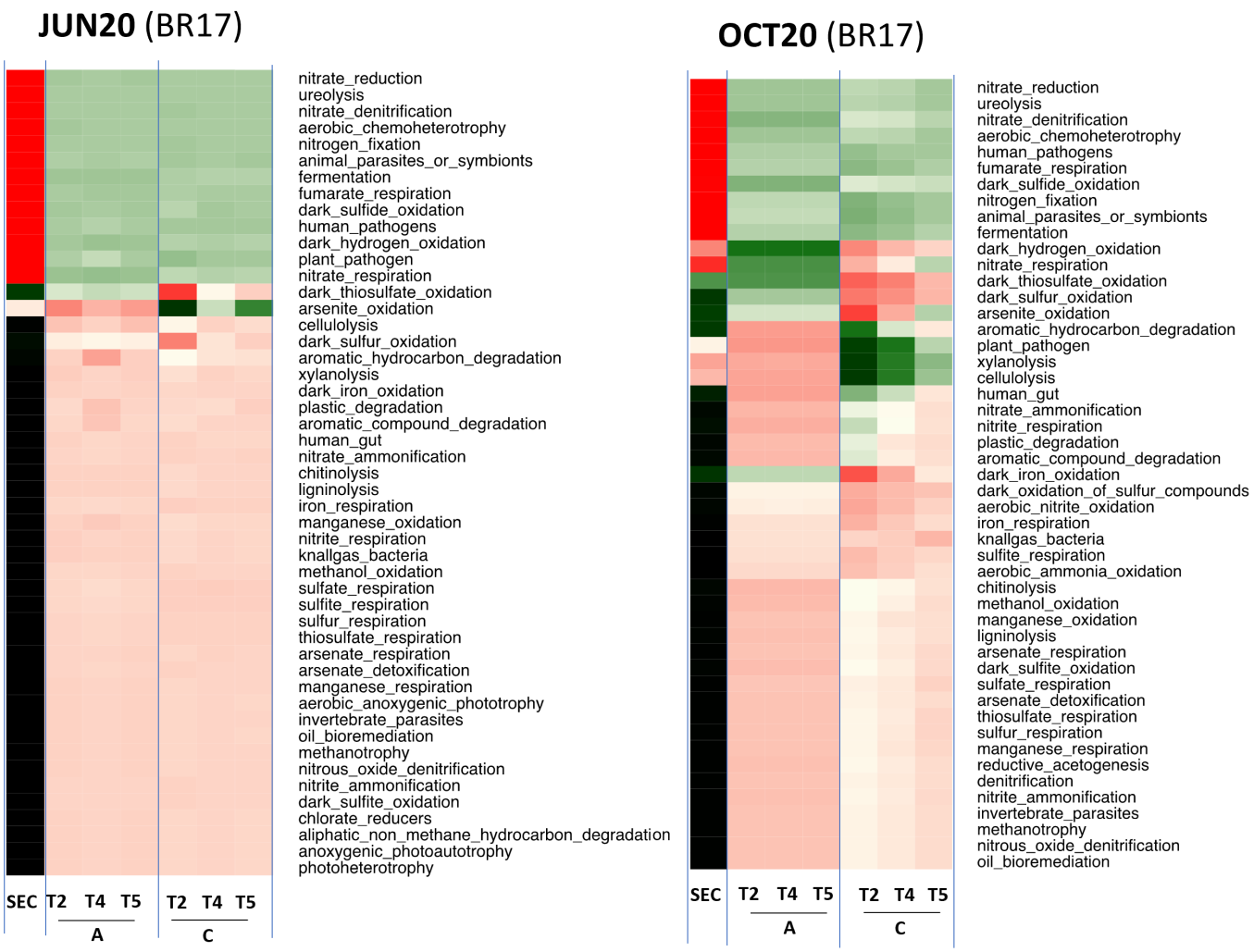

harboring bacteria from the total population, either by elimination or by their displacement by other bacterial groups.

4. Discussion

The filtration process through the reactive barriers reduced the microbial load in water samples and affected the cytometric profiles regardless the recharge period and the presence and composition of reactive barrier. The removal of total microbial cells was in line with values reported for different filtration units and LNA cells were likely to dominate the microbial community after filtering (Amalfitano et al., 2018; Jenkins et al., 2011; Lautenschlager et al., 2014). LNA cells have been associated to oligotrophic environments (Hu et al., 2020), as their compact genomes represent a competitive advantage over HNA cells in conditions of nutrient limitation (Longnecker et al., 2005; Santos et al., 2019; Servais et al., 2003). Therefore, we interpret the replacement of HNA by LNA bacterial groups as indicative of substitution of bacterial enteric groups by natural soil and groundwater-linked microbial populations.

Despite the notable reduction in total microbial

Figure 6. Heatmaps representing the sum of relative abundances of ASVs associated to given metabolic groups in the FARPROTAX database for each sampling campaign (shown at the right of each plot). Note that a given ASV could belong to a more than a single metabolic group. Black, green, and red sectors indicate absence or low to high relative abundance values, respectively (column scaled).

cells, the detection of potential pathogens in sampled waters can represent a matter of concern, since their occurrence may limit the application of several treatment options at the full-scale level (Kumari, 2017). That being said, the abundance of waterborne opportunistic pathogens like *Legionella* spp and *Pseudomonas* spp in SAT, can be extremely variable depending on a number of factors, comprising the time of year, local public-health and social-economic status and water per capita use (Regnery et al., 2017).

Constructed aquifers demonstrated to be able to remove ARGs and microbial loads from WWTP effluents by 90-95% or more in almost all cases. This compares favorably with most of current tertiary-treatment methods, particularly with those not using membrane technology (**Supplementary Table ST11**).

Metagenomic analyses provided insights about the mechanism of the removal of ARGs and pathogens by the system. It is clear that the barrier itself, that is, the first meter of the system in which there is either sand or a mixture of sand and different reactive materials, appears to block many of the influent ASVs, along with the genetic element they carry, and allows the substitution of the initial microbiome, rich in gut-related bacteria like Bacteroidota and Campylobacterota, by other

groups, including Archaea, Proteobacteria and Patescibacteria, apparently different from those present in the origin. At the end, less than 95% of human-related ASVs found in SEC samples were present in the samples from zone C.

We observed poor removal ratios for *bla*$_{TEM}$ in the JUN20 campaign and for sul1 in the OCT20 and SEP21 campaigns. Our data suggest that these figures were associated to the growth of specific bacteria in the aquifer, as most groups whose abundance better explain the observed ARG loads were not found at the systems' inflow (SEC) samples. Integron *int*I1, *sul*1, and *bla*$_{TEM}$ have been found present in many environments, including forest and remote soils (Cerqueira et al., 2019; Forsberg et al., 2014). While the origin of these aquifer-dwelling bacterial groups is to be determined yet, a suitable hypothesis being that they may arrived into the aquifers during the long period of time in which the systems had been operating (three years in the case of JUN20 and OCT20 campaigns, seven months for the SEP21 campaign).

The different composition of the barriers did not seem to have a crucial role in the removal of ARG or pathogens. It is clear that all RBs removed a substantial part of the incoming bacteria, but the reference system, consisting solely of sand, also did. That being said, best reduction ratios were obtained in RB enhanced SATs. Similarly, the effect of the recharging regime (continuous vs. pulsating) is presently unclear. One of the problems inherent of the use of such a pilot scale is that the influent material changes constantly, constituting a confounding factor that may complicate the global interpretation of the results. Another factor to be considered is the period of time the barriers have been operating. In this regard, the SEP21 recharge period, (operated only seven months after the rebuilding of the barriers) showed higher total bacteria loads and more differentiation between the different SAT systems than the other two campaigns, performed on SATs let operating for more than three years. While these differences may reflect the long time needed for bacteria to re-colonize the systems, it must be pointed out that the overall removal performance of the systems was essentially identical in the three campaigns.

Our data indicates the establishment of an ecological succession of bacterial groups along the SATs, and that this seems to be the major determinant on the removal of ARG and pathogens. The changes in microbial population we observed (HNA/LNA ratio, metabolic profiles, etc.) are consistent with a transition from hypertrophic, nutrient rich environments, such is wastewater, even after the WWTP secondary treatment, to the eutrophic conditions of our sand tanks. We conjecture that the shift will be further enhanced in natural aquifers, as water reaches the typical groundwater oligotrophic conditions. This process is equivalent to a mineralization of the recharged water and consistent with the removal of CECs and other chemical pollutants by SAT (Valhondo et al., 2020b, 2020a).The pass through the SATs had a much stronger effect on changing the microbiome composition than the WWTP treatment, and this is probably one decisive feature of the system, not necessarily shared by other passive methods, like wetlands. The fact that the SATs performed even better than some active, disinfecting methodologies, like advanced oxidation, ozonation, and UV-treatment on removing ARGs (Leiva et al., 2021) (see also **Supplementary Table ST11**) suggests that the spontaneous substitution of wastewater-related microbiota by natural soil and groundwater-linked and ARG-poor microbial populations may be a more efficient water regeneration process than their active removal by chemical methods. It is worth noting that the rate of most ARG removal by the aquifers (more than 95%) is close to the practical limit of many membrane-based methodologies, due to pores and other defects of the material.

Taking into account that the setup used here was a relatively a small scale one, which aim

was to provide a testing site to gain insight on the processes controlling the evolution of the recharged water, the excellent performance of this systems could be enhanced with an expansion of both, the reactive barriers and the aquifers, at a relatively low cost. This scalation should take place (in terms of ARGs removal) defining the optimal recharge regime, considering all the temporal and climatic variations, the time necessary for the stabilization and bacterial colonization of the reactive barriers, and the total operating time of the systems.

Acknowledgements

This work was supported by grants from the Spanish Ministry of Science and Innovation (MCIN/AEI/10.13039/113760501100011033, grant RTI2018-096175-B-I00), and the Generalitat de Catalunya (2017SGR902), the EU (Water JPI project MARadentro, PCI2019-103603), and the Catalan Water Agency (project RESTORA, CA210/18/00040). CSL was supported by a FI predoctoral fellowship from the Generalitat de Catalunya and the European Social Fund (2018 FI B 00368, ESF Investing in your future). IDAEA-CSIC is a Center of Excellence Severo Ochoa (Spanish Ministry of Science and Innovation, Project CEX2018-000794-S, ERDF A way of making Europe).

Bibliography

Aeschbach-Hertig, W., Gleeson, T., 2012. Regional strategies for the accelerating global problem of groundwater depletion. Nat. Geosci. 2012 512 5, 853–861. https://doi.org/10.1038/ngeo1617

Amalfitano, S., Fazi, S., Ejarque, E., Freixa, A., Romaní, A.M., Butturini, A., 2018. Deconvolution model to resolve cytometric microbial community patterns in flowing waters. Cytom. Part A 93, 194–200. https://doi.org/10.1002/cyto.a.23304

Arad, I., Ziner, A., Ben Moshe, S., Weisbrod, N., Furman, A., 2022. Improving soil aquifer treatment efficiency using air injection into the subsurface. Hydrol. Earth Syst. Sci. Discuss. 2022, 1–24. https://doi.org/10.5194/hess-2022-376

Bray, J.R., Curtis, J.T., 1957. An Ordination of the Upland Forest Communities of Southern Wisconsin. Ecol. Monogr. 27, 325–349. https://doi.org/10.2307/1942268

Callahan, B.J., McMurdie, P.J., Rosen, M.J., Han, A.W., Johnson, A.J.A., Holmes, S.P., 2016. DADA2: High-resolution sample inference from Illumina amplicon data. Nat. Methods 13, 581–+. https://doi.org/10.1038/nmeth.3869

CDC, 2021. Antibiotic / Antimicrobial Resistance | CDC [WWW Document]. URL https://www.cdc.gov/drugresistance/ (accessed 8.8.22).

Cerqueira, F., Matamoros, V., Bayona, J., Piña, B., 2019. Antibiotic resistance genes distribution in microbiomes from the soil-plant-fruit continuum in commercial Lycopersicon esculentum fields under different agricultural practices. Sci. Total Environ. 652, 660–670. https://doi.org/10.1016/j.scitotenv.2018.10.268

Dillon, P., 2005. Future management of aquifer recharge. Hydrogeol. J. 13, 313–316. https://doi.org/10.1007/S10040-004-0413-6/TABLES/1

Elkayam, R., Aharoni, A., Vaizel-Ohayon, D., Sued, O., Katz, Y., Negev, I., Marano, R.B.M., Cytryn, E., Shtrasler, L., Lev, O., 2017. Viral and Microbial Pathogens, Indicator Microorganisms, Microbial Source Tracking Indicators, and Antibiotic Resistance Genes in a Confined Managed Effluent Recharge System. J. Environ. Eng. 144, 05017011. https://doi.org/10.1061/(ASCE)EE.1943-7870.0001334

Forsberg, K.J., Patel, S., Gibson, M.K., Lauber, C.L., Knight, R., Fierer, N., Dantas, G., 2014. Bacterial phylogeny structures soil resistomes across habitats. Nature 509, 612–616. https://doi.org/10.1038/nature13377

Gat, D., Mazar, Y., Cytryn, E., Rudich, Y., 2017. Origin-Dependent Variations in the Atmospheric Microbiome Community in Eastern Mediterranean Dust Storms. Environ. Sci. Technol. 51, 6709–6718. https://doi.org/10.1021/acs.est.7b00362

Gurdak, J.J., 2017. Climate-induced pumping. Nat. Geosci. 2017 102 10, 71–71. https://doi.org/10.1038/ngeo2885

Hara-Kudo, Y., Yoshino, M., Kojima, T., Ikedo, M., 2005. Loop-mediated isothermal amplification for the rapid detection of Salmonella. FEMS Microbiol. Lett. 253, 155–161. https://doi.org/10.1016/j.femsle.2005.09.032

Hu, C., Chen, X., Yu, L., Xu, D., Jiao, N., 2020. Elevated Contribution of Low Nucleic Acid Prokaryotes and Viral Lysis to the Prokaryotic Community Along the Nutrient Gradient From an Estuary to Open Ocean Transect. Front. Microbiol. 11, 3174. https://doi.org/10.3389/FMICB.2020.612053/BIBTEX

Jenkins, M.W., Tiwari, S.K., Darby, J., 2011. Bacterial , viral and turbidity removal by intermittent slow sand filtration for household use in

developing countries : Experimental investigation and modeling. Water Res. 45, 6227–6239. https://doi.org/10.1016/j.watres.2011.09.022

Konikow, L.F., Kendy, E., 2005. Groundwater depletion: A global problem. Hydrogeol. J. 13, 317–320. https://doi.org/10.1007/s10040-004-0411-8

Kumar, M., Ngasepam, J., Dhangar, K., Mahlknecht, J., Manna, S., 2022. Critical review on negative emerging contaminant removal efficiency of wastewater treatment systems: Concept, consistency and consequences. Bioresour. Technol. 352, 127054. https://doi.org/10.1016/j.biortech.2022.127054

Kumari, C.F.N.S., 2017. Status of pathogens , antibiotic resistance genes and antibiotic residues in wastewater treatment systems. Rev. Environ. Sci. Bio/Technology 16, 491–515. https://doi.org/10.1007/s11157-017-9438-x

Laht, M., Karkman, A., Voolaid, V., Ritz, C., Tenson, T., Virta, M., Kisand, V., 2014. Abundances of Tetracycline, Sulphonamide and Beta-Lactam Antibiotic Resistance Genes in Conventional Wastewater Treatment Plants (WWTPs) with Different Waste Load. PLoS One 9. https://doi.org/10.1371/journal.pone.0103705

Lautenschlager, K., Hwang, C., Ling, F., Egli, T., Liu, W., Boon, N., Oliver, K., Hammes, F., 2014. Abundance and composition of indigenous bacterial communities in a multi-step biofiltration-based drinking water treatment plant 2. https://doi.org/10.1016/j.watres.2014.05.035

Leiva, A.M., Piña, B., Vidal, G., 2021. Antibiotic resistance dissemination in wastewater treatment plants: a challenge for the reuse of treated wastewater in agriculture. Rev. Environ. Sci. Biotechnol. 20, 1043–1072. https://doi.org/10.1007/s11157-021-09588-8

Longnecker, K., Sherr, B.F., Sherr, E.B., 2005. Activity and phylogenetic diversity of bacterial cells with high and low nucleic acid content and electron transport system activity in an upwelling ecosystem. Appl. Environ. Microbiol. 71, 7737–7749. https://doi.org/10.1128/AEM.71.12.7737-7749.2005/ASSET/CF56D038-E762-4024-AE02-15C0183EA1F3/ASSETS/GRAPHIC/ZAM0120561920006.JPEG

Louca, S., Parfrey, L.W., Doebeli, M., 2016. Decoupling function and taxonomy in the global ocean microbiome. Science 353, 1272–1277. https://doi.org/10.1126/SCIENCE.AAF4507

Pei, M., Zhang, B., He, Y., Su, J., Gin, K., Lev, O., Shen, G., Hu, S., 2019. State of the art of tertiary treatment technologies for controlling antibiotic resistance in wastewater treatment plants. Environ. Int. 131, 105026. https://doi.org/10.1016/J.ENVINT.2019.105026

Quast, C., Pruesse, E., Yilmaz, P., Gerken, J., Schweer, T., Yarza, P., Peplies, J., Glöckner, F.O., 2013. The SILVA ribosomal RNA gene database project: Improved data processing and web-based tools. Nucleic Acids Res. 41, 590–596. https://doi.org/10.1093/nar/gks1219

Regnery, J., Gerba, C.P., Dickenson, E.R. V, Drewes, J.E., 2017. The importance of key attenuation factors for microbial and chemical contaminants during managed aquifer recharge: A review. Crit. Rev. Environ. Sci. Technol. 47, 1409–1452. https://doi.org/10.1080/10643389.2017.1369234

Santos, M., Oliveira, H., Pereira, J.L., Pereira, M.J., Gonçalves, F.J.M., Vidal, T., 2019. Flow cytometry analysis of low/high DNA content (LNA/HNA) bacteria as bioindicator of water quality evaluation. Ecol. Indic. 103, 774–781. https://doi.org/10.1016/j.ecolind.2019.03.033

Servais, P., Casamayor, E.O., Courties, C., Catala, P., Parthuisot, N., Lebaron, P., 2003. Activity and diversity of bacterial cells with high and low nucleic acid content. Aquat. Microb. Ecol. 33, 41–51. https://doi.org/10.3354/AME033041

Szczepanowski, R., Linke, B., Krahn, I., Gartemann, K.-H., Gützkow, T., Eichler, W., Pühler, A., Schlüter, A., 2009. Detection of 140 clinically relevant antibiotic-resistance genes in the plasmid metagenome of wastewater treatment plant bacteria showing reduced susceptibility to selected antibiotics. Microbiology 155, 2306–2319. https://doi.org/https://doi.org/10.1099/mic.0.028233-0

Tamminen, M., Karkman, A., Lohmus, A., Muziasari, W.I., Takasu, H., Wada, S., Suzuki, S., Virta, M., 2011. Tetracycline Resistance Genes Persist at Aquaculture Farms in the Absence of Selection Pressure. Environ. Sci. Technol. 45, 386–391. https://doi.org/10.1021/es102725n

Valhondo, C., Carrera, J., 2019. Chapter 1 - Water as a finite resource: From historical accomplishments to emerging challenges and artificial recharge, in: Galanakis, C.M., Agrafioti, E.B.T.-S.W. and W.P. (Eds.), . Elsevier, pp. 1–17. https://doi.org/https://doi.org/10.1016/B978-0-12-816170-8.00001-6

Valhondo, C., Carrera, J., Martínez-Landa, L., Wang, J., Amalfitano, S., Levantesi, C., Díaz-Cruz, M.S., 2020a. Reactive barriers for renaturalization of reclaimed water during soil aquifer treatment. Water (Switzerland) 12. https://doi.org/10.3390/W12041012

Valhondo, C., Martínez-Landa, L., Carrera, J., Díaz-Cruz, S.M., Amalfitano, S., Levantesi, C., 2020b. Six artificial recharge pilot replicates to gain insight into water quality enhancement processes. Chemosphere 240. https://doi.org/10.1016/j.chemosphere.2019.124826

Wada, Y., Van Beek, L.P.H., Van Kempen, C.M., Reckman, J.W.T.M., Vasak, S., Bierkens, M.F.P., 2010. Global depletion of groundwater resources. Geophys. Res. Lett. 37. https://doi.org/10.1029/2010GL044571

WHO, 2014. Antimicrobial resistance. Global report on surveillance. World Heal. Organ. 61, 12–28. https://doi.org/10.1007/s13312-014-0374-3

Detoxification of wastewater plant effluents by soil aquifer treatment methodologies

Claudia Sanz[1], Adrià Sunyer-Caldú[1], Marta Casado[1], Sylvia Mansilla[1], Lurdes Martinez-Landa[2,3], Cristina Valhondo[1,2,4], Ruben Gil-Solsona[1], Pablo Gago-Ferrero[1], Jose Portugal[1], M. Silvia Diaz-Cruz[1], Jesús Carrera[1,2], Benjamin Piña[1], Laia Navarro-Martín[1]

1) IDAEA-CSIC, Jordi Girona, 18. E-08034, Barcelona, Spain.

2) Associated Unit: Hydrogeology Group (UPC-CSIC)

3) Dept. of Civil and Environmental Engineering. Universitat Politècnica de Catalunya, Barcelona, Spain

4) Geosciences Montpellier, Université de Montpellier, CNRS, Montpellier, France

5) Water Research Institute, National Research Council of Italy (IRSA-CNR), Monterotondo, Rome, 00015, Italy

To be submitted.

Abstract

Soil Aquifer Treatment (SAT) is recognized as a cost-effective approach to reduce contaminants of emerging concern from Wastewater Treatment Plant (WWTP) effluents. However, its efficiency in removing the associated biological effects is still poorly understood. In this study, we evaluated the efficiency of three pilot SAT systems equipped with and without reactive barriers and containing different proportions of sand and organic materials to remove toxicity associated to the presence of chemicals of emerging concern. SATs were fed with secondary effluents from the Palamós WWTP (N.E. Spain) during two consecutive campaigns scheduled before and after the summer of 2020. Fifteen water samples were collected from the WWTP effluent, below the barriers and at the end of the aquifer. Transcriptomic analyses of zebrafish embryos exposed to the corresponding water extracts revealed a wide range of toxic activities in the WWTP effluents. Results demonstrated that the associated responses were reduced by more than 70% by SAT, achieving control levels in some cases. Similar results were obtained when human HepG2 hepatic cells were tested for cytotoxic and dioxin-like responses. Toxicity reduction appeared to be partially determined by the reactive barrier composition and/or SAT managing and was correlated with the removal of contaminants of emerging concern by SAT. In conclusion, SAT appears as a very promising approach for efficiently reducing the effects of recalcitrant pollutants from WWTP secondary effluents on the environment and human health.

1. Introduction

The ongoing climate crisis dramatically impacts water availability in many areas of the world. Increased extreme weather events reduces the natural recharge and increases the exploitation of aquifers, affecting the groundwater dependent ecosystems such as rivers and wetlands. Projected in the near future, this will translate into limited global freshwater access, that will result in severe water scarcity for the ever-growing human population (Hristov et al., 2021). Mediterranean regions will be especially affected by these phenomena, as their basins have a strong climate seasonality remaining dry for most of the year (Ricart et al., 2021). This predicted decrease in freshwater availability will also have a strong impact on agricultural productivity that, together with the urban-tourist development, will induce agriculture, households, tourism, and industry sectors and the environment to compete for water use. Water scarcity has been traditionally addressed by accumulating water in reservoirs during periods of excess, installing desalination plants in coastal cities, and performing inter-basin water transfer. However, the required investment in energy, materials, and human resources is quite limited, mainly by the geographic location and topography (He et al., 2021).

To face water scarcity by minimizing resource consumption, we need to improve the efficiency of water use and reuse. One of the proposed strategies for the effective management of water is wastewater recycling (Valhondo et al., 2020b; Vymazal et al., 2021; Zhu et al., 2021). Although this might seem a sustainable and cost-effective strategy to alleviate the stress on water resources, it could also compromise the environment and human health due to the high loads of contaminants of emerging concern (CECs) present in the wastewater treatment plants (WWTPs) effluents (Valhondo and Carrera, 2019). CECs present in WWTPs effluents, encompasses a wide range of chemicals including pesticides, pharmaceuticals and personal care products (PPCPs), sex hormones, or per- and polyfluoroalkyl substances (PFASs), among others. Furthermore, WWTPs effluents can also carry relevant microbial hazards like antibiotic-resistant bacteria (ARBs) that can potentially spread antibiotic resistance genes (ARGs) across waterbodies microbiomes (Kumar et al., 2022; Valhondo et al., 2020b).

The reuse of reclaimed water requires optimizing the present procedures to monitor and remove the presence of CECs in wastewater since conventional WWTPs were not designed for this purpose (Kumar et al., 2022; Rout et al., 2022). Managed aquifer recharge (MAR) technologies consisting in the induction of superficial impaired water recharge into aquifers, allows groundwater-dependent regions to maintain, enhance and protect their water resources with limited use of energy and materials (Dillon et al., 2019). Among the different available MAR techniques, soil aquifer treatment (SAT) has been proposed as a useful tool to improve the quality of WWTPs effluents. SAT systems, that involve artificial recharge of the aquifers with wastewater, can be boosted with the installation of reactive barriers (RB) based on organic substrates in the recharge areas of the systems (Valhondo et al., 2020c, 2020b).

In the present study, we analyzed the capacity of SAT to reduce the potential toxicity associated with WWTP effluents using classic toxicological zebrafish and human cell bioassays. We analyzed their response to the water extracts from water samples collected before and after SAT. These analyses were complemented with wide-scope screening for the measurement of CECs loads.

2. Methods

2.1 Soil aquifer treatments (SATs): Location,

description and water sampling

The pilot SAT systems were built in a WWTP situated on the Spanish Mediterranean coastal area. The WWTP integrates a pre-treatment, primary treatment, and biologic secondary treatment (activated sludge). The quality of this WWTP effluent varies considerably throughout the year since it collects wastewater from different coastal municipalities (high seasonal population increase) (Valhondo et al., 2020c) A detailed description of the SAT systems can be found elsewhere (Valhondo et al., 2020c). In brief, the SAT systems (hereinafter referred to as BR17) were built in 2017 and consisted of a recharge area (1.5 width x 2.38 length m^2) with vertical flow connected to an artificial aquifer (1.5 width x 15 length x 1.5 high m^3) filled with sand and characterized by horizontal flow (**Figure 1**). Before entering the SAT system, the WWTP effluent was stored in a reservoir for homogenization (10 m^3 with a residence time of around 24 h, continuously re-filled from the base with the WWTP effluent water) and pumped through a pipe. SATs started infiltrating on January 2018, going through diverse wet and dry recharge periods during three consecutive years. Specifications on average flow into the systems, duration of wet and dry phases and total recharged volume during the BR17' recharge period are described in detail elsewhere (Paper IV and (Valhondo et al., 2020c)). The inflow was allocated continuously (along all the wet period) or in pulses (controlled by a programmable digital timer), pumped with PRIUS dosing pumps (EMEC, Rieti, Italy) and continuously monitored by ISOIL MS600 electromagnetic flowmeters (ISOIL industria, Milan, Italy). The water level of the outflow of the systems was controlled by the elevation of the discharge pipe and the discharge volume monitored by ETWD 110mm DN15 volumetric water meters (ZENNER, Saarbrücken, Germany). A set of piezometers were installed in each SAT to monitor and sample recharged water along the flow paths (Valhondo et al., 2020c). This included piezometers installed between 60-70 cm from the system base and located 1.5 m and 12.5 m away from the recharge area respectively that were used to obtain water samples. Wild grasses and weeds grew spontaneously in the recharge area of all the systems.

Figure 1 shows a simplified scheme of the SAT system and indicates in color the three SAT systems used in the present study (color coding followed in the upcoming figures) and the collected samples. The recharge zone of these three SAT systems was composed by only sand (T2), sand with compost as RB (T4), or sand with woodchips as RB (T5). Water was collected from: 1) the influent of the WWTP (PRIM); 2) the influent water feeding the systems (SEC); and the monitoring points 3) immediately after passing through the vadose zone to evaluate possible differences between the installed barriers per se (AT) and 4) close to the systems discharge (CT). A total of 5 L of water per each sampling point was collected in amber glass bottles. Two sets of samples were collected in June and October 2020 (further referred to as JUN20, and OCT20, respectively) during a recharge period with a continuous allocated inflow and a recharge period with a pulsating allocated inflow. Cumulative precipitation, temperature and conductivity as well as recharge period lengths during the experimental intervals appear in **Supplementary Figure SF1**. In the present study we selected the most different reactive barriers amongst the SAT pilot system and scheduled sampling based on the transit time of the recharged water to each monitoring point (B in **Supplementary Figure SF1**). Physicochemical parameters, including dissolved organic carbon, nitrates, nitrites and phosphates loads among others, were routinely measured in the water samples as described elsewhere (see Figure 3 in Valhondo et al., 2020b, and Supplementary Figure SF4 in Paper IV).

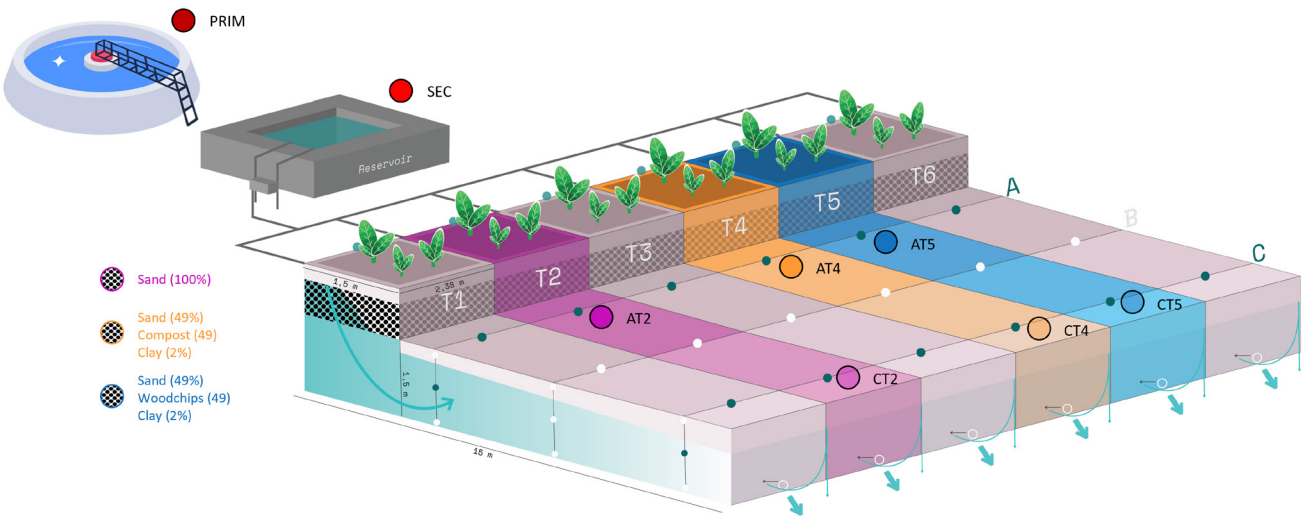

Figure 1. Simplified scheme of the installed SAT system. The three SAT systems studied in the present work are marked in color. Color pink codes for the SAT without reactive barrier filled only with sand, color orange codes for the SAT with a reactive barrier made of sand (49%), compost (49), clay (2%) and color blue codes for the SAT with a reactive barrier made of sand (49%), woodchips (49), clay (2%), Samples were taken prior WWTP treatment (PRIM), after WWTP at the effluent reservoir (SEC), after the immediate passage through the reactive barrier (AT), and at the very end of the systems (CT). Two sets of samples were taken in June 2020 and October 2020 (further referred as JUN20, and OCT20, respectively) through a recharge period with a continuous allocated inflow and a recharge period with a pulsating allocated inflow.

2.2 Solid Phase Extraction (SPE) of Contaminants of Emerging Concern (CECs)

Water samples were stored overnight at 4ºC, to allow the sedimentation of coarse particle aggregates, and subsequently decanted, centrifuged and filtered before the solid phase extraction (SPE) as described in Paper IV (see Sample processing and DNA extraction from the Methods section). SPE was performed according to (Downs et al., 2022), with some minor modifications. The extraction was optimized in order to extract non-polar and polar CECs separately out of the same 5L water samples. Briefly, 6 g Oasis HLB cartridges (Waters Corporation) were sequentially conditioned with ethyl acetate:dichlorometane (1:1; 3x20 mL, HPLC-grade); methanol (3x20 mL, HPLC-grade), methanol:water (1:1; 3x20 mL, HPLC-grade), and HPLC-grade water (3x20 mL). Then, samples were loaded onto the cartridges and were subsequently eluted. The polar CECs were extracted from the cartridge using methanol (3 X 20 mL) and the less polar using ethyl acetate:dichlorometane (1:1; 3 X 20 mL). Polar and non-polar extract fractions were evaporated to dryness under vacuum. Afterwards, the eluates were washed with HPLC-grade ethanol and dried under a N_2 stream. Polar and non-polar residue fractions were reconstituted with 1 mL HPLC-grade ethanol each and stored under Ar atmosphere at -20ºC. A control water sample (hereinafter referred to as CTRL) consisted of 5 L of Millipore Milli-Q water processed as the rest of the water samples.

2.3 Zebrafish toxicity assay

Rearing conditions

Zebrafish adult individuals (wild-type Danio rerio, 12–18 months old, fed twice per day with dry flakes from TetraMin (Tetra, Germany)) were naturally mated to obtain eggs. Mating was performed in 500 mL small breeding tanks using a ratio of three

females and two males (3:2 proportion). Eggs were collected 2 h post fertilization (hpf), transferred to a methylene blue solution (0.01%) for 5 min, then rinsed and checked for fertilization. At 3 days post fertilization (dpf) embryos were placed in six-well plates (10 individuals per well) in 3 mL of clean fish water (reverse-osmosis purified water containing 90 µg/mL of Instant Ocean (Aquarium Systems, Sarrebourg, France) and 0.58 mM of $CaSO_4 \cdot 2H2O$ at 28 ºC) and kept under standard conditions (28.0 ± 1.0 °C, photoperiod of 12L:12D). All experimental procedures were conducted under the license DAMM 7669, 7964 from the competent authority in accordance with the institutional guidelines. These were approved by the Institutional Animal Care and Use Committees of the Research and Development Centre (CID) of the Spanish National Research Council (CSIC).

Zebrafish eleutheroembryos exposures to wastewater extracts

In all cases, zebrafish eleutheroembryos were exposed for 24 h from 4 to 5 dpf. Polar and non-polar fractions of the water extract were combined in a single flask, evaporated and reconstituted in the appropriate volume of fish water. Preliminary dose-response exposures to the WWTP influent (PRIM) extracts (0.3X, 0.8X, 1X, 3X, 8X, and 20X concentration factors) of both campaigns were performed to assess general toxicity (**Supplementary Figure SF2**). In parallel, eleutheroembryos were exposed to 3X and 20X SEC extracts, 1 µM of β-naphthoflavone (BNF, CAS#: 6051-87-2, ≥98.0% purity, Sigma-Aldrich) and 1 µM 17-β-estradiol (E2, CAS#: 50-28-2, ≥98.0% purity, Sigma-Aldrich) in order to evaluate optimal SEC extract exposures. In this experiment BNF and E2 were used as positive controls for dioxin-like and estrogenic responses, respectively and Dimethyl sulfoxide (DMSO) was used as a vehicle (0.2%).

A concentration factor of 20X was chosen as the working concentration for the final exposures to water extracts from both JUN20 and OCT20 campaigns since the responses to SEC extracts were closer to the ones observed for BNF and E2 (**Supplementary Figure SF3**). Thus, the final experimental groups were: Control (CTRL, as described in Section 2.1); influent water (SEC); monitoring points AT, located after the vadose zone for SAT systems with sand (AT2), sand+compost (AT4), sand+woodchips (AT5); and CT, located close to the systems discharge for SATs with sand (CT2), sand+compost (CT4), sand+woodchips (CT5) (see **Figure 1**).

Anatomical development of embryos was followed as described in Kimmel et al., (1995). Survival and swim bladder inflation rates were recorded after the exposures for both the dose-response (**Supplementary Figure SF2**) and the final exposure (**Supplementary Figure SF4**). Eight replicates per treatment (10 zebrafish embryos per replicate) were collected, snap-frozen in dry ice and stored at −80 °C until further procedures.

Sample processing for transcriptomic assessment: RNA extraction, high-throughput RNA sequencing and target transcriptomics by real-time RT-PCR

Total RNA was extracted by using the TRIzol Reagent (Invitrogen Life Technologies, Carlsbad, CA, USA). RNA concentration and quality was measured spectrophotometrically using a NanoDrop™ ND-8000 spectrophotometer (Fisher Scientific). After DNase I treatment, total RNA was retro-transcribed to cDNA using a Transcriptor First Strand cDNA Synthesis Kit (Roche Diagnostics) following the manufacturer's protocol.

RNA-sequencing was performed in five CTRL and SEC replicates from both campaigns to assess global transcriptomic changes caused by exposure to the wastewater extract. Previous to library construction, RNA quantity and quality of samples was determined by Qubit RNA BR

Table 1. Main biological pathways, gene symbol, complete gene description and corresponding primer sequences of the chosen biomarkers. Color red codes for up-regulated genes and color blue codes for down-regulated genes. Information extracted from https://zfin.org/.

Pathway	Gene symbol	Gene description	Forward (5' → 3')	Reverse (5' → 3')
Detoxification: Drug-metabolizing enzyme mediator of phase I oxidative reactions.	(*cyp1a*)	cytochrome P450, family 1, subfamily A	GGTTAAAGTTCACCGGGATGC	CTGTGGTGTGACCCGAAGAAG
Detoxification: Drug-metabolizing enzimes that mediate phase II conjugative reactions.	(*ugt1a1*) (*ugt5a4*) (*gstp2*)	UDP glucuronosyltransferase 1 family, polypeptide A1 UDP glucuronosyltransferase 5 family, polypeptide A4 Glutathione S-transferase pi 2	CGTTTGATTCCTTGTCGTCTTG GAGGCGTTGAAGGAAGTGTTG CTGCCCAACGAGTTCAAACC	AACCACTGGAGTAGCGAGGC TGGTGCAGCTTGGACAGTCT TGATCACCGACCAGGAATCC
Cellular response to xenobiotic stimulus: organic acid and xenobiotic metabolism, steroid hydroxylation, regulation of apoptotic process, antimicrobial humoral immune response, animal organ development, regulation of transcription by RNA polymerase II.	(*cyp2k18*) (*cyp3a65*) (*cidec*) (*cxcl19*) (***anxa1c***) (***ahrra***)	cytochrome P450, family 2, subfamily K, polypeptide 18 cytochrome P450, family 3, subfamily A, polypeptide 65 cell death inducing DFFA like effector c chemokine (C-X-C motif) ligand 19 *annexin A1c* *aryl-hydrocarbon receptor repressor a*	CTGCATTCATCCAAGACCCAGT GTCATGGTGCCGACCTACG GCCAAGGAAAGATGTTGCCA GGCTACAACAGCCGCTGTGT GAGGGCGAGCTGAGTGGAC TCGTCCACTCCATCAAACAGG	TGGACACGCTCTGGGTTTG TCGGGTTTGAAGCTCTCCG GGCAGCCAATAAAATCCTGTG ACTCGCCGCAGGTTATCCT GCAGGTTTATTCCAAGCAGCC GCTCCCGCAGCTCATCAT
Transmembrane transport: ATPase-coupled transmembrane and phosphate ion transport.	(***abcc12***) (***slc34a2a***)	ATP-binding cassette, sub-family C (CFTR/MRP), member 12 solute carrier family 34 member 2a	CATCGGCACCGTCAGGTATAA CGGCTGGCAGGTACTCATG	CTAAAGCCAGCCAAAGCTCTTC TGTTGACAATGATGGCGAAGAT
Response to oxidative stress: Regulation of respiratory gaseous exchange and response to hypoxia.	(***hmox1a***)	heme oxygenase 1a	CAGCTCTCCAGCCCTT CAGT	CGTAAACTCCCATGCCAACC
Response to abiotic stimulus: endoplasmic reticulum stress, light stimulus and phototransduction response, production of gadusol, circadian gene expression and locomotor rhythm regulation, neutrophil differentiation, retinol metabolism	(***hsp70.2***) (***opn1mw1***) (***eevs***) (***nr1d1***) (***alas1***) (***lrata***)	heat shock cognate 70-kd protein, tandem duplicate 2 opsin 1 (cone pigments), medium-wave-sensitive, 1 2-epi-5-epi-valiolone synthase nuclear receptor subfamily 1, group d, member 1 aminolevulinate, delta-, synthase 1 lecithin retinol acyltransferase	TCCCGCAGATCGAAGTGAC TCAAGACCATACATGTCCACCTAAA ACTGGTTGACTTTGGGCACC CGAACCCTCGTCAGCAAGAG ACTCCCAAGATTGTGGCCTTT GCTTTGGCTTGGCACCTTC	GTTTTCCGGTGCTTTTGTCC TTAACCTCAGACCCATCGGC CACCGTGGAGAAGAGCTGGT TCAGGAAGTTTGAGCAGCAGC CACAGCTGCTCCAGTGGACA TCAACCAGCCATCCACAAAA
Small molecule metabolism: carnitine biosynthetic process.	(***bbox***)	butyrobetaine (gamma), 2-oxoglutarate dioxygenase	CAGCAACAATGCAAATGTAGCTC	AAGCCCAATGGAGAAGGTCA
Specific responses: response to estradiol, estrogen and steroid hormone, thiopurine drugs metabolism, response to drugs that modulate gluconeogenesis.	(***cyp19a1b***) (***tpmt.2***) (***tspo***)	cytochrome P450, family 19, subfamily A, polypeptide 1b thiopurine S-methyltransferase, tandem duplicate 2 translocator protein	GCAAAGGGGACAAACCTAATC CTGTTGCGGGACACTTTGG GGTATCCCATCAGCCGCAC	CCTTCGTCATCACCATAGCA TTGCCGATCACATGGGTTTA GCTGGTGGCGACACACAAC

Assay kit (Thermo Fisher Scientific) and RNA 6000 Nano Assay on a Bioanalyzer 2100 (Agilent Technologies). RNA concentration in all samples was higher than 200 ng/µL, free of DNA and with RNA integrity number (RIN) >8. Library construction and RNA-sequencing (RNA-seq) was performed by the National Center for Genomic Analysis (CNAG, Barcelona, Spain). The RNA-Seq library was prepared with KAPA Stranded mRNA-Seq Illumina Platforms Kit (Roche) following the manufacturer´s recommendations using Illumina platform compatible adaptors with unique dual indexes and unique molecular identifiers (Integrated DNA Technologies). The final library was validated on an Agilent 2100 Bioanalyzer with the DNA 7500 assay. The libraries were sequenced on NovaSeq 6000 (Illumina) with a read length of 2x51bp following the manufacturer's protocol for dual indexing. Image analysis, base calling and quality scoring of the run were processed using the manufacturer's software Real Time Analysis (RTA v3.4.4) and followed by generation of FASTQ sequence files.

After identifying the main transcriptomic biomarkers of exposure to the SEC water extract by RNA-seq analysis, an assessment of the effectiveness of the SAT systems to remove associated toxicity (restoration of normal transcriptomic levels) was carried out by real-time RT-PCR. The selected biomarkers included robust markers for: *dioxin-like* activity with the cytochrome P450 family 1, subfamily A (*cyp1a*) and the aryl- hydrocarbon receptor repressor (*ahrra*) (Chamorro et al., 2018; Mesquita et al., 2016; Olivares et al., 2013; Pelayo et al., 2011); estrogenic activity (brain aromatase (*cyp19a1b*)) (Chamorro et al., 2018; Ortiz-Villanueva et al., 2017; Sposito et al., 2018) and another 20

additional biomarkers related to xenotoxicity and embryotoxic responses (*ugt1a1, ugt5a4, gstp2, cyp2k18, cyp3a65, cidec, cxcl19, anxa1c, abcc12, slc34a2a, hmox1a, hsp70.2, opn1mw1, eevs, nr1d1, alas1, bbox, lrata, tpmt.2, tspo*). The housekeeping gene, *ppia2* was selected as an internal control. Appropriated primer sequences (**Table 1**) were obtained from published sources or designed using Primer Express 2.0 software (Applied Biosystems, Foster City, CA, USA) and the Primer-Blast server (http://www.ncbi.nlm.nih.gov/Tools/primer-blast), and synthesized by Sigma-Aldrich. Total RNA of all samples was retrotranscribed to cDNA using the Transcriptor First Strand cDNA Synthesis Kit (Roche Diagnostics) following the manufacturer's protocol. Every sample was run in duplicate in 96-well plates in a volume of 20 µl. Every reaction contained: 1µg of RNA transformed to cDNA (2 µl) and a master mix with 10 µL of SYBR Green Master (Roche Diagnostics), 300 nM (2 µl) of the appropriate primer set and 6 µL of nuclease-free water. Reactions were performed using a LightCycler 480 Real-Time PCR System (Roche Diagnostics). The cycling parameters consisted of 10 min at 95 ºC followed by 45 cycles of 10 s at 95 ºC and 30 s at 60 ºC. After amplification, a dissociation analysis was conducted to evaluate the specificity of the reaction. Two negative controls, non-template and RT-minus, were included on each plate to confirm the absence of primer dimers or genomic DNA contamination. The amplification reaction efficiency was evaluated for each primer pair by serial dilutions of cDNA under the same conditions. Amplification curves yielded an efficiency of 100 ± 10% (slope between −3.1 and −3.6) and r^2>0.98.

2.4 Human HepG2 hepatic cell line assays

Cell culture and exposure

The human HepG2 hepatic cell line (ATTC, HB 8065) was used as a model system to evaluate in vitro toxicity since it displays many of the genetic/metabolic features of hepatic cells (Choi et al., 2015; Schoonen et al., 2005). HepG2 cells were grown in RPMI 1640 medium (Invitrogen) containing 2 mM L-glutamine, supplemented with 10% fetal bovine serum (Invitrogen), and 100 U/ml penicillin/100 µg/ml streptomycin, at 37 °C in a humidified atmosphere with 5% CO_2. Cells were subcultured after reaching approximately 80% confluency. In all cases, cells were trypsinized and seeded in flat-bottomed 96-well plates (50 µl of cell suspension at a density of 2.5 × 10^4 cells/well) and allowed to attach for 24 h. Extracts were reconstituted in RPMI-1640 medium without phenol red to a final concentration of 3000x (equivalent to 3000 ml of water sample). Successive serial dilutions in the 20x-2000x range were obtained (equivalent to 20, 70, 200, 700, or 2000 ml of wastewater). Cells were exposed in triplicate to the different dilutions for 24 h. Negative controls consisted of HepG2 cells incubated with 50 µl supplemented RPMI-1640 medium without phenol red.

Cell proliferation assay

Cell proliferation was evaluated by the resazurin reduction (AlamarBlue) assay, which monitors functional metabolic activity. Cells were exposed to water extracts or 5% DMSO as a positive control. After 24 h exposure, cells were rinsed with PBS and incubated for 1h with 100 µl 5% v/v AlamarBlue reagent (Biosource, Invitrogen, Spain) in phenol red-free RPMI-1640 medium without FBS. AlamarBlue metabolization, a parameter for cell proliferation, was recorded spectrofluorimetrically using a microplate reader (Synergy 2 Multi-Mode Microplate Reader, BioTek Instruments, Vermont, USA), at the excitation/emission wavelengths of 530/590 nm. Results are expressed as the mean percentage of cell proliferation compared to unexposed control cells ± SEM of at least three replicates.

EROD activity measurement

The enzymatic activity of the CYP1A gene product was determined by the spectrofluorometric micro-EROD assay as published (Ouellet et al., 2020; Rudzok et al., 2010), with minor modifications. In brief, HepG2 cells were exposed in triplicate to various concentrations of water samples or 4 µM β-naphthoflavone as a positive control. After exposure, the medium was removed from the wells, and cells were rinsed with PBS and 100 µL of a 100-fold ethoxyresorufin solution 0.5 µM 7-ethoxyresorufin (Resorufin ethyl ether, Sigma), 10 µM dicoumarol (3,3´-Methylene-bis(4-hydroxycoumarin), Sigma) in cell culture medium without FBS was added in every well. Resorufin production was measured fluorometrically at 530 nm excitation and 590 nm emission. The amount of resorufin produced was determined by comparison to a calibration curve of known resorufin concentrations (resorufin sodium salt, Sigma), ranging from 0 to 300 nM. Enzymatic activity was normalized for total protein concentration, determined by the Bradford assay (Bio-Rad). For protein extraction, cells were washed twice with PBS, and, after drying at room temperature, 25 ul 0.1 M sodium hydrogen phosphate buffer (pH 7.8) was added per well. Plates were kept at −80 °C and lysates were obtained after a threefold freeze-thaw-cycle (−80 °C, 25 °C). Total protein was measured spectrophotometrically at 570 nm using a calibration curve made with bovine seroalbumin (BSA). Specific EROD activity was expressed as pmol of resorufin formed per hour per milligram of protein (pmol/h/mg protein) (mean ± SEM; n=3).

2.5 Chemical analysis and semi-quantification of CECs

Aliquots from the same water extracts used for toxicity assays were analyzed by liquid chromatography coupled to HRMS following the steps and conditions used elsewhere (Gil-Solsona et al., 2021). Briefly, separation was performed with a CORTECS UHPLC BEH C18 (100 mm x 2.1 mm, 2.7 µm) column (Waters Corporation) with a precolumn of the same material (5 mm x 2.1 mm, 2.7 µm) in an Acquity ultra-high performance liquid chromatographic system (UHPLC) (Waters Corporation) coupled to an electrospray source (ESI) to a Q-Exactive Orbitrap mass analyser (Thermo Scientific). ESI ionization operated in positive (ESI+) and negative (ESI-) ionization modes in two different injections. Samples were analysed twice with different acquisition modes i.e. Data Dependent Acquisition (DDA), where the 5 most intense ions from the low energy scan (4 eV) were selected and fragmented again at high collision energy (35 eV) to acquire MS/MS (excluding already selected ions for the next 30 seconds), and Data Independent Acquisition (DIA) using a ramp of 10-40 eV of collision energy (CE) for the high energy function.

A home-made database of 726 compounds usually found in water bodies was used (spreadsheet with the compounds, m/z values and SMILES is available in **Supplementary Table ST1**). It compiled pharmaceuticals and personal care products, pesticides and a wide range of industrial chemicals such as plasticizers, flame retardants or PFAS, among others. Data processing of the samples started with the transformation of the DIA files from proprietary (*.raw) format to generic (*.mzML) with ProteoWizard v. 3.0.2 (Kessner et al., 2008). Then, (*.mzML) files were uploaded to mzMine2 software v. 2.53 (Pluskal et al., 2010), and the home-made database was used to check for possible matches. After processing, 428 features matched the database input, but after (I) blank subtraction, (II) fragment ions checking and (II) manual checking of each feature, 166 compounds were kept as confirmed in the water samples. After confirmation, a semi-quantification protocol, retrieved from the work published by Liigand et al., (2020) was used to estimate concentrations of the identified chemicals (see **Supplementary**

Materials and Methods for more details).

2.6 Data analysis

Zebrafish data

Statistical analysis and plots for the zebrafish phenotypic and transcriptomic data were performed under the R environment (version 4.2.1; http://www.rproject.org/). Unless specified, data processing and plotting were performed using tidyverse, dyplr and factoextra packages (Irnawati et al., 2020; Lee et al., 2020; Yarberry, 2021) in the R environment.

Survival and swim bladder inflation rates

To determine differences in the survival and swim bladder inflation of the eleutheroembryos triggered by exposure to the different water extracts, analysis of variance (ANOVA) and Tukey's B post-hoc test for multiple tests were carried out in the normally distributed data (Levene´s test) using *ggpubr* package (Yang et al., 2021) in the R environment.

Trancriptomic data

RNA-Seq reads were aligned to the *Danio Rerio* reference genome (GRCz11) using the STAR software version 2.7.8a (Dobin et al., 2013) with ENCODE parameters. The total sequencing output was 60 million paired end reads for each sample and 100% mapped properly to the reference genome. Quality control of the mapping was performed with Samtools and Gemtools. Detailed description of mapping quality statistics is presented in **Supplementary Table ST2**. The majority mapped to protein-coding genes and exonic regions, with a total of 32.520 genes detected per sample (**Supplementary Table ST2**). The RSEM software version 1.3.0 (Li and Dewey, 2011) was used for the quantification of the annotated genes (using default parameters). Counts were normalized with the DESeq2 (v.1.10.1) R package (Love et al., 2014), which normalizes for sequencing depth and RNA composition using the median of ratios method. RNA-seq data was deposited in NCBI's Gene Expression Omnibus (Edgar et al., 2002) and are accessible through GEO (data to be submitted) Statistical analysis to determine differentially expressed genes (DEGs) between CTRL and SEC treatment groups was carried out with the DESeq2 (v.1.10.1) R package Wald test analysis both regardless of the campaign and in each campaign separately (Love et al., 2014). DEGs enrichment analysis of the common genes was performed using DAVID 2021 Bioinformatic resources (https://david.ncifcrf.gov/) using the default Danio Rerio background and considering the GO:Biological Process and KEGG (Kyoto Encyclopedia of Genes and Genomes) datasets. Network analysis was performed only with pathways that contained at least five hits using the *reshape2*, *igraph* packages (Li and Yan, 2018; Robinson et al., 2017). Lollipop charts were created using ShinyGO 0.76 (http://bioinformatics.sdstate.edu/go/) chart tool and normalized counts heatmaps using *ggplot2* package in R environment.

Relative mRNA abundances of different genes assessed by real-time RT-PCR were calculated based on the second derivative maximum of their respective amplification curves (Cp, calculated by duplicate). Cp values for the target genes (Cp_{tg}) were normalized to the average Cp values of the reference gene (*ppia2*), following the equation $\Delta Cp_{tg} = Cp_{ppia2} - Cp_{tg}$. To calculate the differences between mRNA abundances we used the ΔΔCp method (Pfaffl, 2001) using ΔCp_{tg} values from samples the different experimental groups exposed to water extracts and samples from the control group following the equation:

$\Delta\Delta Cp_{tg} = \Delta Cp_{tg\_control} - \Delta Cp_{tg\_exposed\ waters}$.

Data normality was tested by Levene's test

and diferences in mRNA abundance between experimental groups assessed by ANOVA and Tukey's B post-hoc test for multiple tests in R environment.

Human HepG2 hepatic cells data

Origin 6.0 software was used to adjust response curves in the AlamarBlue cell proliferation assays to non-linear regression slope models and calculate the IC_{50} (concentrations causing a 50% decline in cell proliferation). Significant differences in EROD activity among samples were determined by one-way ANOVA followed by Tukey's post hoc test, carried out in the R environment.

CECs and RT-PCR data correlations

From the 166 confirmed compounds (sheet "confirmed compounds" in **Supplementary Table ST1**) we removed those whose contribution to the blank was higher than to the rest of samples, ending up with 127 semi-quantified compounds (**Supplementary Table ST3**). To find the main compounds that best predicted the biological effects in JUN20 and OCT20, we run an Analysis of Variance-Partial Least Square with 2 components (ANOVA-PLS2) test using the *mixOmics* package in R environment (A. F. Santos et al., 2020). Briefly, this analysis consisted of a decomposition of the combined (chemical+transcriptomic) data matrixes for all treatments through a linear model that considers the experimental design (SEC, ATs, CTs,), and builds a regression between the matrices obtained in the first linear decomposition (x) and a vector (y) defining the class membership of the samples. This analysis allowed to identify 70 and 38 Variables Important for Prediction (VIP compounds) for JUN20 and OCT20 campaigns, respectively, that significantly best described the differences between groups ($p \leq 0.05$). Afterwards, we performed a linear Pearson`s correlation using the package psych in R environment (Revelle, 2016) to assess correlations between the concentration of the identified VIP CECs and the biological responses measured as changes in mRNA (transcriptomic data assessed by real-time RT-PCR), Finally, to assess the spatial distribution of the RT-PCR and chemical samples, we undertook PCA analyses for each campaign separately using *factoextra* in R (Kassambara and Mundt, 2017)

3. Results

3.1 Zebrafish general toxicity assays

Survival analysis showed, as expected, that extracts from PRIM water samples were much more toxic than extracts from SEC samples (**Supplementary Figure SF2**). This was especially notorious for OCT20 PRIM extract, which showed a significant toxic effect at 1X concentration factor and 0% survival at 8X. In contrast, the JUN20 PRIM extract showed 100% survival at 1X, 85% survival at the 3X, and 20% survival at the 8X (**Supplementary Figure SF2**). Regarding the swim bladder inflation rates, findings were similar to the ones observed in survival. There was a significant decrease at 8X for JUN20, and 1X and 3X for OCT20 (**Supplementary Figure SF2**). In contrast, the rest of water extracts (including SEC, ATs and CTs), showed only a marginal decrease in survival even at the 20X concentration (**Supplementary Figure SF4**). A slightly significant decrease in survival was observed for SEC in both JUN20 and OCT20 campaigns (90% and 80% of survival, respectively). No significant alterations of the swim bladder inflation rates were observed for neither of the two campaigns (**Supplementary Figure SF4**).

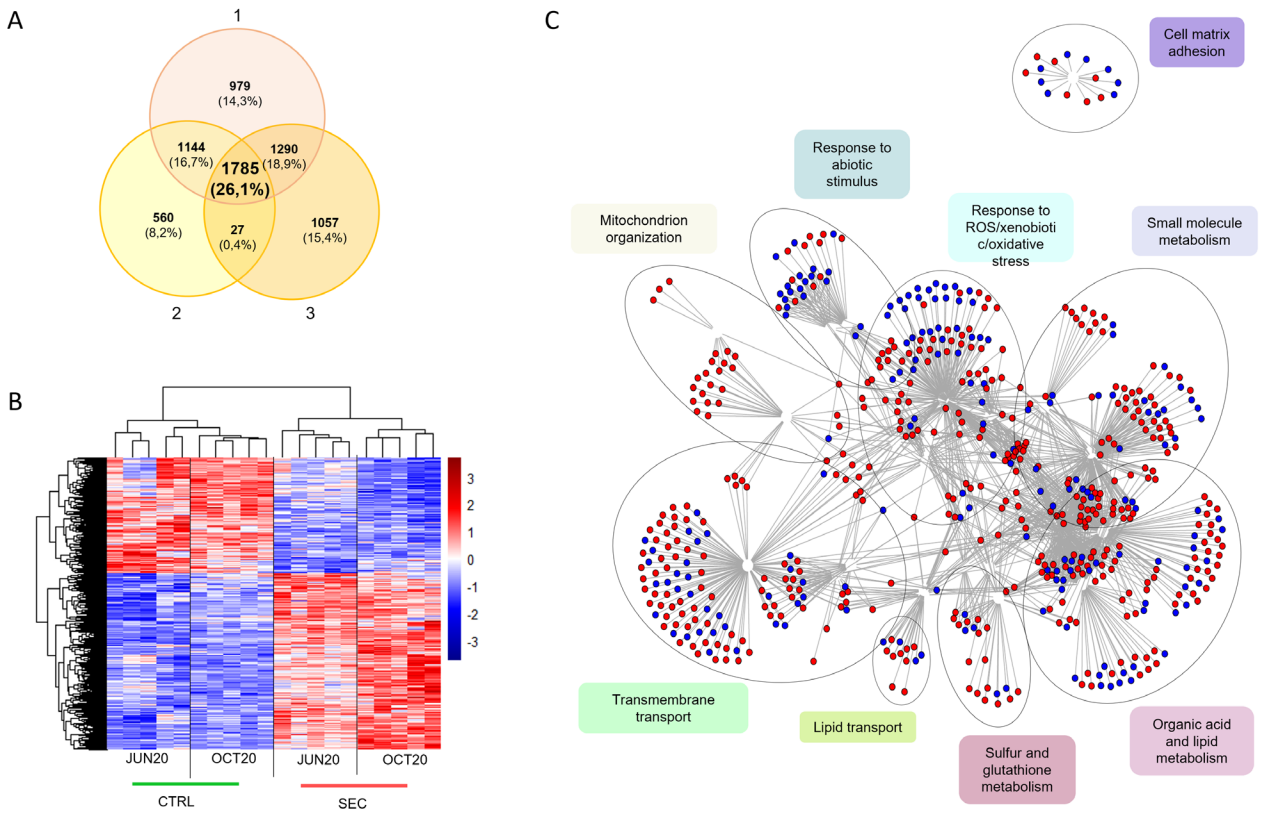

Figure 2. Normalized counts and enrichment analysis of the common 1785 DEGs. **A)** Venn diagram highlights the common 1785 DEGs within the total DEGs from the three approaches (1. DEGs regardless of campaign, 2. JUN20 DEGs, 3. OCT20 DEGs). **B)** Heatmap shows the normalized count data for the common DEGs in both campaigns. C) Enrichment analysis for the 1785 common DEGs. Network displays all the enriched biological processes, illustrating the mutual interaction between the different pathways. Note that similar nodes have been grouped into broader, easy to interpret functional descriptions. Red and blue colors in network code for up and down regulated genes respectively.

3.2 Transcriptomic analysis

DESeq2 workflow analysis identified 5199 DEGs when the Wald analysis was carried out regardless of campaign, 4160 DEGs for JUN20 samples and 3516 DEGs for OCT20 samples (**Table ST4**). Venn Diagram revealed that the three approaches rendered 1785 common DEGs (**Figure 2A**), with 1077 of them being up-regulated and 708 down-regulated compared to CTRL samples (**Figure 2B**). When carrying enrichment pathway analysis over the general 5199 DEGs, the JUN20 4160 DEGs, the OCT20 3516 DEGs and the 1785 common DEGs, we observed that the top 20 significant pathways of the common DEGs were always within the top 20 significant pathways of all the other approaches (**Supplementary Figure SF5**). Consequently, further analysis and biomarker discovery focused in the common DEGs enriched pathways (**Supplementary Figure SF5**). Enrichment analysis of the common DEGs identified 19 pathways, mainly implicated in different detoxification mechanisms (general detoxification and xenobiotic metabolism and detoxification), transmembrane transport, and reaction to extreme abiotic conditions (see lollipop graph for common genes in **Supplementary Figure SF5** and **Supplementary Table ST5**). The network in **Figure 2C** illustrates the mutual interaction between the different enriched pathways for the common genes. Note that similar nodes have been grouped into broader, easy to interpret functional descriptions (eg: "response to reactive oxygen species/ xenobiotic stimulus/ oxidative stress", "Small molecule metabolism", "Organic

acid and lipid metabolism", "Sulfur and glutathione metabolism", "Lipid transport", "Transmembrane transport", "Mitochondrion organization", "Response to abiotic stimulus" and "Cell matrix adhesion"). Most of the involved genes were up-regulated with a small fraction of down-regulated ones.

Targeted mRNA abundance analyses by real-time RT-PCR were consistent with the RNA-seq results (**Figure 3**), showing a stronger response of zebrafish eleutheroembryos exposed to SEC water extracts from OCT20. A general recovery of the control levels was seen for most of the analyzed transcripts due to SAT, corresponding to a reduction of the observed transcriptomic effects caused by SEC of 50-100% for JUN20 and 70-100% for OCT20 samples (**Table 2**). The reduction of the three strongest toxic responses observed in SEC samples i.e. estrogenic response (*cyp19a1b*), xenobiotic metabolism (*cyp2k18*) and *dioxin-like* (*cyp1a, ahrra)* was especially remarkable (**Table 2**, **Supplementary Figure SF6**. In general, our results show that most of this reduction already occurred in the reactive barriers, since similar reduction levels were found in both AT and CT extracts, except for the AT2 JUN20 sample (**Figure 3**, **Table 2**).

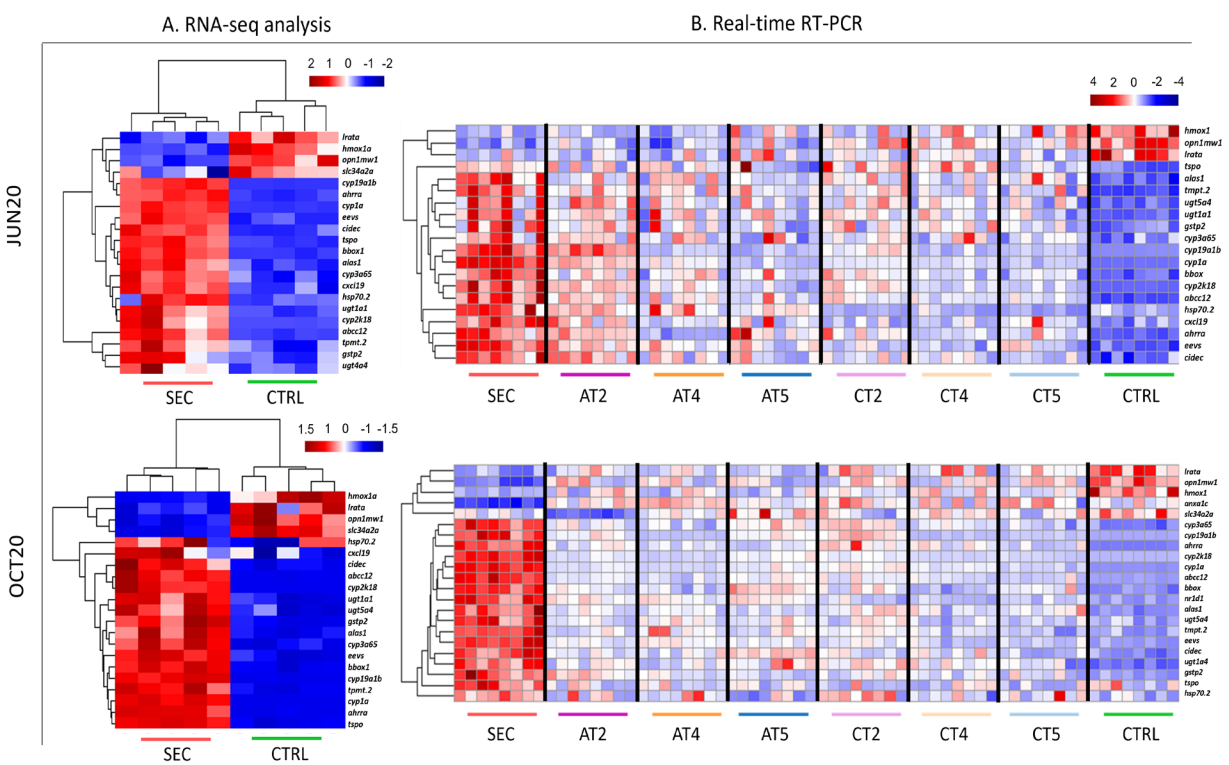

Figure 3. Abundance of mRNA biomarkers before and after SAT treatment for both JUN20 and OCT20 campaigns. **A)** Heatmaps with the selected transcriptomic biomarker´s RNA-seq data from SEC and CTRL water extracts. **B)** Heatmaps showing fold change transcriptomic data obtained by real time RT-PCR of SEC, ATs, CTs and CTRL water extracts. In both cases, data was scaled and centered before plotting data.

Table 2. Reduction percentage of the targeted biomarkers in ATs and CTs samples for both campaigns with its respective SEC sample (Fold Change +- SEM) value. Black boxes highlight those percentages statistically indistinguishable from their respective CTRL value. Red and blue color in gene name code for up-regulated and down-regulated genes respectively. Genes are ordered by their highest toxic response in each campaign (highest SEC (Fold Change +- SEM) value). Minimum and maximum reduction percentage values for each sample are shown at the end of the table.

JUN20

Gene Name	SEC (FC ± SEM)	AT2	AT4	AT5	CT2	CT4	CT5
cyp19a1b	**47,1 ± 4,9**	24%	**82%**	**86%**	60%	**84%**	**83%**
cyp2k18	**15,1 ± 2,1**	41%	61%	**75%**	49%	69%	72%
cyp1a	**11,2 ± 0,5**	49%	67%	80%	70%	74%	79%
ahrra	**4,9 ± 0,5**	25%	**77%**	23%	40%	**64%**	51%
abcc12	3,6 ± 0,4	41%	52%	56%	51%	58%	60%
ugt1a1	3,2 ± 0,3	36%	43%	50%	42%	51%	**65%**
gstp2	3,2 ± 0,5	43%	**54%**	**71%**	45%	46%	**67%**
hsp70.2	3,2 ± 0,4	51%	52%	**67%**	**100%**	**100%**	**100%**
eevs	3 ± 0,16	41%	53%	55%	68%	71%	63%
bbox	2,9 ± 0,2	53%	59%	59%	50%	68%	**72%**
cxcl19	2,5 ± 0,2	48%	**77%**	**63%**	**86%**	**84%**	**64%**
tpmt.2	2,5 ± 0,2	39%	45%	46%	42%	55%	53%
alas1	2,4 ± 0,2	50%	44%	61%	40%	59%	46%
ugt5a4	2,3 ± 0,3	18%	47%	**53%**	34%	**50%**	**58%**
cidec	2,3 ± 0,2	23%	54%	59%	55%	59%	**69%**
cyp3a65	2 ± 0,2	33%	**49%**	**53%**	**48%**	**50%**	**66%**
tspo	1,9 ± 0,1	**18%**	**18%**	**28%**	0%	0%	**46%**
lrata	0,6 ± 0,04	0%	0%	31%	8%	19%	2%
opn1mw1	0,5 ± 0,04	20%	7%	26%	**61%**	55%	40%
hmox1a	0,4 ± 0,04	8%	3%	32%	20%	38%	**51%**
anxa1c	bql	bql	bql	bql	bql	bql	bql
slc34a2a	bql	bql	bql	bql	bql	bql	bql
nr1d1	bql	bql	bql	bql	bql	bql	bql
	min	0%	0%	23%	0%	0%	2%
	max	53%	82%	86%	100%	100%	100%

OCT20

Gene Name	SEC (FC ± SEM)	AT2	AT4	AT5	CT2	CT4	CT5
cyp2k18	**81,7 ± 6**	87%	**93%**	79%	83%	**91%**	**92%**
cyp19a1b	**55,2 ± 6,5**	74%	**93%**	71%	55%	**94%**	**91%**
ahrra	**29,5 ± 2,4**	64%	71%	73%	46%	60%	73%
cyp1a	**21,5 ± 0,9**	77%	81%	72%	65%	75%	82%
abcc12	10,4 ± 0,7	79%	**84%**	71%	74%	81%	**84%**
nr1d1	6,6 ± 0,6	64%	**67%**	62%	**85%**	**90%**	**84%**
gstp2	6,4 ± 0,9	52%	**73%**	**82%**	**69%**	**76%**	**80%**
eevs	5,5 ± 0,4	75%	68%	74%	75%	**87%**	**84%**
bbox	5,1 ± 0,2	69%	79%	47%	64%	**87%**	69%
ugt1a1	4,5 ± 0,3	56%	65%	39%	44%	53%	68%
cidec	4,2 ± 0,3	70%	69%	44%	71%	64%	**83%**
tpmt.2	3,8 ± 0,3	**79%**	58%	**73%**	69%	**80%**	**94%**
ugt5a4	3,5 ± 0,4	**83%**	**73%**	**75%**	**73%**	**91%**	**89%**
alas1	3,4 ± 0,4	**70%**	**71%**	**76%**	57%	**70%**	61%
cyp3a65	2,7 ± 0,1	66%	75%	56%	49%	68%	**79%**
tspo	1,7 ± 0,2	**100%**	**100%**	**100%**	**100%**	**100%**	**100%**
hsp70.2	1,6 ± 0,1	70%	49%	100%	18%	83%	43%
anxa1c	0,4 ± 0,03	**100%**	**100%**	**100%**	**100%**	**100%**	**100%**
slc34a2a	0,4 ± 0,04	92%	**100%**	**100%**	**100%**	**100%**	**100%**
lrata	0,4 ± 0,04	36%	31%	16%	49%	**54%**	40%
hmox1a	0,3 ± 0,02	31%	21%	12%	24%	39%	25%
opn1mw1	0,2 ± 0,04	54%	53%	42%	58%	51%	58%
cxcl19	bql	bql	bql	bql	bql	bql	bql
	min	31%	21%	12%	18%	39%	25%
	max	100%	100%	100%	100%	100%	100%

3.3 Human HepG2 hepatic cell line assays

HepG2 hepatic cells proliferation profiles (**Supplementary Figure SF2B**) upon addition of PRIM extracts revealed that the OCT20 PRIM extracts had a higher toxicity than the JUN20 PRIM extracts. Analysis of samples before and after SAT (**Supplementary Figure SF4B**) indicated a reduction of the observed toxicity (i.e., inhibition of cell proliferation) aligned with the zebrafish data. In this case, SAT T4 was the most efficient one, particularly in OCT20 (IC_{50} values are indicated in **Supplementary Figure SF4**).

Specific toxic effects in HepG2 cells were explored by analyzing the CYP1A/EROD activity in cells exposed to the water extracts (**Figure 4**). EROD significantly increased in cells exposed to SEC samples while it was significantly reduced in both the ATs and CTs extracts. As seen with *cyp1a* activity in zebrafish larvae, the T2 SAT was less efficient in removing EROD than the other two SATs, especially in OCT20 samples (**Figure 4**) and EROD reduction mainly occurred at the RB (**Figure 4**), highlighting the operative capacity of RBs.

3.4 CECs analysis and correlation with biological data

A total of 127 CECs were identified by LC-HRMS-based screening in SEC, ATs, and CTs water extracts, which included pharmaceuticals and pesticides, among others, as well as related transformation products (**Supplementary Table ST3**). ANOVA-PLS2 carried out for JUN20 and OCT20 samples separately, identified 70 and 38 CECs, respectively that best predicted changes in the transcriptomic data for each campaign. Hierarchical clustering in the heatmaps built from the correlation values between the selected CECs and the RT-PCR data revealed two well differentiated clusters (A and B) for the two campaigns (**Figure 5A&D**). In both campaigns all the compounds that significantly correlated with the presence of the evaluated toxic responses (understanded as up-regulation of genes not normally activated in controls, and inhibition/down-regulation of genes normally activated in controls appeared in cluster A. On the other hand, compounds from cluster B negatively correlated to the up-regulation of genes not

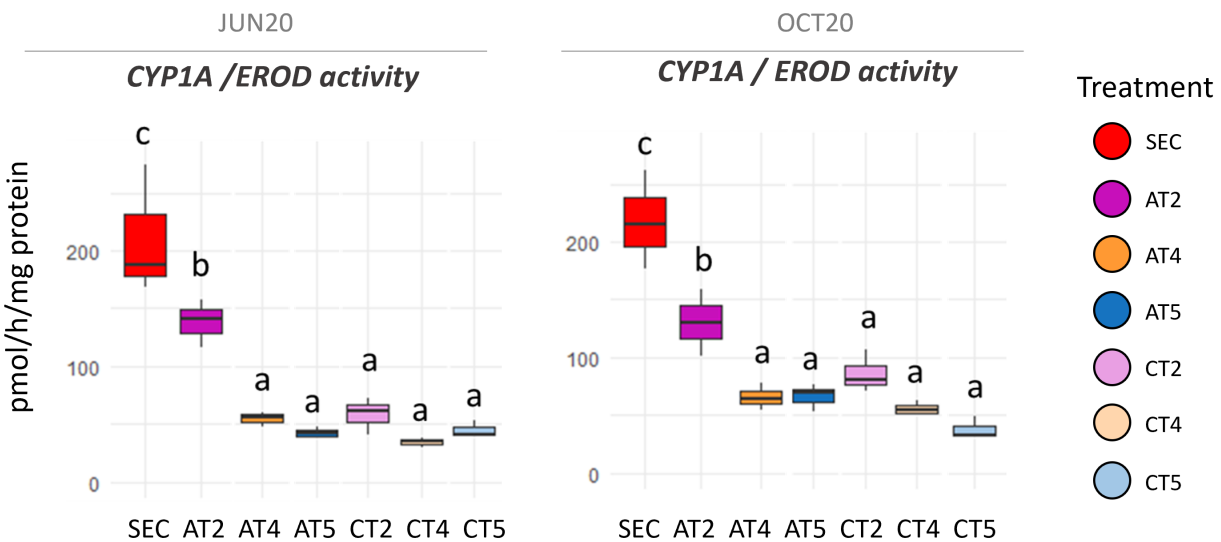

Figure 4. EROD activity of HepG2 cells exposed to SEC, AT, and CT extracts. Letters denote statistical differences amongst experimental groups (ANOVA test, followed by pairwise comparisons using Tukey's test, p<0.05).

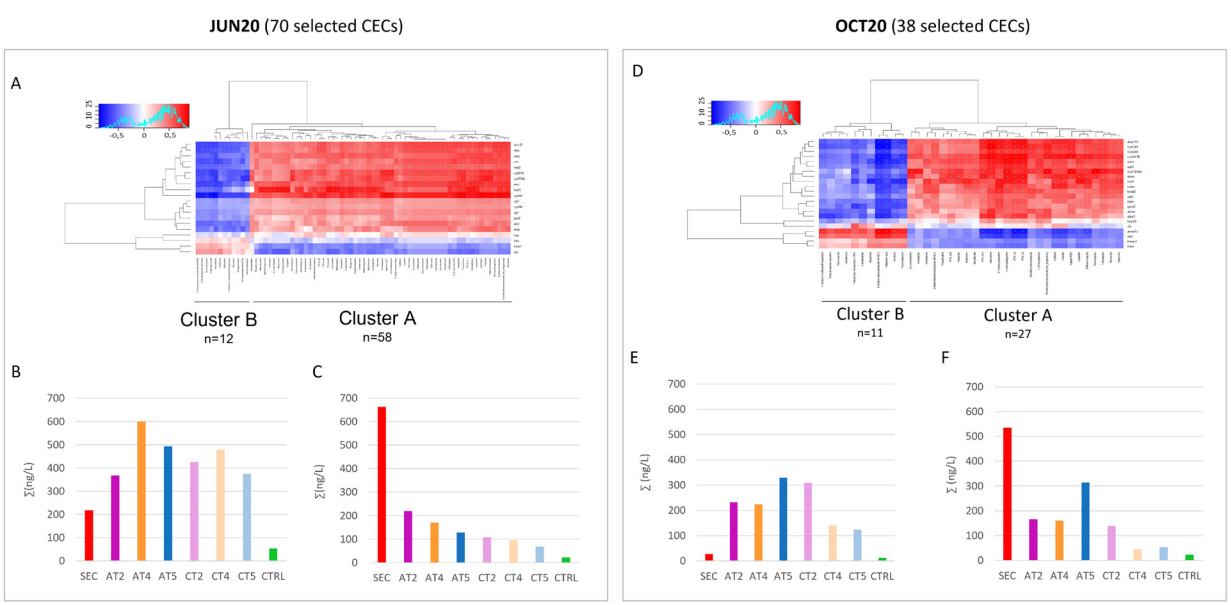

Figure 5. Heatmap showing Pearson's correlation between real-time RT-PCR transcriptomic data and ANOVA-PLS2 selected CECs loads for JUN20 (A) and OCT20 (D) campaigns respectively. Pearson's correlations validated ANOVA-PLS2 analysis finding significative correlations between the selected CECs that best predicted the transcriptomic responses and the biological data. Color code denotes Pearson's correlation values (red positive correlation, blue negative correlation) and asterisks represents significant correlations (p< 0.05). Bar plot graphs, show the CECs summatory concentration (in ng/L), for each experimental group, of the compounds allocated in clusters A (C and F graphs) and B (B and E graphs) spotted in the respective heatmaps of correlation values.

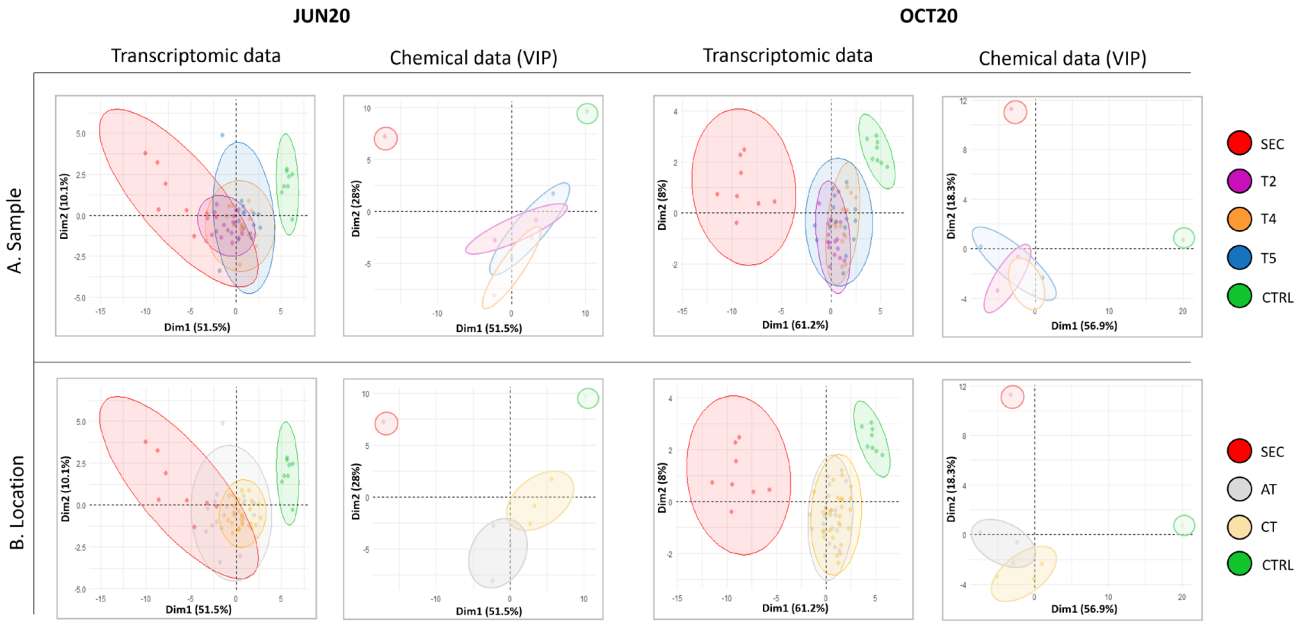

Figure 6. Principal Component Analysis (PCA) of the biological and the chemical data for JUN20 and OCT20 campaigns. A) Color coding differentiates between sampling location between SEC, SATs, and CTRL samples. B) Color coding differentiates between sampling location including SEC, AT, CT and CTRL samples.

normally activated in controls, and in most cases positively correlated with the activation of genes normally expressed in controls. The total loads of CECs from cluster A (58 CECs and 27 CECs for JUN20 and OCT20 campaigns respectively) experienced an outstanding reduction in SATs, finding their highest concentration in SEC extracts and the lowest in CTs extracts (**Figure 5C&F**). Conversely, the total loads of CECs from cluster B (12 CECs and 11 CECs for JUN20 and OCT20 campaigns respectively) were highly concentrated in the SAT samples, not being removed during treatment (**Figure 5B&E**).

The graphical distribution of the biological (transcriptomics) and chemical (selected CECs by ANOVA-PLS2) data by PCA analysis showed a clear separation between both SEC and CTRL extracts for both campaigns (**Figure 6A**). Water extracts from SAT systems were positioned in the PCA plot in between SEC and CTRL extracts, with no clear differences amongst their distributions. A partial overlap between SEC and SAT extracts was observed in the case of JUN20 transcriptomic data. On the other hand, PCA analysis was also plotted considering the sampling location within the SAT system (immediately after passing the vadose zone (AT) or close to the system discharge (CT)), regardless of the composition of the SAT (**Figure 6B**). In this case, ATs and CTs extracts overlapped when plotting transcriptomic data, while a clear separation between both could be observed when plotting the selected CECs data.

4. Discussion

It is generally acknowledged that WWTP are highly efficient in removing loads of carbon, nitrogen and phosphorous from influent wastewaters, and very efficient in removing pathogens, but they were not designed to eliminate other contaminants such as CECs (Margot et al., 2015; Tisler et al., 2021). This has fueled the need for supplementary treatment steps (the so-called tertiary treatments) to eliminate the hazardous activities associated to these quantitatively minor, but potentially dangerous pollutants. In the present study, we were capable to identify a total of 127

chemicals, with a wide range of physicochemical properties, by using wide-scope HRMS-based screening, including pharmaceuticals (PhACs) (e.g. metformin or venlafaxine), plastic additives (e.g. bisphenol S or phthalate metabolites), food related chemicals (such as caffeine, theobromine or theophylline), pesticides (e.g. imidacloprid or acetamiprid), as well as other types of chemicals typically found in urban or industrial wastewaters (e.g. nicotine, the UV filter benzophenone-3 or polypropylene glycols). The levels of the identified compounds observed in the SEC extracts were consistent with those usually found in wastewater effluents worldwide (Gago-Ferrero et al., 2020; Sunyer-Caldú et al., 2023; Tisler et al., 2021). This study used zebrafish embryos to analyze toxic effects associated to the presence of CECs in the wastewater extracts, as they represent an excellent model for both animal and human toxicity (Raldúa et al., 2012). Our results showed that exposure to SEC extracts was linked with a general triggering of detoxification pathways and the disruption of embryo general development.

In particular we observed the activation of cellular responses related to the exposure to xenobiotics, mainly related to both Phase I and Phase II detoxification pathways. On the other hand, exposure to SEC extracts also activated a "*dioxin-like*" response, which is associated with the presence of ligands to the aryl hydrocarbon receptors (AhR), and is characterized as both response to, and primary driver of, poisoning by dioxins (Pelayo et al., 2011). This specific response, was not only observed by the upregulation of *cyp1a* and *ahrra* mRNA levels in zebrafish, but also observed by the induction of EROD activity in human HepG2 hepatic cells exposed to SEC extracts. Estrogenicity is often associated to urban and industrial wastewaters, due to the presence of a variety of pollutants, such as natural and synthetic estrogens, pharmaceuticals, pulp mill residues or industrial wastes (Cooper et al., 2021a, 2021b; Romana et al., 2021). It represents one of the major limitations on the reuse and direct discharge of treated wastewater, because of their potential detrimental effects on fish and other vertebrate species (i.e, impaired sexual maturation, feminization, immune system modulation (Milla et al., 2011; Robitaille et al., 2022). The effects on humans are presently unclear, although it is assumed to have potential long terms effects for exposed children and fetuses (Aksglaede et al., 2006). The effect is mediated by interaction of natural or artificial compounds to the estrogen receptor (ER), present in all vertebrates. Given their rather high potency, with EC_{50} values within the picomolar or nanomolar range, ER agonists are rarely detected or quantified in wastewaters by chemical analyses (Brion et al., 2019). It is well known that the induction of the brain aromatase *cyp19a1b* (Chamorro et al., 2018; Martínez et al., 2020; Sposito et al., 2018) in zebrafish larvae is a direct marker of exposure to estrogenic compounds, so is a proven excellent biomarker of estrogenicity. In this regard, the present study showed a 50-fold increase of *cyp19a1b* mRNA levels in zebrafish embryos exposed to the SEC extracts, demonstrating once again, the estrogenic capacity of WWTP effluents. In addition to Phase I and II detoxification responses and estrogenic activity, our results showed that exposure to SEC extracts caused alterations in lipid metabolism and transport, transmembrane transport and mitochondrion organization, cellular response to light stimulus and phototransduction, retinol metabolism, circadian rhythm and locomotion, amongst others. Alterations in lipid metabolism and transport could impair cell membrane or dysregulate embryonic development (Martínez et al., 2020; Ortiz-Villanueva et al., 2018; Vremere et al., 2022) and they are also typically linked to endocrine disruption (Maradonna and Carnevali, 2018; Ortiz-Villanueva et al., 2018). Activation of the transmembrane transport can be linked to recovering homeostasis by regulating pH or chloride levels (Xu et al., 2016). The activation

of mitochondrion organization pathways might compensate mitochondrial dysfunctions (Imran et al., 2022). The latter effect usually correlates with alterations in heme and iron homeostasis, involvement of aryl hydrocarbon receptor (AhR) signaling and oxidative stress (Imran et al., 2022), in a response that partially overlaps the detoxification mechanisms. Circadian rhythm network is vital to mediate cellular and physiological processes such as the neurodevelopment and visual function (Li and Dowling, 2000). Therefore, we suggest that alterations on the transcriptomic profile of the 'visual and rythmic' pathways could be related to general embryotoxicity. Particularly, exposure to SEC decreased transcriptomic abundance of *opn1mw1* (involved in the cellular response to light stimulus and phototransduction) and *lrata* (involved in retinol metabolism). Eyes and brain are important sensory organs with high intensity of oscillations, and are sensitive to the external influence (Shi et al., 2022). Hence, we suggest that transcriptomic biomarkers related to light stimulus and photoreception, such as *opn1mw1,* can be used as sensitive markers of exposure to CECs. Finally, it is well known the involvement of the retinoid pathway in eye development (Bohnsack et al., 2012; Valdivia et al., 2016), which could explain alterations in photoreception, vision and behavior. Altogether, our results demonstrate that exposure of WWTP effluents extracts is capable to trigger the activation of detoxification pathways, estrogenicity and disruption of embryo general development in zebrafish.

The main finding of this study was that SAT treatment of the WWTP effluents provoked a major reduction of the evaluated toxic responses. For instance, in the case of the *dioxin-like* responses, *cyp1a* and *ahrra* mRNA levels in exposed larvae were significantly decreased thanks to the SAT treatment with a maximum of 82% removal, and this reduction was further observed with the reduction of EROD activity induction in exposed HepG2 hepatic cells. Remarkably, the SAT systems were also capable to reduce estrogenicity (induction of *cyp19a1b*) caused by exposure to SEC extracts by 83-92%, reaching control levels after the SAT treatment. It is worth mentioning that WWTP have been deemed as almost unable to eliminate estrogenic compounds from wastewaters (Meade et al., 2022), thus the relevance of this capability of SAT cannot be underestimated. We observed a major decrease on CECs loads in extracts obtained after the vadose zone, although this removal was still noticed through the SAT system. In concordance with these results, we observed that the major reduction of toxicological effects was already observed in water extracts obtained immediately after the vadose zone. This suggests that the retention/degradation of the most toxic compounds present in the SEC effluent might mainly occur passed the recharge areas. Correlation analysis of both the transcriptomic and the chemical data validated ANOVA-PLS2 analysis confirming that the abundance of a total of 108 CECs significantly predicted the observed changes in transcriptomic responses along the SAT treatment. The majority of this CECs (67), which included, caffeine, losartan, bisoprolol among others, experienced a considerable removal after the SAT treatment, which was significantly correlated with a decrease in the transcriptomic toxic responses. Altogether these results support the effectiveness of SATs in removing toxic CECs. On the other hand, a smaller number of CECs (17), like benzotriazole, melamine and some transformation products, such as 2-hydroxybenzothiazole, or valsartan acid were not removed or even increased their levels after the SAT treatment. As observed in the studied SATs, some of these CECs also appear recalcitrant to current wastewater treatments (Akao et al., 2022; Javadi et al., 2018). These results could explain the fact that although high rates of toxicity reduction were achieved after the SAT treatment, in some cases, control levels were not achieved, suggesting that the remaining toxicity could be

due to the presence of recalcitrant CECs in the SATs discharge waters.

Another aspect to highlight based on the results of this study is that the T2 system, which did not include an RB and was composed only by sand, was slightly less efficient in removing CECs and presented a lower performance in terms of toxicity removal than the systems that included RBs with different types organic matter. No apparent differences were observed between the SAT system that included woodchips or compost. Therefore, our results need to support the hypothesis that the provision of organic matter in the RBs located in the recharge areas of SATs could be required to boost SATs' performance in removing CECs and associated toxicity. In fact, the implementation of permeable reactive barriers has already proven efficient in increasing the removal of several CECs during SAT operations (Valhondo et al., 2020a, 2015, 2014) reaffirming their capability of improving water quality in short times, facilitating its application as tertiary treatments. Beyond toxicity and contaminants removal, SAT technologies have a beneficial ecological impact since they contribute to aquifer's recovering promoting in this way the exchange of groundwaters and surface waters (hyporheic exchange) in rivers and the associated ecosystems (Sunyer-Caldú et al., 2023). In summary, we conclude that the proposed SAT systems significantly improved CECs removal and its associated toxicological effects, demonstrating their effectiveness as cost-effective green tertiary treatments. That being said, additional follow-up studies are needed to evaluate new strategies in order to make SAT systems even more efficient and capable of removing recalcitrant CECs.

To the best of author's knowledge this is the first study that couples both *in vitro* and *in vivo* assays with wide-scope CECs suspect screening successfully evaluating the fate of CECs and their associated toxicity in WWTP effluents and the role of SAT treatment in their removal. The comparative approach followed in this study appears as an efficient and integrative tool for a representative biomonitoring of both WWTP effluents and SATs performance that could be easily implemented in future wastewater regeneration and effluents surveillance projects.

5. Conclusions

In summary, our results showed that exposure to SEC extracts caused alterations in lipid metabolism and transport, transmembrane transport and mitochondrion organization, cellular response to light stimulus and phototransduction, retinol metabolism, circadian rhythm and locomotion, amongst others. Simultaneously, we have demonstrated that the infiltration of WWTP effluents through the SAT systems enhanced the quality of the WWTP effluent by efficiently reducing between 46-100% toxicity responses such as general detoxification, estrogenicity and *dioxin-like* in zebrafish eleutheroembryos and human dioxin-like responses in HepG2 hepatic cells (markers heavily associated with detrimental effects on environmental and human health). This decrease in the detoxification response correlated with a 50-100% reduction of CECs cumulative loads. Our results demonstrated that the implementation of SAT holds great potential to reduce CECs loads and attenuate the toxic effects associated with WWTP effluents, allowing their safer disposal or potential use in aquifer recharge schemes. Identifying recalcitrant CECs and observing residual toxicity after SAT, aligned with the fact that the degradation of CECs seems to be compound-dependent, appear as key elements to consider in future SAT optimizations. We suggest designing and implementing combinations of barrier materials that can optimize the SAT, thereby improving the removal of possible toxic recalcitrant hazards. By integrating toxicogenomic analysis

with wide-scope suspect screening chemical analysis, we were able to link CECs removal with a reduction of associated toxic effects by the SAT treatments. We provide strong evidences that promote the implementation of enhanced SAT systems as a very promising approach to reduce, in a cost-efficient and ecofriendly manner, the environmental and human health effects of recalcitrant pollutants present in WWTP effluents.

Acknowledgements

This work was supported by the Water Catalan Agency Project RESTORA (ACA210/18/00040), the Spanish Research Agency Severo Ochoa Project (CEX2018-000794-S), and the projects BRAWR (RTI 2018-096175-B-I00), and JPI MARADENTRO (PCI2019-103603). We also thank the Consorci d'Aigües de la Costa Brava Girona (CACBGi) for facilitating access to the WWTP. CS was supported by a personal investigador predoctoral en formació (FI) fellow (2018 FI B 00368) awarded by the Secretary for Universities and Research of the Ministry of Economy and Knowledge of the Government of Catalonia.

Bibliography

A. F. Santos, E., C. S. Cruz, E., C. Ribeiro, H., D. Barbosa, L., S. Zandonadi, F., & Sussulini, A. (2020). Multi-omics: An Opportunity to Dive into Systems Biology. Brazilian Journal of Analytical Chemistry, 7(29), 18–44. https://doi.org/10.30744/brjac.2179-3425.rv-03-2020

Akao, P. K., Kaplan, A., Avisar, D., Dhir, A., Avni, A., & Mamane, H. (2022). Removal of carbamazepine, venlafaxine and iohexol from wastewater effluent using coupled microalgal-bacterial biofilm. Chemosphere, 308, 136399. https://doi.org/https://doi.org/10.1016/j.chemosphere.2022.136399

Almuktar, S. A. A. A. N., Abed, S. N., & Scholz, M. (2018). Wetlands for wastewater treatment and subsequent recycling of treated effluent: a review. Environmental Science and Pollution Research, 25(24), 23595–23623. https://doi.org/10.1007/s11356-018-2629-3

Bohnsack, B. L., Kasprick, D. S., Kish, P. E., Goldman, D., & Kahana, A. (2012). A Zebrafish Model of Axenfeld-Rieger Syndrome Reveals That pitx2 Regulation by Retinoic Acid Is Essential for Ocular and Craniofacial Development. Investigative Ophthalmology & Visual Science, 53(1), 7–22. https://doi.org/10.1167/iovs.11-8494

Brion, F., De Gussem, V., Buchinger, S., Hollert, H., Carere, M., Porcher, J. M., Piccini, B., Féray, C., Dulio, V., Könemann, S., Simon, E., Werner, I., Kase, R., & Aït-Aïssa, S. (2019). Monitoring estrogenic activities of waste and surface waters using a novel in vivo zebrafish embryonic (EASZY) assay: Comparison with in vitro cell-based assays and determination of effect-based trigger values. Environment International, 130(June), 104896. https://doi.org/10.1016/j.envint.2019.06.006

CADD Group Chemoinformatics Tools and User Services. (2022). Cactus Chemical Identifier Resolver.

Chamorro, S., Barata, C., Piña, B., Casado, M., Schwarz, A., Sáez, K., & Vidal, G. (2018). Toxicological Analysis of Acid Mine Drainage by Water Quality and Land Use Bioassays. Mine Water and the Environment, 37(1), 88–97. https://doi.org/10.1007/s10230-017-0472-2

Choi, J. M., Oh, S. J., Lee, S. Y., Im, J. H., Oh, J. M., Ryu, C. S., Kwak, H. C., Lee, J. Y., Kang, K. W., & Kim, S. K. (2015). HepG2 cells as an in vitro model for evaluation of cytochrome P450 induction by xenobiotics. Archives of Pharmacal Research, 38(5), 691–704. https://doi.org/10.1007/s12272-014-0502-6

Cooper, R., David, A., Kudoh, T., & Tyler, C. R. (2021). Seasonal variation in oestrogenic potency and biological effects of wastewater treatment works effluents assessed using ERE-GFP transgenic zebrafish embryo-larvae. Aquatic Toxicology, 237(January), 105864. https://doi.org/10.1016/j.aquatox.2021.105864

Cooper, R., David, A., Lange, A., & Tyler, C. R. (2021). Health Effects and Life Stage Sensitivities in Zebra fi sh Exposed to an Estrogenic Wastewater Treatment Works Effluent. 12(April), 1–16. https://doi.org/10.3389/fendo.2021.666656

Couto, C. F., Lange, L. C., & Amaral, M. C. S. (2019). Occurrence, fate and removal of pharmaceutically active compounds (PhACs) in water and wastewater treatment plants—A review. Journal of Water Process Engineering, 32, 100927. https://doi.org/https://doi.org/10.1016/j.jwpe.2019.100927

Delli Compagni, R., Gabrielli, M., Polesel, F., Turolla, A., Trapp, S., Vezzaro, L., & Antonelli, M. (2020). Risk assessment of contaminants of emerging concern in the context of wastewater reuse for irrigation: An integrated modelling approach. Chemosphere, 242, 125185. https://doi.org/10.1016/j.chemosphere.2019.125185

Deng, H., & Runger, G. (2012). Feature Selection via Regularized Trees. https://doi.org/10.48550/arxiv.1201.1587

Dillon, P., Stuyfzand, P., Grischek, T., Lluria, M., Pyne, R. D. G., Jain, R. C., Bear, J., Schwarz, J., Wang, W., Fernandez, E., Stefan, C., Pettenati, M.,

van der Gun, J., Sprenger, C., Massmann, G., Scanlon, B. R., Xanke, J., Jokela, P., Zheng, Y., … Sapiano, M. (2019). Sixty years of global progress in managed aquifer recharge. Hydrogeology Journal, 27(1), 1–30. https://doi.org/10.1007/s10040-018-1841-z

Dobin, A., Davis, C. A., Schlesinger, F., Drenkow, J., Zaleski, C., Jha, S., Batut, P., Chaisson, M., & Gingeras, T. R. (2013). STAR: Ultrafast universal RNA-seq aligner. Bioinformatics, 29(1), 15–21. https://doi.org/10.1093/bioinformatics/bts635

Downs, C. A., Bishop, E., Diaz-Cruz, M. S., Haghshenas, S. A., Stien, D., Rodrigues, A. M. S., Woodley, C. M., Sunyer-Caldú, A., Doust, S. N., Espero, W., Ward, G., Farhangmehr, A., Tabatabaee Samimi, S. M., Risk, M. J., Lebaron, P., & DiNardo, J. C. (2022). Oxybenzone contamination from sunscreen pollution and its ecological threat to Hanauma Bay, Oahu, Hawaii, U.S.A. Chemosphere, 291(November 2021). https://doi.org/10.1016/j.chemosphere.2021.132880

Ghimire, U., Nandimandalam, H., Martinez-Guerra, E., & Gude, V. G. (2019). Wetlands for wastewater treatment. Water Environment Research, 91(10), 1378–1389. https://doi.org/10.1002/wer.1232

Gil-Solsona, R., Nika, M. C., Bustamante, M., Villanueva, C. M., Foraster, M., Cosin-Tomás, M., Alygizakis, N., Gómez-Roig, M. D., Llurba-Olive, E., Sunyer, J., Thomaidis, N. S., Dadvand, P., & Gago-Ferrero, P. (2021). The Potential of Sewage Sludge to Predict and Evaluate the Human Chemical Exposome. Environmental Science and Technology Letters, 8(12), 1077–1084. https://doi.org/10.1021/acs.estlett.1c00848

He, C., Liu, Z., Wu, J., Pan, X., Fang, Z., Li, J., & Bryan, B. A. (2021). Future global urban water scarcity and potential solutions. Nature Communications, 12(1), 1–11. https://doi.org/10.1038/s41467-021-25026-3

Hristov, J., Barreiro-Hurle, J., Salputra, G., Blanco, M., & Witzke, P. (2021). Reuse of treated water in European agriculture: Potential to address water scarcity under climate change. Agricultural Water Management, 251(January 2020). https://doi.org/10.1016/j.agwat.2021.106872

Imran, M., Chalmel, F., Sergent, O., Evrard, B., Le Mentec, H., Legrand, A., Dupont, A., Bescher, M., Bucher, S., Fromenty, B., Huc, L., Sparfel, L., Lagadic-Gossmann, D., & Podechard, N. (2022). Transcriptomic analysis in zebrafish larvae identifies iron-dependent mitochondrial dysfunction as a possible key event of NAFLD progression induced by benzo[a]pyrene/ethanol co-exposure. Cell Biology and Toxicology, 0123456789. https://doi.org/10.1007/s10565-022-09706-4

Irnawati, I., Riswanto, F. D. O., Riyanto, S., Martono, S., & Rohman, A. (2020). The use of software packages of R factoextra and FactoMineR and their application in principal component analysis for authentication of oils. Indonesian Journal of Chemometrics and Pharmaceutical Analysis, 1(1), 1. https://doi.org/10.22146/ijcpa.482

Iyanagi, T. (2007). Molecular Mechanism of Phase I and Phase II Drug-Metabolizing Enzymes: Implications for Detoxification. International Review of Cytology, 260(06), 35–112. https://doi.org/10.1016/S0074-7696(06)60002-8

Javadi, N. H. S., Baghdadi, M., Mehrdadi, N., & Mortazavi, M. (2018). Removal of benzotriazole from secondary municipal wastewater effluent by catalytic ozonation in the presence of magnetic alumina nanocomposite. Journal of Environmental Chemical Engineering, 6(5), 6421–6430. https://doi.org/https://doi.org/10.1016/j.jece.2018.09.063

Kassambara, A., & Mundt, F. (2017). Package 'factoextra.' Extract and Visualize the Results of Multivariate Data Analyses, 76(2).

Kessner, D., Chambers, M., Burke, R., Agus, D., & Mallick, P. (2008). ProteoWizard: Open source software for rapid proteomics tools development. Bioinformatics, 24(21), 2534–2536. https://doi.org/10.1093/bioinformatics/btn323

Kimmel, C. B., Ballard, W. W., Kimmel, S. R., Ullmann, B., & Schilling, T. F. (1995). Stages of embryonic development of the zebrafish. Developmental Dynamics, 203(3), 253–310. https://doi.org/10.1002/aja.1002030302

Kumar, M., Ngasepam, J., Dhangar, K., Mahlknecht, J., & Manna, S. (2022). Critical review on negative emerging contaminant removal efficiency of wastewater treatment systems: Concept, consistency and consequences. Bioresource Technology, 352(February), 127054. https://doi.org/10.1016/j.biortech.2022.127054

Lee, S., Sriutaisuk, S., & Kim, H. (2020). Using the Tidyverse Package in R for Simulation Studies in SEM. Structural Equation Modeling: A Multidisciplinary Journal, 27(3), 468–482. https://doi.org/10.1080/10705511.2019.1644515

Li, B., & Dewey, C. N. (2011). RSEM: accurate transcript quantification from RNA-Seq data with or without a reference genome. BMC Bioinformatics, 12(1), 323. https://doi.org/10.1186/1471-2105-12-323

Li, K., & Yan, E. (2018). Co-mention network of R packages: Scientific impact and clustering structure. Journal of Informetrics, 12(1), 87–100. https://doi.org/10.1016/j.joi.2017.12.001

Li, L., & Dowling, J. E. (2000). Disruption of the olfactoretinal centrifugal pathway may relate to the visual system defect in night blindness b mutant zebrafish. Journal of Neuroscience, 20(5), 1883–1892. https://doi.org/10.1523/jneurosci.20-05-01883.2000

Lian, L., Yan, S., Yao, B., Chan, S.-A., & Song, W. (2017). Photochemical Transformation of Nicotine in Wastewater Effluent. Environmental Science & Technology, 51(20), 11718–11730. https://doi.org/10.1021/acs.est.7b03223

Liigand, J., Wang, T., Kellogg, J., Smedsgaard, J., Cech, N., & Kruve, A. (2020). Quantification for non-targeted LC/MS screening without standard substances. Scientific Reports, 10(1), 1–10. https://doi.org/10.1038/s41598-020-62573-z

Love, M. I., Huber, W., & Anders, S. (2014). Moderated estimation of fold change and dispersion for RNA-seq data with DESeq2. Genome Biology, 15(12), 1–21. https://doi.org/10.1186/s13059-014-0550-8

Maradonna, F., & Carnevali, O. (2018). Lipid metabolism alteration by endocrine disruptors in animal models: An overview. Frontiers in Endocrinology, 9(November), 1–14. https://doi.org/10.3389/fendo.2018.00654

Margot, J., Rossi, L., Barry, D. A., & Holliger, C. (2015). A review of the fate of micropollutants in wastewater treatment plants. WIREs Water, 2(5), 457–487. https://doi.org/https://doi.org/10.1002/wat2.1090

Martínez, R., Codina, A. E., Barata, C., Tauler, R., Piña, B., & Navarro-Martín, L. (2020). Transcriptomic effects of tributyltin (TBT) in zebrafish eleutheroembryos. A functional benchmark dose analysis. Journal of Hazardous Materials, 398(May). https://doi.org/10.1016/j.jhazmat.2020.122881

Martínez, R., Navarro-Martín, L., van Antro, M., Fuertes, I., Casado, M., Barata, C., & Piña, B. (2020). Changes in lipid profiles induced by bisphenol A (BPA) in zebrafish eleutheroembryos during the yolk sac absorption stage. Chemosphere, 246. https://doi.org/10.1016/j.chemosphere.2019.125704

Martínez, R., Tu, W., Eng, T., Allaire-Leung, M., Piña, B., Navarro-Martín, L., & Mennigen, J. A. (2020). Acute and long-term metabolic consequences of early developmental Bisphenol A exposure in zebrafish (Danio rerio). Chemosphere, 256. https://doi.org/10.1016/j.chemosphere.2020.127080

Meade, E. B., Iwanowicz, L. R., Neureuther, N., LeFevre, G. H., Kolpin, D. W., Zhi, H., Meppelink, S. M., Lane, R. F., Schmoldt, A., Mohaimani, A., Mueller, O., & Klaper, R. D. (2022). Transcriptome signatures of wastewater effluent exposure in larval zebrafish vary with seasonal mixture composition in an effluent-dominated stream. Science of The Total Environment, 856(September 2022), 159069. https://doi.org/10.1016/j.scitotenv.2022.159069

Mesquita, S. R., Dachs, J., van Drooge, B. L., Castro-Jiménez, J., Navarro-Martín, L., Barata, C., Vieira, N., Guimarães, L., & Piña, B. (2016). Toxicity assessment of atmospheric particulate matter in the Mediterranean and Black Seas open waters. Science of the Total Environment, 545–546. https://doi.org/10.1016/j.scitotenv.2015.12.055

Morin-Crini, N., Lichtfouse, E., Fourmentin, M., Ribeiro, A. R. L., Noutsopoulos, C., Mapelli, F., Fenyvesi, É., Vieira, M. G. A., Picos-Corrales, L. A., Moreno-Piraján, J. C., Giraldo, L., Sohajda, T., Huq, M. M., Soltan, J., Torri, G., Magureanu, M., Bradu, C., & Crini, G. (2022). Removal of emerging contaminants from wastewater using advanced treatments. A review. In Environmental Chemistry Letters (Vol. 20, Issue 2). Springer International Publishing. https://doi.org/10.1007/s10311-021-01379-5

Ofori, S., Puškáčová, A., Růžičková, I., & Wanner, J. (2021). Treated wastewater reuse for irrigation: Pros and cons. Science of the Total Environment, 760. https://doi.org/10.1016/j.scitotenv.2020.144026

Olivares, A., Van Drooge, B. L., Casado, M., Prats, E., Serra, M., Van Der Ven, L. T., Kamstra, J. H., Hamers, T., Hermsen, S., Grimalt, J. O., & Piña, B. (2013). Developmental effects of aerosols and coal burning particles in zebrafish embryos. Environmental Pollution, 178, 72–79. https://doi.org/10.1016/j.envpol.2013.02.026

Ortiz-Villanueva, E., Jaumot, J., Martínez, R., Navarro-Martín, L., Piña, B., & Tauler, R. (2018). Assessment of endocrine disruptors effects on zebrafish (Danio rerio) embryos by untargeted LC-HRMS metabolomic analysis. Science of the Total Environment, 635, 156–166. https://doi.org/10.1016/j.scitotenv.2018.03.369

Ortiz-Villanueva, E., Navarro-Martín, L., Jaumot, J., Benavente, F., Sanz-Nebot, V., Piña, B., & Tauler, R. (2017). Metabolic disruption of zebrafish (Danio rerio) embryos by bisphenol A. An integrated metabolomic and transcriptomic approach. Environmental Pollution, 231, 22–36. https://doi.org/10.1016/j.envpol.2017.07.095

Ouellet, J., Gembé, C., Buchinger, S., Reifferscheid, G., Hollert, H., & Brinkmann, M. (2020). Validation of the micro-EROD assay with H4IIE cells for assessing sediment contamination with dioxin-like chemicals. Environmental Pollution, 265. https://doi.org/10.1016/j.envpol.2020.114984

Pelayo, S., López-Roldán, R., González, S., Casado, M., Raldúa, D., Cortina, J. L., & Piña, B. (2011). A zebrafish scale assay to monitor dioxin-like activity in surface water samples. Analytical and Bioanalytical Chemistry, 401(6), 1861–1869. https://doi.org/10.1007/s00216-011-5288-5

Pfaffl, M. (2001). Development and Validation of an Externally Standardised Quantitative Insulin-like Growth Factor-1 RT-PCR Using LightCycler SYBR Green I Technology BT - Rapid Cycle Real-Time PCR: Methods and Applications (S. Meuer, C. Wittwer, & K.-I. Nakagawara (eds.); pp. 281–291). Springer Berlin Heidelberg. https://doi.org/10.1007/978-3-642-59524-0_30

Pluskal, T., Castillo, S., Villar-Briones, A., & Oresic, M. (2010). MZmine 2: modular framework for processing, visualizing, and analyzing mass spectrometry-based molecular profile data. BMC Bioinformatics, 11, 395. https://doi.org/10.1186/1471-2105-11-395

Raldúa, D., Barata, C., Casado, M., Faria, M., Navas, J. M., Olivares, A., Oliveira, E., Pelayo, S., Thienpont, B., & Piña, B. (2012). Zebrafish as a Vertebrate Model to Assess Sublethal Effects and Health Risks of Emerging Pollutants. In Handbook of Environmental Chemistry (Vol. 20, pp. 395–414). https://doi.org/10.1007/698_2011_124

Revelle, W. (2016). How to: Use the psych package for factor analysis and data reduction. Evanston, IL: Northwestern University, Department of Psychology.

Ricart, S., Villar-Navascués, R. A., Hernández-Hernández, M., Rico-Amorós, A. M., Olcina-Cantos, J., & Moltó-Mantero, E. (2021). Extending natural limits to address water scarcity? The role of non-conventional water fluxes in climate change adaptation capacity: A review. Sustainability (Switzerland), 13(5), 1–31. https://doi.org/10.3390/su13052473

Robinson, S., Finel, H., Boumendil, A., Tilly, H., Salles, G., Corradini, P., Cairoli, R., Pytlik, R., Schouten, H. C., Lewerin, C., Thieblemont, C., Metzner, B., Rambaldi, A., Ringhoffer, M., Lown, R., Rossi, G., Bittenbring, J. T., Bloor, A., Illés, A., … Montoto, S. (2017). In the era of chemoimmunotherapy, relapse post autologous stem cell transplantation for follicular lymphoma is associated with prolonged overall survival. An analysis by the lymphoma working party of the European Society for Blood and Marrow Transplantati. Blood, 130, 4818. https://doi.org/10.1182/blood.V130.Suppl

Romana, P., Mounteer, A. H., Benjamin, A., Rodrigues, E., Vitorino, F., Arcanjo, G., & Rodrigues, V. (2021). Evaluation of toxicity and estrogenicity

in UASB - Treated municipal sewage. Chemosphere, 268, 1–9. https://doi.org/10.1016/j.chemosphere.2020.128778

Rout, P. R., Mohanty, A., Aastha, Sharma, A., Miglani, M., Liu, D., & Varjani, S. (2022). Micro- and nanoplastics removal mechanisms in wastewater treatment plants: A review. Journal of Hazardous Materials Advances, 6(April), 100070. https://doi.org/10.1016/j.hazadv.2022.100070

Rudzok, S., Schlink, U., Herbarth, O., & Bauer, M. (2010). Measuring and modeling of binary mixture effects of pharmaceuticals and nickel on cell viability/cytotoxicity in the human hepatoma derived cell line HepG2. Toxicology and Applied Pharmacology, 244(3), 336–343. https://doi.org/10.1016/j.taap.2010.01.012

Sandoval, L., Zamora-Castro, S. A., Vidal-Álvarez, M., & Marín-Muñiz, J. L. (2019). Role of wetland plants and use of ornamental flowering plants in constructed wetlands for wastewater treatment: A review. Applied Sciences (Switzerland), 9(4), 1–17. https://doi.org/10.3390/app9040685

Schoonen, W. G. E. J., De Roos, J. A. D. M., Westerink, W. M. A., & Débiton, E. (2005). Cytotoxic effects of 110 reference compounds on HepG2 cells and for 60 compounds on HeLa, ECC-1 and CHO cells. II Mechanistic assays on NAD(P)H, ATP and DNA contents. Toxicology in Vitro, 19(4), 491–503. https://doi.org/10.1016/j.tiv.2005.01.002

Shi, W. J., Long, X. B., Li, S. Y., Ma, D. D., Liu, F., Zhang, J. G., Lu, Z. J., & Ying, G. G. (2022). Dydrogesterone and levonorgestrel at environmentally relevant concentrations have antagonist effects with rhythmic oscillation in brain and eyes of zebrafish. Aquatic Toxicology, 248(March), 106177. https://doi.org/10.1016/j.aquatox.2022.106177

Sorinolu, A. J., Tyagi, N., Kumar, A., & Munir, M. (2021). Antibiotic resistance development and human health risks during wastewater reuse and biosolids application in agriculture. Chemosphere, 265, 129032. https://doi.org/10.1016/j.chemosphere.2020.129032

Sposito, J. C. V., Montagner, C. C., Casado, M., Navarro-Martín, L., Jut Solórzano, J. C., Piña, B., & Grisolia, A. B. (2018). Emerging contaminants in Brazilian rivers: Occurrence and effects on gene expression in zebrafish (Danio rerio) embryos. Chemosphere, 209, 696–704. https://doi.org/10.1016/j.chemosphere.2018.06.046

Sunyer-Caldú, A., Sepúlveda-Ruiz, P., Salgot, M., Folch-Sánchez, M., Barcelo, D., & Diaz-Cruz, M. S. (2022). Reclaimed water in agriculture: a plot-scale study assessing crop uptake of emerging contaminants and pathogens. Journal of Environmental Chemical Engineering, 108831. https://doi.org/https://doi.org/10.1016/j.jece.2022.108831

Thieulant, M., Mouriec, K., Gueguen, M., Manuel, C., Pakdel, F., & Kah, O. (2009). Androgens Upregulate cyp19a1b (Aromatase B) Gene Expression in the Brain of Zebrafish (Danio rerio) Through Estrogen Receptors. 896(January), 889–896. https://doi.org/10.1095/biolreprod.108.073643

Tisler, S., Liang, C., Carvalho, P. N., & Bester, K. (2021). Identification of more than 100 new compounds in the wastewater: Fate of polyethylene/polypropylene oxide copolymers and their metabolites in the aquatic environment. Science of The Total Environment, 761, 143228. https://doi.org/https://doi.org/10.1016/j.scitotenv.2020.143228

Valdivia, L. E., Lamb, D. B., Horner, W., Wierzbicki, C., Tafessu, A., Williams, A. M., Gestri, G., Krasnow, A. M., Vleeshouwer-Neumann, T. S., Givens, M., Young, R. M., Lawrence, L. M., Stickney, H. L., Hawkins, T. A., Schwarz, Q. P., Cavodeassi, F., Wilson, S. W., & Cerveny, K. L. (2016). Antagonism between Gdf6a and retinoic acid pathways controls timing of retinal neurogenesis and growth of the eye in zebrafish. Development, 143(7), 1087–1098. https://doi.org/10.1242/dev.130922

Valhondo, C., Mart, L., & Wang, J. (2020). Reactive Barriers for Renaturalization of Reclaimed. Water, 12 (4), 10.

Valhondo, C., Martínez-Landa, L., Carrera, J., Díaz-Cruz, S. M., Amalfitano, S., & Levantesi, C. (2020). Six artificial recharge pilot replicates to gain insight into water quality enhancement processes. Chemosphere, 240. https://doi.org/10.1016/j.chemosphere.2019.124826

Vremere, A., Merola, C., Fanti, F., Sergi, M., Perugini, M., Compagnone, D., Mikhail, M., Lorenzetti, S., & Amorena, M. (2022). Oxysterols profiles in zebrafish (Danio rerio) embryos exposed to bisphenol A. Food and Chemical Toxicology, 165(December 2021), 113166. https://doi.org/10.1016/j.fct.2022.113166

Vymazal, J. (2020). Removal of nutrients in constructed wetlands for wastewater treatment through plant harvesting – Biomass and load matter the most. Ecological Engineering, 155(July), 105962. https://doi.org/10.1016/j.ecoleng.2020.105962

Vymazal, J., Zhao, Y., & Mander, Ü. (2021). Recent research challenges in constructed wetlands for wastewater treatment: A review. Ecological Engineering, 169(March), 106318. https://doi.org/10.1016/j.ecoleng.2021.106318

Wang, W., & Kannan, K. (2017). Mass loading and emission of benzophenone-3 (BP-3) and its derivatives in wastewater treatment plants in New York State, USA. Science of The Total Environment, 579, 1316–1322. https://doi.org/https://doi.org/10.1016/j.scitotenv.2016.11.124

Westlund, P., & Yargeau, V. (2017). Investigation of the presence and endocrine activities of pesticides found in wastewater effluent using yeast-based bioassays. Science of The Total Environment, 607–608, 744–751. https://doi.org/https://doi.org/10.1016/j.scitotenv.2017.07.032

Xu, T., Zhao, J., Xu, Z., Pan, R., & Yin, D. (2016). The developmental effects of pentachlorophenol on zebrafish embryos during segmentation: A systematic view. Scientific Reports, 6(May). https://doi.org/10.1038/srep25929

Yang, M. feng, Long, X. X., Hu, H. sai, Bin, Y. ling, Chen, X. ming, Wu, B. hua, Peng, Q. zhou, Wang, L. sheng, Yao, J., & Li, D. feng. (2021). Comprehensive analysis on the expression profile and prognostic values of Synaptotagmins (SYTs) family members and their methylation levels in gastric cancer. Bioengineered, 12(1), 3550–3565. https://doi.org/10.1080/21655979.2021.1951059

Yap, C. W. (2011). PaDEL-descriptor: An open source software to calculate molecular descriptors and fingerprints. Journal of Computational Chemistry, 32(7), 1466–1474. https://doi.org/https://doi.org/10.1002/jcc.21707

Yarberry, W. (2021). DPLYR BT - CRAN Recipes: DPLYR, Stringr, Lubridate, and RegEx in R (W. Yarberry (ed.); pp. 1–58). Apress. https://doi.org/10.1007/978-1-4842-6876-6_1

Zhu, T., Gao, J., Huang, Z., Shang, N., Gao, J., Zhang, J., & Cai, M. (2021). Comparison of performance of two large-scale vertical-flow constructed wetlands treating wastewater treatment plant tail-water: Contaminants removal and associated microbial community. Journal of Environmental Management, 278(P1), 111564. https://doi.org/10.1016/j.jenvman.2020.111564

CHAPTER FOUR.

GENERAL DISCUSSION AND CONCLUSIONS

General discussion and conclusions

Sanz, Claudia[1]; Navarro-Martin, Laia[1]; Piña, Benjamin[1]

1) IDAEA-CSIC, Jordi Girona, 18. E-08034, Barcelona, Spain

1. General Discussion

The work presented in this thesis adds new information on the risks associated to the use of regenerated materials on the environment. We focused in two aspects of this use: the application of biosolids to agricultural fields and the recharge of aquifers using reclaimed wastewater. We contributed with new insights into ARG loads transmission and potential microbiome alterations under realistic conditions. In addition, we assessed the role of WWTP effluents in ARG, CECs and associated toxic responses spreading and their potential removal after SAT treatment, in order to attenuate their impact in receiving underground and surficial water bodies.

A particular strength of this thesis resides in the provision of experimental data on the impact linked to the reuse of a large variety of biosolids for the fertilization of different target soils and crops. Additionally, we explored the effects of consecutive wastewater regeneration episodes, a piece of information specially lacking in field studies that is urgently required by policy-makers, since it represents an essential information for a complete assessment of WWTP effluents associated risk monitoring and reduction (Bondarczuk et al., 2016). Specifically, the publications of the second Chapter surveilled the occurrence of ABs, ARGs and ARBs in different agroecosystems under organic fertilization and the fate of these hazards in both fertilizers and fertilized soils and crops. On the other hand, the publications of the third Chapter helped us gain insight on the occurrence of ARGs, ARBs, and associated toxic responses in a given WWTP effluent through successive sampling campaigns and the potential role of SAT techniques in their removal. In the light of the obtained results, we developed a guide of different risk mitigation strategies for both reusing biosolids as organic fertilizers and handling wastewater effluents for water regeneration purposes.

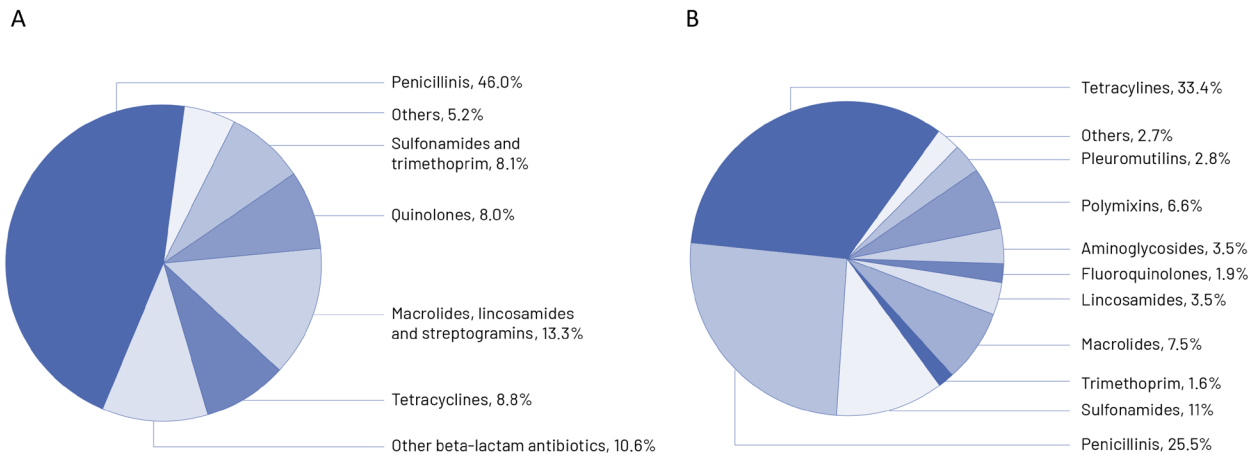

Figure 1. A) European consumption of antibiotics in human medicine (community and hospital sector) by classes in thirty European countries in 2015, expressed in daily defined doses (DDD)/1000 inhabitants/day. (ECDC, 2015). **B)** European consumption of antibiotics for food-producing animals by classes in twenty-nine European countries in 2014, expressed as percentage of the total sales in mg/population correction unit (PCU) (ECDC, 2014). Adapted from Pan and Chu (2017).

1.1 Occurrence of ABs, ARGs and ARBs in the studied agroecosystems. From ABs use to AR in foodstuffs

In the reports published by the European Center for Disease Prevention and Control (ECDC) on the specific prescription of antibiotics in human medicine (defined daily doses, DDD), a gradual increase was observed between 2000 and 2015. By 2015, Penicillins accounted for 46% of the total consumed ABs, followed by other β-lactams, macrolides, tetracyclines, quinolones, and sulfonamides (Pan and Chu, 2017, **Figure 1A**). Conversely, the ECDC observed large inter-country variations in antibiotic sales for food-producing activities (Pan and Chu, 2017). Tetracyclines accounted for approximately 33,4% of total AB consumption for food-producing animals in twenty-nine European countries, followed by penicillins, sulfonamides, macrolides, and polymixins (**Figure 1B**). Both the parent and metabolite forms of these ABs enter the environment via sewage (human urine and feces) and animal manure (90% excreted in urine, 75% in feces (Sarmah et al., 2006)). These residues contaminate soil, and surface and ground waters through leaching, runoff or, more directly, through soil fertilization with these matrices (Ezzariai et al., 2018; Gao et al., 2020; Michael et al., 2013).

The low-volatility and high persistence rates of a wide variety of ABs determine their accumulation in soil and their uptake by crops. They can be translocated and reallocated in different plant tissues depending on the plant genotype, on its physiological state, and on the presence of other stressors (Matamoros et al., 2022). Pan & Chu compilated in their review of 2017 a battery of studies that quantified different ABs in animal manure, other biosolids, soils and crops. Their results showed AB concentrations ranging from 10000 to 80000 ng/g (dry weight, dw) in animal manure, 300 to 1500 ng/g dw in other biosolids, 700 to 20 ng/g dw in soil and 500 to 10 ng/g dw in crop tissues. Tetracyclines appeared as the predominant family in the case of animal manure, soils, and crops, whereas quinolones were predominant in other biosolids (**Figure 2**). This accumulation pattern was also observed in the results from Chapter Two (see ST6 in Paper I, Tables 1 and 2 in Matamoros et al., (2022) and ST6 in Paper III), where the highest ABs concentrations were found in pig-based fertilizers followed by sewage biosolids, target soils, and,

Figure 2. Average concentrations range of different antibiotic families measured in animal manure, other biosolids, soil and crops across available literature. Data from Table S1 in Pan and Chu (2017).

lastly, crops. We observed that the treatment of pig-slurry did have a strong impact on ABs concentration, corresponding the lowest AB loads to solid fractions and digested slurries, and the highest ones to liquid fractions and raw pig slurries. Nonetheless, the loads of tetracyclines and lincosamides in pig-based fractions were around 4000 ng/g fw on average even in digested slurries. Consistently with the data in the Pan & Chu review, our results showed that quinolones were the highest AB family in sewage biosolid while any AB was quantified in the organic fraction of municipal solid waste (OFMSW). Regarding fertilized soils, tetracyclines reached their highest values in soils fertilized with solid fraction of pig slurry. For edible crops, ABs were only detected in lettuces and radishes at very low concentrations for all ABs families with a predominance of tetracyclines in the case of radish (Matamoros et al., 2022; Sanz et al., 2022a). On the other hand, no AB residues were found in corn, suggesting that the uptake capacity of cereals and grains ranged from moderate to low (Christou et al., 2019; Eggen and Lillo, 2012). Taken together, these results reveal that tetracyclines and quinolones and, to a lower extent, sulfonamides and lincosamides, are widespread amongst biosolids effectively reaching fertilized soils and crops. The potential propagation of ARGs and ARBs in the fertilizer-soil-crop continuum derived from ABs use/presence and their subsequent selective pressure still remain insufficiently characterized, with only a handful of available mesocosms studies that approach ARGs distribution over several compartments (Chen et al., 2018; Zhang et al., 2019a; Zhu et al., 2017). In contrast, the potential effects of ABs residues in soils and crops have been quite intensively assessed in literature, including inhibition of bacterial growth, bacterial respiration, toxic effects on meso and macrofauna and phytotoxicity (Conde-Cid et al., 2020; Li et al., 2011). In this context, the information retrieved in our laboratory over the past few years (Cerqueira et al., 2020, 2019b, 2019c, 2019a) and the results derived from this thesis (Sanz et al., 2022a, 2022b, 2021) become highly relevant.

Culture-independent qPCR methods allowed us to identify the possible sources of AR in agroecosystems with the screening of AR-associated genetic elements (ARGs and *intI1*). **Supplementary Table ST1**, summarizes the quantified genetic elements average abundance in all the analyzed matrices in the works included in Chapter Two. Fertilizers showed highest loads of all detected genes, particularly in raw pig slurry and processed pig slurry fractions, with a clear predominance of *int*I1, *sul*1 and *tet*M in all cases. This data is consistent with the fact that ABs administration enhances the prevalence of ARBs and ARGs in animal manure, as seen in a large body of studies (Looft et al., 2012; You and Silbergeld, 2014; Zhu et al., 2017). For instance, in the study by Zhu and collaborators (2013), manure samples from large-scale commercial swine farms showed three to four orders of magnitude more ARGs than manure samples from animals not exposed to antibiotics. Consistently with our results, many reports on agriculture-associated ARGs found high prevalence of tetracycline (i.e *tet*G, *tet*M, *tet*PB) and sulphonamide resistance genes (i.e, *sul*1, *sul*2) in animal manures (Wang et al., 2015; Zhao et al., 2019; Zhou et al., 2017), as well as a high prevalence of integrons, transposons, plasmids, and other MGEs (Cheng et al., 2013; Johnson et al., 2016; Xie et al., 2016; Zhu et al., 2013). Our finding that different ARG profiles can be found amongst animal wastes reinforces the hypothesis that animal handling and farm conditions have a fundamental role in determining the loads of released ARGs. The fact that *sul*1 and *tet*M were widespread amongst all analyzed wastes, while loads of markers of quinolones and beta lactams resistance were relatively low, reveals that the past use and abuse of this "classical ABs" lead to the presence of their corresponding resistance genes in wastes, even in animals not currently treated with this ABs. New ABs families may not be so widely used and thus their prevalence may still depend on continuous selective pressure. As a possible example, the relatively minor *qnr*S1 gene showed the strongest correlations with the high loads of quantified quinolones in Paper I (Sanz et al., 2021). Any relaxation in the use of quinolones and other ABs could translate in their respective resistance genes becoming part of the "general" resistome in animal and human guts. Our data confirms that the potential selective pressure associated to organic fertilizers may be enough to favor the soil colonization by antibiotic-resistant bacteria from either the same fertilizers or from the pre-existing soil microbial community. In Paper II & III (Sanz et al., 2022a, 2022b), ARG total loads and ARG profiles depended on the fertilizer type, and they were influenced by time between fertilization and sampling. In general, ARG loads were higher in the amended soils than in the minerally fertilized ones, although their levels appeared unstable and transient. For crops, and as observed for ABs, AR-related genetic elements were relatively low in all cases, particularly in radish and corn samples, although *int*I1 and *sul*1 and *tet*M achieved significantly high loads in lettuce when pig slurry was used as fertilizer (**Supplementary Table ST1**). *int*I1, *sul*1, and *tet*M were the genetic markers with highest loads in all three compartments analyzed (fertilizers, soils and crops). This correlates with works that identified tetracycline (*tet*) and sulfonamide (*sul*) resistances genes as the predominant resistance determinants in livestock waste and manured agricultural soils (He et al., 2020; Radu et al., 2021) followed by macrolide (*erm*) and β-lactam (*bla*) ARGs (Radu et al., 2021). The highest loads of these elements were found in raw pig slurry, its fractions, and in soils and crops fertilized with these materials. This suggests that pig slurry-based amendments have a strong potential for influencing ARG loads and increasing HGT in soils and crops, consistently with previous data on pig manure fertilization (Chen et al., 2019; Rahman et al., 2018; Zhang et al., 2021).

Knowing which fraction of the total bacterial communities qualify as ARG-harboring is a

really difficult task. This notwithstanding, the taxonomical information retrieved in works from Chapter Two with the sequencing of the 16S rDNA gene, allowed us to correlate ARG loads with the respective microbiome composition in the same samples. Moreover, we were able to compare fertilizers' microbiome to target soils' and crops' microbiomes in order to track potential contributions. A number of previous studies have shown that bacterial phylogeny and taxonomic structure significantly correlate with resistome composition in animal manure (Xie et al., 2018a), sewage sludge (Cai et al., 2022), and soils (Forsberg et al., 2014; Wang et al., 2020a). Pig-slurry microbiomes in Paper I (Sanz et al., 2021) showed the expected predominance of facultative anaerobic bacteria with a strong contribution of Firmicutes, mainly the Clostridia group, which includes some species related to serious foodborne diseases for man and animals. Minor contributors were Bacteroidetes (widely distributed in the environment and highly abundant in the gastrointestinal animal microbiome) and Spirochaetes groups. A similar composition have been described for fecal microbiomes elsewhere (Lamendella et al., 2011; Zhang et al., 2019b). Microbiota from the fertilizers from Paper II (Sanz et al., 2022a) also showed the predominance of Firmicutes and Bacteroidota groups. In contrast, a significant fraction of Archaea (mostly Crenarchaeota and Halobacterota, thermophilic and methanogenic taxa, respectively) appeared in sewage sludge and pig slurry, whilst Proteobacteria were only predominant in the sludge microbiome. Pig-based fertilizers from Paper III (Sanz et al., 2022b) found again Bacteroidota and Firmicutes as their predominant bacterial Phyla, along with methanogenic and thermophilic archaeal groups (Halobacterota and Thermoplasmatota). For fertilized soils and crops, Proteobacteria were the dominant bacterial Phyla in soils, corn leaves, and corn grains, with variable representations of Actinobacteriota, Bacteroidota, Acidobacteriota, Gemmatimonadota and a small fraction of Firmicutes, groups described elsewhere as being highly prevalent in soils (Karimi et al., 2018).

With the retrieved taxonomical information, we aimed to evaluate 1) the impact of fertilizers microbiome in the nature and distribution of sequenced taxa in soils, and 2) the occurrence of bacterial strains positively related with higher ARG loads in soils after fertilization. In Paper II & Paper III (Sanz et al., 2022a, 2022b), ASV sequence identification allowed us to identify small, but significant contributions of fertilizer microbiomes to the receiving soils, indicating a moderate persistence of gut bacteria in soil conditions. However, as observed with ARG loads, these alterations of the soil microbiome appeared to be transient, returning to a normal soil-like bacterial distribution in a matter of months. This aligns with recent evidence describing the strong capacity of agricultural soils to recover their basal ARG profiles after application of organic fertilizers. Radu and collaborators (2021) showed that ARG concentrations after manure amendment returned to baseline levels within a crop growing season. In the work from Muurinen et al., (2017), manure predominant ARGs were detected in soil short after application, but their abundance decreased over time, with many of them becoming undetectable, suggesting that the observed increase after fertilizing was temporary. That being said, we observed in both Paper I & II a cumulative effect of fertilizers on ASV distribution in soils from the second fertilization periods. The same effect was observed when analyzing the correlations between ARG loads and sequenced taxa. Organic fertilization increased the occurrence of bacterial strains positively correlated with ARG loads in treated soils, mainly belonging to the Proteobacteria, Actinobacteria and Firmicutes phyla. Some of these groups were also linked to high ARGs loads in the fertilizers analyzed in Paper I (Sanz et al., 2021) and to high ARG prevalence in soils, plants, and fruits in other

publications (Cerqueira et al., 2019b; Fogler et al., 2019). However, the majority of the identified members are normally found in soils (Karimi et al., 2018), in agreement with the evidence that the long-term influence of fertilizers on soil resistomes takes place primarily through the alteration of native bacterial composition, rather than through the direct introduction of manure-borne bacteria (Chu et al., 2007; Sun et al., 2015; Xun et al., 2016). Altogether, these results suggest that consecutive fertilization practices do have an additive effect on soil microbiome distribution and diversification. This evidence underscores the importance of respecting the optimal time between fertilization and harvest and of controlling the fertilization rates in order to decrease the risk of ARGs transmission and microbiome alterations over consecutive campaigns.

Another relevant observation extracted from the taxonomical and ARG data correlations carried in this thesis, is the effect of processing wastes on bacterial composition and its potential repercussion on ARG loads in both fertilizers and amended soils. When looking at the bacterial profile of more processed pig wastes in Paper I and Paper III (Sanz et al., 2022b, 2021), we observed the appearance of methanogenic and thermophilic taxa that could indicate the maturation of the initial swine slurry microbiome profile although this shift did not always translate into a lower ARG prevalence. In Paper II (Sanz et al., 2022a), more processed fertilizers (OFMSW and sewage sludge) showed a more soil-like bacterial profile along with a lower ARG prevalence (specially for *tet*M) when compared with raw pig slurry. Soils amended with these fractions also showed lower ARG prevalence than those fertilized with pig slurry. In conclusion we suggest that the implementation of treatments (e.g., composting or digestion) to the initial waste might promote bacterial succession and decrease ARG loads. There is growing evidence on the effect of thermophilic composting on the reduction of ARGs, and especially tetracycline resistance genes, in pig manure (Liu et al., 2020) in poultry manure (Esperón et al., 2020; Subirats et al., 2020) and on the removal of ARGs and MGEs in sewage sludge (Liao et al., 2018).

The ability of AR-associated genetic elements and ARB to colonize the gut microbiome of exposed humans and animals through foodstuffs is still largely unknown (Piña et al., 2020). The potential ARG transmission rate and ARB propagation in animal and human's guts will largely depend on the selective pressure posed by their ABs use/consumption. ABs subinhibitory concentrations and the combination of trace residues from both parental compounds and transformation products can have a dramatic effect on the maintenance of ARBs in the guts of farm animals and humans (Piña et al., 2020). The monitoring of AB residues through food chains is still a developing field, although we can find some works that quantified and estimated exposure rates of other pollutants. A seminal study demonstrated that the antiepileptic drug carbamazepine and its metabolites can be detected at considerable concentrations in the urine of people consuming wastewater irrigated vegetables (Paltiel et al., 2016). Another study showed that children resident in urban areas of Israel (Freeman et al., 2016) showed higher potential exposures rates to food-borne pesticides than the general population for several target compounds, with ten of them exceeding the Acceptable Daily Intake values. Therefore, the current evidence indicates that micropollutants can effectively disseminate from wastes to soil and crops reaching consumers and, consequently, that the general public exposure to ABs and ARG/ARB through food needs to be investigated.

In light of the results of this thesis, pig-slurry fertilizers were identified as the waste category with the highest risk associated to ARG/ARB transmission for both exposed workers and final consumers. Despite the limited capacity of bacterial colonization of this type of wastes, we confirmed that they have a strong potential

for influencing ARG loads and HGT in target soils and crops. Thus, the setting of legal requirements regarding their handling/treatment and the intensity and timing of their application appear crucial for their safe use as fertilizers. An interesting recent study shed some light on the occupational ARG exposure related to farms and slaughterhouses (Yang et al., 2022). The study monitored aph(3')-III, ermB, sul2 and tetW genes in animal faeces, farm-produced meat, environmental samples (electrostatic dustfall collector and gloves of slaughterhouse workers) and faeces from humans occupationally exposed to pigs or broilers at Dutch and German farms and slaughterhouses. They found a high variation of ARG abundance across animal species, environmental samples and human individuals. They concluded that the ARG abundance in the environmental samples significantly correlated with ARG abundance in the exposed human's faeces, fact that highlights the threat that raw pig-slurry handling might be already posing farm workers. However, they found a decreasing trend in the 'farm to fork' transmission of ARGs, partially attributed to recent farm biosecurity levels and regulation of ABs use.

In conclusion, our data validates the hypothesis that the simultaneous presence of AB residues and ARG loads in fertilizers, makes them important vectors of AR transmission through organic fertilization, especially with pig-based fertilizers. Although the observed increase in ARG loads and the modulation of fertilized soils microbiome appeared as transient impacts, the cumulative effect observed in the microbial distribution and diversification in soils from the second cycles highlight the importance of establishing adequate fertilization rates and properly scheduling harvest after organic fertilization. That being said, further studies are needed in order to fully evaluate the AR risk associated to organic fertilization based on the monitoring of AR residues and AR-associated genetic elements through food chains.

1.2. Occurrence of ARGs, ARB and toxic responses in wastewater effluents

Another potential risk to exposed environments evaluated in this thesis is that related to the handling of WWTP effluents in the context of water scarcity. The use of reclaimed wastewater represents a reliable source of water supply when weather variability and water over-abstraction compromise a sustainable water access. Nonetheless, WWTPs were initially designed to remove organic matter, pathogens and reducing ammonium loads and their effluents still contain high loads of both chemical and biological unregulated hazards after wastewater depuration, highly compromising a safe use/discharge without proper treatment.

The recent advances in analytical chemistry allowed the detection of a wide range of unregulated compounds, including ABs (Rodriguez-Mozaz et al., 2020), pharmaceuticals (de Oliveira et al., 2020), and plasticizers (Okoffo et al., 2019) in WWTP effluents. However, the analysis of the biological relevance derived from their presence in effluents is still an on-going task. In the context of AR transmission, a growing effort is being made in order to understand the potential role of WWTP effluents in this problematic (Alexander et al., 2020). The simultaneous presence of ABs and ARB makes WWTP effluents dangerous hotspots for antibiotic resistance spreading (Pazda et al., 2019). The persistent selective pressure from antibiotic residues at subinhibitory concentrations, along with the high density and diversity of microorganisms sustained by a nutrient rich environment create favorable conditions for antibiotic resistance dissemination (Rizzo et al., 2013). Antibiotics have been detected in WWTPs at concentrations ranging from < 10 to 7900 ng/l for influent wastewater and < 10 to 5600 ng/l in effluent wastewater (Omuferen et al., 2022). Among the most-detected compounds we find clarithromycin, erythromycin, azithromycin, roxithromycin, sulfamethoxazole,

trimethoprim, ofloxacin, ciprofloxacin, norfloxacin and tetracycline, probably due to the fact that these antibiotics are the most frequently prescribed and have a relatively stable structure (Wang et al., 2020b). However, their frequency and concentrations are heavily influenced by seasonal changes, usually achieving higher levels in winter than in summer correlated to a higher prescription rate (Wu et al., 2016). Other factor that could contribute to their seasonal variability is the regional socioeconomic context, like in the case of massive touristic areas (Cocozza et al., 2023).

The presence of ABs residues is likely related to the significant enrichment of ARGs encoding resistance to macrolides (*ere*A, *erm*B, *erm*C, *erm*43), sulfonamides (*sul*1, *sul*2, *dhfr*1), quinolones (*qnr*S, *qnr*C, *qnr*D), tetracyclines (*tet*A, *tet*B, *tet*E, *tet*G, *tet*H, *tet*S, *tet*T, *tet*X, *tet*M), and to a lower extent, β-lactam (bla_{CTXM} , bla_{TEM}, bla_{OXA-A}, bla_{SHV}, *mec*A) observed in WWTP effluents and WWTP activated sludges, with the latter usually presenting the highest concentrations (Mao et al., 2015; Munir et al., 2011; Wang et al., 2020b). Moreover, mobile elements such as plasmids, transposons, and integrons carrying ARGs have also been detected in effluents and activated sludge samples, indicating that gene transfer may occur in these environments (Guo et al., 2017; Zhuang et al., 2015). The ARG presence monitored in the effluents from Paper IV is consistent with this evidence, finding the highest relative abundance for *sul*1 followed by *tet*M, *qnr*S1 and bla_{TEM} genes. The integron *int*I1 was the genetic element with highest prevalence in effluent samples for all sampling campaigns, suggesting gene-transfer activities in the studied microbiomes. Several studies have monitored the presence of ARG in both WWTP influent and effluent to assess the role of wastewater treatment in ARG removal. Contradictory results have been reported with some of them describing a significant decrease in ARGs after wastewater treatment with activated sludge (Hultman et al., 2018; Laht et al., 2014), while others showed ARG enrichment in the WWTP effluent (Alexander et al., 2015; Amador et al., 2015; Bengtsson-Palme et al., 2016). Results from Paper IV revealed that in our study, the maximal values of ARG prevalence were observed in both influent and effluent samples for all sampling campaigns and the comparison between their respective values indicated that the WWTP treatment reduced ARG loads only by a relatively minor fraction in one sampling episode.

With the aim of characterizing the multi-faceted biological impact of WWTP effluents, different approaches have been taken for toxicity monitoring (Robitaille et al., 2022). This included in vitro cell assays that encompassed simple cytotoxicity tests (Žegura et al., 2009), biomarker studies (Gagné et al., 2013) and metabolomic methods (Žegura et al., 2009; Zhen et al., 2018). In these studies, wastewater effluents from diverse origin appeared cytotoxic, increased the expression of stress-related genes and disrupted energy and lipid metabolism in exposed cells. The magnitude of the observed effects depended on the size of population served by the WWTP, the influent flow rate, and the wastewater treatment method applied in each case. In Paper V, we also observed a dramatic effect of effluent extracts on HepG2 cell proliferation rate and on the induction of EROD activity, a highly sensitive indicator of contaminant exposure/detoxification that provides evidence of a AhR -mediated induction of the *cyp1a* subfamily (Dehn et al., 2004).

Although *in vitro* cell assays represent a great option for monitoring specific modes of action and they are able to predict and model exposure risks related to WWTP effluents, they do not consider synergistic or counter-regulatory processes within whole organisms, whose study requires a systemic approach. (Prasse et al., 2015). This can been achieved by coupling in vitro assays with the search of transcriptomic signatures of WWTP effluents exposure in in vivo assays (Meade et al., 2022). A battery of physiological effects has been

linked to surface water gradients in WWTP effluents chemistry by means of transcriptomics. This includes alterations in reproductive, endocrine and immunological functions in zebrafish and fathead minnow (Berninger et al., 2014; Zhang et al., 2018) as well as genotoxicity and disruption of vascular development in zebrafish (Zhang et al., 2018). This is consistent with the evidence found in Paper V, were the exposure of zebrafish embryos to WWTP effluent extracts induced estrogenic and phase I and II detoxification responses, impaired lipid metabolism and transport, alteration of cellular response to light stimulus and phototransduction, among other potentially adverse effects. It is important to note that robust transcriptomic biomarkers of CECs exposure in effluents are still lacking, since pathway-based impacts of exposure in fish models are not well characterized beyond those that involve steroidal reproductive hormones (Meade et al., 2022).

In summary, the information collected in Papers IV & V underscores the risk associated to WWTP effluents derived from their role in ARG transmission and their proven ability to induce toxic responses in both *in vitro* and *in vivo* assays. Characterizing the toxicity linked to the complex mixtures of chemical compounds present in effluents is still an on-going task where future efforts should be centered in finding robust exposure biomarkers for a complete comprehension of the toxic effects. Additionally, given the high risk associated with effluents discharges, the optimization of cost-effective tertiary treatments capable of removing both chemical and biological hazards appears as a clear challenge.

1.3 Risk mitigation strategies in fertilizers and wastewater effluents handling

The knowledge gained in the studies carried in this thesis contributed to the development of a set of risk mitigation strategies in order to ensure the safety of organic fertilizers and WWTP' effluents reuse.

Organic fertilizers handling.

In light of evidence, the first step for minimizing the risk associated with organic fertilization, in terms of antibiotic resistance dissemination, should be the exhaustive control of AB usage. A hopeful example is the decreasing trend in the ARG transmission observed in farms and attributed to ABs prescription regulations. Given that the spread of ARB/ARGs is dependent on selective pressure, relaxing this regulation might increase the microbiome resistance to new ABs, therefore reducing their effectiveness.

Simultaneously to regulating AB prescriptions, we support the idea that the treatment of generated wastes at the sources also represents a fundamental tool to reduce AB loads and tackle ARG transmission. Our work demonstrated that the handling and processing of farm wastes plays an instrumental role in reducing their AB loads, modulating their microbiome profile, lowering their ARG levels, and diminishing the impact on fertilized soils. Waste treatment should take place under conditions that do not favor typical intestinal/fecal microbiomes (represented by orders like Lactobacillales, Eubacteriales, Bacteroidales, and others (Chen et al., 2021)) and that favor ecological succession towards soil-related taxa normally correlated to low ARG prevalence (Bacillales, Xanthomonadales, Rhizobiales, etc. (Fierer, 2017)) and to the degradation of organic compounds (Cellulomonas, Pseudomonas, Bacillales, etc. (Rastogi et al., 2020)). Some of the key elements promoting this transition are pH, quality and quantity of organic carbon, redox status, moisture, and nitrogen and phosphorus availability, since they are the factors that majorly influence soil bacterial composition (Fierer, 2017). Thermophilic composting has proven very efficient in lowering ARG loads and reducing MGEs in a wide range of wastes, and there is also a growing

body of knowledge regarding its potential to promote compositional and functional succession of bacterial and fungal communities. For instance, the change in abiotic properties during pig-manure composting promoted the substitution of the initially dominant cellulose degrading bacteria by saprophytic fungi specialized in recalcitrant substrates on the latter stages (Wang et al., (2021). In another study by Lei and colaborators (2021), changes in pH during swine composting were the main drivers of bacterial and fungal communities succession, explaining about 60% of their total variation. In this study *Turicibacter* and *Terrisporobacter* genera, predominant in the initial phase, were substituted by *Bacillus* and *Ureibacillus*, thermotolerant bacteria with an active role in the degradation of waste materials, while the fungal genera *Thermomyces* and *Dipodascus* were substituted by *Mycothermus*, involved in the degradation of cellulose and hemicellulose.

Second only to the proper processing of wastes, the timing of application constitutes a key element to minimize the risk of ARG transmission to soils. Despite the known high re-naturalization capacity of soils, we observed a greater impact in soil ARG loads and ASV distribution by the second fertilization cycles when compared with their respective first cycles. This long-term impact was also observed on a bigger scale in the study by (Xie et al., 2018b), in which 25 years application of pig manure dramatically increased the diversity and abundance of ARGs in soil over the years in comparison with minerally fertilized plots, through both exogenous ARGs introduction and boosting of indigenous ARGs. In this case, ARG distribution seemed relatively independent from bacterial phylogeny, suggesting that the impact on ARG loads was mainly driven by HGT (stimulated with manure additions) rather than by microbiome modulation. Considering this evidence, we propose that organic fertilization cycles need to be paced in order to allow soil re-naturalization while minimizing cumulative impacts on soils.

Wastewater effluents handling. Soil Aquifer Treatment role and performance.

Taken together, the studies included in Chapter Three demonstrate the associated toxicity of WWTP effluents and their role as reservoirs of both ARGs and CECs, highlighting their potential risk to human and environmental health. As in the case of ABs, we propose that the first step on diminishing the toxicity risk should be limiting CECs use and uncontrolled disposal. Upcoming regulations aim to control the use of some emerging compounds, but the impact of their complex mixtures has never been contemplated, and the regulation of such a few members appears to be insufficient to tackle this problem. In this context, wastewater regeneration practices are presented as an almost indispensable tool for the safe use and discharge of WWTP effluents (Valhondo et al., 2020a, 2020b; Vymazal et al., 2021).

Similarly to the composting processes, a water regeneration system that favors the displacement of gut-related, copiotrophic bacteria by oligotrophic or mesotrophic microbiomes seems to play a big role on water depuration in terms of ARGs removal. The potential role of bacterial succession in wastewater regeneration was identified in Paper IV, where SAT systems enhanced with reactive barriers appeared as suitable tertiary treatments to promote a microbiome shift likely leading to a reduction of ARG loads. Functional analysis revealed that aerobic chemoheterotrophs, nitrate reducers and human pathogens present in the effluent were eventually substituted at the end of the systems by groundwater-like bacterial groups able to perform iron, manganese, arsenate, sulfur and nitrogen respiration. This microbial succession most likely contributed to the outstanding 90-95% ARG removal observed across all three sampling campaigns. As mentioned in Paper IV, this ARG removal favorably compares with most of current tertiary-treatment methods (Advance Oxidation, Membrane-based procedures, etc. (Leiva et al., 2021). Moreover,

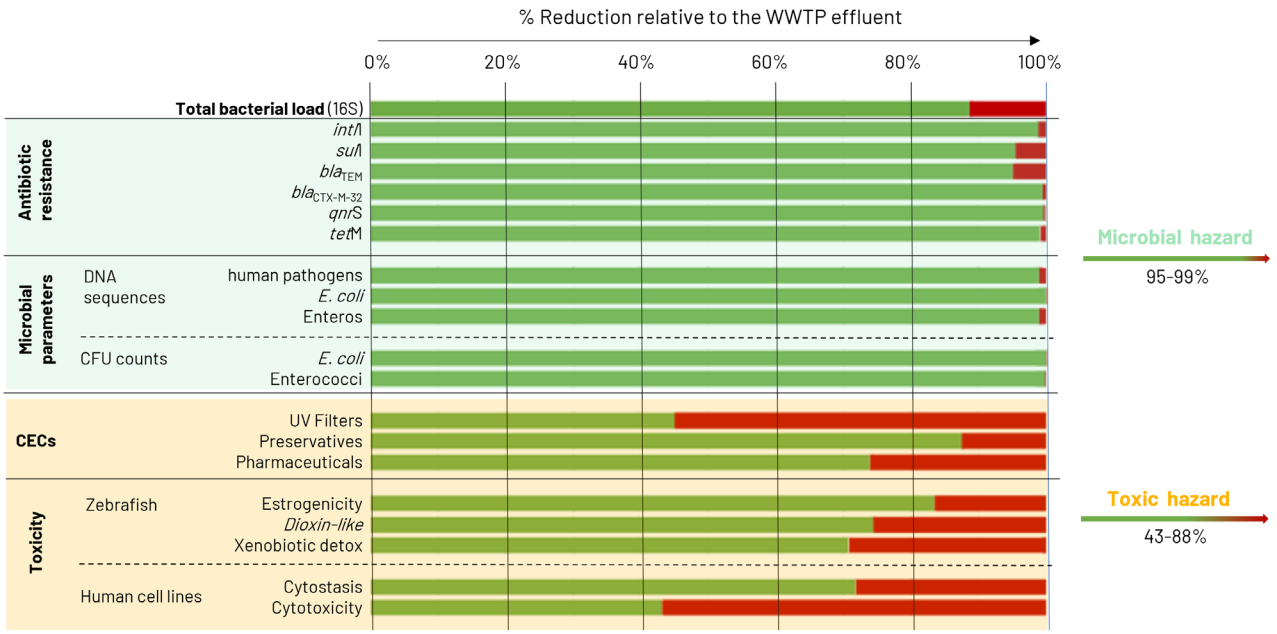

Figure 3. Percentage of reduction of microbial and toxic hazards relative to the WWTP effluent by SATs monitored in this thesis. Supplementary data from Valhondo et al., (2020a) and some unpublished data.

the enhanced SAT systems studied in this thesis have proven capable of not only removing ARGs but both CECs and pathogen indicators (Valhondo et al., 2020a, 2020b, **Figure 3**). We believe that the diversification of bacterial communities facilitate the degradation of compounds and the precluding growth of enteric bacteria (Paper IV). Paper V helped us gain insight into the biological repercussion of the removal of toxic hazards by SATs in two independent biological systems (**Figure 3**). Comparative approaches that integrate information from different biological systems through target and non-target methodologies are highly recommended for a representative biomonitoring of WWTP effluents (Meade et al., 2022). Following this approach, the integration of target and non-target RNA analysis, enzymatic activities, and CEC wide-scope suspect screening allowed us to link the removal of the toxic hazards cocktail by SATs to a reduction, of more than 70% on average, of the associated toxic effects.

To our knowledge, a simultaneous reduction of ARG and CEC loads and estrogenic, dioxin-like and detoxification responses has never been reported for any tertiary treatment. This could be due to the fact that (1) the combined screening of these parameters has never been contemplated in wastewater monitoring (2) the role of microbiome substitution has never been assessed in this context which can explain the failure of tertiary treatments in eliminating many relevant hazards. We promote the use of SATs as appropriate tertiary treatments able to reduce the risk associated with wastewater effluents allowing their safe discharge or their potential use in aquifer recharge schemes or agricultural irrigation, among many other uses. For instance, the safety of SAT-regenerated water for agricultural irrigation was monitored by our project partners in terms of CECs and pathogens uptake in comparison with untreated effluent water irrigation (Sunyer-Caldú et al., 2022). In this work, irrigating crops with SAT-regenerated water drastically reduced the loads of pathogens and CECs transferred to crops, especially in plots under sprinkler irrigation, underscoring the potential role of these systems as water providers in agriculture. The benefits derived from the use of

SATs as tertiary treatments extend beyond toxicity and hazards removal since they promote aquifer's recovering facilitating hyporheic exchange in rivers, fact that makes them environmentally friendly, efficient, and cost-effective techniques to improve recharge wastewater quality while increasing fresh water reserves (Valhondo et al., 2020b).

The work carried in Paper IV & V demonstrate the feasibility of monitoring simultaneously the risk of ARG transmission and the risk of inducing toxic responses. These two endpoints were evaluated following a complementary methodology that provided the scientific community with valuable experimental information regarding wastewater regeneration by SAT that could be easily implemented in the evaluation of other potentially suitable tertiary treatments and in the regulated biomonitoring of WWTP effluents.

2. Conclusions

The main conclusions of the thesis are described below.

1. The potential selective pressure associated to the application of fertilizers in soil is enough to favor the soil colonization by antibiotic-resistant bacteria, either from the same fertilizers or from the pre-existing soil microbial community.

2. *int*I1, *sul*1 and *tet*M appeared as the AR-associated genetic elements with higher prevalence across fertilizers, target soils and crops.

3. Pig slurry-based amendments show the strongest potential for influencing ARG loads and increasing HGT in target soils and crops

4. Corn appears as a particularly adequate crop for animal slurry-based fertilizers, given its low uptake capacity for ARG-harboring bacteria.

5. Animal handling and farm conditions play a fundamental role in biosolids ARG loads, so the strict control of AB use at source combined with the processing of the generated waste promoting bacterial succession represent valuable tools to decrease the risk of ARG transmission through organic fertilization.

6. Both increased ARG loads and fertilizers microbiome contributions in soils appear as transient impacts although consecutive fertilization practices do have an additive effect on microbiome distribution and diversification.

7. SAT systems constitute a cost-effective alternative to power-consuming tertiary wastewater treatments and their efficiency on removing biological hazards, and particularly ARG loads, appears to match the state-of-the art current membrane and advanced-oxidation technologies.

8. Reactive barriers do not seem to play a relevant role in microbiome modulation and ARG removal but they do influence CECs loads and associated toxic activities, with the control barrier (sand) appearing as the less effective treatment in some cases.

9. The displacement of gut-related, copiotrophic bacteria by groundwater-like microbiomes in SATs seems to play a big role on ARGs, CECs, and toxic responses removal.

10. The identification of both recalcitrant CECs and potentially associated residual toxicity after SAT treatment in two consecutive campaigns call for further implementations on barrier materials combinations for an optimal removal performance of these systems.

3. Future research perspectives

The current ability to describe whole microbiomes by high throughput DNA sequencing opened complete new ways of monitoring alterations, anthropogenic or not, on the ecosystems. In our work, microbial metabolism and growth appeared central in the process of depuration of water bodies and polluted soils. During this thesis, we observed in different field studies how the microbiome was changed by the presence of anthropogenic pollution and how its reversal to a normal microbial profile took place under distinct scenarios. This process occurred after the exposure to both biological (ARG/ARBs) and chemical hazards (CECs). Future efforts should be made in order to gain insight on the role of microbiota as drivers and markers of water and soil pollution and recovery. We propose microbiome analysis as a way to monitor the pollution of impacted sites and, at the same time, a guide to develop treatment schemes favoring bacterial succession.

On the other hand, in Paper IV we observed a larger diversification in taxonomic and functional profiles in SEP21 SATs in comparison with JUN20 and OCT20 mature SATs. Thus, a further line of investigation could be centered on the progressive monitoring of bacterial colonization in SAT systems and how it compromises ARG, CECs and associated toxic responses removal over time. A suitable way to accomplish this goal could take place through the successive sampling of reactive barrier material from the monitored SATs, following in this way bacterial colonization/succession, locating key bacterial shifts for an accurate estimation of SATs optimal operational time.

Lastly, given the fact that the pilot scale of the studied SATs was indeed a confounding factor from which only preliminary conclusions could be drawn, the same complementary monitoring of ARG, CECs and toxic responses removal carried in Chapter Three should take place in larger experimental SATs in order to understand the role of scale in the monitored processes.

Bibliography

Alexander, J., Bollmann, A., Seitz, W., Schwartz, T., 2015. Microbiological characterization of aquatic microbiomes targeting taxonomical marker genes and antibiotic resistance genes of opportunistic bacteria. Sci. Total Environ. 512, 316–325.

Alexander, J., Hembach, N., Schwartz, T., 2020. Evaluation of antibiotic resistance dissemination by wastewater treatment plant effluents with different catchment areas in Germany. Sci. Rep. 10, 8952.

Amador, P.P., Fernandes, R.M., Prudêncio, M.C., Barreto, M.P., Duarte, I.M., 2015. Antibiotic resistance in wastewater: Occurrence and fate of Enterobacteriaceae producers of Class A and Class C β-lactamases. J. Environ. Sci. Heal. Part A 50, 26–39.

Bengtsson-Palme, J., Hammaren, R., Pal, C., Östman, M., Björlenius, B., Flach, C.-F., Fick, J., Kristiansson, E., Tysklind, M., Larsson, D.G.J., 2016. Elucidating selection processes for antibiotic resistance in sewage treatment plants using metagenomics. Sci. Total Environ. 572, 697–712.

Berninger, J.P., Martinović-Weigelt, D., Garcia-Reyero, N., Escalon, L., Perkins, E.J., Ankley, G.T., Villeneuve, D.L., 2014. Using transcriptomic tools to evaluate biological effects across effluent gradients at a diverse set of study sites in Minnesota, USA. Environ. Sci. Technol. 48, 2404–2412.

Bondarczuk, K., Markowicz, A., Piotrowska-Seget, Z., 2016. The urgent need for risk assessment on the antibiotic resistance spread via sewage sludge land application. Environ. Int. 87, 49–55.

Cai, C., Huang, X., Dai, X., 2022. Differential variations of intracellular and extracellular antibiotic resistance genes between treatment units in centralized sewage sludge treatment plants. Water Res. 222, 118893.

Cerqueira, F., Christou, A., Fatta-Kassinos, D., Vila-Costa, M., Bayona,

J.M., Piña, B., 2020. Effects of prescription antibiotics on soil-and root-associated microbiomes and resistomes in an agricultural context. J. Hazard. Mater. 400, 123208.

Cerqueira, F., Matamoros, V., Bayona, J., Elsinga, G., Hornstra, L.M., Piña, B., 2019a. Distribution of antibiotic resistance genes in soils and crops. A field study in legume plants (Vicia faba L.) grown under different watering regimes. Environ. Res. 170, 16–25.

Cerqueira, F., Matamoros, V., Bayona, J., Piña, B., 2019b. Antibiotic resistance genes distribution in microbiomes from the soil-plant-fruit continuum in commercial Lycopersicon esculentum fields under different agricultural practices. Sci. Total Environ. https://doi.org/10.1016/j.scitotenv.2018.10.268

Cerqueira, F., Matamoros, V., Bayona, J.M., Berendonk, T.U., Elsinga, G., Hornstra, L.M., Piña, B., 2019c. Antibiotic resistance gene distribution in agricultural fields and crops. A soil-to-food analysis. Environ. Res. 177, 108608.

Chen, C., Zhou, Y., Fu, H., Xiong, X., Fang, S., Jiang, H., Wu, J., Yang, H., Gao, J., Huang, L., 2021. Expanded catalog of microbial genes and metagenome-assembled genomes from the pig gut microbiome. Nat. Commun. 12, 1106.

Chen, Q.L., An, X.L., Zheng, B.X., Ma, Y.B., Su, J.Q., 2018. Long-term organic fertilization increased antibiotic resistome in phyllosphere of maize. Sci. Total Environ. https://doi.org/10.1016/j.scitotenv.2018.07.260

Chen, Z., Zhang, W., Yang, L., Stedtfeld, R.D., Peng, A., Gu, C., Boyd, S.A., Li, H., 2019. Antibiotic resistance genes and bacterial communities in cornfield and pasture soils receiving swine and dairy manures. Environ. Pollut. 248, 947–957.

Cheng, W., Chen, H., Su, C., Yan, S., 2013. Abundance and persistence of antibiotic resistance genes in livestock farms: a comprehensive investigation in eastern China. Environ. Int. 61, 1–7.

Christou, A., Papadavid, G., Dalias, P., Fotopoulos, V., Michael, C., Bayona, J.M., Pina, B., Fatta-Kassinos, D., 2019. Ranking of crop plants according to their potential to uptake and accumulate contaminants of emerging concern. Environ. Res. 170, 422–432. https://doi.org/10.1016/j.envres.2018.12.048

Chu, H., Lin, X., Fujii, T., Morimoto, S., Yagi, K., Hu, J., Zhang, J., 2007. Soil microbial biomass, dehydrogenase activity, bacterial community structure in response to long-term fertilizer management. Soil Biol. Biochem. 39, 2971–2976.

Cocozza, C., Di Iaconi, C., Murgolo, S., Traversa, A., De Mastro, F., De Sanctis, M., Altieri, V.G., Cacace, C., Brunetti, G., Mascolo, G., 2023. Use of constructed wetlands to prevent overloading of wastewater treatment plants. Chemosphere 311, 137126.

Conde-Cid, M., Núñez-Delgado, A., Fernández-Sanjurjo, M.J., Álvarez-Rodríguez, E., Fernández-Calviño, D., Arias-Estévez, M., 2020. Tetracycline and sulfonamide antibiotics in soils: presence, fate and environmental risks. Processes 8, 1479.

de Oliveira, M., Frihling, B.E.F., Velasques, J., Magalhães Filho, F.J.C., Cavalheri, P.S., Migliolo, L., 2020. Pharmaceuticals residues and xenobiotics contaminants: occurrence, analytical techniques and sustainable alternatives for wastewater treatment. Sci. Total Environ. 705, 135568.

Dehn, P.F., White, C.M., Conners, D.E., Shipkey, G., Cumbo, T.A., 2004. Characterization of the human hepatocellular carcinoma (hepg2) cell line as an in vitro model for cadmium toxicity studies. Vitr. Cell. Dev. Biol. 40, 172–182.

Eggen, T., Lillo, C., 2012. Antidiabetic II drug metformin in plants: uptake and translocation to edible parts of cereals, oily seeds, beans, tomato, squash, carrots, and potatoes. J. Agric. Food Chem. 60, 6929–6935.

Esperón, F., Albero, B., Ugarte-Ruíz, M., Domínguez, L., Carballo, M., Tadeo, J.L., del Mar Delgado, M., Moreno, M.Á., de la Torre, A., 2020. Assessing the benefits of composting poultry manure in reducing antimicrobial residues, pathogenic bacteria, and antimicrobial resistance genes: a field-scale study. Environ. Sci. Pollut. Res. 27, 27738–27749.

Ezzariai, A., Hafidi, M., Khadra, A., Aemig, Q., El Fels, L., Barret, M., Merlina, G., Patureau, D., Pinelli, E., 2018. Human and veterinary antibiotics during composting of sludge or manure: Global perspectives on persistence, degradation, and resistance genes. J. Hazard. Mater. https://doi.org/10.1016/j.jhazmat.2018.07.092

Fierer, N., 2017. Embracing the unknown: disentangling the complexities of the soil microbiome. Nat. Rev. Microbiol. 15, 579–590.

Fogler, K., Guron, G.K.P., Wind, L.L., Keenum, I.M., Hession, W.C., Krometis, L.A., Strawn, L.K., Pruden, A., Ponder, M.A., 2019. Microbiota and Antibiotic Resistome of Lettuce Leaves and Radishes Grown in Soils Receiving Manure-Based Amendments Derived From Antibiotic-Treated Cows. Front. Sustain. Food Syst. 3, 1–17. https://doi.org/10.3389/fsufs.2019.00022

Forsberg, K.J., Patel, S., Gibson, M.K., Lauber, C.L., Knight, R., Fierer, N., Dantas, G., 2014. Bacterial phylogeny structures soil resistomes across habitats. Nature 509, 612–616. https://doi.org/10.1038/nature13377

Freeman, S., Kaufman-Shriqui, V., Berman, T., Varsano, R., Shahar, D.R., Manor, O., 2016. Children's diets, pesticide uptake, and implications for risk assessment: An Israeli case study. Food Chem. Toxicol. 87, 88–96.

Gagné, F., Smyth, S.A., André, C., Douville, M., Gélinas, M., Barclay, K., 2013. Stress-related gene expression changes in rainbow trout hepatocytes exposed to various municipal wastewater treatment influents and effluents. Environ. Sci. Pollut. Res. 20, 1706–1718.

Gao, F.Z., He, L.Y., He, L.X., Zou, H.Y., Zhang, M., Wu, D.L., Liu, Y.S., Shi, Y.J., Bai, H., Ying, G.G., 2020. Untreated swine wastes changed antibiotic resistance and microbial community in the soils and impacted abundances of antibiotic resistance genes in the vegetables. Sci. Total Environ. 741. https://doi.org/10.1016/j.scitotenv.2020.140482

Guo, J., Li, J., Chen, H., Bond, P.L., Yuan, Z., 2017. Metagenomic analysis reveals wastewater treatment plants as hotspots of antibiotic resistance genes and mobile genetic elements. Water Res. 123, 468–478.

He, Y., Yuan, Q., Mathieu, J., Stadler, L., Senehi, N., Sun, R., Alvarez, P.J.J., 2020. Antibiotic resistance genes from livestock waste: Occurrence, dissemination, and treatment. NPJ Clean Water 3, 1–11.

Hultman, J., Tamminen, M., Pärnänen, K., Cairns, J., Karkman, A., Virta, M., 2018. Host range of antibiotic resistance genes in wastewater treatment plant influent and effluent. FEMS Microbiol. Ecol. 94, fiy038.

Johnson, T.A., Stedtfeld, R.D., Wang, Q., Cole, J.R., Hashsham, S.A., Looft, T., Zhu, Y.-G., Tiedje, J.M., 2016. Clusters of antibiotic resistance genes enriched together stay together in swine agriculture. MBio 7, e02214-15.

Karimi, B., Terrat, S., Dequiedt, S., Saby, N.P.A., Horrigue, W., Lelièvre, M., Nowak, V., Jolivet, C., Arrouays, D., Wincker, P., 2018. Biogeography of soil bacteria and archaea across France. Sci. Adv. 4, eaat1808.

Laht, M., Karkman, A., Voolaid, V., Ritz, C., Tenson, T., Virta, M., Kisand, V., 2014. Abundances of Tetracycline, Sulphonamide and Beta-Lactam Antibiotic Resistance Genes in Conventional Wastewater Treatment Plants (WWTPs) with Different Waste Load. PLoS One 9, 1–8. https://doi.org/10.1371/journal.pone.0103705

Lamendella, R., Santo Domingo, J.W., Ghosh, S., Martinson, J., Oerther, D.B., 2011. Comparative fecal metagenomics unveils unique functional capacity of the swine gut. BMC Microbiol. 11. https://doi.org/10.1186/1471-2180-11-103

Lei, L., Gu, J., Wang, X., Song, Z., Wang, J., Yu, J., Hu, T., Dai, X., Xie, J., Zhao, W., 2021. Microbial succession and molecular ecological networks response to the addition of superphosphate and phosphogypsum during swine manure composting. J. Environ. Manage. 279, 111560.

Leiva, A.M., Piña, B., Vidal, G., 2021. Antibiotic resistance dissemination in wastewater treatment plants: a challenge for the reuse of treated wastewater in agriculture. Rev. Environ. Sci. Biotechnol. https://doi.org/10.1007/s11157-021-09588-8

Li, Y.-W., Wu, X.-L., Mo, C.-H., Tai, Y.-P., Huang, X.-P., Xiang, L., 2011. Investigation of sulfonamide, tetracycline, and quinolone antibiotics in vegetable farmland soil in the Pearl River Delta area, southern China. J. Agric. Food Chem. 59, 7268–7276.

Liao, H., Lu, X., Rensing, C., Friman, V.P., Geisen, S., Chen, Z., Yu, Z., Wei, Z., Zhou, S., Zhu, Y., 2018. Hyperthermophilic composting accelerates the removal of antibiotic resistance genes and mobile genetic elements in sewage sludge. Environ. Sci. Technol. 52, 266–276.

Liu, W., Ling, N., Guo, J., Ruan, Y., Wang, M., Shen, Q., Guo, S., 2021. Dynamics of the antibiotic resistome in agricultural soils amended with different sources of animal manures over three consecutive years. J. Hazard. Mater. 401, 123399.

Liu, Y., Cheng, D., Xue, J., Weaver, L., Wakelin, S.A., Feng, Y., Li, Z., 2020. Changes in microbial community structure during pig manure composting and its relationship to the fate of antibiotics and antibiotic resistance genes. J. Hazard. Mater. 389, 122082.

Looft, T., Johnson, T.A., Allen, H.K., Bayles, D.O., Alt, D.P., Stedtfeld, R.D., Sul, W.J., Stedtfeld, T.M., Chai, B., Cole, J.R., 2012. In-feed antibiotic effects on the swine intestinal microbiome. Proc. Natl. Acad. Sci. 109, 1691–1696.

Mao, D., Yu, S., Rysz, M., Luo, Y., Yang, F., Li, F., Hou, J., Mu, Q., Alvarez, P.J.J., 2015. Prevalence and proliferation of antibiotic resistance genes in two municipal wastewater treatment plants. Water Res. 85, 458–466.

Matamoros, V., Casas, M.E., Mansilla, S., Tadić, Đ., Cañameras, N., Carazo, N., Portugal, J., Piña, B., Díez, S., Bayona, J.M., 2022. Occurrence of antibiotics in Lettuce (Lactuca sativa L.) and Radish (Raphanus sativus L.) following organic soil fertilisation under plot-scale conditions: Crop and human health implications. J. Hazard. Mater. 436, 129044.

Meade, E.B., Iwanowicz, L.R., Neureuther, N., LeFevre, G.H., Kolpin, D.W., Zhi, H., Meppelink, S.M., Lane, R.F., Schmoldt, A., Mohaimani, A., Mueller, O., Klaper, R.D., 2022. Transcriptome signatures of wastewater effluent exposure in larval zebrafish vary with seasonal mixture composition in an effluent-dominated stream. Sci. Total Environ. 856, 159069. https://doi.org/10.1016/j.scitotenv.2022.159069

Michael, I., Rizzo, L., McArdell, C.S., Manaia, C.M., Merlin, C., Schwartz, T., Dagot, C., Fatta-Kassinos, D., 2013. Urban wastewater treatment plants as hotspots for the release of antibiotics in the environment: a review. Water Res. 47, 957–995.

Munir, M., Wong, K., Xagoraraki, I., 2011. Release of antibiotic resistant bacteria and genes in the effluent and biosolids of five wastewater utilities in Michigan. Water Res. 45, 681–693.

Muurinen, J., Stedtfeld, R., Karkman, A., Pärnänen, K., Tiedje, J., Virta, M., 2017. Influence of Manure Application on the Environmental Resistome under Finnish Agricultural Practice with Restricted Antibiotic Use. Environ. Sci. Technol. 51, 5989–5999. https://doi.org/10.1021/acs.est.7b00551

Okoffo, E.D., O'Brien, S., O'Brien, J.W., Tscharke, B.J., Thomas, K. V, 2019. Wastewater treatment plants as a source of plastics in the environment: a review of occurrence, methods for identification, quantification and fate. Environ. Sci. Water Res. Technol. 5, 1908–1931.

Omuferen, L.O., Maseko, B., Olowoyo, J.O., 2022. Occurrence of antibiotics in wastewater from hospital and convectional wastewater treatment plants and their impact on the effluent receiving rivers: current knowledge between 2010 and 2019. Environ. Monit. Assess. 194, 306.

Paltiel, O., Fedorova, G., Tadmor, G., Kleinstern, G., Maor, Y., Chefetz, B., 2016. Human exposure to wastewater-derived pharmaceuticals in fresh produce: a randomized controlled trial focusing on carbamazepine. Environ. Sci. Technol. 50, 4476–4482.

Pan, M., Chu, L.M., 2017. Fate of antibiotics in soil and their uptake by edible crops. Sci. Total Environ. 599, 500–512.

Pazda, M., Kumirska, J., Stepnowski, P., Mulkiewicz, E., 2019. Antibiotic resistance genes identified in wastewater treatment plant systems–a review. Sci. Total Environ. 697, 134023.

Piña, B., Bayona, J.M., Christou, A., Fatta-Kassinos, D., Guillon, E., Lambropoulou, D., Michael, C., Polesel, F., Sayen, S., 2020. On the contribution of reclaimed wastewater irrigation to the potential

exposure of humans to antibiotics, antibiotic resistant bacteria and antibiotic resistance genes - NEREUS COST Action ES1403 position paper. J. Environ. Chem. Eng. 8. https://doi.org/10.1016/j.jece.2018.01.011

Prasse, C., Stalter, D., Schulte-Oehlmann, U., Oehlmann, J., Ternes, T.A., 2015. Spoilt for choice: A critical review on the chemical and biological assessment of current wastewater treatment technologies. Water Res. 87, 237–270.

Radu, E., Woegerbauer, M., Rab, G., Oismüller, M., Strauss, P., Hufnagl, P., Gottsberger, R.A., Krampe, J., Weyermair, K., Kreuzinger, N., 2021. Resilience of agricultural soils to antibiotic resistance genes introduced by agricultural management practices. Sci. Total Environ. 756, 143699.

Rahman, M.M., Shan, J., Yang, P., Shang, X., Xia, Y., Yan, X., 2018. Effects of long-term pig manure application on antibiotics, abundance of antibiotic resistance genes (ARGs), anammox and denitrification rates in paddy soils. Environ. Pollut. 240, 368–377.

Rastogi, M., Nandal, M., Khosla, B., 2020. Microbes as vital additives for solid waste composting. Heliyon 6, e03343.

Rizzo, L., Manaia, C., Merlin, C., Schwartz, T., Dagot, C., Ploy, M.C., Michael, I., Fatta-Kassinos, D., 2013. Urban wastewater treatment plants as hotspots for antibiotic resistant bacteria and genes spread into the environment: a review. Sci. Total Environ. 447, 345–360.

Robitaille, J., Denslow, N.D., Escher, B.I., Kurita-Oyamada, H.G., Marlatt, V., Martyniuk, C.J., Navarro-Martín, L., Prosser, R., Sanderson, T., Yargeau, V., 2022. Towards regulation of Endocrine Disrupting chemicals (EDCs) in water resources using bioassays-A guide to developing a testing strategy. Environ. Res. 205, 112483.

Rodriguez-Mozaz, S., Vaz-Moreira, I., Della Giustina, S.V., Llorca, M., Barceló, D., Schubert, S., Berendonk, T.U., Michael-Kordatou, I., Fatta-Kassinos, D., Martinez, J.L., 2020. Antibiotic residues in final effluents of European wastewater treatment plants and their impact on the aquatic environment. Environ. Int. 140, 105733.

Sanz, C., Casado, M., Navarro-Martin, L., Cañameras, N., Carazo, N., Matamoros, V., Bayona, J.M., Piña, B., 2022a. Implications of the use of organic fertilizers for antibiotic resistance gene distribution in agricultural soils and fresh food products. A plot-scale study. Sci. Total Environ. 815, 151973. https://doi.org/10.1016/j.scitotenv.2021.151973

Sanz, C., Casado, M., Navarro-Martin, L., Tadić, Đ., Parera, J., Tugues, J., Bayona, J.M., Piña, B., 2021. Antibiotic and antibiotic-resistant gene loads in swine slurries and their digestates: Implications for their use as fertilizers in agriculture. Environ. Res. 194. https://doi.org/10.1016/j.envres.2020.110513

Sanz, C., Casadoi, M., Tadic, Đ., Pastor-López, E.J., Navarro-Martin, L., Parera, J., Tugues, J., Ortiz, C.A., Bayona, J.M., Piña, B., 2022b. Impact of organic soil amendments in antibiotic levels, antibiotic resistance gene loads, and microbiome composition in corn fields and crops. Environ. Res. 214. https://doi.org/10.1016/j.envres.2022.113760

Sarmah, A.K., Meyer, M.T., Boxall, A.B.A., 2006. A global perspective on the use, sales, exposure pathways, occurrence, fate and effects of veterinary antibiotics (VAs) in the environment. Chemosphere 65, 725–759.

Subirats, J., Murray, R., Scott, A., Lau, C.H.-F., Topp, E., 2020. Composting of chicken litter from commercial broiler farms reduces the abundance of viable enteric bacteria, Firmicutes, and selected antibiotic resistance genes. Sci. Total Environ. 746, 141113.

Sun, R., Zhang, X.-X., Guo, X., Wang, D., Chu, H., 2015. Bacterial diversity in soils subjected to long-term chemical fertilization can be more stably maintained with the addition of livestock manure than wheat straw. Soil Biol. Biochem. 88, 9–18.

Sunyer-Caldú, A., Sepúlveda-Ruiz, P., Salgot, M., Folch-Sánchez, M., Barcelo, D., Diaz-Cruz, M.S., 2022. Reclaimed water in agriculture: a plot-scale study assessing crop uptake of emerging contaminants and pathogens. J. Environ. Chem. Eng. 108831. https://doi.org/https://doi.org/10.1016/j.jece.2022.108831

Valhondo, C., Carrera, J., Martínez-Landa, L., Wang, J., Amalfitano, S., Levantesi, C., Diaz-Cruz, M.S., 2020a. Reactive barriers for renaturalization of reclaimed water during soil aquifer treatment. Water (Switzerland) 12. https://doi.org/10.3390/W12041012

Valhondo, C., Martínez-Landa, L., Carrera, J., Díaz-Cruz, S.M., Amalfitano, S., Levantesi, C., 2020b. Six artificial recharge pilot replicates to gain insight into water quality enhancement processes. Chemosphere 240. https://doi.org/10.1016/j.chemosphere.2019.124826

Vymazal, J., Zhao, Y., Mander, Ü., 2021. Recent research challenges in constructed wetlands for wastewater treatment: A review. Ecol. Eng. 169, 106318. https://doi.org/10.1016/j.ecoleng.2021.106318

Wang, F., Han, W., Chen, S., Dong, W., Qiao, M., Hu, C., Liu, B., 2020. Fifteen-year application of manure and chemical fertilizers differently impacts soil ARGs and microbial community structure. Front. Microbiol. 11, 62.

Wang, J., Ben, W., Zhang, Y., Yang, M., Qiang, Z., 2015. Effects of thermophilic composting on oxytetracycline, sulfamethazine, and their corresponding resistance genes in swine manure. Environ. Sci. Process. Impacts 17, 1654–1660.

Wang, J., Chu, L., Wojnárovits, L., Takács, E., 2020. Occurrence and fate of antibiotics, antibiotic resistant genes (ARGs) and antibiotic resistant bacteria (ARB) in municipal wastewater treatment plant: An overview. Sci. Total Environ. 744, 140997.

Wang, X., Wan, J., Jiang, G., Yang, T., Banerjee, S., Wei, Z., Mei, X., Friman, V.-P., Xu, Y., Shen, Q., 2021. Compositional and functional succession of bacterial and fungal communities is associated with changes in abiotic properties during pig manure composting. Waste Manag. 131, 350–358.

Wu, M., Que, C., Tang, L., Xu, H., Xiang, J., Wang, J., Shi, W., Xu, G., 2016. Distribution, fate, and risk assessment of antibiotics in five wastewater treatment plants in Shanghai, China. Environ. Sci. Pollut. Res. 23, 18055–18063.

Xie, W.-Y., Yang, X.-P., Li, Q., Wu, L.-H., Shen, Q.-R., Zhao, F.-J., 2016. Changes in antibiotic concentrations and antibiotic resistome during

commercial composting of animal manures. Environ. Pollut. 219, 182–190.

Xie, W. Y., Shen, Q., Zhao, F.J., 2018. Antibiotics and antibiotic resistance from animal manures to soil: a review. Eur. J. Soil Sci. 69, 181–195. https://doi.org/10.1111/ejss.12494

Xie, Wan Ying, Yuan, S.T., Xu, M.G., Yang, X.P., Shen, Q.R., Zhang, W.W., Su, J.Q., Zhao, F.J., 2018. Long-term effects of manure and chemical fertilizers on soil antibiotic resistome. Soil Biol. Biochem. 122, 111–119. https://doi.org/10.1016/j.soilbio.2018.04.009

Xun, W., Zhao, J., Xue, C., Zhang, G., Ran, W., Wang, B., Shen, Q., Zhang, R., 2016. Significant alteration of soil bacterial communities and organic carbon decomposition by different long-term fertilization management conditions of extremely low-productivity arable soil in S outh C hina. Environ. Microbiol. 18, 1907–1917.

Yang, D., Heederik, D.J.J., Scherpenisse, P., Van Gompel, L., Luiken, R.E.C., Wadepohl, K., Skarżyńska, M., Van Heijnsbergen, E., Wouters, I.M., Greve, G.D., 2022. Antimicrobial resistance genes aph (3')-III, erm (B), sul2 and tet (W) abundance in animal faeces, meat, production environments and human faeces in Europe. J. Antimicrob. Chemother. 77, 1883–1893.

You, Y., Silbergeld, E.K., 2014. Learning from agriculture: understanding low-dose antimicrobials as drivers of resistome expansion. Front. Microbiol. 5, 284.

Yu, Y., Wu, B., Jiang, L., Zhang, X.-X., Ren, H.-Q., Li, M., 2019. Comparative analysis of toxicity reduction of wastewater in twelve industrial park wastewater treatment plants based on battery of toxicity assays. Sci. Rep. 9, 3751.

Žegura, B., Heath, E., Černoša, A., Filipič, M., 2009. Combination of in vitro bioassays for the determination of cytotoxic and genotoxic potential of wastewater, surface water and drinking water samples. Chemosphere 75, 1453–1460.

Zhang, D., Liu, H., Wang, S., Zhang, W., Wang, J., Tian, H., Wang, Y., Ji, H., 2019. Fecal microbiota and its correlation with fatty acids and free amino acids metabolism in piglets after a Lactobacillus strain oral administration. Front. Microbiol. 10, 1–13. https://doi.org/10.3389/fmicb.2019.00785

Zhang, R.-M., Liu, X., Wang, S.-L., Fang, L.-X., Sun, J., Liu, Y.-H., Liao, X.-P., 2021. Distribution patterns of antibiotic resistance genes and their bacterial hosts in pig farm wastewater treatment systems and soil fertilized with pig manure. Sci. Total Environ. 758, 143654.

Zhang, Y.-J., Hu, H.-W., Chen, Q.-L., Singh, B.K., Yan, H., Chen, D., He, J.-Z., 2019. Transfer of antibiotic resistance from manure-amended soils to vegetable microbiomes. Environ. Int. 130, 104912.

Zhang, Z., Liu, W., Qu, Y., Quan, X., Zeng, P., He, M., Zhou, Y., Liu, R., 2018. Transcriptomic profiles in zebrafish liver permit the discrimination of surface water with pollution gradient and different discharges. Int. J. Environ. Res. Public Health 15, 1648.

Zhao, X., Wang, Jinhua, Zhu, L., Wang, Jun, 2019. Field-based evidence for enrichment of antibiotic resistance genes and mobile genetic elements in manure-amended vegetable soils. Sci. Total Environ. 654, 906–913.

Zhen, H., Ekman, D.R., Collette, T.W., Glassmeyer, S.T., Mills, M.A., Furlong, E.T., Kolpin, D.W., Teng, Q., 2018. Assessing the impact of wastewater treatment plant effl

SUPPORTING INFORMATION.

Paper I: Antibiotic and antibiotic-resistant gene loads in swine slurries and their digestates: implications for their use as fertilizers in agriculture

Sanz, Claudia[1]; Casado, Marta[1]; Navarro-Martin, Laia[1]; Tadić, Đorđe[1]; Parera, Joan[2]; Tugues, Jordi[2]; Bayona, Josep M[1]; Piña, Benjamin[1]

1) IDAEA-CSIC, Jordi Girona, 18. E-08034, Barcelona, Spain

2) DARP Catalunya Central, GENCAT, Carrer de la Llotja, s/n (Recinte Firal El Sucre) 08500, Vic, Spain

Supporting Figures

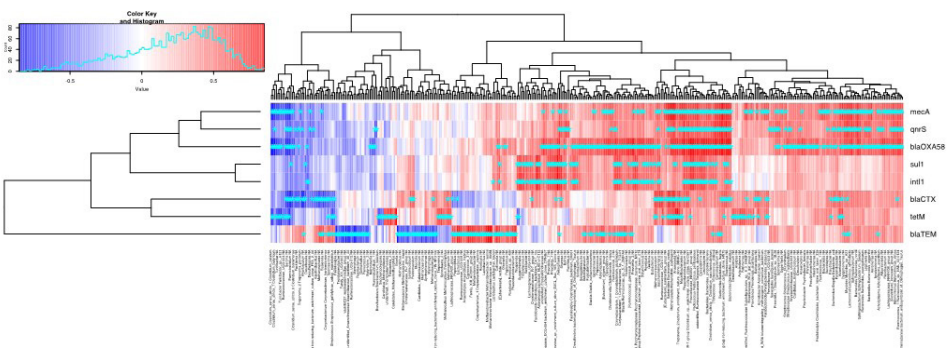

Supplementary Figure SF1. Pearson correlations between ARG prevalence and relative abundance of bacterial entities identified at least at the Genus level. Blue and red sectors represent positive and negative correlations, respectively; asterisks indicate significant correlations (5% FDR).

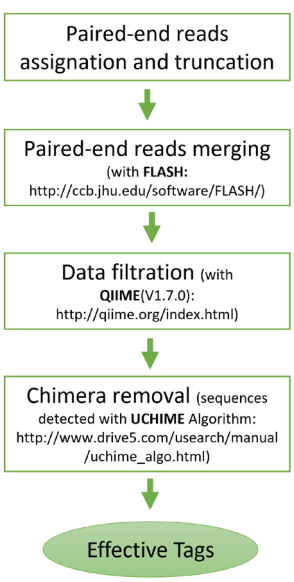

Supplementary Figure SF2. Paired-end reads assembly and quality control.

Supporting Tables

Supplementary Table ST1. Characterization of the slurries, fractions and digestates.

Samples	Code	nº of samples	Dry Matter (%)	N total (kg/t)	P Olsen (kg/t)	K total (kg/t)
Pregnant sow slurry	A	47	3.6±1.6	3.0±0.9	0.9±0.6	1.5±0.6
Pregnant & nursing sow slurry	B	17	4.6±1.7	2.6±1.5	1.2±0.4	1.8±0.5
Transition piglet slurry	C,D	7	8.47±4.2	5.06±1.9	2.08±0.9	2.67±1.3
Fatting piglet slurry	E,F	5	8.77±3.0	7.32±0.7	1.47±0.6	4.72±0.3
Digested sow slurry + slaughter sludge + waste cake industry + barley waste	G	14	3.92±2.8	4.24±1.2	0.8±0.6	1.19±0.4
Liquid fraction from sow slurry	H	6	1.96±1.6	2.63±0.6	0.81±0.4	1.41±0.3
Solid fraction from sow slurry	J	2	26.49±4.0	6.9±0.7	6.4±4.4	3.46±0.4
Liquid fraction from sow slurry	K	2	1.07±0.7	1.61±0.5	3.45±1.1	18.44±5.7
Fatting piglet slurry	L	1	5.83	3.81	1.74	4.7
Digested sow slurry + sludge+chicken waste	M	4	3.3±1.6	4.26±0.6	0.71±0.4	0.86±0.2

Data correspond to historical records for each type of material and farm, except for those from samples A and B, which correspond to a neighbouring farm with similar management procedures and genetic background of the animals

Supplementary Table ST2. Plasmid, primers and LOQs used for detection and quantifications of antibiotic resistance genes in amendments.

Target gene	Plasmid	LOQ (gene copies/ul)	Primers	Sequence (5'-> 3')	Amplicon size (bp)	Tm(ºC)	Reference
16S rDNA	pNORM1 (3324 bp)	1000	331F	TCCTACGGGAGGCAGCAGT	195	60	Bräuer et al., 2011
			518R	ATTACCGCGGCTGCTGG			
intI1		100	intI1LC5	GATCGGTCGAATGCGTGT	196	60	Barraud et al., 2010
			intI1LC1	GCCTTGATGTTACCCGAGAG			
sul1		100	sul1-FW	CGCACCGGAAACATCGCTGCAC	162	60	Pei et al., 2006
			sul1-RV	TGAAGTTCCGCCGCAAGGCTCG			
qnrS1		100	qnrSrtF11	GACGTGCTAACTTGCGTGAT	118	60	Marti & Balcázar, 2013
			qnrSrtR 11	TGGCATTGTTGGAAACTTG			
tetM	pUC19 (2882 bp)	1000	tetMF	GCAATTCTACTGATTTCTGC	186	60	Tamminen & Karkman, 2011
			tetMR	CTGTTTGATTACAATTTCCGC			
mecA	pUC19 (2871 bp)	1000	mecAF	AAAAAGATGGCAAAGATATTCAA	185	63	Szczepanowski et al., 2009
			mecAR	TTCTTCGTTACTCATGCCATACA			
bla_{TEM}	pNORM1 (3324 bp)	1000	blaTEM-F	TTCCTGTTTTTGCTCACCCAG	113	60	Di Cesare et al., 2016
			blaTEM -R	CTCAAGGATCTTACCGCTGTTG			
$bla_{CTX-M-32}$		100	ctx-m-32-FW	CGTCACGCTGTTGTTAGGAA	156	60	Hembach et al., 2017
			ctx -m-32-R	CGCTCATCAGCACGATAAAG			
bla_{OXA-58}	pUC19 (2838 bp)	1000	OXA58F	GCAATTGCCTTTTAAACCTGA	152	63	Laht et al., 2014
			OXA58R	CTGCCTTTTCAACAAAACCC			

References

O. Barraud, M.C. Baclet, F. Denis, M.C. Ploy, J. Antimicrob. Chemother. 65 (2010) 1642–1645. doi:10.1093/jac/dkq167.

S.L. Bräuer, C. Adams, K. Kranzler, D. Murphy, M. Xu, P. Zuber, H.M. Simon, A.M. Bapsta, B.M. Tebo, Environ. Microbiol. 13 (2011) 589–603. doi:10.1111/j.1462-2920.2010.02360.x.

A. Di Cesare, C. Losasso, L. Barco, E.M. Eckert, D. Conficoni, G. Sarasini, G. Corno, A. Ricci, Sci. Rep. 6 (2016) 1–9. doi:10.1038/srep28759.

N. Hembach, F. Schmid, J. Alexander, C. Hiller, E.T. Rogall, T. Schwartz, Front. Microbiol. 8 (2017) 1–11. doi:10.3389/fmicb.2017.01282.

M. Laht, A. Karkman, V. Voolaid, C. Ritz, T. Tenson, M. Virta, V. Kisand, PLoS One. 9 (2014) 1–8. doi:10.1371/journal.pone.0103705.

E. Martí, J.L. Balcázar, Appl. Environ. Microbiol. 79 (2013) 1743–1745.

R. Pei, S.C. Kim, K.H. Carlson, A. Pruden, Water Res. 40 (2006) 2427–2435. doi:10.1016/j.watres.2006.04.017

R. Szczepanowski, B. Linke, I. Krahn, K.H. Gartemann, T. Gützkow, W. Eichler, A. Pühler, A. Schlüter, Microbiology. 155 (2009) 2306–2319. doi:10.1099/mic.0.028233-0.

M. Tamminen, A. Karkman, Environmental Science & Technology, 45 (2011) 386-391.doi:10.1021/es102725n.

Supplementary Table ST3. Sequencing quality control parameters.

Sample	Raw PE(#)	Combined(#)	Qualified(#)	Nochime(#)	Base(nt)	AvgLen(nt)	Q20	Q30	GC%	Effective%
A1	134,043	117,979	116,117	96,513	39,776,023	412	98.14	94.16	52.92	72
A2	134,057	121,886	120,226	99,499	40,969,549	412	98.27	94.49	52.87	74.22
A3	133,788	122,464	120,593	97,703	40,224,798	412	98.29	94.54	52.91	73.03
B1	133,335	121,675	119,826	96,704	39,803,142	412	98.26	94.48	52.63	72.53
B2	144,280	130,458	128,447	104,245	42,943,001	412	98.16	94.18	52.58	72.25
B3	134,075	120,875	119,254	96,245	39,582,814	411	98.28	94.47	52.63	71.78
C1	139,085	125,799	123,519	93,344	38,773,001	415	98.08	93.99	52.41	67.11
C2	140,036	127,132	124,986	94,917	39,440,475	416	98.17	94.25	52.38	67.78
C3	137,072	124,250	121,992	97,228	40,436,026	416	98.12	94.1	52.29	70.93
D1	145,242	133,804	132,038	106,144	43,924,053	414	98.36	94.66	53.12	73.08
D2	134,308	120,989	119,076	93,642	38,747,710	414	98.15	94.18	53.18	69.72
D3	134,938	121,844	119,727	96,058	39,674,581	413	97.87	93.33	53.27	71.19
E1	132,557	120,272	118,321	91,754	37,647,398	410	98.11	94.1	52.61	69.22
E2	145,429	132,602	130,342	101,063	41,462,727	410	98.11	94.06	52.66	69.49
E3	135,637	123,836	121,750	93,165	38,213,269	410	98.14	94.19	52.67	68.69
F1	148,048	135,630	133,572	101,598	41,595,210	409	98.2	94.27	52.65	68.63
F2	142,027	128,998	126,896	97,076	39,766,318	410	98.15	94.18	52.56	68.35
F3	135,725	123,858	121,865	93,453	38,304,838	410	98.18	94.25	52.58	68.85
G1	142,555	130,847	129,045	114,078	46,476,022	407	98.19	94.27	53.68	80.02
G2	138,291	126,396	124,676	109,775	44,624,084	407	98.14	93.99	53.85	79.38
G3	137,525	119,192	117,265	101,807	41,772,030	410	98.17	94.23	53.71	74.03
H1	136,712	124,430	122,409	101,417	41,844,440	413	98.22	94.34	52.61	74.18
H2	143,404	130,874	128,773	99,232	40,893,727	412	98.17	94.25	52.57	69.2
H3	146,204	133,144	130,968	102,789	42,448,548	413	98.22	94.37	52.49	70.31
J1	148,047	134,882	132,659	98,711	40,500,822	410	98.17	94.23	53.04	66.68
J2	134,215	121,718	119,791	89,087	36,531,784	410	98.26	94.45	53.05	66.38
J3	140,604	126,969	124,896	96,175	39,485,733	411	98.09	93.99	52.88	68.4
K1	132,096	118,919	116,859	95,984	39,493,021	411	98.07	93.95	53.49	72.66
K2	141,328	127,191	125,183	110,880	45,517,917	411	97.98	93.68	53.73	78.46
K3	142,848	131,951	130,181	111,789	45,876,618	410	98.35	94.61	53.53	78.26
L1	134,322	120,907	118,923	102,929	42,355,210	411	98.2	94.32	52.86	76.63
L2	130,946	119,384	117,582	99,345	40,804,527	411	98.13	94.06	52.94	75.87
L3	132,799	121,502	119,603	98,983	40,606,697	410	98.19	94.33	53	74.54
M1	131,644	119,884	117,834	102,700	42,321,571	412	98.03	93.82	53.13	78.01
M2	133,500	122,285	120,432	105,394	43,442,059	412	98.18	94.27	53.07	78.95
M3	140,858	127,695	125,669	110,734	45,534,935	411	98.14	93.99	53.15	78.61

Supplementary Table ST4. Taxonomic sequencing results.

Sample	Uniq_tag	Tax_tag	Unclassified	Chloroplast	Mitochondria
A1	17144	79369	0	168	109
A2	16891	82608	0	168	34
A3	19374	78328	1	200	34
B1	14057	82644	3	0	0
B2	15070	89174	1	0	0
B3	13248	82996	1	0	0
C1	15438	77902	4	12	6
C2	16372	78545	0	0	0
C3	15256	81971	1	0	0
D1	17619	88522	3	183	121
D2	15836	77805	1	173	120
D3	15004	81054	0	200	49
E1	15353	76401	0	146	39
E2	16835	84228	0	0	0
E3	15463	77702	0	0	0
F1	14390	87208	0	0	0
F2	14061	83013	2	5	9
F3	13152	80301	0	1	0
G1	13853	100223	2	0	0
G2	15051	94720	4	165	112
G3	13135	88672	0	378	223
H1	11434	89969	14	316	64
H2	16005	83218	9	281	64
H3	20161	82625	3	1	0
J1	16377	82332	2	0	0
J2	13518	75565	4	0	1
J3	13596	82574	5	16	16
K1	18280	77696	8	2	0
K2	15867	94928	85	1	0
K3	20195	91556	38	202	159
L1	13251	89659	19	533	353
L2	12812	86529	4	582	235
L3	15799	83150	34	523	209
M1	20026	82674	0	117	133
M2	19586	85805	3	117	93
M3	17870	92861	3	159	160

Supplementary Table ST5. Quantitative pPCR results for all amplified genetic elements and samples.

Group Name	Site code	rDNA_16s	intI1	blaTEM	sul1	tetM	qnrS	blaOXA58	blaCTX	mecA
A	Site 1	1.83E+11	1.49E+09	4.64E+07	1.64E+09	3.37E+10	1.81E+05	2.25E+06	5.89E+04	1.80E+05
A	Site 1	2.65E+11	2.16E+09	7.02E+07	2.57E+09	4.84E+10	2.57E+05	3.65E+06	8.29E+04	2.47E+05
A	Site 1	1.63E+11	1.30E+09	4.37E+07	1.63E+09	3.00E+10	1.50E+05	2.12E+06	3.90E+04	1.56E+05
B	Site 1	3.88E+11	3.89E+09	4.25E+07	5.42E+09	3.01E+10	4.87E+05	2.09E+06	1.96E+05	2.68E+05
B	Site 1	5.75E+11	5.57E+09	6.22E+07	6.73E+09	3.47E+10	3.19E+05	3.12E+06	3.67E+05	4.04E+05
B	Site 1	4.16E+11	4.59E+09	4.70E+07	5.25E+09	3.83E+10	3.52E+05	2.70E+06	4.20E+05	3.18E+05
C	Site 2	7.89E+10	1.18E+09	2.29E+08	1.29E+09	2.29E+10	2.23E+07	2.49E+07	8.02E+05	2.33E+07
C	Site 2	1.06E+11	1.24E+09	2.94E+08	1.52E+09	3.32E+10	2.22E+07	2.82E+07	1.30E+06	3.00E+07
C	Site 2	5.11E+10	6.82E+08	1.38E+08	7.40E+08	1.64E+10	1.09E+07	1.41E+07	5.66E+05	1.35E+07
D	Site 2	1.81E+11	9.06E+09	1.13E+08	1.03E+10	3.86E+10	5.37E+06	5.46E+07	5.70E+05	9.96E+06
D	Site 2	1.74E+11	8.33E+09	9.42E+07	8.87E+09	3.52E+10	4.59E+06	4.76E+07	5.96E+05	8.25E+06
D	Site 2	2.50E+11	1.28E+10	1.43E+08	1.34E+10	5.03E+10	7.99E+06	7.85E+07	8.57E+05	1.13E+07
E	Site 3	3.47E+11	1.74E+09	1.09E+09	2.29E+09	4.75E+10	3.39E+05	1.77E+06	1.77E+04	2.35E+05
E	Site 3	3.85E+11	2.08E+09	1.24E+09	2.63E+09	5.10E+10	8.11E+04	2.34E+06	1.38E+04	2.92E+05
E	Site 3	3.01E+11	1.57E+09	9.94E+08	2.08E+09	4.58E+10	1.87E+05	1.97E+06	6.23E+04	2.71E+05
F	Site 3	4.80E+11	3.77E+09	7.41E+08	4.61E+09	3.16E+10	6.13E+05	2.61E+06	2.97E+04	3.18E+05
F	Site 3	5.28E+11	4.80E+09	8.58E+08	5.16E+09	3.71E+10	6.58E+05	2.45E+06	3.74E+04	3.35E+05
F	Site 3	5.30E+11	3.88E+09	7.59E+08	4.85E+09	3.50E+10	9.41E+05	2.27E+06	1.97E+04	3.10E+05
G	Site 4	1.79E+11	1.40E+09	7.01E+06	1.21E+09	1.12E+10	2.34E+05	2.59E+06	4.83E+04	3.66E+05
G	Site 4	1.47E+11	1.15E+09	5.79E+06	9.64E+08	9.84E+09	3.11E+05	2.55E+06	5.87E+04	3.05E+05
G	Site 4	1.09E+11	8.71E+08	6.18E+06	7.35E+08	8.23E+09	3.78E+05	1.55E+06	2.07E+04	1.94E+05
H	Site 5	4.29E+11	6.73E+09	1.50E+08	7.34E+09	1.62E+10	7.78E+06	4.41E+06	8.71E+05	2.53E+05
H	Site 5	4.44E+11	6.08E+09	1.36E+08	6.46E+09	2.58E+10	6.76E+06	4.65E+06	8.90E+05	2.58E+05
H	Site 5	1.79E+11	2.94E+09	4.52E+07	3.21E+09	2.04E+10	2.63E+06	2.15E+06	2.95E+05	1.57E+05
J	Site 5	4.37E+11	6.95E+09	1.01E+08	7.24E+09	2.56E+10	6.64E+06	6.62E+06	7.36E+05	1.66E+06
J	Site 5	3.30E+11	5.21E+09	8.33E+07	5.23E+09	1.90E+10	7.44E+06	5.62E+06	6.14E+05	2.61E+07
J	Site 5	3.68E+11	5.95E+09	8.98E+07	5.95E+09	2.19E+10	6.14E+06	5.13E+06	7.29E+05	7.64E+05
K	Site 6	1.45E+11	2.32E+09	3.26E+07	2.96E+09	6.28E+10	476676.60	5058507.2	404751.09	4.55E+05
K	Site 6	1.36E+11	2.11E+09	3.81E+07	2.55E+09	5.50E+10	453572.00	3726878.71	405011.03	3.99E+05
K	Site 6	2.05E+11	2.80E+09	4.30E+07	3.85E+09	8.46E+10	659002.79	6117127.77	637269.02	5.91E+05
L	Site 7	2.87E+11	1.79E+09	8.01E+07	2.88E+09	5.61E+10	848255.76	1435044.72	350687.47	5.94E+05
L	Site 7	3.14E+11	1.96E+09	1.01E+08	2.74E+09	7.36E+10	999394.78	1718599.55	486266.36	6.75E+05
L	Site 7	2.32E+11	1.53E+09	7.30E+07	1.88E+09	5.59E+10	747258.53	3215548.27	193751.70	5.66E+05
M	Site 8	2.15E+11	1.92E+09	1.53E+07	2.30E+09	5.93E+10	1053099.64	2066222.89	576771.02	5.15E+06
M	Site 8	2.87E+11	2.20E+09	1.96E+07	3.44E+09	7.54E+10	1691162.79	5607834.37	1040093.61	6.30E+06
M	Site 8	2.41E+11	2.19E+09	1.82E+07	2.80E+09	6.61E+10	1808229.70	2425668.95	1429651.63	6.03E+06

Sectors in red correspond to values below quantification limits

Supplementary Table ST6. Concentrations of antibiotics detected at pig slurry samples at ng/g dw by LC-MS/MA and confirmed by LC-HRMS and authentic standards.

			Sample Codes									
Antibiotic	Antibiotic class	MSC[a] (µg/L)	B	C	D	F	G	I	J	K	L	M
Azithromycin	macrolide	0.25	32	98	<LOD	<LOD	67	<LOD	<LOD	<LOD	<LOD	<LOD
Enrofloxacin	fluoroquinolone	0.064	<LOD	2396	6780	<LOD	<LOD	4765	1065	<LOD	21048	133
Ciprofloxacin	fluoroquinolone	0.064	59	11980	2680	28	149	464	78	<LOD	612	44
Tetracyline	tetracicyline	1	396	2144	36	<LOD	133	6055	308	<LOD	<LOD	<LOD
Doxyciline	tetracicyline	2	<LOD	<LOD	<LOD	<LOD	<LOD	<LOD	<LOD	<LOD	<LOD	<LOD
Oxytetracycline	tetracicyline	0.5	<LOD	<LOD	4634	<LOD	2524	49	13	<LOD	<LOD	<LOD
Sulfadiazine	sulfonamide	16[b]	122	<LOD	22	<LOD	37	<LOD	<LOD	<LOD	<LOD	<LOD
Sulfametoxazole	sulfonamide	16	<LOD	<LOD	<LOD	<LOD	<LOD	<LOD	<LOD	<LOD	<LOD	<LOD
Lincomycin	lincosamide	2	<LOD	<LOD	CD	2427	2324	<LOD	<LOD	1000	2806	4333
Sample humidity (%)			98	97	90	95	93	97	69	98	93.8	95.5

LOD: limit of detection; CD: conflicting data (detected by HRMS at high abundance but not by MS/MS)

a) MSC values from Bengstsson-Palme and Larsson 2016, 10.1016/j.envint.2015.10.015

b) MSC value estimated for values from other sulfonamides

Supplementary Table ST7. Taxon abundance, at the family level.

Kingdom	Phylum	Class	Order	Family	Number of OTUs	Total reads
Archaea	Euryarchaeota	Methanomicrobia	Methanomicrobiales	Methanomicrobiaceae	8	47061
		Methanobacteria	Methanobacteriales	Methanobacteriaceae	19	40056
		Thermoplasmata	Thermoplasmatales	Thermoplasmatales incertae sedis	17	25302
Bacteria	Actinobacteria	unidentified_Actinobacteria	Corynebacteriales	Corynebacteriaceae	26	202790
		unidentified_Actinobacteria	Propionibacteriales	Propionibacteriaceae	29	14093
	Bacteroidetes	Bacteroidia	Bacteroidales	Porphyromonadaceae	193	104259
		Bacteroidia	Bacteroidales	Bacteroidaceae	36	48761
		Bacteroidia	Bacteroidales	Bacteroidales UCG-001	10	44664
		Bacteroidia	Bacteroidales	Bacteroidetes incertae sedis	197	33345
		Bacteroidia	Bacteroidales	Marinilabiaceae	25	14628
		Bacteroidia	Bacteroidales	Rikenellaceae	108	11481
	Cloacimonetes	GZKB75	NA	Cloacimonetes incertae sedis	48	110176
	Firmicutes	Clostridia	Clostridiales	Clostridiaceae	162	693935
		Clostridia	Clostridiales	Firmicutes incertae sedis	859	306528
		Clostridia	Clostridiales	Ruminococcaceae	871	139038
		Clostridia	Clostridiales	Lachnospiraceae	241	68753
		Clostridia	Clostridiales	Syntrophomonadaceae	97	62088
		Clostridia	Clostridiales	Christensenellaceae	192	47116
		Erysipelotrichia	Erysipelotrichales	Erysipelotrichaceae	202	38541
		Clostridia	Clostridiales	Clostridia Family XI	219	36265
		Clostridia	Clostridiales	Clostridia Family XIII	65	24514
		Clostridia	Clostridiales	Eubacteriaceae	49	21766
		Bacilli	Lactobacillales	Aerococcaceae	13	20134
		Bacilli	Lactobacillales	Enterococcaceae	14	16253
		Bacilli	Lactobacillales	Carnobacteriaceae	23	13402
		Clostridia	Clostridiales	Peptostreptococcaceae	51	10865
	Proteobacteria	Gammaproteobacteria	Pseudomonadales	Pseudomonadaceae	34	24677
		Gammaproteobacteria	Pseudomonadales	Moraxellaceae	25	14287
	Spirochaetes	unidentified_Spirochaetes	Spirochaetales	Spirochaetaceae	138	100024
	Synergistetes	Synergistia	Synergistales	Synergistaceae	56	81997
	Tenericutes	Mollicutes	Acholeplasmatales	Acholeplasmataceae	59	19799
	Verrucomicrobia	Opitutae	Puniceicoccales	Puniceicoccaceae	2	20532
Unknown	Unknown	Unknown	Unknown	Unknown	402	34012
Only families with more than 10,000 reads are included						

Paper II: Implications of the use of organic fertilizers for Antibiotic Resistance Gene distribution in agricultural soils and fresh food products. A plot-scale study

Claudia Sanz[1], Marta Casado[1], Laia Navarro-Martin[1], Núria Cañameras[2], Núria Carazo[2], Victor Matamoros[1], Josep Maria Bayona[1], Benjamin Piña[1]

1) IDAEA-CSIC, Jordi Girona, 18. E-08034, Barcelona, Spain

2) Department of Agri-Food Engineering and Biotechnology DEAB-UPC, Esteve Terrades 8, Building 4, Castelldefels, 08860, Spain

Supporting Figures

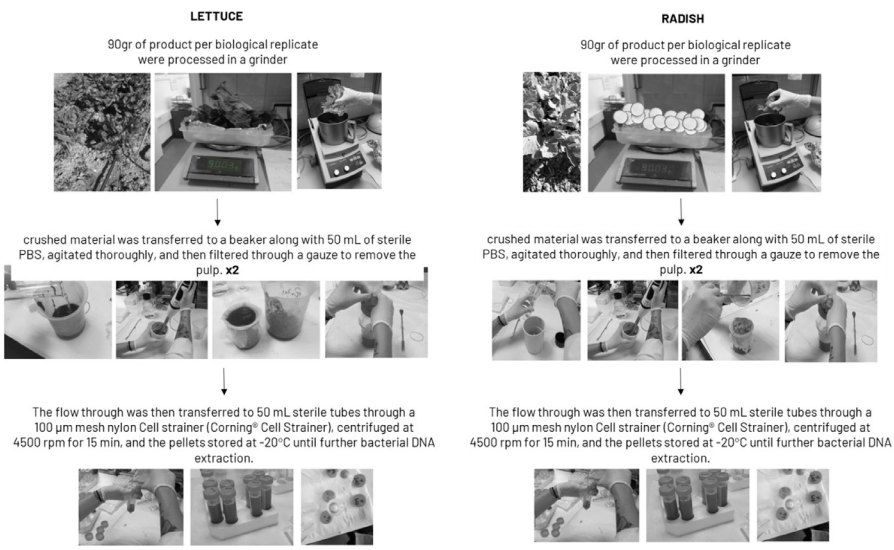

Supplementary Figure S1. Processing of lettuce and radish samples.

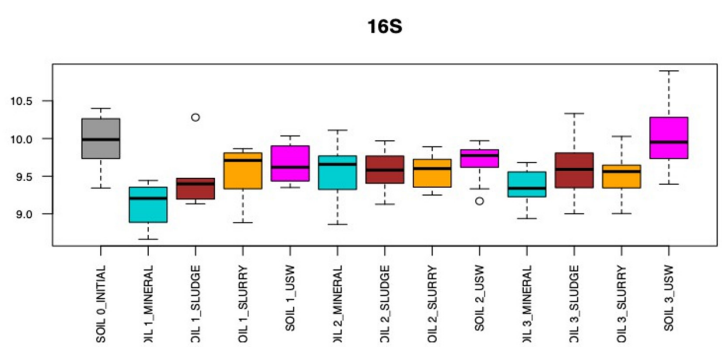

Supplementary Figure S2. Absolute abundance 16S rDNA values for the different groups of samples. Boxes are color-coded by the type of fertilizer used in the amendment: grey, none (initial soil), pale blue, mineral fertilizer; brown, sludge; orange, slurry; magenta, USW. Data are expressed as copies of 16S rDNA sequences per gram of soil. Thick black line, boxes and whiskers represent the median, first-to third percentiles and total distribution of samples, respectively.

Supporting Tables

Supplementary Table S1. Main physico-chemical properties of organic fertilizers in this study. Analyses were done by Eurofins Agroambiental, S.A. Lleida (Spain) under standard methods.

PARAMETERS	FERTILIZERS		
	OFMSW	SLUDGE	SLURRY
Dry matter (% f.w.)	88.8	20.9	4.8
Total N (% d.w..)	2.71	2.77	3.14
Organic N (% d.w..)	2.46	51.5	2.80
NH_4-N (% d.w..)	0.25	1.34	0.34
Total P (% d.w..)	0.52	1.55	0.98
Total K (% d.w..)	92.51	0.207	0.99

Supplementary Table S2. Key physico-chemical properties of experimental soils after a cycle. prior to the new biosolid application. Analyses were done by Eurofins Agroambiental, S.A. Lleida (Spain) under standard methods.

PARAMETERS	FROM 1_{ST} CYCLE TO 2_{ND} CYCLE			
	MINERAL SOIL	OFMSW SOIL	SLUDGE SOIL	SLURRY SOIL
Humidity (%)	1.44	1.48	1.48	1.47
Total N (% d.w..)	0.121	0.156	0.108	0.125
N-NO_3 (mg/kg d.w.)	13.0	18.8	14.8	17,7
Total P (mg/kg d.w.)	22	28	35	23
Total K (mg/kg d.w.)	366	476	295	384
Ca (mg/kg d.w.)	6130	6381	6424	6267
Mg (ext. ac. amònic) (mg/kg d.w..)	426	445	416	440
Na (mg/kg d.w..)	117	121	125	121

Supplementary Table S3. Plasmid, primers and LOQs used for detection and quantifications of antibiotic resistance genes in amendments.

Target gene	Plasmid	LOQ (gene copies/ul)	Primers	Sequence (5'-> 3')	Amplicon size (bp)	Tm(ºC)	Reference
16S rDNA	pNORM1 (3324 bp)	1000	331F	TCCTACGGGAGGCAGCAGT	195	60	Bräuer et al., 2011
			518R	ATTACCGCGGCTGCTGG			
*intI*1		100	intI1LC5	GATCGGTCGAATGCGTGT	196	60	Barraud et al., 2010
			intI1LC1	GCCTTGATGTTACCCGAGAG			
*sul*1		100	sul1-FW	CGCACCGGAAACATCGCTGCAC	162	60	Pei et al., 2006
			sul1-RV	TGAAGTTCCGCCGCAAGGCTCG			
*qnr*S1		100	qnrSrtF11	GACGTGCTAACTTGCGTGAT	118	60	Marti & Balcázar, 2013
			qnrSrtR 11	TGGCATTGTTGGAAACTTG			
*tet*M	pUC19 (2882 bp)	1000	tetMF	GCAATTCTACTGATTTCTGC	186	60	Tamminen & Karkman, 2011
			tetMR	CTGTTTGATTACAATTTCCGC			
*mec*A	pUC19 (2871 bp)	1000	mecAF	AAAAAGATGGCAAAGATATTCAA	185	63	Szczepanowski et al., 2009
			mecAR	TTCTTCGTTACTCATGCCATACA			
bla_{TEM}	pNORM1 (3324 bp)	1000	blaTEM-F	TTCCTGTTTTTGCTCACCCAG	113	60	Di Cesare et al., 2016
			blaTEM -R	CTCAAGGATCTTACCGCTGTTG			
$bla_{CTX-M-32}$		100	ctx-m-32-FW	CGTCACGCTGTTGTTAGGAA	156	60	Hembach et al., 2017
			ctx -m-32-R	CGCTCATCAGCACGATAAAG			
bla_{OXA-58}	pUC19 (2838 bp)	1000	OXA58F	GCAATTGCCTTTTAAACCTGA	152	63	Laht et al., 2014
			OXA58R	CTGCCTTTTCAACAAAACCC			

References

O. Barraud, M.C. Baclet, F. Denis, M.C. Ploy, J. Antimicrob. Chemother. 65 (2010) 1642–1645. doi:10.1093/jac/dkq167.

S.L. Bräuer, C. Adams, K. Kranzler, D. Murphy, M. Xu, P. Zuber, H.M. Simon, A.M. Bapsta, B.M. Tebo, Environ. Microbiol. 13 (2011) 589–603. doi:10.1111/j.1462-2920.2010.02360.x.

A. Di Cesare, C. Losasso, L. Barco, E.M. Eckert, D. Conficoni, G. Sarasini, G. Corno, A. Ricci, Sci. Rep. 6 (2016) 1–9. doi:10.1038/srep28759.

N. Hembach, F. Schmid, J. Alexander, C. Hiller, E.T. Rogall, T. Schwartz, Front. Microbiol. 8 (2017) 1–11. doi:10.3389/fmicb.2017.01282.

M. Laht, A. Karkman, V. Voolaid, C. Ritz, T. Tenson, M. Virta, V. Kisand, PLoS One. 9 (2014) 1–8. doi:10.1371/journal.pone.0103705.

E. Martí, J.L. Balcázar, Appl. Environ. Microbiol. 79 (2013) 1743–1745.

R. Pei, S.C. Kim, K.H. Carlson, A. Pruden, Water Res. 40 (2006) 2427–2435. doi:10.1016/j.watres.2006.04.017

R. Szczepanowski, B. Linke, I. Krahn, K.H. Gartemann, T. Gützkow, W. Eichler, A. Pühler, A. Schlüter, Microbiology. 155 (2009) 2306–2319. doi:10.1099/mic.0.028233-0.

M. Tamminen, A. Karkman, Environmental Science & Technology, 45 (2011) 386-391.doi:10.1021/es102725n.

Supplementary Table S4. Quality parameters of sequencing results.

Sample ID	Total reads	Combined reads	Uncombined reads	Percent combined (%)	Combined base (bp)	Min length (bp)	Max length (bp)	Avg legth (bp)
S0_NONE	130,006	122,111	7,895	93.93	51,100,412	44	441	418
S0_NONE	136,992	122,665	14,327	89.54	51,234,756	122	441	418
S0_NONE	148,661	135,761	12,900	91.32	56,822,060	227	441	419
S1_MINERAL	133,134	126,013	7,121	94.65	52,851,689	44	441	419
S1_MINERAL	102,744	97,861	4,883	95.25	40,831,724	49	441	417
S1_MINERAL	142,510	133,924	8,586	93.98	56,169,356	59	441	419
S1_MINERAL	144,339	126,426	17,913	87.59	52,827,782	48	444	418
S1_SLUDGE	134,099	126,165	7,934	94.08	52,759,443	122	441	418
S1_SLUDGE	144,639	137,136	7,503	94.81	57,372,173	158	441	418
S1_SLUDGE	105,072	100,319	4,753	95.48	41,997,396	49	441	419
S1_SLUDGE	132,761	117,389	15,372	88.42	48,905,727	44	443	417
S1_SLURRY	117,679	111,551	6,128	94.79	46,690,724	44	441	419
S1_SLURRY	110,192	104,375	5,817	94.72	43,675,752	78	441	418
S1_SLURRY	134,613	127,386	7,227	94.63	53,220,571	44	441	418
S1_SLURRY	126,262	119,997	6,265	95.04	50,212,097	261	441	418
S1_SLURRY	142,270	126,231	16,039	88.73	52,791,974	44	443	418
S1_USW	138,029	130,075	7,954	94.24	54,476,000	222	441	419
S1_USW	147,502	138,115	9,387	93.64	57,900,034	44	441	419
S1_USW	103,378	98,501	4,877	95.28	41,174,311	205	441	418
S1_USW	134,123	121,809	12,314	90.82	50,872,266	60	441	418
S2_MINERAL	137,061	130,301	6,760	95.07	54,478,482	44	441	418
S2_MINERAL	145,028	135,258	9,770	93.26	56,490,786	82	441	418
S2_MINERAL	140,597	132,833	7,764	94.48	55,258,266	150	441	416
S2_MINERAL	149,589	141,893	7,696	94.86	59,233,634	45	441	417
S2_MINERAL	132,037	122,470	9,567	92.75	51,144,856	242	441	418
S2_MINERAL	136,455	128,479	7,976	94.15	53,588,700	65	441	417
S2_SLUDGE	143,357	134,555	8,802	93.86	56,234,066	35	441	418
S2_SLUDGE	142,319	133,570	8,749	93.85	55,821,618	65	441	418
S2_SLUDGE	137,874	129,990	7,884	94.28	54,348,325	44	441	418
S2_SLUDGE	135,145	127,912	7,233	94.65	53,604,414	65	441	419
S2_SLUDGE	143,082	129,828	13,254	90.74	54,250,987	67	444	418
S2_SLUDGE	130,229	113,607	16,622	87.24	47,440,757	49	442	418
S2_SLURRY	143,061	134,663	8,398	94.13	56,316,359	88	441	418
S2_SLURRY	140,215	131,747	8,468	93.96	55,245,496	44	441	419
S2_SLURRY	135,546	128,051	7,495	94.47	53,412,478	44	441	417
S2_SLURRY	143,125	134,944	8,181	94.28	56,273,129	44	442	417
S2_SLURRY	136,879	123,506	13,373	90.23	51,771,987	44	441	419
S2_SLURRY	139,599	126,275	13,324	90.46	52,808,509	45	443	418
S2_USW	138,728	130,153	8,575	93.82	54,336,217	49	441	417

Supplementary Table S4. Continued.

S2_USW	135,423	127,163	8,260	93.9	53,184,789	49	441	418
S2_USW	132,340	124,260	8,080	93.89	52,041,359	44	441	419
S2_USW	144,533	135,176	9,357	93.53	56,366,578	44	441	417
S2_USW	130,037	122,866	7,171	94.49	51,540,825	49	441	419
S2_USW	137,696	130,000	7,696	94.41	54,312,520	44	441	418
S3_MINERAL	140,657	129,939	10,718	92.38	54,295,274	44	441	418
S3_MINERAL	131,421	123,590	7,831	94.04	51,611,457	83	442	418
S3_MINERAL	137,159	129,505	7,654	94.42	54,107,635	44	441	418
S3_MINERAL	142,501	132,383	10,118	92.9	55,332,420	44	441	418
S3_MINERAL	146,904	134,637	12,267	91.65	56,256,887	43	441	418
S3_MINERAL	149,600	134,687	14,913	90.03	56,331,396	65	444	418
S3_SLUDGE	133,098	125,391	7,707	94.21	52,390,787	245	441	418
S3_SLUDGE	132,279	123,625	8,654	93.46	51,723,738	262	441	418
S3_SLUDGE	146,376	137,986	8,390	94.27	57,766,722	44	441	419
S3_SLUDGE	141,273	132,997	8,276	94.14	55,971,049	244	441	421
S3_SLUDGE	133,002	125,433	7,569	94.31	52,543,431	65	441	419
S3_SLUDGE	143,947	136,099	7,848	94.55	56,869,282	44	441	418
S3_SLURRY	144,022	135,853	8,169	94.33	56,742,024	44	441	418
S3_SLURRY	140,529	132,217	8,312	94.09	55,047,827	238	441	416
S3_SLURRY	143,144	134,887	8,257	94.23	56,292,353	44	442	417
S3_SLURRY	146,818	138,128	8,690	94.08	57,909,078	49	441	419
S3_SLURRY	137,361	129,609	7,752	94.36	54,094,000	65	441	417
S3_SLURRY	149,803	141,471	8,332	94.44	59,071,742	183	441	418
S3_USW	144,653	134,951	9,702	93.29	56,527,048	44	441	419
S3_USW	145,161	136,403	8,758	93.97	57,167,386	44	441	419
S3_USW	138,095	130,181	7,914	94.27	54,610,026	44	441	419
S3_USW	149,916	141,531	8,385	94.41	59,248,191	64	441	419
S3_USW	138,400	130,198	8,202	94.07	54,686,204	269	441	420
S3_USW	144,234	136,486	7,748	94.63	57,151,097	64	442	419
Sludge	141,649	130,020	11,629	91.79	54,203,483	272	441	417
Slurry	148,669	136,658	12,011	91.92	55,801,716	64	440	408
USW	121,959	108,369	13,590	88.86	45,488,814	51	444	420

Supplementary Table S5. Annotation statistics.

	# of Taxa	% Annotation
Kingdom	2	100%
Phylum	68	100%
Class	167	98%
Order	382	93%
Family	559	84%
Genus	1536	59%
Species	1652	13%

Supplementary Table S6. PERMANOVA ADONIS tests.

Two-way ADONIS, Sampling x Treatment				
	Df	F	*p*	
Sampling	2	2.8935	0.001	***
Treatment	3	1.7692	0.001	***
Sampling x Treatment	6	1.2556	0.001	***
One-way ADONIS, Treatment				
Soil 1 ~ Treatment	3	1.3354	0.002	**
Soil 2 ~Treatment	3	1.1465	0.016	*
Soil 3 ~ Treatment	3	1.7274	0.001	***
One-way ADONIS, Sampling				
Mineral ~ Sampling	2	1.5088	0.003	**
Sludge ~ Sampling	2	1.7012	0.001	***
Slurry ~ Sampling	2	1.5167	0.001	***
USW ~ Sampling	2	1.9266	0.001	***

*, p<0.05; **, p<0.01;***, p<0.001

Df, degrees of freedom

Paper III: Impact of organic soil amendments in antibiotic levels, antibiotic resistance gene loads, and microbiome composition in corn fields and crops

Sanz, Claudia[1]; Casado, Marta[1]; Đorde Tadic[1]; Pastor-López, Edward J[1].; Navarro-Martin, Laia[1]; Parera, Joan[2]; Tugues, Jordi[2]; Ortiz, Carlos A.[2], Bayona, Josep M.[1]; Piña, Benjamin[1]

1) IDAEA-CSIC, Jordi Girona, 18. E-08034, Barcelona, Spain

2) DACC, Departament d'Acció Climàtica, Alimentació i Agenda Rural, Generalitat de Catalunya, Gran Via de les Corts Catalanes, 612-614, E-08007, Barcelona, Spain

Supporting Figures

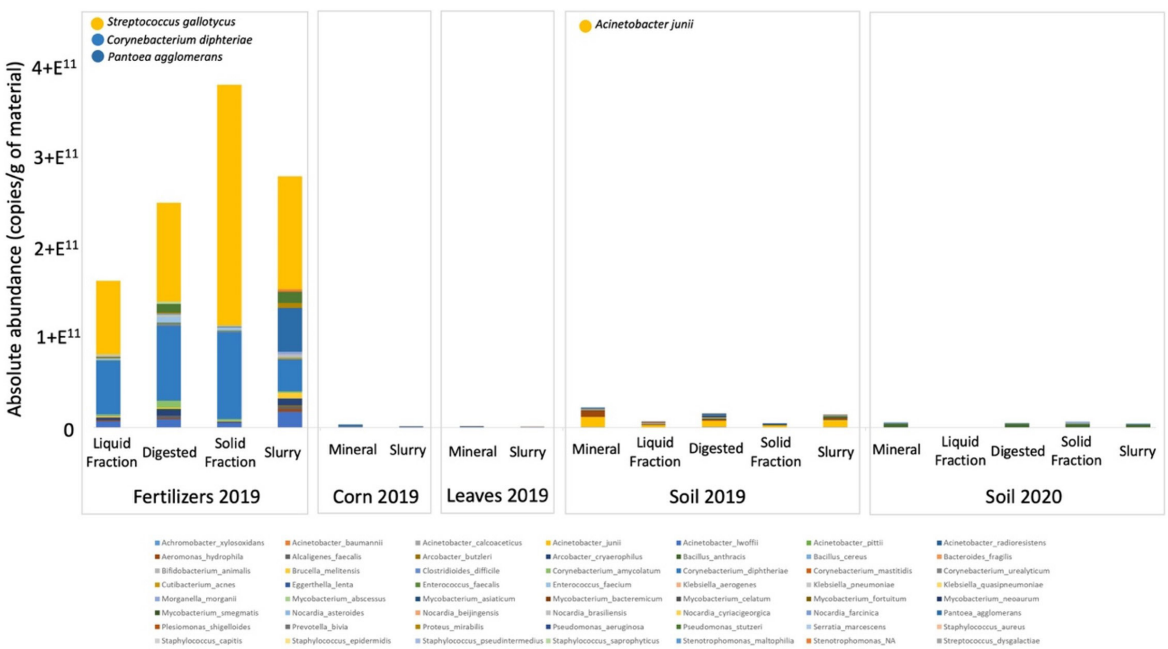

Supplementary Figure SF1. Absolute abundance of bacterial taxa classified as pathogenic in the FAPROTAX database (http://www.zoology.ubc.ca/louca/FAPROTAX).

Supporting Tables

Supplementary Table ST1. Initial soil characterization of the different plots (0-30 cm).

PARAMETERS	Initial soil			
	n=1	n=2	n=3	n=4
pH	7.9	7.7	7.7	7.7
Electric conductivity	0.7	1.8	1.9	2.1
$CaCO_3$	29	30	29	30
NO_3–	9	12	13	13
Total P (mg/kg)	56	64	59	55
Total K (mg/kg)	191	204	192	195
Organic matter (%)	1.91	1.99	2.08	2.17

Supplementary Table ST2. Composition of soil amendments for the 2019 and 2010 productive cycles.

PARAMETERS	2019				2020			
	Solid Fraction	Liquid Fraction	Digested	Slurry	Solid Fraction	Liquid Fraction	Digested	Slurry
Dry matter (% s.m.f)	23.6	1.8	4.5	5.8	31.9	-	1.64	14.08
Organic matter (% s.m.f)	73.6	65.4	65.7	63.5	69.5	-	54.3	67.4
Total N (% s.m.s.)	1.7	2.9	3.8	2.8	1.6	-	3.71	2.13
Organic N (% s.m.s.)	2.6	13.2	11.3	6.5	2.2	-	16.43	-
NH_4-N (% s.m.s.)	0.97	10.5	7.2	3.8	0.7	-	12.72	2.68
Total P_2O_5 (% s.m.s.)	4.02	2.8	2.2	3.0	2.5	-	1.41	2.957
Total K_2O (% s.m.s.)	1.3	8.1	6.7	8.0	0.8	-	13.95	3.483

Supplementary Table ST3. Plasmid, primers and LOQs used for detection and quantifications of antibiotic resistance genes in amendments.

Target gene	Plasmid	LOQ (gene copies/ul)	Primers	Sequence (5'-> 3')	Amplicon size (bp)	Tm(ºC)	Reference
16S rDNA	pNORM1 (3324 bp)	1000	331F	TCCTACGGGAGGCAGCAGT	195	60	Bräuer et al., 2011
			518R	ATTACCGCGGCTGCTGG			
*int*I1		100	intI1LC5	GATCGGTCGAATGCGTGT	196	60	Barraud et al., 2010
			intI1LC1	GCCTTGATGTTACCCGAGAG			
*sul*1		100	sul1-FW	CGCACCGGAAACATCGCTGCAC	162	60	Pei et al., 2006
			sul1-RV	TGAAGTTCCGCCGCAAGGCTCG			
*qnr*S1		100	qnrSrtF11	GACGTGCTAACTTGCGTGAT	118	60	Marti & Balcázar, 2013
			qnrSrtR 11	TGGCATTGTTGGAAACTTG			
*tet*M	pUC19 (2882 bp)	1000	tetMF	GCAATTCTACTGATTTCTGC	186	60	Tamminen & Karkman, 2011
			tetMR	CTGTTTGATTACAATTTCCGC			
*mec*A	pUC19 (2871 bp)	1000	mecAF	AAAAAGATGGCAAAGATATTCAA	185	63	Szczepanowski et al., 2009
			mecAR	TTCTTCGTTACTCATGCCATACA			
bla_{TEM}	pNORM1 (3324 bp)	1000	blaTEM-F	TTCCTGTTTTTGCTCACCCAG	113	60	Di Cesare et al., 2016
			blaTEM -R	CTCAAGGATCTTACCGCTGTTG			
$bla_{CTX\text{-}M\text{-}32}$		100	ctx-m-32-FW	CGTCACGCTGTTGTTAGGAA	156	60	Hembach et al., 2017
			ctx -m-32-R	CGCTCATCAGCACGATAAAG			
$bla_{OXA\text{-}58}$	pUC19 (2838 bp)	1000	OXA58F	GCAATTGCCTTTTAAACCTGA	152	63	Laht et al., 2014
			OXA58R	CTGCCTTTTCAACAAAACCC			

References

O. Barraud, M.C. Baclet, F. Denis, M.C. Ploy, J. Antimicrob. Chemother. 65 (2010) 1642–1645. doi:10.1093/jac/dkq167.

S.L. Bräuer, C. Adams, K. Kranzler, D. Murphy, M. Xu, P. Zuber, H.M. Simon, A.M. Bapsta, B.M. Tebo, Environ. Microbiol. 13 (2011) 589–603. doi:10.1111/j.1462-2920.2010.02360.x.

A. Di Cesare, C. Losasso, L. Barco, E.M. Eckert, D. Conficoni, G. Sarasini, G. Corno, A. Ricci, Sci. Rep. 6 (2016) 1–9. doi:10.1038/srep28759.

N. Hembach, F. Schmid, J. Alexander, C. Hiller, E.T. Rogall, T. Schwartz, Front. Microbiol. 8 (2017) 1–11. doi:10.3389/fmicb.2017.01282.

M. Laht, A. Karkman, V. Voolaid, C. Ritz, T. Tenson, M. Virta, V. Kisand, PLoS One. 9 (2014) 1–8. doi:10.1371/journal.pone.0103705.

E. Martí, J.L. Balcázar, Appl. Environ. Microbiol. 79 (2013) 1743–1745.

R. Pei, S.C. Kim, K.H. Carlson, A. Pruden, Water Res. 40 (2006) 2427–2435. doi:10.1016/j.watres.2006.04.017

R. Szczepanowski, B. Linke, I. Krahn, K.H. Gartemann, T. Gützkow, W. Eichler, A. Pühler, A. Schlüter, Microbiology. 155 (2009) 2306–2319. doi:10.1099/mic.0.028233-0.

M. Tamminen, A. Karkman, Environmental Science & Technology, 45 (2011) 386-391.doi:10.1021/es102725n.

Supplementary Table ST4. Quality control parameters for high throughput sequencing results.

Sample	MATRIX	TREATMENT	YEAR	Raw PE(#)	Combined(#)	Qualified(#)	Nochime(#)	Base(nt)	AvgLen(nt)	Q20	Q30	GC%	Effective%
M25.1	FERTILIZER	Digestate	2019	131,644	119,884	117,834	102,700	42,321,571	412	98.03	93.82	53.13	78.01
M25.2	FERTILIZER	Digestate	2019	133,500	122,285	120,432	105,394	43,442,059	412	98.18	94.27	53.07	78.95
M25.3	FERTILIZER	Digestate	2019	140,858	127,695	125,669	110,734	45,534,935	411	98.14	93.99	53.15	78.61
K21.1	FERTILIZER	Liquid Fraction	2019	132,096	118,919	116,859	95,984	39,493,021	411	98.07	93.95	53.49	72.66
K21.2	FERTILIZER	Liquid Fraction	2019	141,328	127,191	125,183	110,880	45,517,917	411	97.98	93.68	53.73	78.46
K21.3	FERTILIZER	Liquid Fraction	2019	142,848	131,951	130,181	111,789	45,876,618	410	98.35	94.61	53.53	78.26
L23.1	FERTILIZER	Slurry	2019	134,322	120,907	118,923	102,929	42,355,210	411	98.2	94.32	52.86	76.63
L23.2	FERTILIZER	Slurry	2019	130,946	119,384	117,582	99,345	40,804,527	411	98.13	94.06	52.94	75.87
L23.3	FERTILIZER	Slurry	2019	132,799	121,502	119,603	98,983	40,606,697	410	98.19	94.33	53	74.54
J17.4	FERTILIZER	Solid Fraction	2019	148,047	134,882	132,659	98,711	40,500,822	410	98.17	94.23	53.04	66.68
J17.5	FERTILIZER	Solid Fraction	2019	134,215	121,718	119,791	89,087	36,531,784	410	98.26	94.45	53.05	66.38
J17.6	FERTILIZER	Solid Fraction	2019	140,604	126,969	124,896	96,175	39,485,733	411	98.09	93.99	52.88	68.4
FS.CF	FERTILIZER	Solid Fraction	2020	136,381	132,734	131,041	95,269	39,929,996	419	98.68	95.38	53.32	69.86
AGRI34	CORN	Mineral	2019	136,804	122,933	121,499	119,247	48,452,650	406	98.36	94.71	55.26	87.17
AGRI35	CORN	Slurry	2019	139,116	122,125	120,325	105,695	43,335,435	410	98.31	94.66	54.84	75.98
AGRI32	LEAVES	Mineral	2019	136,166	102,709	100,785	77,074	32,023,787	415	98.21	94.43	55.39	56.6
AGRI33	LEAVES	Slurry	2019	131,721	119,611	118,217	99,395	41,192,664	414	98.54	95.2	54.61	75.46
AGRI13	SOIL	Digestate	2019	141,171	109,488	107,344	77,370	32,339,762	418	98.43	94.91	56.25	54.81
AGRI14	SOIL	Digestate	2019	136,865	104,814	102,510	72,004	30,074,945	418	98.15	94.29	56.32	52.61
AGRI24	SOIL	Digestate	2019	144,246	114,391	111,936	83,563	34,971,989	419	98.27	94.54	56.9	57.93
AGRI25	SOIL	Digestate	2019	133,698	102,716	100,746	74,801	31,192,366	417	98.37	94.76	56.18	55.95
AGRI3	SOIL	Digestate	2019	141,319	109,353	107,247	74,159	30,973,982	418	98.16	94.25	56.48	52.48
AGRI4	SOIL	Digestate	2019	146,774	111,374	109,258	73,060	30,474,692	417	98.2	94.35	56.12	49.78
CF20.1	SOIL	Digestate	2020	108,067	97,590	96,171	73,805	30,846,727	418	98.41	94.74	55.52	68.3
CF20.2	SOIL	Digestate	2020	117,887	109,496	108,123	84,376	35,290,540	418	98.54	95.12	55.57	71.57
CF20.3	SOIL	Digestate	2020	104,781	97,434	96,225	72,297	30,136,973	417	98.56	95.21	55.75	69
CF20.4	SOIL	Digestate	2020	115,736	104,922	103,210	79,807	33,249,621	417	98.34	94.64	55.56	68.96
CF20.5	SOIL	Digestate	2020	113,974	105,409	104,120	76,787	32,029,715	417	98.51	95.05	55.62	67.37
CF20.6	SOIL	Digestate	2020	106,939	99,920	98,663	77,275	32,256,092	417	98.54	95.11	55.36	72.26
AGRI11	SOIL	Liquid Fraction	2019	144,381	108,213	105,703	72,254	30,225,267	418	98.16	94.29	56.31	50.04
AGRI12	SOIL	Liquid Fraction	2019	145,878	107,408	104,535	74,865	31,257,218	418	98.14	94.19	56.76	51.32
AGRI22	SOIL	Liquid Fraction	2019	131,725	93,974	90,535	68,703	28,624,180	417	98.17	94.23	56.45	52.16
AGRI23	SOIL	Liquid Fraction	2019	147,045	113,586	110,921	76,326	31,890,084	418	98.14	94.26	56.3	51.91
AGRI5	SOIL	Liquid Fraction	2019	132,653	102,063	100,266	68,366	28,521,226	417	98.52	95.08	55.94	51.54
AGRI6	SOIL	Liquid Fraction	2019	133,045	102,427	100,667	67,408	28,119,943	417	98.46	94.94	56.4	50.67
AGRI1	SOIL	Mineral	2019	149,907	115,377	113,341	79,451	33,219,709	418	98.4	94.8	56.3	53
AGRI15	SOIL	Mineral	2019	149,343	113,851	111,438	81,272	34,012,978	419	98.12	94.16	57.51	54.42
AGRI16	SOIL	Mineral	2019	140,944	108,391	106,124	74,786	31,326,361	419	98.33	94.7	56.44	53.06
AGRI2	SOIL	Mineral	2019	139,652	106,697	104,702	69,322	28,964,531	418	98.18	94.33	56.12	49.64
AGRI26	SOIL	Mineral	2019	145,603	114,213	112,000	80,292	33,486,002	417	98.14	94.26	56.06	55.14
AGRI27	SOIL	Mineral	2019	146,161	113,394	111,057	79,099	32,927,302	416	98.2	94.39	56.96	54.12
CF21.1	SOIL	Mineral	2020	118,540	106,721	105,062	81,348	33,973,334	418	98.38	94.63	55.33	68.62
CF21.2	SOIL	Mineral	2020	106,355	98,511	97,283	72,094	30,134,174	418	98.52	95.06	55.67	67.79
CF21.3	SOIL	Mineral	2020	100,692	93,605	92,472	71,705	29,891,330	417	98.56	95.15	55.66	71.21
CF21.4	SOIL	Mineral	2020	110,845	101,568	100,246	82,802	34,515,171	417	98.47	94.94	55.4	74.7
CF21.5	SOIL	Mineral	2020	101,574	95,088	94,021	72,236	30,152,225	417	98.6	95.2	55.48	71.12
CF21.6	SOIL	Mineral	2020	113,726	103,807	102,006	48,475	20,229,842	417	98.26	94.52	56.32	42.62
AGRI10	SOIL	Slurry	2019	134,988	102,150	100,208	73,994	30,965,360	418	98.22	94.33	56.24	54.82
AGRI17	SOIL	Slurry	2019	136,014	105,741	103,677	71,440	29,835,179	418	98.47	95	56.16	52.52
AGRI18	SOIL	Slurry	2019	148,039	114,264	112,144	75,926	31,706,195	418	98.34	94.63	56.31	51.29
AGRI19	SOIL	Slurry	2019	142,653	109,653	107,513	77,644	32,388,736	417	98.33	94.7	57.14	54.43
AGRI28	SOIL	Slurry	2019	146,670	111,671	109,588	77,861	32,441,742	417	98.22	94.42	56.74	53.09
AGRI29	SOIL	Slurry	2019	137,674	106,545	104,591	77,403	32,343,491	418	98.39	94.83	56.49	56.22
AGRI9	SOIL	Slurry	2019	132,888	97,124	94,929	68,004	28,344,463	417	98.2	94.28	56.3	51.17
CF22.1	SOIL	Slurry	2020	100,944	92,791	91,339	64,446	26,964,190	418	98.4	94.74	55.72	63.84
CF22.2	SOIL	Slurry	2020	115,207	107,716	106,053	69,896	29,264,519	419	98.51	95.08	56.11	60.67
CF22.3	SOIL	Slurry	2020	104,128	95,382	93,874	61,748	25,763,638	417	98.39	94.83	56.11	59.3
CF22.4	SOIL	Slurry	2020	116,009	105,228	103,309	68,472	28,557,598	417	98.26	94.43	55.72	59.02
CF22.5	SOIL	Slurry	2020	115,902	106,711	105,000	67,336	28,101,743	417	98.43	94.88	55.82	58.1
CF22.6	SOIL	Slurry	2020	111,233	102,583	101,068	68,529	28,615,148	418	98.43	94.87	55.73	61.61
AGRI20	SOIL	Solid Fraction	2019	138,677	105,432	103,436	75,343	31,333,718	416	98.3	94.63	56.98	54.33
AGRI21	SOIL	Solid Fraction	2019	131,749	108,075	106,039	83,051	34,442,059	415	98.38	94.86	56.24	63.04
AGRI30	SOIL	Solid Fraction	2019	136,802	103,894	101,854	69,720	29,079,290	417	98.28	94.49	56.42	50.96
AGRI31	SOIL	Solid Fraction	2019	142,647	108,352	106,233	75,902	31,640,290	417	98.21	94.38	56.9	53.21
AGRI7	SOIL	Solid Fraction	2019	145,557	111,889	109,661	74,318	31,109,373	419	98.34	94.68	56.35	51.06
AGRI8	SOIL	Solid Fraction	2019	136,563	105,090	103,195	74,487	31,083,065	417	98.39	94.82	56.47	54.54
CF24.1	SOIL	Solid Fraction	2020	102,240	93,763	92,227	60,768	25,372,528	418	98.43	94.8	55.67	59.44
CF24.2	SOIL	Solid Fraction	2020	108,112	101,424	100,044	65,182	27,223,147	418	98.48	95	56.16	60.29
CF24.3	SOIL	Solid Fraction	2020	116,172	108,572	106,931	68,810	28,728,464	418	98.47	94.97	55.96	59.23
CF24.4	SOIL	Solid Fraction	2020	104,490	95,223	93,692	69,313	28,923,430	417	98.35	94.67	55.4	66.33
CF24.5	SOIL	Solid Fraction	2020	110,024	103,983	102,620	67,632	28,227,398	417	98.5	94.97	55.28	61.47
CF24.6	SOIL	Solid Fraction	2020	118,386	96,320	93,843	67,634	28,250,445	418	97.7	93.03	56.24	57.13

Supplementary Table ST5. Annotation statistics.

	# of Taxa	% Annotation
Kingdom	2	99.9%
Phylum	67	98.6%
Class	165	96.5%
Order	388	90.1%
Family	557	77.8%
Genus	1500	52.3%
Species	1576	8.6%

Supplementary Table ST6. Detection and quantification limits, and absolute recoveries (%) of the analysed antibiotics.

Matrix	Antibiotics															
	Lincomycin				Tetracycline				Doxycycline				Oxytetracycline			
	LOD	LOQ	%Rabs Lv 1*	%Rabs Lv 2*	LOD	LOQ	%Rabs Lv 1*	%Rabs Lv 2*	LOD	LOQ	%Rabs Lv 1*	%Rabs Lv 2*	LOD	LOQ	%Rabs Lv 1*	%Rabs Lv 2*
Fertiliser	2.4	5.5	40±8	-	2.0	3.1	53±1	-	1.5	1.8	51±21	-	2.3	3.1	71±3	-
Corn (grain)	4.3	5.7	67±5	75±2	5.3	6.7	48±5	55±10	7.7	8.0	73±14	38±4	4.3	15.0	75±3	84±4
Soil**	1.4	2.3	15±2	15±4	4.0	16.2	46±7	40±8	8.2	16.3	34±4	34±8	2.6	7.2	61±2	59±1

*Fertiliser – Spike Lv 1: 100 ng/g w.w, *Corn – Spike Lv 1: 50 ng/g w.w and spike Lv 2: 5 ng/g w.w and *Soil – Spike Lv 1: 172 ng/g w.w and spike Lv 2: 46 ng/g w.w.
**Soil values were extrapolated from dry weight values using %humidity of the samples (14%±3).

Supplementary Table ST7. ARG loads in corn and leaves samples Values in italic were below quantification limit and 0 were below detection limit.

		Total loads (copies/g of tissue). Mean±SD (number of positive samples)					
	n	*sulI*1	*intI*1	*qnrS*1	*tet*M	bla_{TEM}	$bla_{CTX\text{-}M\text{-}32}$
Mineral (Corn 2019)	3	*<5.6E+4*	*<5.6E+4*	*0*	*<5.6E+4*	*<5.6E+4*	*0*
Mineral (Corn 2020)	3	*<5.6E+4*	*<5.6E+4*	*0*	*<5.6E+4*	*<5.6E+4*	*0*
Digested (Corn 2019)	3	*<5.6E+4*	*<5.6E+4*	*0*	*<5.6E+4*	*<5.6E+4*	*0*
Digested (Corn 2020)	3	*<5.6E+4*	*<5.6E+4*	*0*	*<5.6E+4*	*<5.6E+4*	*0*
Liquid fraction (Corn 2019)	3	*<5.6E+4*	*<5.6E+4*	*0*	*<5.6E+4*	*<5.6E+4*	*0*
Solid fraction (Corn 2019)	3	*<5.6E+4*	*<5.6E+4*	*0*	*<5.6E+4*	*<5.6E+4*	*0*
Solid fraction (Corn 2020)	3	*<5.6E+4*	*<5.6E+4*	*0*	*<5.6E+4*	*<5.6E+4*	*0*
Slurry (Corn 2019)	3	*<5.6E+4*	*<5.6E+4*	*0*	*<5.6E+4*	*<5.6E+4*	*0*
Slurry (Corn 2020)	3	*<5.6E+4*	*<5.6E+4*	*0*	*<5.6E+4*	*<5.6E+4*	*0*
Mineral (Leaves 2019)	7	2.17E+5± 1.08E+5 (7)	1.16E+5± 9.11+4 (7)	2.23E+5 (2)	*<5.6E+4*	*<5.6E+4*	2,63E+5 (1)
Digested (Leaves 2019)	7	2,60E+5± 1,22E+5 (7)	1.01E+5± 7,60E+4 (7)	1,82E+5± 1,49E+5 (3)	*<5.6E+4*	*<5.6E+4*	3,12E+5 (1)
Liquid fraction (Leaves 2019)	7	3,49E+5± 4,32E+5 (7)	2,03E+5± 3,22E+5 (7)	7.04E+5 (2)	*<5.6E+4*	*<5.6E+4*	*0*
Solid fraction (Leaves 2019)	7	2,50E+5± 1,71E+5 (7)	1,31E+5± 1,24E+5 (7)	4,50+5± 3,20E+5 (3)	*<5.6E+4*	*<5.6E+4*	1,82E+5 (2)
Slurry (Leaves 2019)	7	4,01+5± 2,52+5 (7)	1,80E+5± 1,41E+5 (7)	4,14E+5± 4,59E+5 (3)	*0*	*0*	1.89E+5 (1)

Supplementary Table ST8. Plastid fraction of sequenced samples.

		Total counts	Mitochondrial fraction	Chloroplast fraction	Plastid fraction	Average plastid fraction (%)
AGRI34	Mineral Corn	107292	0,398	0,574	0,971	85,38%
AGRI35	Slurry Corn	82675	0,285	0,451	0,736	
AGRI32	Mineral Leaves	52109	0,000	0,004	0,004	0,61%
AGRI33	Slurry Leaves	78884	0,001	0,006	0,008	
AGRI1	Mineral Soil	53597	0,000	0,002	0,002	
AGRI15	Mineral Soil	50951	0,000	0,001	0,001	
AGRI16	Mineral Soil	49918	0,000	0,001	0,001	
AGRI2	Mineral Soil	44082	0,000	0,002	0,002	
AGRI26	Mineral Soil	50746	0,000	0,001	0,002	
AGRI27	Mineral Soil	50610	0,000	0,003	0,004	
CF21.1	Mineral Soil	59402	0,001	0,002	0,002	
CF21.2	Mineral Soil	54036	0,001	0,002	0,003	
CF21.3	Mineral Soil	54711	0,000	0,004	0,005	
CF21.4	Mineral Soil	62626	0,001	0,005	0,005	
CF21.5	Mineral Soil	54629	0,000	0,001	0,002	
CF21.6	Mineral Soil	32949	0,000	0,001	0,001	
AGRI13	Digested Soil	52604	0,000	0,001	0,001	
AGRI14	Digested Soil	45364	0,000	0,001	0,001	
AGRI24	Digested Soil	53831	0,001	0,001	0,002	
AGRI25	Digested Soil	49919	0,000	0,002	0,002	
AGRI3	Digested Soil	47290	0,000	0,002	0,002	
AGRI4	Digested Soil	46116	0,000	0,003	0,003	
CF20.1	Digested Soil	54058	0,001	0,005	0,006	0,46%
CF20.2	Digested Soil	63986	0,001	0,001	0,002	
CF20.3	Digested Soil	54416	0,001	0,003	0,004	
CF20.4	Digested Soil	57652	0,000	0,005	0,006	
CF20.5	Digested Soil	57509	0,001	0,022	0,023	
CF20.6	Digested Soil	59045	0,002	0,003	0,004	
AGRI11	Liquid Fraction Soil	45642	0,000	0,001	0,001	
AGRI12	Liquid Fraction Soil	46716	0,000	0,000	0,001	
AGRI22	Liquid Fraction Soil	43162	0,000	0,001	0,001	
AGRI23	Liquid Fraction Soil	48594	0,000	0,002	0,002	
AGRI5	Liquid Fraction Soil	47317	0,000	0,004	0,004	
AGRI6	Liquid Fraction Soil	45872	0,000	0,001	0,001	
AGRI20	Solid Fraction Soil	49570	0,002	0,001	0,003	
AGRI21	Solid Fraction Soil	57751	0,001	0,001	0,002	
AGRI30	Solid Fraction Soil	44790	0,001	0,002	0,003	
AGRI31	Solid Fraction Soil	49086	0,005	0,086	0,091	
AGRI7	Solid Fraction Soil	49614	0,001	0,003	0,004	
AGRI8	Solid Fraction Soil	50842	0,000	0,001	0,001	
CF24-1	Solid Fraction Soil	43545	0,001	0,001	0,001	

Paper IV: Use of soil-aquifer treatment to efficiently remove microbial pathogens and antibiotic resistance genes from treated wastewaters

Claudia Sanz[1], Marta Casado[1], Lurdes Martinez-Landa[2,3], Cristina Valhondo[1,2,4], Stefano Amalfitano[5], Francesca Di Pippo[5], Caterina Levantesi[5], Jesús Carrera[1,2], Benjamin Piña[1]

1) IDAEA-CSIC, Jordi Girona, 18. E-08034, Barcelona, Spain
2) Associated Unit: Hydrogeology Group (UPC-CSIC)
3) Dept. of Civil and Environmental Engineering. Universitat Politècnica de Catalunya, Barcelona, Spain
4) Geosciences Montpellier, Université de Montpellier, CNRS, Montpellier, France
5) Water Research Institute, National Research Council of Italy (IRSA-CNR), Monterotondo, Rome, 00015, Italy

Supporting Figures

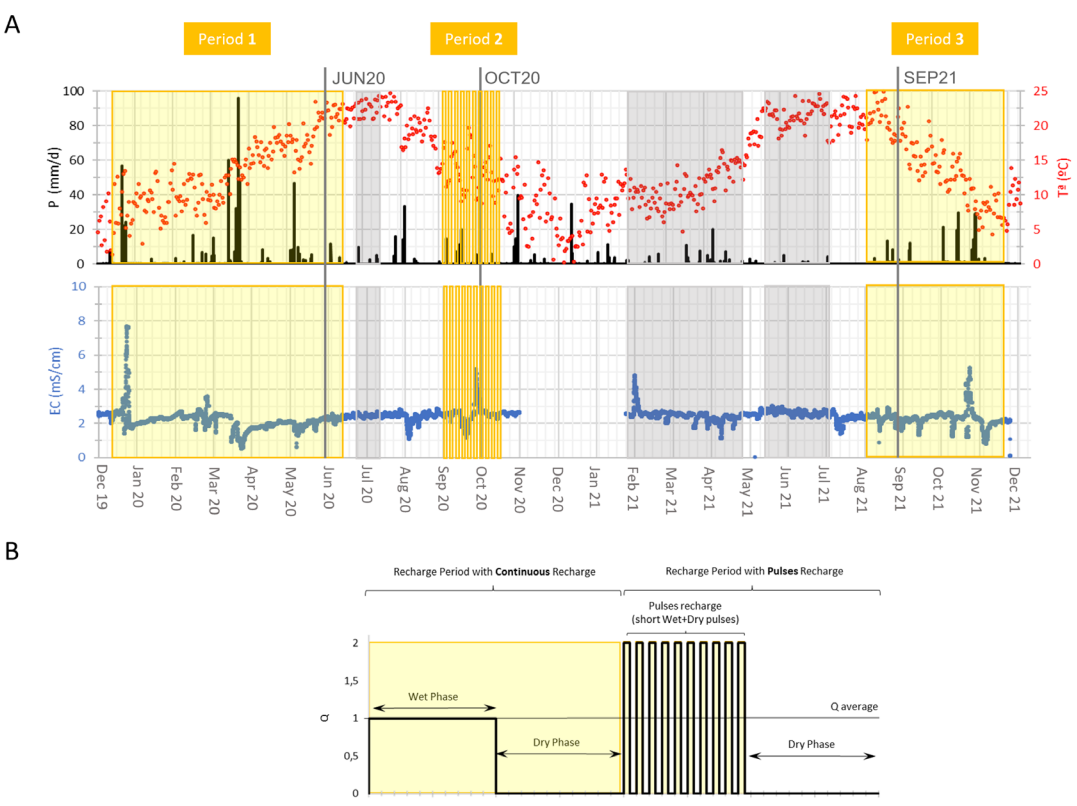

Supplementary Figure SF1. Cumulative precipitation and temperature at the experimental site and SEC´s electrical conductivity (EC) are shown in A. Recharge period lenghts are indicated using solid yellow rectangles for continuous recharge and stripped yellow rectangles for pulse recharge. Gray boxes indicate other continuous recharge periods that took place but were not sampled in this study. The start of the sampling campaigns are marked as a vertical gray line. B displays an scheme of the Recharge Management specifying the phases involved in a continuous and pulse recharge respectively for a better understanding of Supplementary Table ST2.

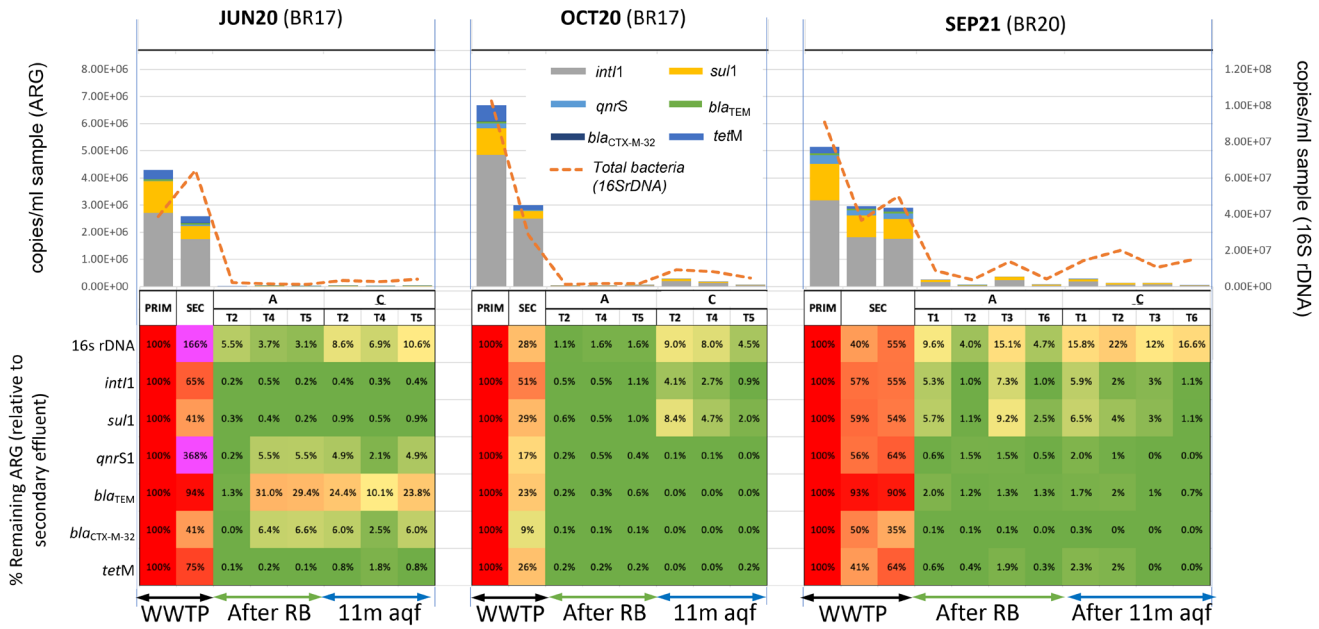

Supplementary Figure SF2. Remaining ARG loads relative to SEC for the analysed samples

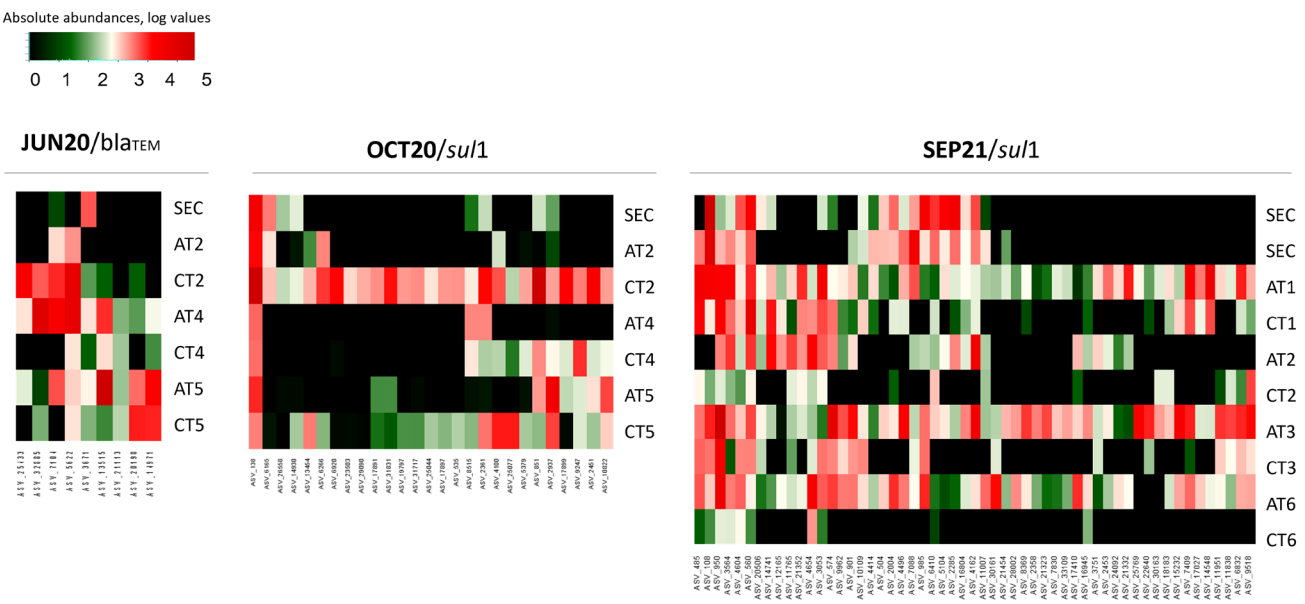

Supplementary Figure SF3. Heatmaps representing absolute abundances (copies per ml of sample, log values) of ASVs significantly correlated with the prevalence of blaTEM in JUN20 (left) or sul1 in OCT20 and SEP21 (middle and left panels, respectively) recharge periods. Each column corresponds to a single ASV, and abundances are color coded, from black (absence) to red (more than 106 copies/ml, see the scale at the bottom). Note that abundance values of the same ASVs in SEC samples is included at the top row(s) of the plot, although these figures were not included in the regression (black sectors in the graph indicate undetected ASVs).

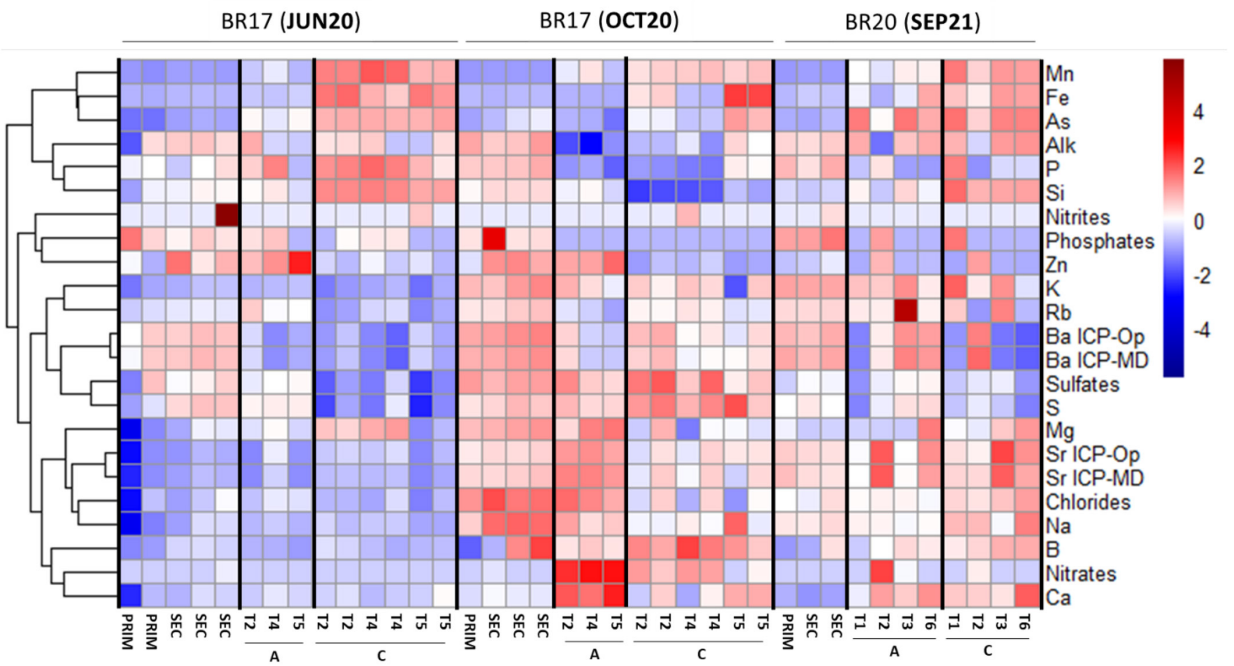

Supplementary Figure SF4. Heatmap of the quantified physico-chemical parameters in the studied samples

Supporting Tables

Supplementary Table ST1. Seasonal average routine physico-chemical parameters measured at the WWTP effluent (SEC) from 2018 to 2021. BOD5 stands for Biochemical Oxygen Demand measured at 5 days, COD stands for Chemical Oxygen Demand, SS stands for Suspended Solids, and COND stands for Electrical Conductivity.

		BOD5	COD	SS	pH	COND	N. Kjeldahl	[NH 4] +	NO2−	NO3-	Total N	Total P
		mg O2/l	mg O2/L	mg/l	ut. pH	µS/cm	mg N/l	mg N-NH4/L	mg N-NO2/L	mg N-NO3/L	mg N/L	mg P/L
2018	jan - march	13,3	76,7	19,7	7,8	3931,0	59,9	51,7	0,1	0,2	60,2	2,8
	apr - jun	13,7	79,7	19,3	7,8	2695,3	51,6	44,0	0,1	0,1	51,8	3,8
	jul - sept	13,7	88,7	19,3	7,8	3025,3	70,3	58,4	0,1	0,1	70,5	4,9
	sept - dic	9,3	55,7	9,3	7,8	2422,3	33,9	29,3	1,4	0,8	36,0	3,0
2019	jan - march	10,0	62,7	14,7	7,9	2709,3	53,9	51,5	0,1	0,2	54,1	3,6
	apr - jun	12,3	65,3	12,7	7,9	2691,0	49,3	42,8	1,7	0,5	51,6	3,1
	jul - sept	16,3	94,7	19,3	7,9	2520,7	59,8	53,9	0,1	0,2	60,1	3,9
	sept - dic	13,0	63,3	14,3	7,9	2637,0	44,3	40,5	0,1	0,1	44,5	3,6
2020	jan - march	12,7	65,0	15,3	7,8	2366,0	42,8	39,6	0,2	0,3	43,3	3,8
	apr - jun	12,0	60,7	10,3	7,8	1866,3	31,3	25,3	0,1	0,2	31,6	3,1
	jul - sept	15,0	90,3	19,0	7,9	2472,0	55,9	48,5	0,0	0,2	56,1	3,1
	sept - dic	12,0	74,3	12,3	7,9	2787,0	45,4	40,3	0,5	0,4	46,3	4,2
2021	jan - march	13,7	71,7	12,3	7,9	2816,3	41,3	36,6	1,0	0,8	43,2	3,3
	apr - jun	14,7	64,7	15,7	7,8	2475,7	50,6	46,6	0,7	0,7	52,0	4,4
	jul - sept	15,7	72,7	17,0	8,0	2335,3	61,5	53,9	0,7	0,6	62,8	4,7
	sept - dic	11,7	54,3	7,7	8,0	2130,0	36,6	31,9	2,8	3,5	42,8	3,5
	average	13,1	71,3	14,9	7,9	2617,5	49,3	43,4	0,6	0,5	50,4	3,7

Supplementary Table ST2. Specification of the recharge conditions during the recharge periods 1, 2 and 3 and the three corresponding samplings.

Set of SATs	Recharge period	Start Wet Phase	End Wet Phase – Start Dry Phase	End Dry Phase	Total Wet Phase (d)	Total Dry Pahse (d)	Total Recharging Time (d)	Total Recharged Volume (m^3)	Q Average (m/d)	Sampling			
										ID	Total Recharging Time (d)	Total Recharged Volume (m^3)	Type of allocated inflow
BR17	Period 1	11/01/20	20/07/20	20/07/20	180	11	191	191,1	0,30	JUN20	151	160	Continuous
BR17	Period 2	29/09/20	11/11/20	17/02/21	43	98	141	63,4	0,42	OCT20	20	29	Pulses
BR20	Period 3	26/08/21	09/12/21	03/03/22	105	84	189	151,2	0,41	SEP21	11	15,84	Continuous

Supplementary Table ST3. Sampling dates were established taking into account hydraulic retention in the WWTP and residence times along the systems.

Set of SATs	Recharge period	Sampling	Sample name	Date
BR17	Period 1	JUN20	PRIM	11/06/20
BR17	Period 1	JUN20	SEC	12/06/20
BR17	Period 1	JUN20	AT2	14/06/20
BR17	Period 1	JUN20	AT4	14/06/20
BR17	Period 1	JUN20	AT5	14/06/20
BR17	Period 1	JUN20	CT2	18/06/20 + 25/06/20
BR17	Period 1	JUN20	CT4	18/06/20 + 25/06/20
BR17	Period 1	JUN20	CT5	18/06/20 + 25/06/20
BR17	Period 2	OCT20	PRIM	19/10/20
BR17	Period 2	OCT20	SEC	19/10/20
BR17	Period 2	OCT20	AT2	21/10/20
BR17	Period 2	OCT20	AT4	21/10/20
BR17	Period 2	OCT20	AT5	21/10/20
BR17	Period 2	OCT20	CT2	24/10/20 + 29/10/20
BR17	Period 2	OCT20	CT4	24/10/20 + 29/10/20
BR17	Period 2	OCT20	CT5	24/10/20 + 29/10/20
BR20	Period 3	SEP21	PRIM	06/09/21
BR20	Period 3	SEP21	SEC (1)	06/09/21
BR20	Period 3	SEP21	SEC (2)	08/09/21
BR20	Period 3	SEP21	AT1	09/9/21
BR20	Period 3	SEP21	AT2	09/9/21
BR20	Period 3	SEP21	AT3	09/9/21
BR20	Period 3	SEP21	AT6	09/9/21
BR20	Period 3	SEP21	CT1	14/09/21
BR20	Period 3	SEP21	CT2	14/09/21
BR20	Period 3	SEP21	CT3	14/09/21
BR20	Period 3	SEP21	CT6	14/09/21

Supplementary Table ST4. Specification of the size fraction analysed in the 69 processed samples.

Set of SATs	Sample name	Size fraction	Sequencing ID
BR17 (**JUN20**)	PRIM	Co	PAL36
		F	PAL37
		UF	PAL38
	SEC	Co	PAL39
		F	PAL40
		UF	PAL41
	T2A	F	PAL43
		UF	PAL42
	T2C	Co	PAL50
		F	PAL51
	T4A	Co	PAL44
		F	PAL45
		UF	PAL46
	T4C	Co	PAL52
		F	PAL53
	T5A	Co	PAL47
		F	PAL48
		UF	PAL49
	T5C	Co	PAL54
		F	PAL55

Set of SATs	Sample name	Size fraction	Sequencing ID
BR17 (**OCT20**)	PRIM	F	OCTINFposo
		UF	OCTPRIN3
	SEC	Co	OCTPRIN0.2
		F	OCTINF3
		UF	OCTINF0.2
	T2A	F	OCTT2A2
	T2C	Co	OCTT2C2poso
		F	OCTT2C23
		UF	OCTT2C20.2
	T4A	F	OCTT4A2
	T4C	Co	OCTT4C2poso
		F	OCTT4C23
		UF	OCTT4C20.2
	T5A	F	OCTT5A2
	T5C	Co	OCTT5C2poso
		F	OCTT5C23

Set of SATs	Sample name	Size fraction	Sequencing ID
BR21 (**SEP21**)	PRIM	Co	PRIN.P
		F	PRIN.3
		UF	PRIN.02
	SEC1	Co	INF06.P
		F	INF08.P
		UF	INF06.3
	SEC2	Co	INF08.3
		F	INF08.02
		UF	INF06.02
	T1A	Co	T1A2.P
		F	T1A2.3
		UF	T1A2.02
	T1C	Co	T3A2.P
		F	T3A2.3
		UF	T3A2.02
	T2A	Co	T1C2.P
		F	T1C2.3
		UF	T1C2.02
	T2C	Co	T3C2.P
		F	T3C2.3
		UF	T3C2.02
	T3A	Co	T2A2.P
		F	T2A2.3
		UF	T2A2.02
	T3C	Co	T6A2.P
		F	T6A2.3
		UF	T6A2.02
	T6A	Co	T2C2.P
		F	T2C2.3
		UF	T2C2.02
	T6C	Co	T6C2.P
		F	T6C2.3
		UF	T6C2.02

Supplementary Table ST5. Plasmid, primers and LOQs used for detection and quantifications of antibiotic resistance genes in samples.

Target gene	Plasmid	LOQ (gene copies/ul)	Primers	Sequence (5'-> 3')	Amplicon size (bp)	Tm(ºC)	Reference
16S rDNA	pNORM1 (3324 bp)	1000	331F	TCCTACGGGAGGCAGCAGT	195	60	Bräuer et al., 2011
			518R	ATTACCGCGGCTGCTGG			
*intI*1		100	intI1LC5	GATCGGTCGAATGCGTGT	196	60	Barraud et al., 2010
			intI1LC1	GCCTTGATGTTACCCGAGAG			
*sul*1		100	sul1-FW	CGCACCGGAAACATCGCTGCAC	162	60	Pei et al., 2006
			sul1-RV	TGAAGTTCCGCCGCAAGGCTCG			
*qnrS*1		100	qnrSrtF11	GACGTGCTAACTTGCGTGAT	118	60	Marti & Balcázar, 2013
			qnrSrtR 11	TGGCATTGTTGGAAACTTG			
*tet*M	pUC19 (2882 bp)	1000	tetMF	GCAATTCTACTGATTTCTGC	186	60	Tamminen & Karkman, 2011
			tetMR	CTGTTTGATTACAATTTCCGC			
*mec*A	pUC19 (2871 bp)	1000	mecAF	AAAAAGATGGCAAAGATATTCAA	185	63	Szczepanowski et al., 2009
			mecAR	TTCTTCGTTACTCATGCCATACA			
bla_{TEM}	pNORM1 (3324 bp)	1000	blaTEM-F	TTCCTGTTTTTGCTCACCCAG	113	60	Di Cesare et al., 2016
			blaTEM -R	CTCAAGGATCTTACCGCTGTTG			
$bla_{CTX\text{-}M\text{-}32}$		100	ctx-m-32-FW	CGTCACGCTGTTGTTAGGAA	156	60	Hembach et al., 2017
			ctx -m-32-R	CGCTCATCAGCACGATAAAG			
$bla_{OXA\text{-}58}$	pUC19 (2838 bp)	1000	OXA58F	GCAATTGCCTTTTAAACCTGA	152	63	Laht et al., 2014
			OXA58R	CTGCCTTTTCAACAAAACCC			

References

O. Barraud, M.C. Baclet, F. Denis, M.C. Ploy, J. Antimicrob. Chemother. 65 (2010) 1642–1645. doi:10.1093/jac/dkq167.

S.L. Bräuer, C. Adams, K. Kranzler, D. Murphy, M. Xu, P. Zuber, H.M. Simon, A.M. Bapsta, B.M. Tebo, Environ. Microbiol. 13 (2011) 589–603. doi:10.1111/j.1462-2920.2010.02360.x.

A. Di Cesare, C. Losasso, L. Barco, E.M. Eckert, D. Conficoni, G. Sarasini, G. Corno, A. Ricci, Sci. Rep. 6 (2016) 1–9. doi:10.1038/srep28759.

N. Hembach, F. Schmid, J. Alexander, C. Hiller, E.T. Rogall, T. Schwartz, Front. Microbiol. 8 (2017) 1–11. doi:10.3389/fmicb.2017.01282.

M. Laht, A. Karkman, V. Voolaid, C. Ritz, T. Tenson, M. Virta, V. Kisand, PLoS One. 9 (2014) 1–8. doi:10.1371/journal.pone.0103705.

E. Martí, J.L. Balcázar, Appl. Environ. Microbiol. 79 (2013) 1743–1745.

R. Pei, S.C. Kim, K.H. Carlson, A. Pruden, Water Res. 40 (2006) 2427–2435. doi:10.1016/j.watres.2006.04.017

R. Szczepanowski, B. Linke, I. Krahn, K.H. Gartemann, T. Gützkow, W. Eichler, A. Pühler, A. Schlüter, Microbiology. 155 (2009) 2306–2319. doi:10.1099/mic.0.028233-0.

M. Tamminen, A. Karkman, Environmental Science & Technology, 45 (2011) 386-391.doi:10.1021/es102725n.

Supplementary Table ST6 Total reads and quality control parameters for the analysed samples.

Recharge period	Sample Name	Total_reads	Combined_reads	Uncombined_reads	Percent_combined(%)	Combined_base(bp)	Min_len(bp)	Max_len(bp)	Avg_len(bp)
BR17-PR7	J20_PRI_Co	145306	129624	15682	89.21	54338238	46	441	419
BR17-PR7	J20_PRI_F	148422	131590	16832	88.66	54785547	49	441	416
BR17-PR7	J20_PRI_UF	146786	132679	14107	90.39	55806475	97	441	421
BR17-PR7	J20_SEC_Co	137958	122861	15097	89.06	51527879	111	441	419
BR17-PR7	J20_SEC_F	136250	121889	14361	89.46	50946450	233	441	418
BR17-PR7	J20_SEC_UF	144149	126271	17878	87.6	52567125	67	441	416
BR17-PR7	J20_T2A_F	144582	130995	13587	90.6	53783838	62	441	411
BR17-PR7	J20_T2A_UF	147691	130834	16857	88.59	54445381	44	441	416
BR17-PR7	J20_T2C_Co	134618	119538	15080	88.8	49698509	109	441	416
BR17-PR7	J20_T2C_F	136540	121856	14684	89.25	50543707	45	441	415
BR17-PR7	J20_T4A_Co	145375	129994	15381	89.42	53866921	53	441	414
BR17-PR7	J20_T4A_F	146259	129375	16884	88.46	53663648	57	441	415
BR17-PR7	J20_T4A_UF	139882	126409	13473	90.37	52748472	213	444	417
BR17-PR7	J20_T4C_Co	136077	120930	15147	88.87	50395534	107	441	417
BR17-PR7	J20_T4C_F	143840	128201	15639	89.13	53411165	63	441	417
BR17-PR7	J20_T5A_Co	146957	127986	18971	87.09	53240759	37	443	416
BR17-PR7	J20_T5A_F	149789	128639	21150	85.88	53256062	46	441	414
BR17-PR7	J20_T5A_UF	137977	121925	16052	88.37	50705325	48	441	416
BR17-PR7	J20_T5C_Co	135787	121449	14338	89.44	50652145	120	441	417
BR17-PR7	J20_T5C_F	149653	133911	15742	89.48	55588925	122	442	415
BR17-PR9	O20_PRI_F	125728	87684	38044	69.74	36659740	65	442	418
BR17-PR9	O20_PRI_UF	130247	103636	26611	79.57	42764700	123	442	412
BR17-PR9	O20_SEC_Co	140169	95957	44212	68.46	40259684	249	441	419
BR17-PR9	O20_SEC_F	143388	96151	47237	67.06	40209247	65	441	418
BR17-PR9	O20_SEC_UF	123702	86056	37646	69.57	35952235	85	442	417
BR17-PR9	O20_T2A_F	122890	93926	28964	76.43	38989103	65	442	415
BR17-PR9	O20_T2C_Co	114996	85724	29272	74.55	35680103	78	442	416
BR17-PR9	O20_T2C_F	110223	79226	30997	71.88	33227042	65	442	419
BR17-PR9	O20_T2C_UF	129579	92568	37011	71.44	39055963	65	442	421
BR17-PR9	O20_T4A_F	147605	114231	33374	77.39	47086810	66	441	412
BR17-PR9	O20_T4C_Co	147259	104244	43015	70.79	43237867	65	442	414
BR17-PR9	O20_T4C_F	110513	74069	36444	67.02	30920669	154	442	417
BR17-PR9	O20_T4C_UF	125413	85940	39473	68.53	35956196	65	442	418
BR17-PR9	O20_T5A_F	138360	103716	34644	74.96	43219662	65	442	416
BR17-PR9	O20_T5C_Co	125173	97460	27713	77.86	40480086	123	442	415
BR17-PR9	O20_T5C_F	143065	107933	35132	75.44	44881147	65	442	415
BR20-PR3	S21_PRIN_Co	80137	73459	6678	91.67	30656596	44	430	417
BR20-PR3	S21_PRIN_F	91003	83092	7911	91.31	34663523	116	430	417
BR20-PR3	S21_PRIN_UF	96039	88146	7893	91.78	36331179	64	430	412
BR20-PR3	S21_SEC06_Co	84436	79180	5256	93.78	32980324	44	430	417
BR20-PR3	S21_SEC06_F	89922	83552	6370	92.92	34710501	44	430	415
BR20-PR3	S21_SEC06_UF	87986	81400	6586	92.51	33839618	44	430	416
BR20-PR3	S21_SEC08_Co	98711	90259	8452	91.44	37672656	44	430	417
BR20-PR3	S21_SEC08_F	83972	77779	6193	92.62	32553161	44	430	419
BR20-PR3	S21_SEC08_UF	83052	76951	6101	92.65	32301600	47	430	420
BR20-PR3	S21_T1A_Co	97879	88950	8929	90.88	37061545	44	430	417
BR20-PR3	S21_T1A_F	90609	82441	8168	90.99	34205716	34	430	415
BR20-PR3	S21_T1A_UF	81591	75156	6435	92.11	31552562	44	430	420
BR20-PR3	S21_T1C_Co	86330	80368	5962	93.09	33804634	44	430	421
BR20-PR3	S21_T1C_F	89602	81935	7667	91.44	34207298	44	430	417
BR20-PR3	S21_T1C_UF	83431	76785	6646	92.03	32209291	44	430	419
BR20-PR3	S21_T2A_Co	99320	89767	9553	90.38	37461764	44	430	417
BR20-PR3	S21_T2A_F	86978	78595	8383	90.36	32948175	64	430	419
BR20-PR3	S21_T2A_UF	96592	86708	9884	89.77	36279455	44	430	418
BR20-PR3	S21_T2C_Co	80608	73165	7443	90.77	30496686	44	430	417
BR20-PR3	S21_T2C_F	83448	77226	6222	92.54	32113929	44	430	416
BR20-PR3	S21_T2C_UF	95989	88930	7059	92.65	37017873	44	430	416
BR20-PR3	S21_T3A_Co	94830	85191	9639	89.84	35192137	44	430	413
BR20-PR3	S21_T3A_F	83806	77341	6465	92.29	32652809	44	430	422
BR20-PR3	S21_T3A_UF	88838	83399	5439	93.88	35137062	44	430	421
BR20-PR3	S21_T3C_Co	93420	84706	8714	90.67	35440106	44	430	418
BR20-PR3	S21_T3C_F	80997	74596	6401	92.1	31059686	122	430	416
BR20-PR3	S21_T3C_UF	93133	86605	6528	92.99	36229747	64	430	418
BR20-PR3	S21_T6A_Co	86085	78706	7379	91.43	32802796	44	430	417
BR20-PR3	S21_T6A_F	89297	82955	6342	92.9	34316180	49	430	414
BR20-PR3	S21_T6A_UF	85582	80508	5074	94.07	34105528	44	430	424
BR20-PR3	S21_T6C_Co	98000	88743	9257	90.55	36923433	59	430	416
BR20-PR3	S21_T6C_F	93895	83864	10031	89.32	35088873	44	430	418
BR20-PR3	S21_T6C_UF	81059	74806	6253	92.29	31228375	64	430	417

Supplementary Table ST7. Total count distribution.

Total Count Distribution	
Archaea	328914
Bacteria	3580051
Chloroplast	6352
Mitochondria	1030

Supplementary Table ST8. Annotation statistics.

	# of Taxa	% Annotation
Kingdom	2	100%
Phylum	76	98%
Class	176	96%
Order	410	88%
Family	595	71%
Genus	1604	49%
Species	1633	13%

Supplementary Table ST9. Presence(+)/absence(-) of pathogenic enterobacteria (Salmonella spp) and opportunistic pathogens (*Legionella* spp and *Pseudomonas aeruginosa*) assessed by LAMP-PCR in samples from JUN20 and OCT20, respectively.

	Salmonella spp.	*Legionella spp.*	*Pseudomonas aeruginosa*
SEC	--	++	+ -
AT2	--	++	++
AT4	--	++	--
AT5	--	++	++
CT2	--	++	+ -
CT4	--	++	+ -
CT5	--	++	--

Supplementary Table ST10. Metabolic groups reduced and increased by the SATs. Orange color stands for positive, white for negative and yellow for conflict (present in different lists depending on the campaign).

	Reduced by treatment		
Metabolic group	**Jun-20**	**Oct-20**	**Sep-21**
aerobic chemoheterotrophy			
aromatic compound degradation			
aromatic hydrocarbon degradation			
animal parasites or symbionts			
dark hydrogen oxidation			
dark sulfide oxidation			
fermentation			
fumarate respiration			
human pathogens			
manganese oxidation			
nitrate denitrification			
nitrate reduction			
nitrate respiration			
nitrogen fixation			
plant pathogen			
plastic degradation			
ureolysis			

	Increased by treatment		
Metabolic group	**Jun-20**	**Oct-20**	**Sep-21**
anammox			
aerobic ammonia oxidation			
aerobic nitrite oxidation			
anoxygenic photoautotrophy			
aromatic compound degradation			
aromatic hydrocarbon degradation			
arsenate detoxification			
arsenate respiration			
arsenite oxidation			
cellulolysis			
chitinolysis			
chlorate reducers			
dark hydrogen oxidation			
dark iron oxidation			
dark oxidation of sulfur compounds			
dark sulfite oxidation			
dark sulfur oxidation			
dark thiosulfate oxidation			
denitrification			
human gut			
invertebrate parasites			
iron respiration			
knallgas bacteria			
ligninolysis			
manganese oxidation			
manganese respiration			
methanogenesis			
methanol oxidation			
methanotrophy			
methylotrophy			
nitrate ammonification			
nitrate respiration			
nitrite ammonification			
nitrite respiration			
nitrous oxide denitrification			
oil bioremediation			
plant pathogen			
plastic degradation			
photoheterotrophy			
plastic degradation			
reductive acetogenesis			
sulfate respiration			
sulfite respiration			
sulfur respiration			
thiosulfate respiration			
xylanolysis			

Supplementary Table ST11. Comparison of removal efficiencies across different tertiary treatments including those studied in this work.

Remaining ARG loads after treatment (% of WWTP influent)

Treatment Class	Treatment	Median	Max	Min
Conventional Treatment	Activated Sludge	3551.44%	18620.69%	0.80%
	Anaerobic-Anoxic-Oxic Tecnhology	456.44%	3033.33%	5.83%
Wetland-based Treatments	Horizontal Subsurface Flow Constructed Wetlands	45.32%	71.21%	23.85%
	Hybrid	28.70%	163.33%	4.76%
	Surface Flow Constructed Wetlands	27.31%	53.13%	16.67%
	Subsurface Flow Constructed Wetlands	20.59%	48.98%	0.87%
Advanced Oxidation	H202-UV / Peroxymonosulfate-UV / Peroxymonosulfate-Fe2+-UV	37.84%	63.10%	12.59%
	UV-Persulfate	35.52%	63.10%	7.94%
	UV/O3/Fenton/Fenton-UV	7.92%	15.85%	0.00%
	Fenton/ UV/H202	1.60%	3.16%	0.03%
	UV-A Assisted Iron-Based/UV-C Driven H2O2, Persulfate; Peroxymonosulfate	0.08%	0.10%	0.05%
Membrane-based procedures	Ultrafiltration/Nanofiltration/Reverse Osmosis	39.72%	79.43%	0.01%
	Microfiltration	0.64%	1.26%	0.01%
	Forward Osmosis Membrane	0.55%	1.00%	0.10%
	Microfiltration-Reverse Osmosis	0.55%	1.00%	0.10%
	Microfiltration-Ultrafiltration-Nanofiltration-Reverse Osmosis	0.00%	0.00%	0.00%
Barriers/aquifer	Aquifer JUN20	1.97%	24.38%	0.31%
	Aquifer OCT20	0.05%	8.45%	0.00%
	Aquifer SEP21	1.94%	6.48%	0.03%

Leiva, A.M., Piña, B., Vidal, G. (2021). Antibiotic resistance dissemination in wastewater treatment plants: a challenge for the reuse of treated wastewater in agriculture. Rev Environ Sci Bio/Technol. https://doi.org/10.1007/s11157-021-09588-8

Paper V: Detoxification of wastewater plant effluents by soil aquifer treatment methodologies

Claudia Sanz[1], Adrià Sunyer-Caldú[1], Marta Casado[1], Sylvia Mansilla[1], Lurdes Martinez-Landa[2,3], Cristina Valhondo[1,2,4], Ruben Gil-Solsona[1], Pablo Gago-Ferrero[1], Jose Portugal[1], M. Silvia Diaz-Cruz[1], Jesús Carrera[1,2], Benjamin Piña[1], Laia Navarro-Martín[1]

1) IDAEA-CSIC, Jordi Girona, 18. E-08034, Barcelona, Spain

2) Associated Unit: Hydrogeology Group (UPC-CSIC)

3) Dept. of Civil and Environmental Engineering. Universitat Politècnica de Catalunya, Barcelona, Spain

4) Geosciences Montpellier, Université de Montpellier, CNRS, Montpellier, France

5) Water Research Institute, National Research Council of Italy (IRSA-CNR), Monterotondo, Rome, 00015, Italy

Supplementary Materials and Methods

Briefly, the SMILES of the confirmed chemicals were obtained from a Chemical Identifier Resolver database (CADD Group Chemoinformatics Tools and User Services, 2022). Those SMILES were uploaded to PaDEL-Descriptor software v. 2.21 (Yap, 2011), which generated more than 1400 descriptors of each structure. The same descriptors were generated for two training sets (positive and negative ionization) of 3139 and 1286 compounds, respectively, of known ionization efficiency (logIE) measured under different conditions (e.g. pH or solvents of the mobile phase, instrument, ionization technique, etc). The most relevant descriptors were retrieved from another study (Liigand et al., 2020), including 450 in positive and 145 in negative ionization, as well as 5 empirical eluent descriptors (viscosity, surface tension, polarity index, pH, and NH4+ content), which were used to create training and results sets. Then, a machine learning algorithm (random forest regression) was used (R package RRF) (Deng & Runger, 2012) to develop different models for the prediction of logIE in positive and negative ionization modes (Liigand et al., 2020), and it was applied to the compounds found in the samples. As the model output was in universal ionization efficiency values, calibration curves were used to transform the predicted logIE values to instrumentation specific quantitative values, accounting for specific matrix effect reduction in each sample type, which was compensated using labelled internal standards. These calibration curves were analysed in the same conditions as the samples. Finally, concentration of each compound in the extract was obtained with the application of Equation 1:

$$\text{Concentration} = \frac{Area\ in\ Sample\ (A.U.)}{Slope\ CC\ (1/ng{\cdot}mL^{-1}){*}Predicted\ \log IE\ (A.U.)} \frac{Area\ IS\ Sample\ (A.U.)}{Area\ IS\ CC\ (A.U.)}$$

Where Area is the response of the instrument for a given compound (the one to be semi-quantified), slope CC is the slope of the semi-quantification calibration curve (created by correlating the predicted logIE for all the chemicals included in the calibration curve and observed area of these chemicals in the curve for a given concentration of 1 ng/mL), the Predicted logIE is the ionization efficiency, Area IS Samples the area of the internal standard in the samples, and Area IS CC the area of the internal standard in the calibration curve. The units of the calculated concentration are the same used for the calibration curves (ng/mL).

Supporting Figures

A

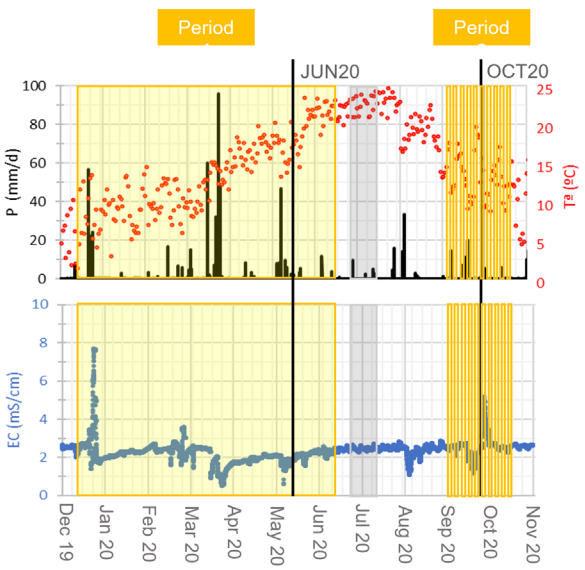

B

Set of SATs	Recharge period	Sampling	Sample name	Date
BR17	Period 1	JUN20	PRIM	11/06/2020
BR17	Period 1	JUN20	SEC	12/06/2020
BR17	Period 1	JUN20	AT2	14/06/2020
BR17	Period 1	JUN20	AT4	14/06/2020
BR17	Period 1	JUN20	AT5	14/06/2020
BR17	Period 1	JUN20	CT2	18/06/2020 + 25/06/2020
BR17	Period 1	JUN20	CT4	18/06/2020 + 25/06/2020
BR17	Period 1	JUN20	CT5	18/06/2020 + 25/06/2020
BR17	Period 2	OCT20	PRIM	19/10/2020
BR17	Period 2	OCT20	SEC	19/10/2020
BR17	Period 2	OCT20	AT2	21/20/2020
BR17	Period 2	OCT20	AT4	21/20/2020
BR17	Period 2	OCT20	AT5	21/20/2020
BR17	Period 2	OCT20	CT2	24/10/2020 + 29/10/2020
BR17	Period 2	OCT20	CT4	24/10/2020 + 29/10/2020
BR17	Period 2	OCT20	CT5	24/10/2020 + 29/10/2020

Supplementary Figure SF1. Cumulative precipitation and temperature at the experimental site and SEC´s electrical conductivity are shown in **A)** Recharge period lenghts are indicated using solid yellow rectangles for continuous recharge and stripped yellow rectangles for pulse recharge. Gray boxes indicate other continuous recharge periods that took place but were not sampled in this study. The start of the sampling campaigns are marked as a vertical gray line. **B)** Specifies the sampling dates for the sampled recharge periods.

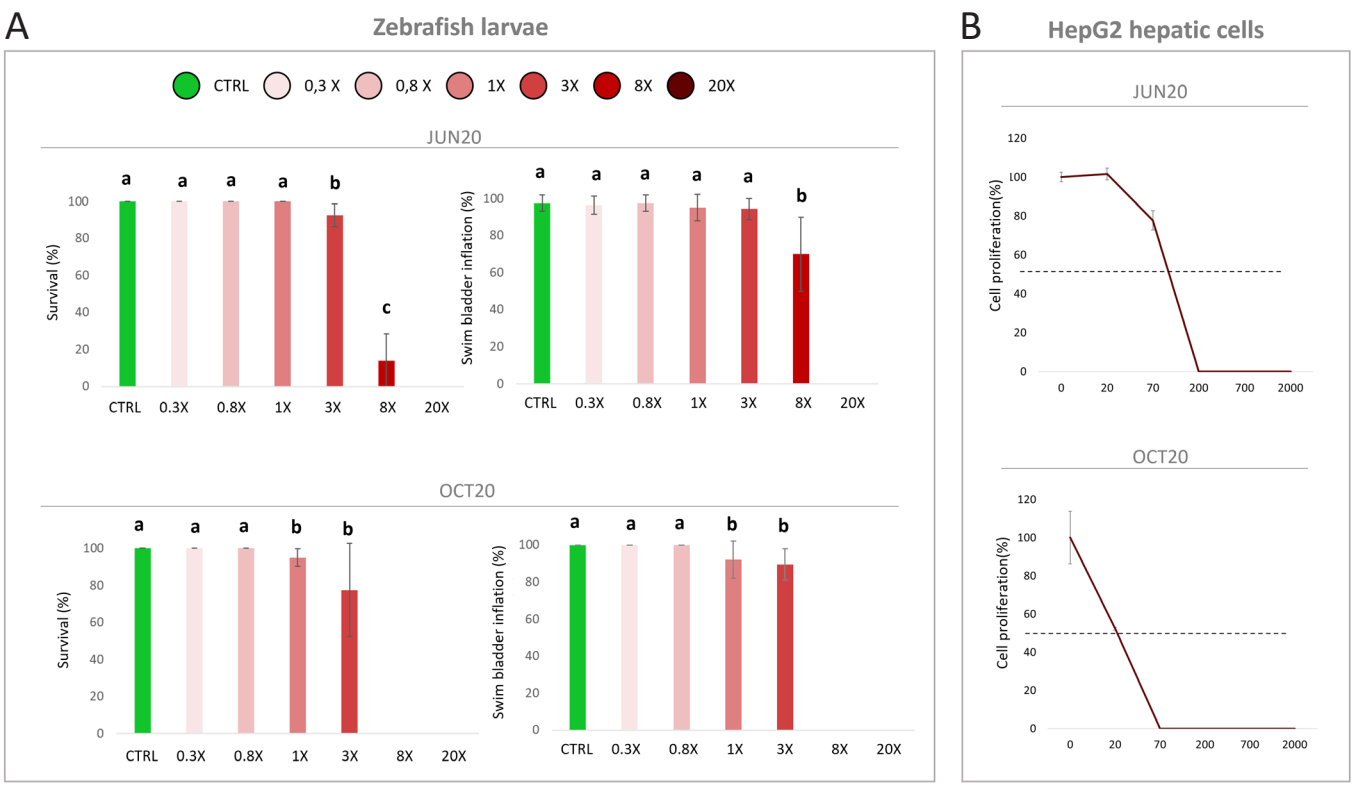

Supplementary Figure SF2. Results of PRIM exposure in both biological models. Figure **A** shows the survival and swim bladder inflation rate in percentage for the dose-response assay on zebrafish larvae for JUN20 and OCT20 campaigns. Figure **B** shows the results of the AlamarBlue cell proliferation assay for PRIM sample in percentage on HepG2 hepatic cells for JUN20 and OCT20 campaigns. Dashed lines in cell proliferation graphs mark the IC_{50} value for each sample expressed as the volume (mL) that inhibits cell proliferation by 50% (95% confidence interval): (JUN20 PRIM: 79 ± 56 ; OCT20 PRIM: 20 ± 1). Letters on bars code for statistical differences amongst samples.

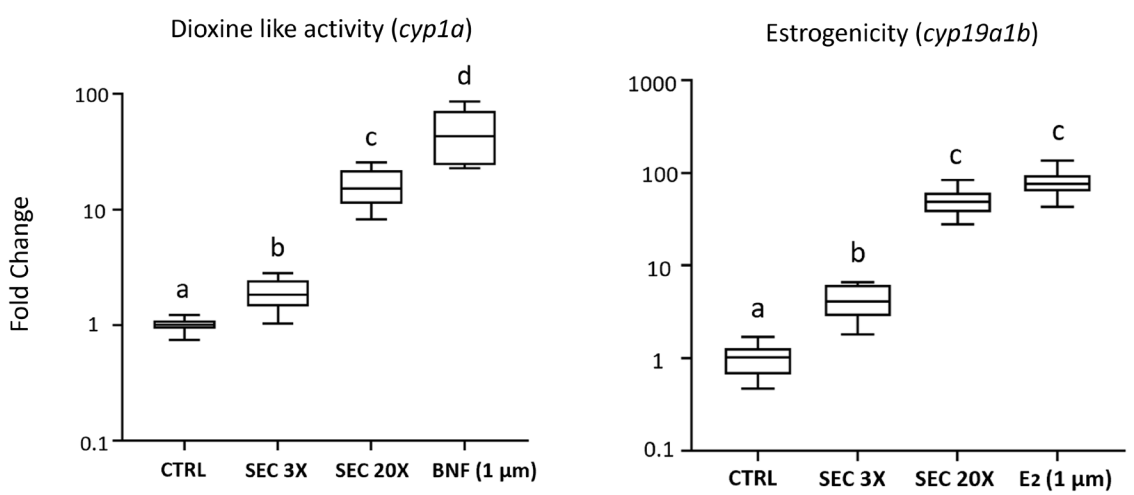

Supplementary Figure SF3. *Dioxin-like* activity biomarker (*cyp1a*) and estrogenicity biomarker (*cyp19a1b*) for the 3x and 20x SEC extracts exposure plus positive control 1 µm β-Naphthoflavone (BNF) and 1µm 17β-estradiol (E2) respectively. Note that DMSO was used as a vehicle, so included control samples (CTRL) were treated with the same concentration of DMSO (0.2%). Letters on boxplots code for statistical differences amongst samples.

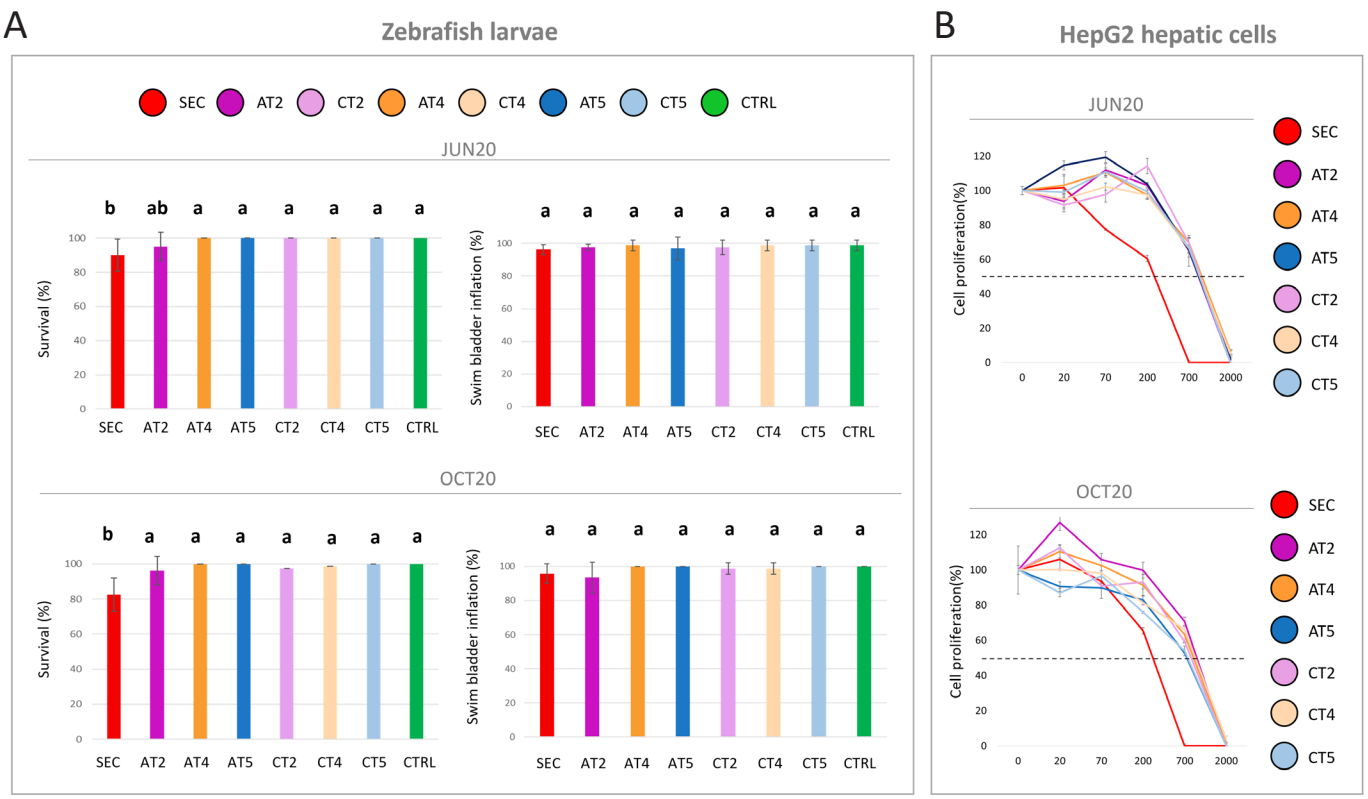

Supplementary Figure SF4. Results regarding exposure to SEC, ATs and CTs samples in both biological models. Figure **A** shows the survival and swim bladder inflation rate in percentage for the 20x exposure on zebrafish larvae for JUN20 and OCT20 campaigns. Figura **B** shows the results of the AlamarBlue cell proliferation assay for SEC, As and Cs samples on HepG2 hepatic cells for JUN20 and OCT20 campaigns. Dashed lines in cell proliferation graphs mark the IC_{50} value for each sample expressed as the volume (mL) that inhibits cell proliferation by 50% (95% confidence interval): JUN20: SEC: 204 ± 35, AT2: 757 ± 102, CT2: 723 ± 108, AT4: 828 ± 98, CT4: 842 ± 53, AT5: 715 ± 113, CT5: 776 ± 96; OCT20: SEC: 232 ± 21, AT2: 592 ± 118, CT2: 599 ± 158, AT4: 713 ± 121, CT4: 851 ± 116, AT5: 632 ± 118, CT5: 587 ± 142. Letters on bars code for statistical differences amongst samples.

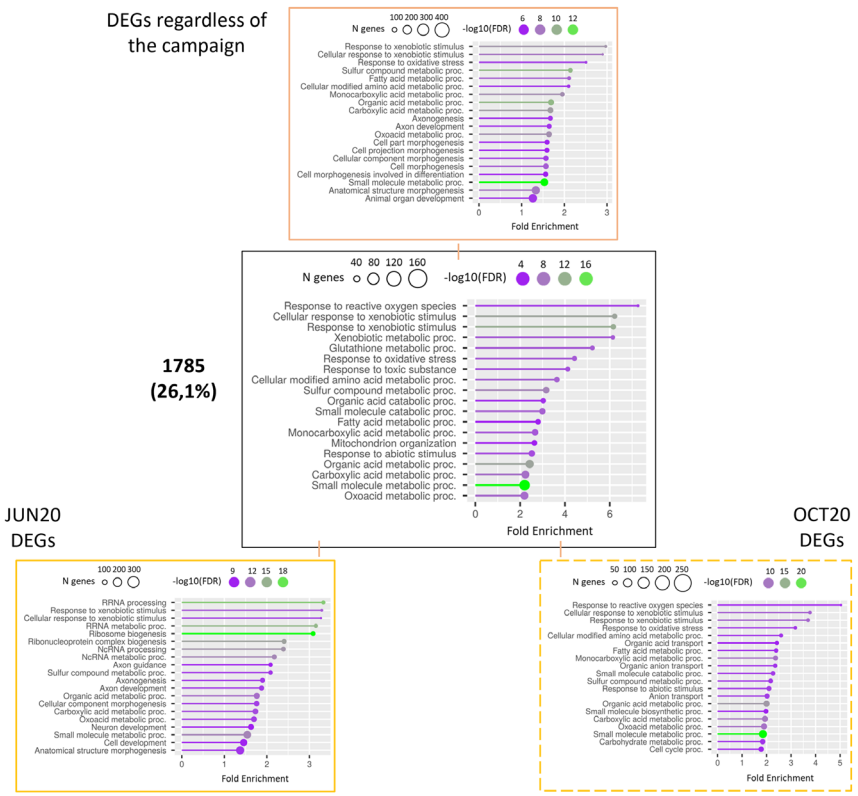

Supplementary Figure SF5. Enrichment analysis of the obtained DEGs. Figure shows the top 20 enriched pathways lollipop graphs (created with ShinyGO 0.76 (http://bioinformatics.sdstate.edu/go/)) for the three approaches and for the common genes.

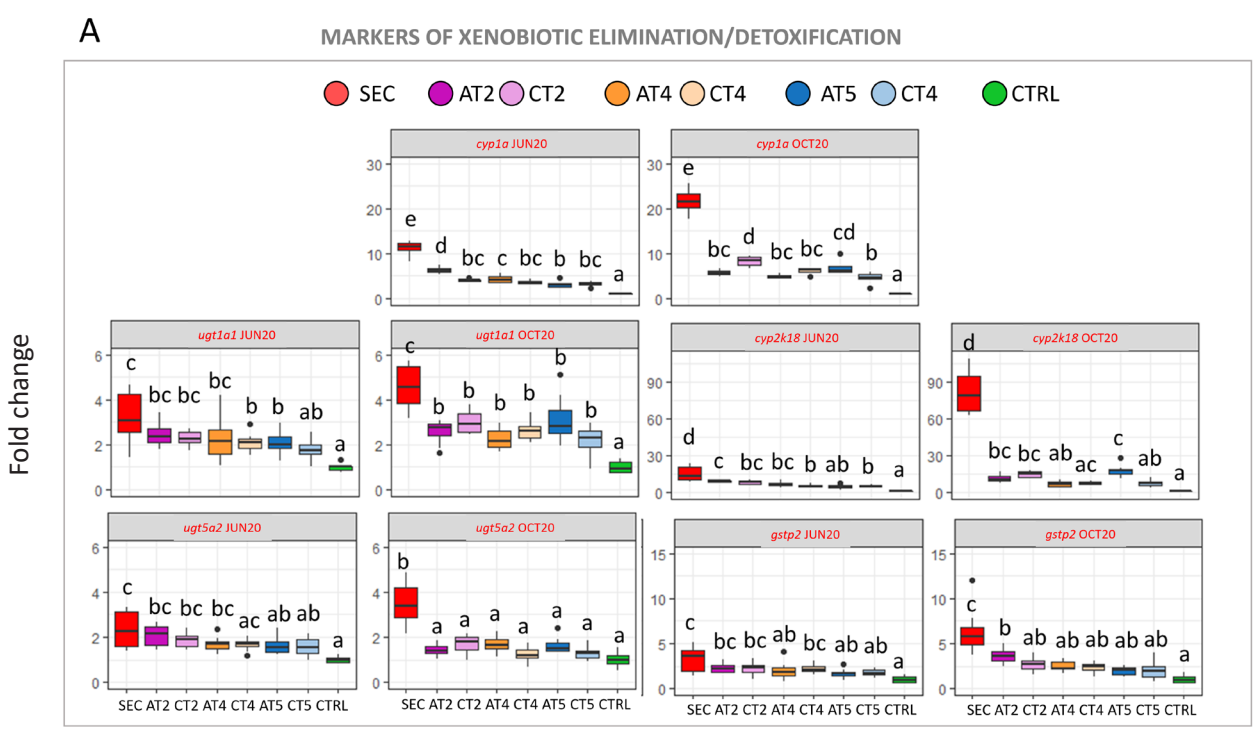

B

TRANSMEMBRANE TRANSPORT + MITOCHONDRIAL DYSFUNCTION
(CORREATED WITH HEME IRON HOMEOSTASIS, AhR SIGNALING AND OXIDATIVE STRESS)

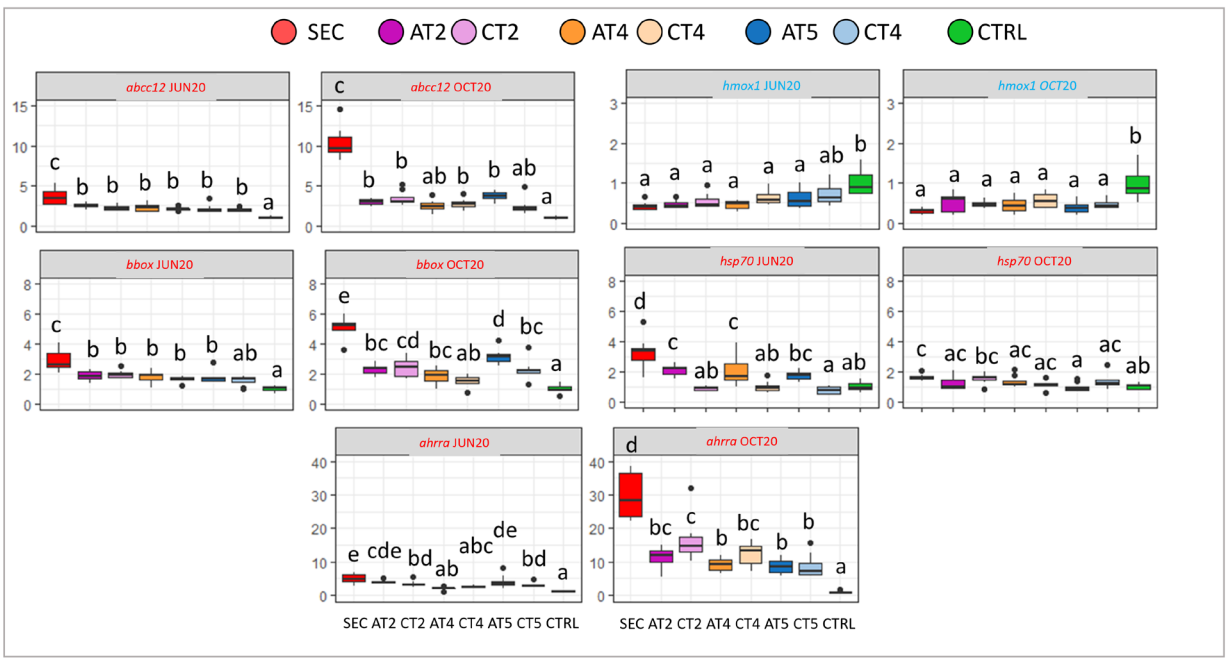

C

EFFECT ON CIRCADIAN RHYTHM AND PHOTOTRANSDUCTION

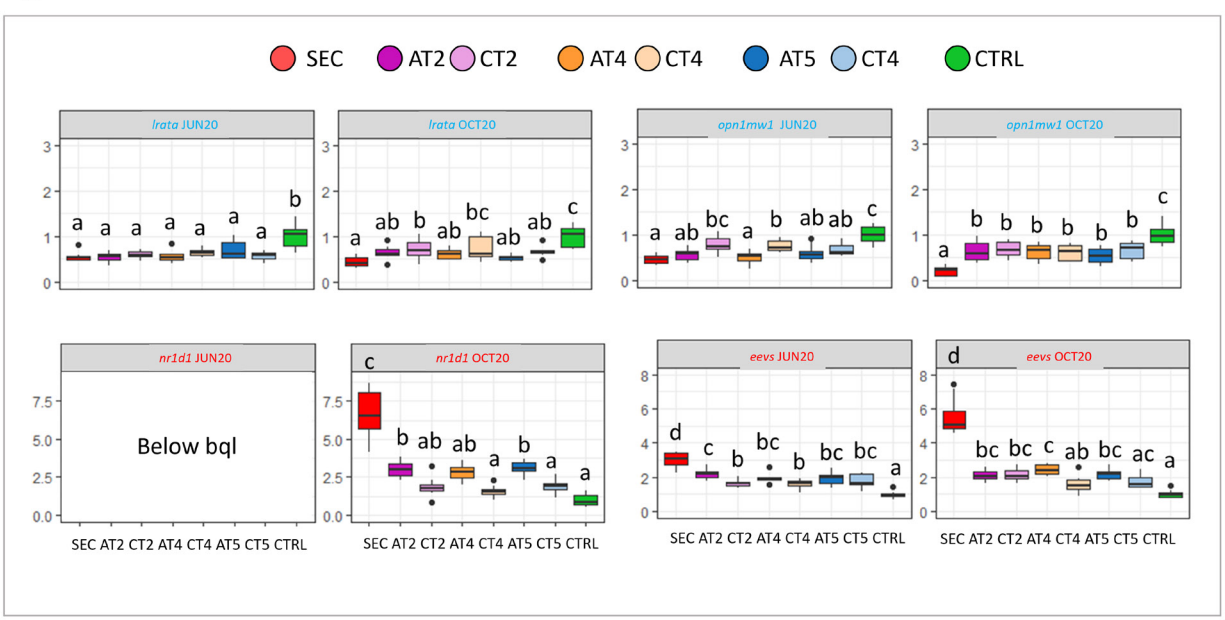

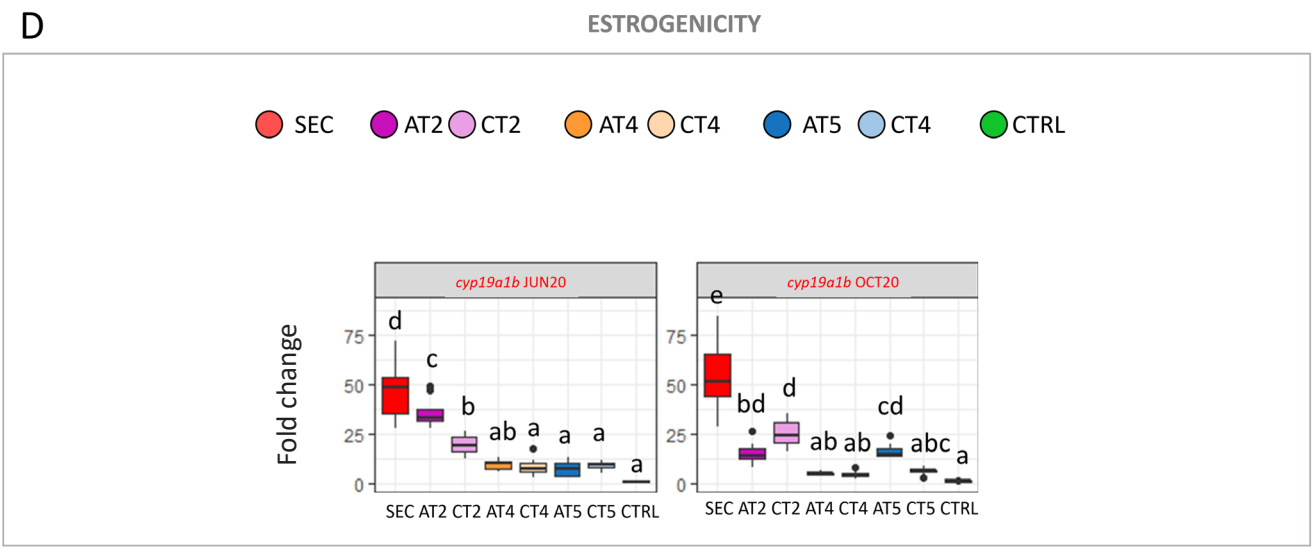

Supplementary Figure SF6. Fold change values for SEC, ATs, CTs and CTRL samples for both campaings of biomarkers of **A)** xenobiotic detoxification, **B)** transmembrane transport, mithochondrial dysfunction, heme iron homeostasis AhR signaling and oxidative stress, **C)** effects on circadian rhythm and phototransduction, **D)** of estrogenicity. Letters on boxplots code for statistical differences amongst samples.

Supporting Tables

Supplementary Table ST1. Home-made database of compounds usually found in water bodies semi-quantified in positive, negative, and resultant confirmed compounds. Available in :
https://www.dropbox.com/scl/fo/l9osr7jywmo802tp2ynja/h?dl=0&rlkey=i5ty4jc7ficyi3lgv9zmctmvu .

Supplementary Table ST2. Description of mapping quality statistics of sequenced samples. Available in :
https://www.dropbox.com/scl/fo/l9osr7jywmo802tp2ynja/h?dl=0&rlkey=i5ty4jc7ficyi3lgv9zmctmvu .

Supplementary Table ST3. Spreadsheet shows the concentration , Predicted No Effect Concentration (PNEC) and chemical structure of the 127 semi-quantified compounds. Sheets 2 and 3 show the VIP compunds identified in the ANOVA-PLS2 analysis for JUN20 and OCT20 samples respectively. Available in :
https://www.dropbox.com/scl/fo/l9osr7jywmo802tp2ynja/h?dl=0&rlkey=i5ty4jc7ficyi3lgv9zmctmvu .

Supplementary Table ST4. Normalized counts and differentially expressed genes (DEGs) for the four approaches. Sheets "1", "2", "3" and "4", show the normalized counts obtained after the Wald analysis regardless of the campaign, for JUN20 campaign, for OCT20 campaign and for the common genes respectively. Sheets "5", "6", "7" and "8", show the DEGs selected after DESeq2 analysis (v.1.10.1) for the four approaches respectively. Available in :
https://www.dropbox.com/scl/fo/l9osr7jywmo802tp2ynja/h?dl=0&rlkey=i5ty4jc7ficyi3lgv9zmctmvu .

Supplementary Table ST5. Enrichment analysis of the common 1785 DEGs performed in DAVID (https://david.ncifcrf.gov/) . Available in :
https://www.dropbox.com/scl/fo/l9osr7jywmo802tp2ynja/h?dl=0&rlkey=i5ty4jc7ficyi3lgv9zmctmvu .

General discussion

SupplementaryTable ST1. Average of the abundance of the different genetic elements in all analyzed matrices in Chapter Two. Data are expressed as copies of each sequence per g of sample. Data in purple highlights average distributions that included estimates from values under the limit of quantitation. Non detected copies were stated as "n.d.".

Type of fertilizer	Paper	Matrix	*int*I1	*sul*1	*tet*M	*qnr*S1	*bla* $_{TEM}$	*bla* $_{CTX-M-32}$	*bla* $_{OXA-58}$	*mec* A
Raw pig slurry	I	Fertilizer	3,90E+09	4,49E+09	3,66E+10	4,33E+06	3,89E+08	3,35E+05	1,54E+07	5,54E+06
Raw pig slurry	II	Fertilizer	1,29E+10	1,10E+10	6,79E+11	4,37E+06	6,05E+07	1,76E+05	4,80E+06	n.d.
Raw pig slurry	III	Fertilizer	1,76E+09	2,50E+09	6,19E+09	8,65E+05	8,48E+07	1,90E+04	1,90E+04	n.d.
Liquid fraction pig slurry	I	Fertilizer	3,14E+09	3,76E+09	5,01E+10	2,37E+06	7,78E+07	5,04E+05	3,61E+06	4,39E+05
Liquid Fraction pig slurry	III	Fertilizer	2,41E+09	3,12E+09	6,75E+09	5,30E+05	3,79E+07	4,82E+05	1,90E+04	n.d.
Solid fraction pig slurry	I	Fertilizer	6,04E+09	6,14E+09	2,21E+10	6,74E+06	9,14E+07	6,93E+05	5,79E+06	9,51E+06
Solid Fraction pig slurry	III	Fertilizer	7,10E+08	5,83E+08	1,37E+09	1,90E+04	3,04E+08	1,90E+04	4,83E+07	n.d.
Digested pig slurry	I	Fertilizer	1,62E+09	1,91E+09	3,84E+10	9,13E+05	1,20E+07	5,29E+05	2,80E+06	3,06E+06
Digested pig slurry	III	Fertilizer	2,10E+09	2,85E+09	6,70E+09	1,52E+06	1,77E+07	1,02E+06	1,90E+04	n.d.
Sewage sludge	II	Fertilizer	2,47E+09	1,52E+09	3,06E+09	8,22E+07	6,41E+06	5,66E+06	1,96E+09	n.d.
OFMSW	II	Fertilizer	5,25E+07	1,03E+08	7,12E+06	3,08E+05	3,18E+05	4,65E+05	1,22E+06	n.d.
Raw pig slurry fertilized soil	II	Soil	2,19E+05	6,92E+05	6,63E+06	1,29E+04	1,01E+03	1,50E+05	1,01E+03	n.d.
Raw pig slurry fertilized soil	III	Soil	6,41E+06	2,59E+06	7,61E+05	4,51E+05	1,78E+06	8,64E+05	2,11E+03	n.d.
Liquid fraction fertilized soil	III	Soil	4,05E+06	2,01E+06	6,80E+05	2,31E+05	1,49E+05	6,02E+05	2,11E+03	n.d.
Solid fraction fertilized soil	III	Soil	2,36E+07	1,12E+07	1,45E+06	3,76E+05	1,49E+06	6,70E+05	2,11E+03	n.d.
Digested pig slurry fertilized soil	III	Soil	5,27E+06	2,78E+06	6,69E+05	5,48E+04	1,66E+06	1,50E+05	2,11E+03	n.d.
Sewage sludge fertilized soil	II	Soil	2,21E+05	5,69E+05	6,55E+06	1,65E+04	5,16E+03	7,53E+04	1,01E+03	n.d.
OFMSW fertilized soil	II	Soil	2,38E+05	5,27E+05	1,09E+07	1,65E+04	1,44E+04	8,78E+04	1,01E+03	n.d.
Minerally fertilized soil	II	Soil	2,64E+05	6,13E+05	6,53E+06	7,18E+04	1,51E+04	3,69E+04	1,00E+03	n.d.
Minerally fertilized soil	III	Soil	4,91E+06	2,05E+06	7,59E+05	8,85E+05	2,98E+06	1,59E+06	2,11E+03	n.d.
Unfertilized soil	II	Soil	1,73E+06	1,88E+06	1,01E+03	1,07E+02	1,01E+03	1,04E+02	1,00E+03	n.d.
Raw slurry fertilized fertilized lettuce	II	Lettuce	8,07E+04	3,84E+04	1,24E+06	1,04E+02	1,00E+03	1,02E+02	1,00E+03	n.d.
Raw slurry fertilized fertilized radish	II	Radish	7,07E+03	1,09E+04	1,00E+03	1,52E+03	1,00E+03	1,68E+03	1,01E+03	n.d.
Raw slurry fertilized corn (leaves)	III	Corn leaves	1,80E+05	4,01E+05	2,11E+03	1,79E+05	2,11E+03	2,88E+04	2,11E+03	n.d.
Liquid fraction fertilized corn (leaves)	III	Corn leaves	2,03E+05	3,49E+05	2,11E+03	2,03E+05	2,11E+03	2,11E+03	2,11E+03	n.d.
Solid fraction fertilized corn (leaves)	III	Corn leaves	1,31E+05	2,50E+05	2,11E+03	1,94E+05	2,11E+03	5,34E+04	2,11E+03	n.d.
Digested pig slurry fertilized corn (leaves)	III	Corn leaves	1,01E+05	2,60E+05	2,11E+03	7,94E+04	2,11E+03	4,71E+04	2,11E+03	n.d.
Sewage sludge fertilized lettuce	II	Lettuce	3,87E+03	9,35E+02	4,47E+04	1,06E+02	1,00E+03	1,03E+02	1,01E+03	n.d.
Sewage sludge fertilized radish	II	Radish	5,05E+03	3,05E+03	1,00E+03	1,06E+02	1,01E+03	1,04E+02	1,61E+04	n.d.
OFMSW fertilized lettuce	II	Lettuce	9,72E+03	6,15E+02	1,75E+04	1,05E+02	1,00E+03	1,06E+02	1,01E+03	n.d.
OFMSW fertilized radish	II	Radish	1,04E+02	1,04E+02	1,01E+03	1,05E+02	1,00E+03	1,05E+02	1,00E+03	n.d.
Minerally fertilized corn (leaves)	III	Corn leaves	1,16E+05	2,17E+05	2,11E+03	6,53E+04	2,11E+03	3,94E+04	2,11E+03	n.d.
Minerally fertilized lettuce	II	Lettuce	5,57E+03	6,37E+02	1,18E+04	1,04E+02	1,00E+03	1,07E+02	1,01E+03	n.d.
Minerally fertilized radish	II	Radish	1,04E+02	1,04E+02	1,00E+03	4,26E+02	1,01E+03	1,06E+02	1,52E+03	n.d.

ACKNOWLEDGMENTS.

THANK YOU• GRÀCIES• GRACIAS

Agradecimientos

"Not a lot, just forever, intertwined, sewn together, like the rock bears the weather"

ADRIANNE LENKER

Tal y como comienzo a rellenar este documento que creé hace cuatro años, me envuelve una sensación de incredulidad combinada con un amor y agradecimiento infinitos. Creo que la única forma que encuentro para ordenar mis emociones es trazar una línea temporal añadiendo con cuidado a las maravillosas personas que me han permitido llegar a este momento.

Todo comenzó cuando mi co-directora Laia Navarro encontró entre sus cien correos mi carta de motivación para el puesto y pensó que encajaría y lo disfrutaría. Gracias Laia por confiar en mi y darme esta oportunidad de evolucionar y crecer en todos los aspectos y por contagiarme tu pasión científica y tu perseverancia, ha sido una tesis accidentada entre pandemias y retos vitales pero lo hemos conseguido y estamos orgullosas del resultado. Estoy segura de que te espera una vida llena de emocionantes proyectos y que conseguirás crear el grupo de investigación con el que sueñas. Y seguidamente debo agradecer a mi director Benjamí Piña, que se dejó convencer para acoger a una doctoranda más, y a pesar de ello no me dejó de guiar, acompañar y enseñar durante todo el proceso. Muchas gracias por darme prioridad cuando la agenda aprieta y por hacer todo lo que estaba en tu mano para que llegara lo más preparada al final de esta etapa.

Cuando recién aterrizaba al laboratorio me encontré con humanos increíbles que se convirtieron en imprescindibles en muy pocos

meses. Rubén, mi doctor antecesor, eres de las personas más bondadosas que he conocido en mi vida, tu facilidad para sorprenderte y apasionarte por la vida y por la ciencia me reconfortó durante aquellos principios difíciles en los que andaba asustada entre eppendorfs. Gracias por estar siempre disponible, por tu amabilidad inagotable y tu cariño. Señora Marta Casado, mi madre gato catalana de Sarrià, has sido mi roca durante todos estos años, me enseñaste los *basics* moleculares pero también los *basics* vitales. Conectamos desde el primer momento (desde que dejaste de darme miedo), y sinceramente no me imagino haber llegado aquí sin ti, sabes bien que esta tesis también es tuya. Te doy las gracias en mi nombre pero también en el nombre de todos los estudiantes que han pasado y pasarán por el laboratorio, gracias por acogernos, querernos y guiarnos cuando ni nosotros mismos sabemos gestionarnos. Ay Inmaculada, qué bien hiciste en cortarte el pelo para que pudiera encontrar una excusa para tomar el café contigo. Cuantísimo cariño, cuidados y consejos me has dado, se me sale el amor por las letras. Cada día que tengo la suerte de que sigas en mi vida mi admiración por ti va creciendo y creciendo. Gracias por escucharme, quererme y sacarme de casa cuándo tenia más ansiedad que amigues. Eres brillante en todos los sentidos. Mir, empezamos con un mes de diferencia, compartimos todas las angustias pero también celebramos todos nuestros logros, empoderándonos a lo largo del proceso. Eres una bola de energía, un cerebro lleno de fórmulas que no entiendo y un corazón bien grande. Juliette, gracias por traer arte, amor y punk a los pasillos de la sexta y acompañarme con tu capacidad para relativizar y tu humor francés que tanta falta le hacia a este edificio. Mel, mi compañera de despacho en la última etapa, i treasured every silly convo we had early in the morning and all the warmth I received from you when my anxiety was kicking in, I adore chu my warrior. Amaita, el agobio de viernes en el baño de la quinta nos unió, y desde ahí no paramos de compartir nuestra vulnerabilidad ni de cuidarnos sin demandas, sin tempos y con mucho mucho amor. Gracias linda. Alex, que afortunada fui de que te pusieras a torturar ratoncillos un domingo de doctorandas pringadas a mi lado y me dieras la oportunidad de conocerte y quererte. Amor entre cotilleos, cine y bizarrismos que más puedo pedir. Crissss mi hermana de pega, acogiste a pollito bajo tu ala ya en el primer muestreo en Palamós y desde entonces no me soltaste. Gracias por tu energía, por lo alto y bonito que te ríes, por siempre regalarme un "pero qué buena cara tienes", un "antes que nada como estás" y alimentarme con guarrerías. Qué ganas de que te mudes a mi barrio.

La ciencia no se sostiene sin los empleados de mantenimiento y limpieza que tanto nos facilitan. Marisa, no se si eres consciente de lo mucho que significaba para mi tu “mira que eres buena y guapa” cada vez que nos cruzábamos en el pasillo. Desde el primer dia supiste ver en mi cosas que ni yo sabia que tenía y no se ni como agradecértelo. Eres un regalo para todas nosotras. Paco, la persona más carismática del edificio. Tu buen humor, tu predisposición inagotable y tu sonrisa eterna sean las cinco de la mañana o de la tarde, marcan la diferencia. Sólo escuchar vuestra voz por los pasillos me hacia sentir en casa. Gracias a los dos. Gracias también al resto de equipo de limpieza que siempre nos regalan su amabilidad y respeto en cada cruce de ascensor.

Y cuando mi corazón ya se iba llenando gracias a todas estas personas, de repente me cayó un regalo del cielo mientras trituraba lechugas. Carlos Barata entra al lab y me pregunta ¿Sabes algo de copépodos? ¿Quieres irte de campaña oceanográfica?. El proyecto ANTOM cambió mi vida por completo. Gracias Carlos, Maria y Jordi por brindarme semejante oportunidad. Dos campañas con la Antártida de por medio. ¿Cómo puedo ser así de afortunada?. Lo que no me esperaba es que aparte de cumplir un sueño, mi familia aumentaría. Nai, nuestro núcleo de abrazos. ¿Qué seria de mi

vida cultural y festivalera sin ti? Gracias por darme el empujón que necesitaba para terminar y por respetar siempre mi espacio y mis necesidades, alegrándote genuinamente por todos mis pequeños logros. Por más aventuras de las señoras del AMPA. Ali, gracias por permitirme graduarme en la escuela Shaolin, por el confesionario intelectual de madrugada, por el baño en nenuco y lejía. Por tu canto desafinado en la cabañita mientras me quedaba ciega muestreando. Por apreciar mi sabiduría de niña vieja. Por tu predisposición a ayudarme, por tu confianza, tus cuidados, tus sopas instantáneas, el chocolate con sal y tus camisetas para que no pareciera una madre en una maratón de domingo. T'estimo y atesoro cada momento contigo. Nur y Jon, gracias por ser tan bonitas, por vuestra energía calmada, sensible, preciosa y vuestra vulnerabilidad y cariño. Os habéis ganado todos nuestros corazones. Gemma y Berta, qué manera tan especial de cuidaros y de cuidarnos tenéis. Gracias por la empatía, por el cariño, los mensajitos de ánimo y preocupación, llenasteis mucho mi corazón. Paraísos míos Pauli y Marta, ANTOM besties, the ultimate queer safe space. Siempre conseguís que me salga la risa de ganso. Gracias por permitirme vivir la fantasía paraíso en alta mar y alimentarme de contrabando. Gracias también al resto de equipo ANTOM. Todxs vosotrxs hicisteis de esta experiencia, algo único e irrepetible.

A parte de estas maravillosas campañas, algo igual de increíble me pasó mientras me tomaba el té de media mañana fue encontrarme con una persona con tatuajes divertidísimos, olor a lavanda y mandarina y risa contagiosa que entró inesperadamente en la salita del café. Era Olga, ¡mi Olga!. Crucé dos palabras con ella y ya sabia que se quedaría en mi vida para siempre. Abriste tu vida entera y me dejaste entrar como si nos conociéramos desde hace años. Eres la bondad, eres el amor, eres la fuerza, eres la red que nos mantiene a todas unidas. Gracias por darme el regalo de compartir la vida contigo. Y gracias por, a través de ti, haberme permitido formar mi familia elegida. Ire, mi otra pequeña bolita de energía, gracias por empatizar, comprender y acompañarme durante estos años de vida ajetreada. Por quererme, cuidarme, por navegar las aguas de crisis vitales y crecer juntas cada día. Por muchos domingos lentos y gustosos de los que nos llenan. Guille, Dj Alto Bicho, escalador guapísimo con un corazón aún más bonito. Convivir con vosotros en la maravillosa casa me hizo sobrevivir a la pandemia sin quedarme calva del estrés. Gracias por tu hospitalidad, amor, y flow que convierten la vida en espontaneidad, risas y tranquilidad. Eres bello. Jaimi marido mío, gracias a ti también por haberme acompañado desde el principio en mi aventura barcelonesa. Si me preguntan que es la felicidad para mí, no puedo describirlo de otra forma que quedarme bailando contigo durante tres horas en la terraza de casa a media tarde. Ya tengo la maleta lista para ir a verte. Gracias también a ti Ross por cuidarnos mutuamente en esta ajetreada cuidad, y por las conversaciones y sueños largos que compartimos. Gracias Mire por tu bondad, consejos, energía y corazón cálidos.

Benjito, my other chosen family. There is no feasible way to summarize how much I appreciate everything you did for me during these years. You nourished me in every sense possible and helped me become the best version of myself. You were on the other side of the line, night and day, even being 5821 miles apart. Thanks for enriching my life with your mere presence.

Y muchas gracias al resto de personitas guapas que llenan mis días y mi corazón y que sin duda estarán presentes en este nuevo renacer post parto académico. Andre bichito, es sólo pensar en ti y ya estoy sonriendo. Por toda una vida de mandarina pelada a tu lado. Gemes Marti y Angi, por fin el círculo está completo. Por fin mi familia elegida valenciana comparte sus vidas conmigo. Qué ganas de todo lo que se viene reinas.

Nito, Nipus, Nispi, Niti. Me has enseñado tantas cosas. Que el amor es entrega, es compromiso, es trabajo, es agradecimiento, es empatía, es crecimiento. Que el amor no duele, no pesa, no se agota. Que todo es relativo, que sólo lo esencial importa. Valentí, regaste tanto mis plantas que tengo la espalda llena de hojas nuevas. Cada noche me acuesto arropada por ellas a tu lado. Cada día es el primero contigo. Cada abrazo es nuevo, único y renovador. Gracias por sostener mis cimientos cuándo tenía la casa en pleno terremoto. Gracias por ayudarme a reconstruirla. El mundo tiene suerte de tenerte en él y nosotras de coexistir contigo.

Mi Carmen, qué años hemos pasado, cuánto crecimiento y dolor, pero siempre juntas, llueva o truene. La videollamada de emergencia siempre activa, la sensación de amor envolvente al despedirnos siempre intacta. Qué ganas de poder seguir siendo testigo de todo lo que irás consiguiendo y experimentando. Te quiero mi continente.

Y papis, un infinito gracias a los dos. Siempre vulnerables, siempre humanos, siempre unidos. Gracias al equipo Sanz Lanzas por quererme y apoyarme tan fervientemente. Gracias mami por las infinitas llamadas y por tu escucha siempre activa. Al final nos reiremos del mundo.

No podría no agradecer el haber compartido plano vital con todos mis bebés peludos. Mi pequeño Lennon, madre Telma, mis bebés Gunti y Marsi, bichis Annie y Lola, linda Mina, bella Bimba, gran Gustavo. Gracias a todas las mascotas que se han dejado acariciar por las calles de Gràcia.

Y un final y amplio gracias al arte por acompañarme desde el primer día que aterricé en Barcelona. Por una vida llena de ilustraciones y escritas sanadoras.

Gracias a todas de corazón, si me he dejado a alguien seguro que te quiero también :)))